

2

AGARD-AG-160-Vol.17

AGARD-AG-160-Vol.17

AD-A171 303

AGARD

ADVISORY GROUP FOR AEROSPACE RESEARCH & DEVELOPMENT

7 RUE ANCELLE 92200 NEUILLY SUR SEINE FRANCE

AGARD AGARDograph No.160 Volume 17

AGARD Flight Test Instrumentation Series Volume 17

on

Analogue Signal Conditioning for Flight Test Instrumentation

by

D.W.Veatch and R.K.Bogue

DISTRIBUTION STATEMENT A

Approved for public release
Distribution Unlimited

DTIC

ELECTE

JUN 11 1986

S

D

B

NORTH ATLANTIC TREATY ORGANIZATION



DISTRIBUTION AND AVAILABILITY
ON BACK COVER

86 611 046

DTIC FILE COPY

NORTH ATLANTIC TREATY ORGANIZATION
ADVISORY GROUP FOR AEROSPACE RESEARCH AND DEVELOPMENT
(ORGANISATION DU TRAITE DE L'ATLANTIQUE NORD)

AGARDograph No.160 Vol.17
ANALOGUE SIGNAL CONDITIONING FOR FLIGHT TEST INSTRUMENTATION
by
D.W.Veatch and R.K.Bogue
A Volume of the
AGARD FLIGHT TEST INSTRUMENTATION SERIES

Edited by
R.K.Bogue

DTIC
ELECTE
S JUN 11 1986 D
B

DISTRIBUTION STATEMENT A
Approved for public release
Distribution Unlimited

THE MISSION OF AGARD

The mission of AGARD is to bring together the leading personalities of the NATO nations in the fields of science and technology relating to aerospace for the following purposes:

- Exchanging of scientific and technical information;
- Continuously stimulating advances in the aerospace sciences relevant to strengthening the common defence posture;
- Improving the co-operation among member nations in aerospace research and development;
- Providing scientific and technical advice and assistance to the Military Committee in the field of aerospace research and development (with particular regard to its military application);
- Rendering scientific and technical assistance, as requested, to other NATO bodies and to member nations in connection with research and development problems in the aerospace field;
- Providing assistance to member nations for the purpose of increasing their scientific and technical potential;
- Recommending effective ways for the member nations to use their research and development capabilities for the common benefit of the NATO community.

The highest authority within AGARD is the National Delegates Board consisting of officially appointed senior representatives from each member nation. The mission of AGARD is carried out through the Panels which are composed of experts appointed by the National Delegates, the Consultant and Exchange Programme and the Aerospace Applications Studies Programme. The results of AGARD work are reported to the member nations and the NATO Authorities through the AGARD series of publications of which this is one.

Participation in AGARD activities is by invitation only and is normally limited to citizens of the NATO nations.

The content of this publication has been reproduced directly from material supplied by AGARD or the authors.

Published April 1986

Copyright © AGARD 1986
All Rights Reserved

ISBN 92-835-1520-X



Printed by Specialised Printing Services Limited
40 Chigwell Lane, Loughton, Essex IG10 3TZ

PREFACE

Soon after its founding in 1952, the Advisory Group for Aerospace Research and Development recognized the need for a comprehensive publication on flight test techniques and the associated instrumentation. Under the direction of the AGARD Flight Test Panel (now the Flight Mechanics Panel), a Flight Test Manual was published in the years 1954 to 1956. The Manual was divided into four volumes: I. Performance, II. Stability and Control, III. Instrumentation Catalog, and IV. Instrumentation Systems.

As a result of developments in the field test instrumentation, the Flight Test Instrumentation Group of the Flight Mechanics Panel was established in 1968 to update Volume III and IV of the Flight Test Manual. Upon the advice of the Group, the Panel decided that Volume III would not be continued and that Volume IV would be replaced by a series of separately published monographs on selected subjects of flight test instrumentation: the AGARD Flight Test Instrumentation Series. The first volume of the Series gives a general introduction to the basic principles of flight test instrumentation engineering and is composed from contributions by several specialized authors. Each of the other volumes provides a more detailed treatise by a specialist on a selected instrumentation subject. Mr W.D.Mace and Mr A.Pool were willing to accept the responsibility of editing the Series, and Prof D.Bosman assisted them in editing the introductory volume. In 1975 Mr K.C.Sanderson succeeded Mr Mace as an editor.

Special thanks and appreciation are extended to Professor T.van Oosterom, NE, who chaired the Group from its inception in 1968 until 1976 and established many of the ground rules under which the Group operated, to the late Mr N.O.Matthews, UK, who chaired the Group during 1977 and 1978 and to Mr F.N.Stoliker, US, who chaired the Group from 1979 until its termination in 1981.

In 1981 the Flight Mechanics Panel decided that the Group should also supervise a new series of monographs in the field of Volumes I and II of the Flight Test Manual. The Group was therefore renamed Flight Test Techniques Group. However, this Group also continues the publication of the volumes in the Flight Test Instrumentation Series. The Group gratefully remembers the way Mr Stoliker chaired the Flight Test Techniques Group during 1981 and 1982 and marked the outlines for future publications.

It is hoped that the Flight Test Instrumentation Series will satisfy the existing need for specialized documentation in the field of flight test instrumentation and as such may promote a better understanding between the flight test engineer and the instrumentation and data processing specialists. Such understanding is essential for the efficient design and execution of flight test programs.

In the preparation of the present volume the members of the Flight Test Techniques Group listed below have taken an active part. AGARD has been most fortunate in finding these competent people willing to contribute their knowledge and time in the preparation of this volume.

Adolph, C.E.	AFFTC/US
Bogue, R.K. (editor)	NASA/US
Borek, R.W.	NASA/US
Bothe, H.	DFVLR/GE
Bull, E.J.	A & AEE/UK
Carabelli, R.	SAI/IT
Galan, R.C.	CEV/FR
Lapchine, N.	CEV/FR
Moreau, J.	CEV/FR
Norris, E.J.	A & AEE/UK
Phillips, A.D.	AFFTC/US
Pool, A.	NLR/NE
Sanderson, K.C.	NASA/US

on For	
RA&I	<input checked="" type="checkbox"/>
B	<input type="checkbox"/>
nced	<input type="checkbox"/>
cation	

J.T.M.van DOORN, NLR/NE
 Member, Flight Mechanics Panel
 Chairman, Flight Test Techniques Group.

ution/
 bility Codes

avail and/or
 Special

Dist



A-1

CONTENTS

	Page
PREFACE	iii
NOMENCLATURE	vi
SUMMARY	
1. INTRODUCTION	1
2. FLIGHT-TEST SIGNAL-CONDITIONING AND THE ENGINEER	2
2.1 THE IDEAL INSTRUMENTATION SYSTEM	2
2.2 THE PRACTICAL INSTRUMENTATION SYSTEM	2
2.2.1 The Measurand	2
2.2.2 The Detection Process	2
2.2.3 Pre-Transduction Signal Conditioning	3
2.2.4 The Transducer	3
2.2.5 The Data-Terminal Device	4
3. GENERAL SIGNAL-CONDITIONING TECHNIQUES	6
3.1 AMPLIFICATION, ATTENUATION, AND ZERO SHIFTING	6
3.1.1 Voltage Amplifier	7
3.1.2 Isolation Amplifier	9
3.1.3 Current Amplifier	10
3.1.4 Charge Amplifier	10
3.1.5 Logarithmic and Antilogarithmic Amplifier	11
3.1.6 Alternating Current Amplifier	12
3.1.7 Amplitude-Modulation Carrier Amplifier System	12
3.2 FILTERS	12
3.2.1 Noise Reduction with Filters	12
3.2.2 Ideal Filters	13
3.2.3 Practical Filters	13
3.2.4 Disadvantages of Filters	18
3.3 DIGITAL SIGNAL CONDITIONING	18
3.3.1 Analog-to-Digital Converter	18
3.3.2 Digital Filter	19
3.3.3 Extracting Data from a Digital Data Bus	19
3.3.4 Signal Conditioning with Microcomputers	20
3.3.5 Signal Conditioning with Minicomputers	20
4. SIGNAL CONDITIONING OPTIMIZED FOR SPECIFIC TRANSDUCTION TECHNIQUES	32
4.1 SELF-GENERATING TRANSDUCER SIGNAL CONDITIONING	32
4.1.1 Piezoelectric Transducer Signal Conditioning	32
4.1.2 Thermocouple Transducer Signal Conditioning	36
4.1.3 Faraday-Law Transducer Signal Conditioning	42
4.2 NON-SELF-GENERATING TRANSDUCER SIGNAL CONDITIONING	43
4.2.1 Variable-Resistance-Transducer Signal Conditioning	44
4.2.2 Variable-Capacitance-Transducer Signal Conditioning	49
4.2.3 Variable-Inductance-Transducer Signal Conditioning	51
4.2.4 Mechano-Optical Effect Transducer Signal Conditioning	56
4.2.5 Force-Balance-Transducer Signal Conditioning	57
5. MULTIPLEXERS AS SIGNAL CONDITIONERS	79
1 TIME-SAMPLED DATA AND ALIASING	79
5.2 FREQUENCY-DIVISION MULTIPLEXING	80
5.2.1 Proportional-Bandwidth FM-Type FDM Systems	80
5.2.2 Constant-Bandwidth FM-Type FDM Systems	82
5.3 TIME-DIVISION MULTIPLEXING	83
5.3.1 Pulse-Amplitude Modulation TDM Systems	83
5.3.2 Pulse-Code Modulation TDM Systems	84
5.4 TIME CORRELATION OF MULTIPLEXED DATA	85
5.5 REMOTE MULTIPLEXING	85
6. SIGNAL CONDITIONING FOR AIRBORNE SIGNAL TERMINAL DEVICES	91
6.1 SIGNAL CONDITIONING FOR MAGNETIC TAPE RECORDERS	91
6.1.1 Direct-Recording Signal Conditioning	91
6.1.2 Wideband-FM Recording Signal Conditioning	92

	Page
6.1.3 PCM-Recording Signal Conditioning	92
6.2 SIGNAL CONDITIONING FOR TELEMETRY TRANSMITTERS	93
6.2.1 FM/PM Pre-Emphasis	94
6.2.2 PCM/FM Systems	95
6.2.3 Pre-Modulation Filter	95
6.3 THE CAMERA	95
6.3.1 Photographic Camera	95
6.3.2 Television Camera	96
6.4 CONTINUOUS-TRACE RECORDER	96
6.5 PILOT AND AIRCREW DISPLAYS	98
6.5.1 Pilot Displays	98
6.5.2 Crew Displays	98
APPENDIX A OPERATIONAL AMPLIFIER	105
A.1 NON-IDEAL OPERATIONAL AMPLIFIER CHARACTERISTICS	106
A.2 ERRORS CAUSED BY FINITE OPEN-LOOP AMPLIFIER GAIN	106
A.3 EFFECTS OF FINITE OPERATIONAL AMPLIFIER OUTPUT IMPEDANCE	106
A.4 EFFECTS OF FINITE OPERATIONAL AMPLIFIER FREQUENCY RESPONSE	106
A.5 EFFECTS OF OPERATIONAL AMPLIFIER FINITE INPUT IMPEDANCE	107
A.6 EFFECTS OF INTERNAL VOLTAGE AND CURRENT BIAS	108
A.7 EFFECTS OF FINITE AMPLIFIER COMMON-MODE REJECTION RATIO	109
A.8 EFFECTS OF OTHER NON-IDEAL FACTORS	109
APPENDIX B SINGLE-ENDED VOLTAGE AMPLIFIER	113
B.1 THE SINGLE-ENDED INVERTING AMPLIFIER	113
B.2 THE SINGLE-ENDED NON-INVERTING AMPLIFIER	114
APPENDIX C INSTRUMENTATION (DIFFERENTIAL) AMPLIFIER	117
APPENDIX D ISOLATION AMPLIFIER	120
APPENDIX E CURRENT AMPLIFIER	122
APPENDIX F CHARGE AMPLIFIER	124
APPENDIX G ALTERNATING CURRENT COUPLED AMPLIFIER	129
APPENDIX H CARRIER-AMPLIFIER SYSTEM	130
APPENDIX I THE ACTIVE FILTER	133
I.1 INTRODUCTION	133
I.2 LOGARITHMIC RATIOS FOR DESCRIBING FILTER RESPONSE	133
I.3 TRANSFER FUNCTION AND FILTERS	134
I.4 SCALING FILTER FREQUENCY AND IMPEDANCE	137
I.5 FILTER CIRCUITS	137
I.5.1 The Zero-offset Low-Pass Filter	138
I.5.2 Voltage-Controlled Voltage-Source Low-Pass Filters	139
I.5.3 Voltage-Controlled Voltage-Source High-Pass Filters	142
I.5.4 Cauer (Elliptic) High-Pass and Low-Pass Filters	145
I.5.5 Commutating Bandpass and Band-Reject Filter	147
I.6 SELECTING COMPONENTS FOR AN ACTIVE FILTER	147
APPENDIX J THERMOCOUPLE PATTERN-CIRCUIT TECHNIQUE	152
APPENDIX K ANALYSIS OF AN ICE-BATH REFERENCE	156
APPENDIX L PROPORTIONAL-CONTROL HEATER FOR THERMOCOUPLE REFERENCE OVENS	157
APPENDIX M THERMOCOUPLE REFERENCE-JUNCTION COMPENSATOR	158
APPENDIX N ANALYSIS OF A STANDARD COPPER CONNECTION IN A THERMOCOUPLE WIRING CIRCUIT	160
APPENDIX O THE PATTERN-CIRCUIT ANALYSIS TECHNIQUE FOR COMPLEX THERMOCOUPLE CIRCUITS	161
REFERENCES	163

NOMENCLATURE

Symbols:		V	voltage
A	area; amplitude gain; amplitude of sinusoidal waveform	X	input measurand
A,B,C	thermoelectric materials	x	a variable
A'	open-loop amplifier gain	Z	impedance
a	acceleration	α	time-phase shift, synchros; angle
a,b	dimensions	β	thermal coefficient of resistivity; thermistor material constant; feedback factor; bandwidth factor (FM modulation)
B	magnetic flux density	ϵ	permittivity; longitudinal strain (dimensionless); dielectric constant
C	capacitance	θ	stator angle
D	deviation ratio; diode	$T^{\text{II AB}}$	Peltier coefficient of materials A and B whose junction is at temperature T
d	damping coefficient; diameter	σ	longitudinal stress; Thompson voltage coefficient
E	Young's modulus; power supply voltage or bias voltage	τ	time constant; group delay
e	variable voltage; natural logarithm base	ϕ	phase shift
F	force	Ω	ohm
f	frequency	ω	angular frequency, $2\pi f$, rad/sec; angular rotational velocity, deg/sec
G	absolute value of transfer function		
g	gap spacing; gravitational acceleration		
H	transfer function		
I	current	Subscripts:	
i	variable current	A	amplifier
i,j	an imaginary number	A,B	resolver output (voltage)
K	a constant; filter gain	A,B,C	thermoelectric materials
k	gauge factor of a strain guage	a,b	network elements (resistors)
L	length; inductance	amb	ambient (temperature)
M	motor	B	battery/bridge (voltage); bias (current)
m,n	an integer	C	cable (resistance/capacitance); calibration (resistance); composite (resistance); carrier (frequency); center (frequency); cutoff (frequency)
N	number of turns on a coil	CH	high cutoff (frequency)
n	gear ratio; normalized position of a potentiometer tap	CL	cable leakage (resistance); low cutoff (frequency)
P	power	CM	common mode (gain/impedance)
Q	electric charge; quality factor defining a filter characteristic sharpness	D	differential (gain/impedance)
R	resistance	e	error
rms	root-mean-square	exp	exponential
S	switch contact; thermocouple sensitivity	F	feedback (resistance/capacitance); fixed (resistance)
s	Laplace operator	G	gauge or galvanometric (resistance)
T	period; temperature; transformer		
t	time		

i	input (voltage/current/resistance/impedance)	CMR	common-mode rejection, dB
J	index (channel)	CMRR	common-mode rejection ratio
K	thermocouple (sensitivity/voltage output)	CR	control receiver
k	index (Bessel function)	CT	control transformer
L	load (resistance/impedance); longitudinal (strain)	CX	control transmitter
log	logarithmic	DAS	data-acquisition system
M	ratio (voltage)	DIN	Deutsche Industrienorm (German Industrial Standard)
m	maximum (frequency)(strain)	FDM	frequency division multiplexing
N	noise (voltage)	FET	field-effect transistor
n	natural frequency	FM	frequency modulation
o	output (voltage/current/resistance/impedance); free-space value (permittivity); base channel (subcarrier array); reference (resistance/voltage)	F.S.	full scale
oe	effective output (impedance)	INS	inertial navigation system
os	offset (voltage)	IRIG	Inter-Range Instrumentation Group (U.S.A.)
P	pattern circuit (voltage); potentiometer (voltage/resistance)	LSB	least significant bit (of a digital word)
p	Peltier voltage	LVDT	linear variable-differential transformer
R	reference (temperature/resistance/voltage)	MSB	most significant bit (of a digital word)
S	source (voltage/current/resistance/impedance); data spectrum maximum frequency; shunt (resistance/capacitance)	NASA	National Aeronautics and Space Administration (U.S.A.)
s	sampling (frequency); signal (frequency)	NBS	National Bureau of Standards (U.S.A.)
T	Thompson (voltage); temperature transducer (voltage/resistance); thermistor (resistance)	NLR	Nationaal Lucht-En Ruimtevaartlaboratorium (National Aerospace Laboratory, the Netherlands)
TL	transducer leakage (resistance)	NRZ	nonreturn to zero
VL	variable line (resistance)	PAM	pulse-amplitude modulation
W	lead wire (resistance)	PBFM	proportional bandwidth FM
x	variable value (voltage/capacitance); excitation (voltage)	PCM	pulse-code modulation
Z	zone (isothermal)	PDM	pulse-duration modulation
1,2,...,n	differentiates between similar items (elements, constants, or phases)	PM	phase modulation
Abbreviations:		PSD	phase-sensitive demodulator
ADC	analog-to-digital converter	RF	radio frequency
ADS	air data system	RS	resolver
AM	amplitude modulation	RTD	resistive temperature detector
BCAC	Boeing Commercial Aircraft Company	RVDT	rotary variable differential transformer
CBFM	constant-bandwidth FM	RZ	return to zero
CDX	control differential transmitter	SAS	stability augmentation system
		SCO	subcarrier oscillator
		S/N	signal-to-noise ratio
		TC	temperature coefficient

TDM	time division multiplexing	TX	torque transmitter
TDR	torque differential receiver	VCO	voltage controlled oscillator
TDX	torque differential transmitter	VDT	variable differential transformer
TR	torque receiver		

ANALOG SIGNAL CONDITIONING FOR FLIGHT-TEST INSTRUMENTATION

Donald W. Veatch*
 Consultant to AGARD Flight Mechanics Panel
 Star Route 2, Box 3060-C
 Tehachapi, California 93561

and

Rodney K. Bogue
 Group Leader, Flight-Test Techniques
 NASA Ames Research Center
 Dryden Flight Research Facility
 P.O. Box 273
 Edwards, California 93523-5000

SUMMARY

This document addresses the application of analog signal conditioning to flight-test data-acquisition systems. Emphasis is placed on practical applications of signal conditioning for the most common flight-test data-acquisition systems. A limited amount of theoretical discussion is included to assist the reader in a more complete understanding of the subject matter.

Nonspecific signal conditioning, such as amplification, filtering, and multiplexing, is discussed. Signal conditioning for various specific transducers and data terminal devices is also discussed to illustrate signal conditioning that is unique to particular types of transducers.

The purpose of this document is to delineate for the reader the various signal-conditioning technique options, together with tradeoff considerations, for commonly encountered flight-test situations.

1. INTRODUCTION

The primary goal of this volume is to acquaint flight-test and instrumentation engineers with the most important signal-conditioning techniques and with the ways in which these techniques can best be applied. The background material provided herein should make it possible for the engineer to understand the rationale behind the selection of optimal signal-conditioning techniques for given applications. (The term "engineer" is used throughout for both flight-test and instrumentation engineers.)

A secondary goal of this volume is to provide the new engineer with a working background in signal-conditioning practices. This material also makes an interesting review for the experienced engineer, and the sections on practical approximations constitute a fruitful area for further discussion. The appendixes contain theoretical, mathematical, and circuit details on several subjects covered more generally in the main text, and the references listed at the end of the volume provide handy guidelines for further study.

Since even experienced engineers do not always agree on what signal conditioning encompasses, signal conditioning must first be defined before it can be discussed. As used in this volume, flight-test signal conditioning is defined as "the signal modifications between the transducer and the input stage of the recording or telemetry system, the indicator, or the airborne computer" (Ref. 1). This is post-transduction signal conditioning and is the subject of this volume.

Although airborne computers and microprocessors can be very powerful signal conditioners, they are not extensively discussed. The airborne computer referred to in the above definition would be a computer such as those used in the flight-controls systems and thus would be defined as a data-acquisition terminal device. A computer can also function as a signal source for the data-acquisition system (DAS), in which case signal conditioning is required.

The purpose of (post-transduction) signal conditioning is to make an optimal match between the transducer output and the input of the aircraft data-acquisition terminal devices: for example, to match a thermocouple to a tape recorder or transmitter. Properly done, this signal conditioning greatly simplifies the airborne data-acquisition and ground data-reduction tasks. For example, pulse-code modulation (PCM) can place many data channels on a single tape-recorder track or on a single transmitter channel and can also match the data conveniently to the modern computerized ground data-reduction systems.

An excellent short overview of signal conditioning is provided in Chapter 5 of Ref. 1. The symbols used herein for electrical circuits conform to those recommended in Ref. 2.

*Head (retired), Instrument Development Branch, NASA Ames Research Center, Dryden Flight Research Facility.

2. FLIGHT-TEST SIGNAL-CONDITIONING AND THE ENGINEER

To understand the need for signal conditioning, the engineer must understand the nature and purpose of each link in the airborne data-acquisition sequence. To illustrate the need for signal conditioning, an "ideal" instrumentation system is compared with a real instrumentation system. By this means it is clearly shown why signal conditioning is required and how it can be used to improve the quality of the data. Flight-test signal conditioning is the subject of this volume and the emphasis is on why the various techniques are selected. The relative merits of each technique are also discussed.

2.1 THE IDEAL INSTRUMENTATION SYSTEM

In an ideal instrumentation system, there is no requirement for signal conditioning. In this ideal world, there exists a measurand, a transducer, and an airborne data-terminal device (Fig. 1). None of these ideal system components introduces a time delay.

The measurand is defined as the physical quantity that is to be measured; for example, strain, pressure, or temperature. The ideal measurand contains no information beyond that required for the application.

The ideal transducer detects the measurand without distorting the measurand. If the measurand is not in a form that optimally matches the on-board data-terminal device, then the transducer provides the airborne terminal device with the desired representation of the measurand. The ideal transducer introduces no distortion or noise.

The airborne data-acquisition terminal device is a recorder, transmitter, indicator, or airborne (terminal-type) computer. The ideal (aircraft) acquisition terminal device requires no signal conditioning, since the transducer optimally matches its input requirements.

2.2 THE PRACTICAL INSTRUMENTATION SYSTEM

Figure 2 is a representation of a practical, one-channel airborne data-acquisition system. This system differs from the ideal system in that each system element, to a greater or lesser degree, "contaminates" the data during the acquisition process. This contamination takes the form of amplitude distortion, time-delay, and additive noise.

Each block in Fig. 2 has an input and an output signal. The relationship between these individual input and output signals is described by a transfer function (see Sec. 3 and Appendix I). The transfer function is a mathematical description of how the input signal is modified during transit through each system element. Most often this description is in the form of an amplitude and time-delay relationship between input and output. It is vital that the engineer know and understand the transfer function of each system element so that the effects of the accumulated transfer functions may be corrected in the data-reduction process.

In addition to the signal modifications by the system elements, noise is introduced within and between each system element, even including the measurand itself. This noise can be introduced by several means — power fluctuations, electrically coupled contamination, and physical vibration. Once this noise is coupled into the data information, it is very difficult or impossible to remove. The most effective way to reduce noise is to prevent its entry into the data channel. This reduction can be accomplished by power-line stabilization, isolation of signal wiring from noise sources, and vibration isolators. These noise-reduction techniques are covered here only in a general manner since they are considered in detail in the literature. Reference 3 is an excellent source of information about practical techniques as applied to aerospace applications. References 4 and 5 cover shielding and grounding techniques for low-level signals used in flight-test applications; Refs. 6 and 7 are also excellent sources of information about these techniques.

2.2.1 The Measurand

The measurand is the physical quantity that the engineer wishes to measure. In a real instrumentation system, the measurand always contains some unwanted information, which in this text is called noise. Sometimes what is noise to one person is data to another. Consider the output of a control-surface hydraulic actuator. One engineer wanted to know the position of the control surface over the range of $\pm 20^\circ$. Another wanted to measure the dither introduced by the drive electronics into the actuator. The dither was expected to have a maximum amplitude of $\pm 0.2^\circ$. Both users had to use the same data source and each considered the other user's data as noise. The control-surface data had a frequency spectrum of 0 to 3 Hz, and the dither data had a spectrum of 4 to 6 Hz. The data spectra of each were too close to permit an ideal separation of the two signals; however, a carefully designed low-pass filter removed much of the dither-induced ripple from the control-surface data, and a bandpass filter considerably improved the dither data by removing most of the large static and quasi-static data excursions.

2.2.2 The Detection Process

The detection process was included in Fig. 2 to emphasize the fact that no real transducer can detect the measurand without introducing some error. One can only hope that the errors introduced in the detection process are truly negligible relative to the required accuracy. In a well-designed system this is usually the case. An even greater problem is that the detection process may be incapable of making the measurand available to the transducer. In the previous example of measuring the control-surface position by means of the position of the hydraulic actuator that drove the control surface, the actual position and shape of the control surface was not truly represented by the measured parameter. That control surface was on a very high speed aircraft and was distorted by airflow pressures, temperature, temperature gra-

dients, and acceleration forces. Obviously, when accurate measurements are required, considerable attention must be devoted to the detection process.

2.2.3 Pre-Transduction Signal Conditioning

Thorough coverage of the subject of pre-transduction signal conditioning would require a volume in itself; however, the importance of this subject to the overall data-acquisition process demands that limited coverage of it be included in this document. The use of pre-transduction signal conditioning offers unique opportunities for system noise reduction and system linearity improvement. It is very important that the engineer be aware of the effects introduced by neglect or unintentional inclusion of pre-transduction signal conditioning.

In some instances, a transducer has a transfer function that distorts the amplitude or phase representation of a measurand. For example, the transducer itself may have a lightly damped resonance characteristic that produces undesirable side effects. In these situations, it is often possible to introduce pre-transduction signal conditioning to compensate for these effects and produce a more well-behaved characteristic. For example, a pneumatic network is sometimes used to modify the undesirable characteristics of a pressure transducer.

On the negative side, the unintentional inclusion of pre-transduction signal conditioning may degrade the performance of what is otherwise an excellent transducer. This occurs commonly in the mounting of accelerometers. The mechanical mounting materials and configuration often modify the acceleration waveform and thereby reduce the apparent peak acceleration recorded by the data system.

As noted previously, the introduction of noise into the data signal must be carefully avoided. Many types of noise cannot be eliminated, or can be eliminated only with great difficulty from the electrical signal downstream of the transducer. It is often easier to eliminate this noise before the transduction process. For example, a vibration isolator will minimize the addition of noise into the signal from a transducer that is sensitive to physical vibration. A power-line conditioner will reduce the introduction of power-line noise from a transducer excited from an unregulated voltage source.

Some real examples of this form of signal conditioning will highlight these kinds of situations. A major aircraft manufacturer wished to study the effects of the shock wave of a supersonic aircraft when it passed close to a flight-test aircraft. To accomplish this, the wings and body of the test aircraft were instrumented with a large number of flush-diaphragm pressure transducers. On the first test flight, almost half of the pressure transducers were destroyed. When the transducer pressure diaphragm is mounted flush with the aircraft skin, the diaphragm is in a highly undamped condition. Any pressure transient or pneumatic noise near the diaphragm's natural frequency can cause the diaphragm to rupture. The solution was to mount the pressure transducer in a fixture that provided an air chamber in front of the flush-diaphragm pressure transducer; this chamber was connected by a section of tubing to a pressure port in the skin (Fig. 3). An analysis of the data can determine the bandwidth required to produce a reasonable reproduction of the data wave shape, in this case a fairly abrupt transient. The pneumatic tubing and air chamber, illustrated in Fig. 3, act as a filter that prevents high-frequency damage to the transducer diaphragm; it also protects the diaphragm from mechanically induced vibrational damage by pneumatically damping the diaphragm. This pneumatic filter is mathematically described in Ref. 8 by equations that are adequate for small-pressure perturbations. These equations illustrate that the frequency response, and particularly the system damping, is strongly dependent on the altitude (ambient pressure). Thus, the system design should be optimized for the test conditions.

In another example, an accelerometer with a frequency response of 0 to 100 Hz was used to measure aircraft body motions. These motions normally occupy a narrow bandwidth from 0 to 3 Hz. When the accelerometer was mounted on a light, flexible, and poorly designed instrumentation shelf, self resonances were produced that were in the passband of the accelerometer. A small, high-frequency shelf deflection in the passband of the accelerometer produced very high acceleration inputs. These inputs made the desired data difficult to interpret and at times saturated the transducer and made the accelerometer output meaningless. The first attempted solution was to provide pre-transduction signal conditioning by stiffening the mounting shelf. This reduced the shelf deflections and, thus, the vibrational noise to the accelerometer. In a severe case, the location was strongly driven by a powerful source of high-frequency vibrations from the aircraft engine; in that instance, the accelerometer had to be moved to another location. In another case of severe vibration, the accelerometer had to be mounted on vibration isolators. Note that post-transduction filtering in this case can remove the high-frequency noise, but this may mask the fact that these high-frequency accelerations are of such a magnitude as to render the accelerometer partially or completely inoperative because of saturation.

All of the above examples illustrate that pre-transduction signal conditioning may be required to achieve useful data or even to save the transducer. Post-transduction signal conditioning, the subject of this volume, can mask a serious condition and obviously will not protect the transducer from damage. Pre-transduction signal conditioning is at best a difficult subject and to the author's knowledge, one that is not covered in any one reference in an adequate manner. The only general rule that can be offered is that when environmental or noise inputs to a transducer limit its capability to produce quality data, pre-transduction signal conditioning may be required.

2.2.4 The Transducer

A transducer is a device that can detect a desired measurand, such as a pressure or temperature, and transform it into an output that is compatible with the data-acquisition system signal conditioning. The transducer uses some energy from the measurand and outputs energy in a usable form, most commonly as an electrical output. In some cases the measurand may be in a form that already has the correct output to match the terminal device, in which case neither a transducer nor signal conditioning would be required.

Typically, a transducer is required, and the output usually requires modification to match the aircraft data terminal device.

Signal conditioning is all too often assumed to require only voltage amplification (or attenuation), zero shifting, impedance matching, or filtering, or combinations thereof. In practice, attention should also be devoted to the nature of the transducer output and to the data terminal input requirements. For example, when the transducer is inherently a current or charge-output device, a voltage amplifier is not the optimum interface. Galvanometers and many indicators are current-sensitive data-terminal devices, whereas most airborne radio frequency (RF) transmitters are voltage-sensitive devices. This means that the optimum signal-conditioning technique requires that the engineer accommodate both the transducer output characteristics and the input characteristics of the terminal device. This volume provides this kind of information for the most popular transduction techniques.

Present-day transducers often contain considerable amounts of signal-conditioning integral with the transducer package. This trend is made possible by the availability of reliable low-power microelectronics. For example, the linear variable-differential transformer (LVDT), which is often used to acquire control-position data, requires an ac power supply and a demodulator. Many LVDT modules are presently available as small units which include the dc to ac power supply, the demodulator, and the required filtering internal to the unit. Since it is impossible to predict just how much signal conditioning will be included with a particular transducer, the text will normally assume that each unit has no internal signal conditioning. Thus, the comments on the kinds of signal conditioning usually encountered with each kind of transduction principle will allow the engineer to determine if additional or different signal conditioning is needed.

Some transducers have particular characteristics of which the engineer must be aware if the signal conditioning is to be effective. These characteristics will be covered in the sections on the various signal conditioners required with specific transduction principles. Signal conditioning is only required when the transducer data outputs require a more optimum match to the aircraft data terminal. Typical examples include data-channel multiplexing and transducer-output optimization (amplification, zero shifting, frequency shaping, demodulation, attenuation, coding, and decoding). Airborne computers may be required to perform a variety of sophisticated signal-conditioning tasks.

Signal conditioning itself may introduce side effects not all of which are desirable. For example, signal conditioners such as simple passive filters can exhibit large impedance changes over the operating frequency range. Multiplexing techniques, such as pulse-code modulation (PCM), usually require upper frequency restrictions on their input and output signals.

Many data users strongly resist the inclusion of signal-conditioning filters in the signal-conditioning process since these filters introduce amplitude- and phase-shift changes to the data. What these data users often do not realize is that each link in the signal-conditioning process has its own complex transfer function which, like a filter, also produces amplitude and phase shifts. Any one of these transfer functions can be more limiting than the filter response. All transducers, for example, have a characteristic frequency response and thus are actually filters.

The development of compact and reliable digital circuitry is revolutionizing the signal conditioning of flight-test data. More and more signal-conditioning functions are being performed by digital techniques. Presently, the main effect seems to be the inclusion of microcomputers into the data-acquisition process to perform sophisticated manipulation of data (see Digital Signal Conditioning in Sec. 3). As more computers are used as airborne data terminals, the growth of computerized signal conditioning will be even more pronounced. The digital filter is also presently becoming more important, a powerful signal-conditioning tool for engineers who require very tight control over time delays and filter stability.

2.2.5 The Data-Terminal Device

The data-terminal devices are indicators, recorders, acquisition systems, telemetry transmitters, or computers. These devices will not be discussed in this volume; however, the special signal-conditioning requirements of many of these terminal devices is covered in Secs. 5 and 6.

Many modern dynamic flight-test programs are presently requiring extremely close time-correlations of many diverse data channels. For example, the National Aerospace Laboratory (NLR) in the Netherlands performed takeoff and landing tests that required that dynamic data be compared with a relative time-accuracy of 1 msec. When correlation accuracy of 1 msec or higher is a requirement, close attention to every portion of the data-acquisition chain is an absolute necessity. As mentioned earlier in this section, each link in the data-acquisition chain, including the data-detection process, can produce time-delays. Particular attention should be given to pre-transduction signal conditioning, the transducer, filters, and multiplexing systems.

When the data to be compared are all of one type, say dynamic pressures, the task is somewhat simpler; this is because constraining each data channel to be in every way identical should keep the relative time-shifts matched. In the example of pressure-data channels, the pre-transduction signal conditioning, including the pneumatic system shown in Fig. 3, should be given particular attention. Different tubing diameters, different tubing lengths, variations in the volume of the air cavity in front of the transducer diaphragm, kinked tubing, and partially obstructed tubing — all can dramatically affect the dynamic response of such a pneumatic pre-transduction signal-conditioning system.

The pressure transducers in the example should all be identical, as should all the signal conditioning. Each channel could be recorded, for example, on constant-bandwidth frequency modulation (CBFM) subcarriers (see Sec. 5) that have identical characteristics with identical output filters, thus maintaining relative time-correlation. The above example could be cited as a near-ideal system. In general, many different kinds of measurements will have to be combined. When diverse data such as

pressure data, acceleration data, and inertial guidance data must be compared in time, the task becomes very difficult. The engineer will soon realize that no block in Fig. 2 can be neglected. If the data are derived from a complex system, such as an inertial navigation system (INS) that is part of a vehicle computerized control system, there is little chance of achieving reasonable time-correlations with other data. An INS with continuously available outputs could permit data correlation once the dynamic characteristics (the transfer function) of the system are defined. When the signal conditioning contains filters, care should be taken to match the filter type and bandwidth. Filters with different bandwidths exhibit different time-delays. Filters of the same bandwidth but differing in type can cause wave-shape variations which make comparisons of events difficult.

As suggested earlier, multiplexing systems introduce significant time-delays. Rigorous interchannel time-correlation of data in proportional bandwidth frequency modulation (PBFM) systems requires compensation for the different output filter time-delays. Interchannel time-correlation of CBFM channels is simpler when the same bandwidth options are used. Mixing bandwidth options among channels to be time-correlated complicates the correlation process.

Time-division multiplexing (TDM) as usually implemented also requires compensation for time-sequencing effects, even if the input pre-sampling filter and the output interpolation filters have identical bandwidths. This is a result of the way most ground stations reconstruct the data. This effect is discussed under Time Correlation of Multiplexed Data in Sec. 5.

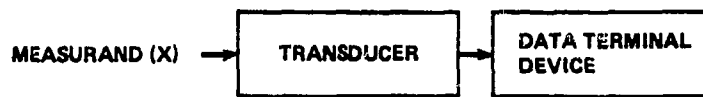


Figure 1. The ideal instrumentation system

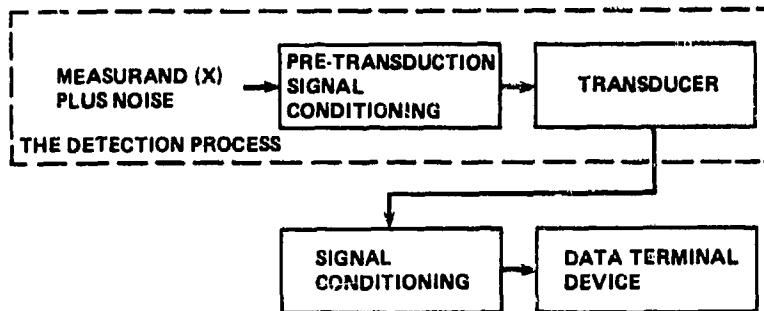


Figure 2. The practical instrumentation system

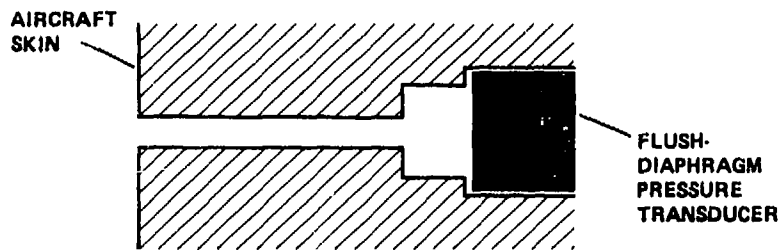


Figure 3. A pneumatic pre-transduction signal-conditioning system

3. GENERAL SIGNAL-CONDITIONING TECHNIQUES

In this section, the general signal-conditioning techniques, such as amplification, attenuation, zero shifting, filtering, modulation, demodulation, and functional operations, are discussed. These techniques can be applied in almost any signal-conditioning application and are, therefore, called general signal-conditioning techniques. Many of these techniques are later used in Secs. 4-6 to illustrate specific examples of how signal-conditioning techniques are applied. Two major categories of signal conditioning (frequency and time-division multiplexing) are discussed in Sec. 5, which covers the signal conditioning required for signal multiplexing.

Common-mode noise and noise-reduction techniques are also discussed in this section. Specific examples of how to apply common-mode noise-reduction techniques are discussed in following sections. Reference 3 covers common-mode problems and grounding techniques in detail.

General signal-conditioning techniques are discussed first so that when they are used later in specific applications, the engineer will be generally familiar with the nature of these techniques. The emphasis here is on signal-conditioning terminology and function, whereas the appendixes expand on specific subjects and practical circuits. References are included for those who wish to delve deeper into specific subjects.

3.1 AMPLIFICATION, ATTENUATION, AND ZERO SHIFTING

One of the most common signal-conditioning situations is a signal source that is not compatible with the device with which it must interface. A transducer, for example, may have a 0-5-V output and the signal encoder to which it must interface may require a ± 2.5 -V input. This requires a zero shift. Frequently, a transducer output voltage does not match the data-terminal device. For example, a 0-20-mV output from a thermocouple is not sufficient for a signal encoder that requires a 5-V input. This situation requires both a scale-factor change (amplification) of 500 and a zero shift. Attenuation is sometimes required to reduce or adjust a signal output for the next stage.

Amplifiers are widely used in signal conditioning because they can provide amplification, attenuation, zero shifting, impedance matching, common-mode voltage rejection, isolation, and other functions. The most common amplifier is the voltage amplifier (voltage-input/voltage-output). This type of amplifier is highly developed and available with many desirable features. However, the voltage amplifier is often used when another type of amplifier would be much more suitable. The charge amplifier (charge-input/voltage-output) is probably the best known "special" amplifier. Many users are not aware that charge amplifiers are available that have charge-inputs and current-outputs, an implementation that is valuable for driving long output lines. Amplifiers are also available, for example, in voltage-input/current-output and current-input/current-output configurations. Again, it is obvious that the signal input/output requirements must be known.

In order to select the appropriate amplifier for each application, the engineer must know the nature of the signal source that drives the amplifier and the nature of the device that the amplifier must drive. Devices that drive a typical amplifier behave as voltage, current, or charge sources. The devices that amplifiers drive behave as voltage, current, or charge sensors which are ideally best driven by amplifier outputs which are, respectively, voltage, current, or charge sources. By combination, there are nine basic amplifier input/output combinations. Most of these combinations are not readily available. Flight-test organizations usually have a large number of "instrumentation" amplifiers that are voltage-input/voltage-output amplifiers. The ready availability of voltage amplifiers has led to their use in inappropriate situations. This misuse has been further encouraged by excessive use of a powerful technique called Thévenin's theorem. Thévenin's theorem makes it possible to convert any two terminal electrical energy sources, no matter how complex, into a simple equivalent voltage source, that is, into a voltage generator in series with an impedance; Fig. 4 illustrates such an equivalent voltage source.

Since all voltage, current, and charge sources can, by Thévenin's theorem, be converted into equivalent voltage sources, voltage amplifiers may be used for these sources. The engineer must be aware of the limitations introduced when, for example, voltage amplifiers are used with current and charge sources, and take these limitations into account in the design process. A simplified current source is shown in Fig. 5a.

When this is a representation of a linear transducer whose generated current I is directly proportional to the input measurand X then

$$I = KX = f(X) \quad (1)$$

When the load impedance Z_L is very much smaller than the source internal impedance Z , essentially all of the available current flows through the load. Note that the internal impedance of the current generator itself is infinite. Normally, the shunt impedance Z of Fig. 5a is very high (often a leakage resistance).

Figure 5b illustrates a voltage source that is an equivalent of the current source of Fig. 5a. This transformation is accomplished in two steps. The first step is to measure the internal impedance Z of the current source with the current generator I removed. This measured impedance Z becomes the voltage-source series impedance Z' in Fig. 5b, and Z' is equal to Z . The second step is to measure the open-circuit output voltage of the total current source, which is

$$e = IZ \quad (2)$$

(Note that if there had been no internal shunt impedance the open-circuit output voltage would have been infinite because the ideal current generator I will keep the current constant with no regard for the size of the load.) The important point to note here is that the output is now

$$e_o = KXZ = f(X, Z) \quad (3)$$

When a current-source output is measured by a voltage sensor, such as a voltage amplifier, the measurand is a function of the current-generator output I , the current-source internal impedance Z , and the voltage-sensor input impedance. Since Z is, in general, not well controlled, simply placing a high input impedance voltage amplifier across the outputs of a current generator is undesirable.

A similar situation evolves when using a voltage amplifier to measure the output of a charge source. Such a charge source, a piezoelectric transducer, is shown later in this section (The Charge Amplifier). In that related figure (Fig. 16), the charge generator itself is defined as having an infinite internal impedance. The capacitance C is often inherent in the construction of the transducer, and R is usually a leakage resistance. From this figure it can readily be shown that the transducer charge Q is a direct function of the measurand X , such as

$$Q = KX = f(X) \quad (4)$$

However, the open circuit voltage output e_o is

$$e_o = Q/C \quad (5)$$

Therefore, by simple algebraic recombination of the above equations, the output, when measured by a voltage amplifier, is a function of

$$e_o = KX/C = f(X, 1/C) \quad (6)$$

The above is a simplification of the situation (the actual problem is analyzed in much greater detail in Appendix F).

In this text, many examples are illustrated in which the signal-conditioning circuits are based on operational amplifiers. Understanding the circuit function does not require that the reader understand operational amplifiers; however, Appendix A presents the theory and practical limitations of operational amplifiers.

3.1.1 Voltage Amplifier

A good general-purpose voltage amplifier (voltage-input/voltage-output) for instrumentation applications has most of the following features: very high input impedance; very low output impedance; appropriate frequency response; and sufficient output drive capability. Figure 4 can be used to represent a transducer with a two-terminal output. The ideal way to measure the internal voltage of a voltage source such as that shown in Fig. 4 is to measure that voltage when no current is being drawn from the voltage source. When a current flows during the measurement, an internal voltage drop occurs across the internal impedance Z , producing an error in the measured output voltage. The above task can be accomplished by presenting to the voltage source a counter-voltage, adjusted until no current flows from the voltage source. When this condition of current null is achieved, the input counter-voltage is exactly equal to and opposite of the equivalent internal voltages of the voltage sources. The mechanical null-balance-voltage measuring instruments are only infrequently used in flight-test instrumentation because of their size, frequency limitations, and electromechanical complexity. All of these disadvantages are a consequence of the electromechanical servomechanisms used to produce the null-balance effect. The servometric null-balance voltmeter is sometimes used in pilot indicators. It can also be used as an amplifier because it can measure low voltages and because the voltage output of the servomechanism can be as large as the power supply permits; however, this is not what is generally meant when one refers to a voltage amplifier.

The modern solid-state voltage amplifier achieves this requirement of zero current drain from the voltage source by drawing so little current from the voltage source that the current-induced errors across the internal impedance are negligible. To do this, the voltage-amplifier input impedance must be very much greater than the voltage-source internal impedance. The voltage amplifier is one of the most commonly used signal-conditioning amplifiers. This is because voltage amplifiers are readily available and because they are the appropriate choice in many applications. When a transducer input measurand X is truly represented by a voltage output, then

$$e_o = f(X) \quad (7)$$

and a voltage amplifier is the obvious choice as a signal conditioner. For example, a thermocouple (Fig. 6) is a true voltage generator and the output voltage e_o is a function of the two temperatures T_1 and T_2

$$e_o = f(T_1, T_2) \quad (8)$$

In this example, a voltage amplifier is the ideal signal conditioner.

Figure 7 illustrates a simplified voltage amplifier driven by a voltage source. For simplicity, all impedances in Fig. 7 are depicted as being resistive. The relationship between the voltage-source internally generated voltage e and the amplifier input voltage e_1 is

$$e_1 = e [R_1 / (R + R_1)] \quad (9)$$

The relationship of e_0 to e_1 is

$$e_0 = Ae_1 [R_L / (R_0 + R_L)] \quad (10)$$

As can be seen from Eq. (9), if R_1 is very much greater than R , then $e_1 \approx e$. Likewise from Eq. (10) it also holds that if R_L is very much greater than R_0 , then $e_0 \approx Ae_1$. When both the above restrictions are valid, then the following equation can be easily derived from Eqs. (9) and (10):

$$e_0 \approx Ae \quad (11)$$

where $R_1 \gg R$, and $R_L \gg R_0$. The relationship shown in Eq. (11) is the justification for selecting a voltage amplifier. Equation (11) states that the output voltage e_0 , is directly proportional to the amplifier gain A , and to the internal voltage e , generated by the voltage generator.

It can be determined from the foregoing that a good general-purpose voltage amplifier for instrumentation signal conditioning should have a very high input-impedance, a very low output-impedance, and a stable amplification factor. It is usually desirable that the amplifier gain A be relatively easy to change to suit test requirements. Typical gain ranges are from 0.1 to 1,000. Zero offset adjustments are also usually required and often voltage amplifiers are capable of offsets of $\pm 100\%$ of full-scale. The frequency bandwidth should be adequate for the task. Appendix B contains a detailed development of several voltage-amplifier circuits with various features and circuit complexities. In addition to the above features, most general-purpose instrumentation amplifiers are differential amplifiers (see Appendix C). A differential amplifier is illustrated in Fig. 8. In an ideal differential amplifier, the output is not affected by common-mode voltage.

As can be seen in Fig. 8, the output voltage e_0 is a function of the difference between the two input voltages, e_1 and e_2 . The amplifier input marked with a negative sign is called the inverting input. The amplifier input marked by a positive sign is called the non-inverting input. If one of the inputs is grounded (that is, e_1 or e_2 is zero) then the amplifier is a simple non-differential inverting (e_2 grounded) or non-inverting (e_1 grounded) amplifier.

The main advantage of a differential amplifier is its ability to reject common-mode noise in a flight-test data-acquisition system. A strain-gauge bridge powered by a battery is a good example of a common-mode voltage generator. When a differential amplifier is used with a strain-gauge bridge, the desired signal is actually a small voltage which is the difference between two large voltages. In Fig. 9, a typical bridge-supply voltage E_B is 12 V; the input voltage, $e_1 - e_2 = e_B$, is typically 0.03 V, maximum. This means that the common-mode voltage, e_{CM} (6 V), is 100 times the maximum input-signal voltage excursion. Figure 10 illustrates another application of a differential amplifier being used to reject common-mode inputs.

Common-mode voltages are often inadvertently introduced (as distinguished from the previous example of a strain-gauge bridge where the common-mode voltage was inherent to the transducer itself) by grounded loops, electromagnetic pickup, and electrostatic pickup. Incorrect system grounding can convert a common-mode signal into a differential signal (Ref. 3). Figure 11 illustrates two examples of how a common-mode signal can be coupled into a circuit via a transducer. In Fig. 11a, a piezoelectric transduction element which is grounded on one side to its case is also mounted directly to the metal aircraft structure. As noted in Ref. 3, on grounding techniques, no two points on an aircraft structure can be expected to have identical potentials, and this potential difference is the common-mode voltage e_{CM} . This common-mode voltage causes current flow in the coaxial cable shield and thus introduces noise into the circuit owing to the shield reactive components. This noise is called common-mode noise, and this circuit is highly susceptible to common-mode noise. In Fig. 11b, the amount of common-mode noise introduced has been considerably reduced by the use of an electrical insulator between the transducer and the aircraft structure, but some common-mode noise is still coupled into the circuit through the insulator case-to-ground capacitance.

The wiring carrying the data signals can also be responsible for the introduction of common-mode signals into the data. Common-mode voltages are often coupled into a circuit electrostatically by stray capacitances. In Appendix B, an amplifier is illustrated that drives the wiring shield to track the signal. This reduces the effect of any shield-to-signal wire capacitances and can significantly reduce the amount of common-mode voltage introduced into long wires. Electromagnetic fields are particularly difficult to discriminate against since the braided copper shielding on signal wires only slightly attenuates these effects. Coupling from strong electromagnetic fields is best avoided by running wire carrying high currents separately from signal wires and by using twisted shielded wire pairs for signal wiring.

Referring back to Fig. 10, the amplifier gain, with respect to the differential input signal e_D is A_D , and its gain with respect to the common-mode signal e_{CM} is A_{CM} . The differential and common-mode gains are defined in the following equations:

$$A_D = e_D/e_C \quad (12)$$

where $e_{CM} = 0$, and

$$A_{CM} = e_D/e_{CM} \quad (13)$$

where $e_D = 0$. The common-mode rejection ratio (CMRR) is defined as

$$CMRR = A_D/A_{CM} \quad (14)$$

The common-mode rejection (CMR), a figure of merit for an amplifier, is usually expressed logarithmically as

$$CMR \text{ (in decibels)} = 20 \log_{10} (CMRR) \quad (15)$$

In many specification sheets, CMRR is also given in units of decibels.

The CMR and CMRR are functions of frequency, input impedance balance, temperature, and signal amplitude to name the most common parameters. Quite often, a manufacturer's specification will state how closely the input impedance in each input line must be matched. The frequency of the common-mode voltage is important. Some differential-amplifier specifications plot CMR versus frequency, whereas many specify the CMR at one frequency. When no frequency is specified, it should be assumed that it is specified at a very low frequency, since CMR decreases with increased frequency. Ordinary differential amplifiers can tolerate common-mode voltages that are limited to something less than the amplifier supply voltages. Over this limit, the input stage malfunctions and the amplifier becomes inoperative. When a high degree of input-voltage isolation is required, isolation amplifiers should be used (see the following subsection).

To take best advantage of the common-mode rejection capabilities of differential amplifiers, the output of a remote transducer should be placed across the differential input leads, the transducer isolated from ground if possible, and the signal wires between the amplifier and transducer shielded. When transducers, which have low-level voltage outputs, require remote amplification, consideration should be given to using a differential amplifier.

It must be emphasized that an amplifier, no matter how good its CMR, will only reject common-mode signals if those signals are truly identical in amplitude and phase on both input lines. Any phase shift or amplitude differences between the signals on each input line will produce a differential signal.

3.1.2 Isolation Amplifier

The term isolation amplifier is usually used to describe an amplifier having a very high input-output ground isolation. Such amplifiers can typically tolerate common-mode voltages of thousands of volts while accurately amplifying low-level dc and low-frequency differential signals. These amplifiers often have isolation resistances in excess of $10^{11} \Omega$ and common-mode rejections of 120 dB.

The name isolation amplifier, as it is commonly used, is confusing, since to a limited extent all amplifiers provide some degree of isolation. Even the single-ended voltage amplifier, to a considerable degree, isolates the voltage source input to the amplifier from load fluctuations presented to the amplifier output. The instrumentation amplifier illustrated in Appendix C has a very high input impedance and a common-mode rejection of over 120 dB at low frequencies; however, these FET (field effect transistor) input instrumentation amplifiers have a typical maximum common-mode input voltage limitation of 10 V. This type of amplifier also requires an input leakage path to the output-common in order to bleed off input bias current.

In flight-test data-acquisition systems, the isolation amplifier can be very useful. Some examples are

1. Physiological studies in which instruments such as electrocardiogram probes are directly connected to human subjects
2. Data taken from flight-critical aircraft subsystems
3. Acquiring data from sources that have or could have common-mode voltages that are considerably higher than the data-acquisition system common ground
4. Retrieving data signals from high-impedance sources in noisy environments
5. Isolation of power transients from the data-acquisition system

Particular care should be exercised when instrumentation is connected directly to a human subject or to a critical flight safety subsystem, as noted in items (1) and (2).

The required input-output isolation can be achieved by many techniques; for example, transformer coupling, light coupling, and Hall-effect magnetic coupling. All of the devices mentioned above show considerable nonlinearity at dc and low frequencies. Linearity-compensation techniques can be used to overcome some of these nonlinearities in the above-mentioned devices; however, the most accurate isolation amplifiers use modulation techniques such as frequency modulation or pulse-width modulation to achieve the desired accuracies.

Isolation amplifiers are often used to protect equipment and people from high, steady-state, ac or transient voltages, and to reliably isolate a critical flight system from other flight-test systems. Fail-safe features and high reliability should be the prime goals in designing or selecting isolation amplifiers. The two most popular configurations are the isolated operational amplifier and the isolated instrumentation amplifier. Figure 12 shows the usual circuit symbols for these types of amplifiers. Appendix D presents a detailed discussion on how one type of isolation amplifier is constructed.

3.1.3 Current Amplifier

Rigorously defined, a current amplifier is an amplifier that takes a current input and produces an amplified current output (that is, a current-input/current-output amplifier); however, in this section the definition has been expanded to include the voltage-input/current-output amplifier (sometimes called a transconductance amplifier, or a voltage-to-current amplifier), and the current-input/voltage-output amplifier (sometimes called a current-to-voltage amplifier). All three types of amplifiers are useful; however, the most commonly used variation is the current-to-voltage amplifier. In fact the current-to-voltage amplifier is so common that it is called a current amplifier in much of the technical literature.

In Fig. 5, it was earlier demonstrated how a true current-source circuit could be represented by Thévenin's theorem be transposed into an equivalent voltage-source circuit. In Fig. 13a current-source circuit is illustrated with a load Z_L . If Z_L is the impedance of a current sensor, such as a galvanometer, and if it is desirable to utilize all of the current-source output I_S , then the source impedance Z_S must be very much larger than the load impedance Z_L . Ideally, a current source has an infinite internal shunt impedance Z_S . In practice, the current source always has a finite, though usually very high, internal shunt impedance. Therefore, it is desirable to have Z_L as low as possible (note that this impedance requirement is just the reverse of that required for an ideally loaded voltage source). For example, in the circuit of Fig. 13, if $Z_L = Z_S$, the available current I_S would be evenly split between Z_L and Z_S and one-half the available current is lost in the source itself.

As a practical example, if Z_S were $10^6 \Omega$, and the current source were driving a current-sensitive device such as a galvanometer that loads the current generator with a $100\text{-}\Omega$ load, then, even if the source impedance Z_S and galvanometer impedance Z_L should change 50%, no appreciable error would be introduced into the current flowing through the galvanometer element. As a comparison, if the above current source had been connected to a voltage amplifier whose load on the current source was $10^{12} \Omega$, nearly all of the generated current I_S would have flowed through the source impedance Z_S . In this case, a $\pm 50\%$ change in Z_S would produce a $\pm 50\%$ change in the input voltage to the amplifier.

The current-input/current-output amplifier (Fig. 14a) is used when a transducer current source is inadequate to drive the required load. For example, a current source has a maximum output of $10 \mu\text{A}$ and must drive a cockpit panel meter that requires 10 mA for a full-scale indication. This would require an amplifier with a current gain of 1,000.

The current-input/voltage-output amplifier is probably the "current" amplifier most encountered in general use (Fig. 14b). When a transducer is a current source, the current-to-voltage amplifier can be used to interface the transducer to the more common voltage-type data-terminal devices used in modern flight-test work. The voltage-input/current-output amplifier (Fig. 14c) is useful when a voltage source must drive a current-sensitive device, such as a galvanometer or an instrument-panel meter. In addition, current-output amplifiers, either current-to-current or voltage-to-current, can be useful when driving long, high-resistance lines. If these high-resistance lines should pass through areas of variable high temperatures, such as an engine compartment, then the line resistances can change. Also, if the wiring must pass through a slip-ring, such as might be required when signals are taken from a helicopter rotor, resistive fluctuations are generated (Ref. 9). Under these conditions, a current-source output amplifier can significantly reduce the line-resistance errors. This technique of using a current source for reduction of system sensitivity to static and dynamic line resistances is illustrated in Fig. 15.

In Fig. 15, R_{VL} is a variable line resistance, ΔR is a resistive noise such as is generated by a slip-ring, I_S and R_S are the equivalent current-source parameters, and R is an accurate termination resistor. The current I_0 is independent of R_{VL} and ΔR when R_S is much larger than the sum of $2R_{VL}$, $2\Delta R$, and R ; therefore, I_0 and e_0 are independent of R_{VL} and ΔR . Another solution (with R removed) is to terminate the wiring of Fig. 15 with a current sensing device, such as a current-to-voltage amplifier.

The various current amplifiers can be very useful when the transducer is a current generator or when the terminal device is a current sensor. In these cases, they may well be the optimum signal-conditioning system. For actual current-amplifier circuits constructed from operational amplifiers, see Appendix E.

3.1.4 Charge Amplifier

The charge amplifier discussed here is the charge-input/voltage-output converter (charge-to-voltage converter). This is a very popular amplifier and one that is frequently used with piezoelectric transducers and variable-capacitance transducers. Charge-to-current and charge-to-charge amplifiers can be constructed but they are used only infrequently and are not discussed here.

Charge amplifiers should be given serious consideration when the signal source generates a charge output. Figure 16 illustrates the electrical representation of a piezoelectric transducer, which is a true charge source. With a true charge source, a fixed amount of charge is generated for a given static value of the input measurand X , and in real flight-test situations, this charge will sooner or later be neutralized through various leakage paths. This means that a charge source cannot be used as a true static

signal generator. For this reason, charge-generating transducers are used for performing dynamic measurements such as vibration, shock, and noise.

The charge amplifier is discussed in detail in Appendix F; however, a summary of the characteristics of a charge amplifier is presented here. The charge amplifier senses the actual charge at its inputs. To accomplish this a feedback capacitor C_f in an operational amplifier is charged until its charge exactly counters the charge Q produced by the charge generator. (See Fig. 131 in Appendix F for a detailed analysis of a charge source connected by coaxial cable to a charge amplifier — charge-input/voltage-output amplifier.) These amplifiers can track high-frequency charge changes, and the output voltage e_o varies directly as

$$e_o = KQ/C_f = f(Q, C_f) \quad (16)$$

The amplifier capacitor C_f must be a precision, stable capacitor. This is in contrast to the application in which a voltage amplifier is used and in which the output voltage is a direct function of the charge-generator output Q and of all shunt-circuit capacitances. These shunt-circuit capacitances are a function of many environmental inputs. In addition, the charge amplifier gives the engineer much better control of the system bandpass frequency response (see Appendix F). Charge amplifiers have many advantages and few disadvantages when used with charge sources; however, the engineer who wishes to use charge-source transducers, such as piezoelectric transducers, should not fail to read Piezoelectric Transducer Signal Conditioning in Sec. 4 and Appendix F.

3.1.5 Logarithmic and Antilogarithmic Amplifier

The logarithmic amplifier and its complementary form, the antilogarithmic (exponential) amplifier, are useful special-purpose signal conditioners. A primary use of them is in the compression/expansion of data that have a wide dynamic range. They are also used to linearize transducers that have exponential or logarithmic data outputs and to perform mathematical operations such as multiplication and division.

Small amplifier units are commercially available or may be constructed from operational amplifiers and external diodes or transistors. However, to make a device that is accurate over a reasonable flight-test temperature range requires careful attention to temperature-compensation techniques. (See Ref. 10 for an analysis of a logarithmic amplifier constructed from an operational amplifier and a diode.) Full temperature compensation involves temperature matching of diodes (or transistors) and the use of temperature-sensitive resistors. These temperature-compensating techniques are time-consuming but can be accomplished.

The logarithmic and antilogarithmic (exponential) functions are

$$e_{\log} = K_1 \log_{10}(K_2 I_1/I_2) \quad (17)$$

$$e_{\exp} = K_3 \exp_{10}(K_4 e_1/e_2) \quad (18)$$

A further explanation of Eqs. (17) and (18) follows.

1. The logarithm and exponential functions are mathematical operators which are defined only for numbers that are dimensionless quantities; therefore, the terms inside the parenthesis in both equations are dimensionless ratios. It is often desirable to derive the logarithm or exponential functions as the ratio of two currents or voltages. In many applications it is necessary to produce a logarithm or exponential function from a single variable; this can be accomplished by placing an appropriate steady-state bias current or voltage on one of the two input terminals.

2. The ratio in Eq. (17) is shown as the current ratio. This ratio can also be a voltage ratio but the dynamic range is decreased (Ref. 10). Typically, a voltage input is limited to four decades of dynamic range, and a current source covers seven decades.

3. In addition, in the case of logarithmic amplifiers even though the output voltage in a practical amplifier can be adjusted to cover a plus and minus range, these amplifiers are unipolar devices, since there is no logarithm for a negative number. As an example, if the sinusoidal vibrational modes of a panel are measured with an accelerometer, then using a logarithmic amplifier to compress the data is not meaningful on the negative half of the bipolar sinusoidal input. Biasing the sinusoidal signal so that it is always positive is not desirable: the amplifiers are usually used because of the wide dynamic range of the input signals. This means that the signal is biased very high, and therefore, is very compressed for high-input signals and expanded for low (previously negative) input signals.

The uses of a logarithmic and antilogarithmic amplifier are implied in the equations; however, there is one interesting "pseudologarithmic" data compressor. As mentioned above, it is difficult to compress a bipolar ac input signal. Figure 17a illustrates an ac data compressor with pseudologarithmic response. In this circuit, taken from Ref. 11, the diodes D_1 and D_2 generate the logarithmic response for the positive and negative output voltages, respectively. The resistor R_f is required because of the discontinuity in the log curves at zero; it modifies the response curve in the vicinity of zero as shown in Fig. 17b. This amplifier cannot be effectively temperature-compensated and thus is useful only under temperature-controlled conditions or for signal compression when high accuracy is not a requirement. As an overscale backup channel to an ordinary linear channel, this circuit can be very useful.

3.1.6 Alternating Current Amplifier

The operational amplifiers and instrument amplifiers illustrated in the appendixes are capable of amplification from steady state to the amplifier upper frequency limit. However, it is often desirable to reject steady-state signals and to discriminate against low frequencies; for example, a transducer that has a low-frequency drift. The ac amplifier provides this capability. The ac amplifier is usually formed by adding a capacitor in series with the input signal; however, other techniques (for example, transformer coupling) can also be used but they are more expensive.

Figure 18 illustrates two dc instrumentation amplifiers that use series blocking capacitors to form economical ac amplifiers. The resistors R_1 and R_2 are required only when the instrumentation amplifier has no appropriate discharge path to amplifier-common. (See Appendix G for actual circuit examples and analysis of the low-frequency cutoff.)

3.1.7 Amplitude-Modulation Carrier Amplifier System

An amplitude-modulation (AM) carrier amplifier system is a very powerful signal-conditioning technique for reducing or eliminating certain very difficult noise problems. When a transducer data spectrum (shown in Fig. 19 as covering the frequency range of zero to f_s) coexists with a harsh electrical noise spectrum, AM techniques are used to translate the data spectrum up to a higher frequency where there is less chance of noise contamination.

AM techniques can be used with both self-generating and non-self-generating transducers, as shown in Fig. 20; however, for the self-generating transducer, a modulator must be introduced at the transducer output as shown in Fig. 20a. (Self-generating and non-self-generating transducers are defined in Sec. 4.) Any noise introduced at the transducer into the wiring leading to the modulator, or at the modulator before modulation, will be included in the modulated signal. The low-pass filter does, however, limit the signal and noise bandwidths into the modulator. When a non-self-generating transducer such as a potentiometer or strain gauge is used, as in Fig. 20b, the modulation is performed within the transducer itself; this has far-reaching implications as will be discussed. The following discussion centers on carrier-amplifier techniques that use non-self-generating transducers as modulating devices.

When a non-self-generating transducer such as a strain-gauge bridge is used as a modulator (see Appendix H), any electrical noise not in the spectrum of the bandpass amplifier will be rejected. This is quite an impressive statement. For example, if the strain-gauge bridge is mounted in a strong temperature gradient near a device that generates considerable 400-Hz energy, the bridge output is likely to contain considerable 400-Hz noise. It is also quite likely to generate very-low-frequency thermoelectric noise outputs. None of this electrical noise spectrum would be amplified. Only those inputs that caused a resistive bridge imbalance are amplified by the carrier-amplifier system. Examples of amplified noise include strains applied to the bridge, which include noise (that is, actual inputs other than the desired measurand) or temperature gradients that produce actual bridge imbalances; see Ref. 3 for examples of carrier techniques. Another advantage of the AM carrier amplifier system is that the bridge output is an ac signal with no steady-state component. This signal is amplified by a bandpass amplifier. Bandpass amplifiers are available with stable high gains. When AM carrier amplifiers are used with a phase-sensitive demodulator, positive and negative outputs are generated with a zero steady-state output at bridge balance. In contrast, when a bridge excited by a dc power supply uses an instrumentation amplifier to increase the signal level, then not only is all the electrical noise to the amplifier input amplified, but the amplifier also contributes low-frequency voltage offsets.

In general, carrier-amplifier systems are used with low-level signals in noisy environments. Usually these systems are used with non-self-generating transducers that produce the amplitude-modulated signal as a by-product of the transduction process. Appendix H examines some actual circuits. The expense and complexity of this type of signal conditioning usually limits its use to premium data channels in a high-noise environment.

3.2 FILTERS

A filter is a frequency-selective, signal-conditioning element that is used to transmit or attenuate a selected frequency or band of frequencies. (An exception is the all-pass network, which is sometimes called a filter and is used only to provide phase corrections). In flight-test data-acquisition systems, the filter is used to reduce the noise outside the data bandwidth. It is also used to isolate certain bands of frequencies in the signal for special analysis. The comb-filter and the airborne spectrum analyzer are examples of frequency-isolation applications.

Figure 21 depicts the "ideal" amplitude response of the four most common types of filters encountered in flight-test data systems. As can be seen, the four basic filter types are the (1) low-pass filter, (2) high-pass filter, (3) bandpass filter, and (4) band-reject filter.

One of the major applications for filters in modern airborne-sampled data-acquisition systems is the anti-aliasing filter (aliasing is discussed in Sec. 5). Although the general characteristics of filters will be discussed in this chapter, the rationale for selecting anti-aliasing filters is presented in Sec. 5 of this report and in Ref. 1.

3.2.1 Noise Reduction with Filters

In the Introduction, noise was defined as any signal not of interest to the engineer. Typically, the engineer specifies a desired data bandwidth (which extends from some low or zero frequency to some upper frequency limit). A filter is then selected that attenuates signal inputs above the upper frequency limit and produces acceptably low distortion below the upper frequency limit. Note that filters are not ordinarily used to reduce the noise inside the data bandwidth; however, pre-emphasis filters used

as the signal-conditioning inputs to tape recorders are used to enhance the signal-to-noise ratio inside the data bandwidth. Selecting a filter that will reduce the noise external to the signal bandwidth requires knowledge of the external noise distribution. There is no way of simply categorizing spectral noise distributions; however, the following types of noise distributions are commonly encountered:

1. Constant spectral density noise (often called white or thermal noise)
2. Noise that increases with frequency
3. Noise that increases inversely with frequency
4. Specific discrete noise frequencies

Constant spectral density noise is a function of the square roots of the data bandwidths: if a first-order, 20-Hz low-pass filter is replaced by a first-order, 10-Hz low-pass filter, the noise reduction is about 30%. Even if an ideal 10-Hz low-pass filter is used, only an additional 20% noise reduction is realized. Most practical filters will achieve considerably less noise reduction than the ideal filter. Increasing the order of a filter beyond second-order is not a particularly effective way to reduce this type of noise.

Noise that changes as a function of the noise frequency is reduced using specialized techniques. With noise that increases with frequency, it is important to locate the high-frequency filter cutoff near the highest frequency of interest. When the noise increases rapidly with frequency, high-order filters may be required. Noise that increases inversely with frequency, such as transistor flicker noise, makes the bandpass filter very desirable. If the data must have steady-state response, then systems must be avoided that introduce this type of noise. The reduction of noise that occurs at a single frequency is discussed under band-reject filters. Very-low-frequency noise usually must be removed with bandpass filters. A steady-state offset can be removed by bandpass filters or by biasing.

3.2.2 Ideal Filters

For the ideal filters depicted in Fig. 21, there is no attenuation in the filter passband and no transmission outside the filter passband. For example, in Fig. 21a the ideal low-pass filter transmits all frequencies from zero to the cutoff frequency f_C without attenuation and passes no other frequencies. Also, the phase shift of an ideal filter is zero everywhere in the passband. The phase-shift outside the filter passband is unimportant since nothing is transmitted.

Ideal low-pass filter. — The ideal low-pass filter (Fig. 21a) as mentioned earlier, transmits all frequencies from zero to f_C and provides infinite attenuation at all frequencies above f_C . Many airborne transducers have a frequency response that extends from zero to some maximum frequency, f_m . These transducers are used to detect measurands that have a frequency spectrum extending from zero to some frequency f_C (in the ideal filter example, $f_C = f_m$). The ideal low-pass filter is a very desirable signal-conditioning element since it rejects noise inputs above f_C .

Ideal high-pass filter. — The ideal high-pass filter shown in Fig. 21b is the inverse of the low-pass filter in that it rejects all frequencies from zero to the cutoff frequency f_C . At first glance, this would seem to be a very useful filter format since not all measurands have useful data near zero frequency, and many transducers have steady-state offset or considerable noise at low frequencies. No measurand has a frequency spectrum extending from f_C to infinity, and all of the bandwidth above the highest frequency of interest to the engineer is a potential source of noise signals. For these reasons a bandpass filter is more desirable than a high-pass filter.

Ideal bandpass filter. — The ideal bandpass filter (Fig. 21c) would pass all frequencies between its low-frequency cutoff f_{CL} and its high-frequency cutoff f_{CH} and reject all other frequencies. When the desired frequency spectrum of the measurand can be defined as being between f_{CL} and f_{CH} , the ideal bandpass filter is the desired signal-conditioning element.

Ideal band-reject filter. — The band-reject filter rejects all frequencies between f_{CL} and f_{CH} and passes all other frequencies, as shown in Fig. 21d. An ideal band-reject filter is used to reject specific noise inputs. For example, with a narrow bandwidth it is used to reject a specific noise input such as the aircraft power frequency. Generally, it would be used in conjunction with a low-pass or bandpass filter.

3.2.3 Practical Filters

The ideal filter does not exist; real filters can only approximate some of the performance characteristics of the ideal filter. The graphs in Fig. 21 represent only the filter amplitude response. In addition, all filters introduce a time-delay characteristic which is manifested as a phase shift and is called the filter phase response. There are two general guidelines about the characteristics of real filters:

1. The closer the real filter amplitude response approximates the ideal filter amplitude response, the less linear will be the real filter phase response
2. Conversely, a real filter with an optimized linear phase response has a less than ideal attenuation characteristic

The optimum wave-shape fidelity for transient data requires a linear change of phase with frequency (constant time-delay). The optimum amplitude response for the steady-state sinusoid is the closest approximation to the ideal filter's rectangular amplitude response. These last two requirements are mutually exclusive. Thus, the more that is known about the data, its noise distribution, and the filter requirements, the easier it is to select an optimum filter for the application.

It is easy to visualize how a sinusoidal signal amplitude will be modified by the curves of Figs. 21 and 22, but it is difficult to visualize how a nonlinear phase characteristic distorts transient data. Using the sinusoid signal analysis as a basis, this understanding can be applied to the analysis of transient data. Transient wave shapes, such as step or pulse inputs, can be represented by a Fourier series as a sequence of sinusoid functions, each with a specific amplitude, frequency, and phase relationship. Each of the sinusoidal components is subjected to the filter transfer function, and each amplitude and phase coefficient is affected differently. The filter output is represented by the summation of these sinusoidal components. A filter with a linear phase characteristic produces low distortion of the input wave shape. The relative phase relationships are maintained while the filter attenuates the signal amplitude coefficients. In a low-pass filter, the attenuation of the high-frequency component coefficients produces a loss of fine detail (corners are "rounded" on step or impulse signals); however, the eye can generally recognize the wave shape. When the same transient is subjected to a filter with a very nonlinear phase response as a function of frequency, the phase of each frequency component is radically shifted and a new wave shape is produced. In extreme cases, the original wave shape is distorted to such a degree that it cannot be recognized.

Real-filter characteristics do not closely approximate those of the ideal filter. The amplitude responses of typical real filters are shown in Fig. 22. These curves require a few words of explanation for those engineers not familiar with presentations of typical filter characteristics. In Fig. 22 the ordinate is called the normalized "amplitude" and is expressed in decibels. It is convenient and conventional to plot filter amplitudes in logarithmic form. To accomplish this, the filter amplitude is converted to a ratio, which is made dimensionless by dividing the filter output amplitude at any given frequency by the filter output signal amplitude at a convenient reference frequency.

In a low-pass filter, the reference is usually the filter steady-state amplitude. In a high-pass filter, the reference amplitude is some frequency far above the filter cutoff frequency f_c . (The cutoff frequency is defined in the next section.) In bandpass filters, the reference amplitude is established at the midband frequency. And finally, in the band-reject filter, the reference amplitude often is the steady-state output amplitude. When this convention is used, the normalized amplitude will be zero dB when the signal ratio equals 1, and will express the filter output as a function of frequency in plus or minus dB.

When the abscissa of the amplitude-response curve is normalized and plotted on a logarithmic scale, it becomes convenient to plot and combine filter characteristics. It is easy to plot, since filter roll-off is expressed in $20n$ dB per decade where n is the order of the filter (see Appendix I). The final filter attenuation asymptotically approaches the $20n$ -dB/decade line. Also, since the normalized amplitude is in decibels, when the filters are noninteractive, the two filter characteristics can be summed directly to provide the overall filter characteristic.

There are many different ways to physically implement filters including such general classifications as, for example, mechanical magneto-strictive filters, crystal filters, discrete-component passive filters, and active filters. Each type of filter mentioned has its own special merits. For example, mechanical and crystal filters are very desirable when bandpass or band-reject filters are required that must have very high rates of band-edge attenuation. Passive filters operate at frequencies higher than those attainable with active filters (because of amplifier response, active filters have high-frequency limitations). Passive filters are constructed using resistors, capacitors, and inductors whereas active filters are constructed from amplifiers, resistors, and capacitors.

Since all filters can be represented by amplitude- and phase-shift characteristics, this section will concentrate on these general characteristics. Appendix I discusses in detail the characteristics and construction of active filters. This section and Appendix I address the filter input-output (transfer) characteristics, and are intended to assist the engineer in understanding other types of filters. This does not mean, however, that the engineer will necessarily have any idea of the internal mechanization, or of the particular advantages or disadvantages. Filters, in all their diversity, constitute a very complex subject, and when the engineer has an unusual requirement, a filter expert should be consulted.

Practical low-pass filter. — Many flight-test engineers intensely dislike utilizing filters in data channels. Figure 23 is included to illustrate the amplitude and phase characteristics that produce these attitudes. The filter illustrated is a simple low-pass filter. It is a first-order filter with a final roll-off of 6 dB/octave (20 dB/decade). In Fig. 23a the normalized amplitude A/A_0 (in dB) is plotted versus the normalized frequency (logarithmic scale), f/f_c . The passband amplitude response of Fig. 23a is -3 dB at the cutoff frequency.

It should be noted that not until 10 times the cutoff frequency does the attenuation approach 20 dB, or 0.1 of the steady-state output. Since most engineers do not utilize data in a logarithmic format, Fig. 23b has been included to illustrate the amplitude response of the filter in a linear form. In this figure, the data have a predictable attenuation of almost 30% of the steady-state value at the cutoff frequency and in fact have an amplitude attenuation of over 10% at $f/f_c = 0.5$.

Figure 23c illustrates that signals passing through a real filter are subjected to substantial phase shifts even within the filter passband ($0 < f < f_c$). The filter illustrated in Fig. 23 is a first-order low-pass filter, and when filters with even larger attenuation outside the passband (higher-order filters)

are used, even larger phase shifts will result. In general, the sharper rates of change of attenuation produce higher phase shifts.

All these amplitude and phase changes mean that an engineer who is striving to minimize overall error may require a sophisticated correction procedure to restore the data integrity. This will be particularly true when the data are transient.

First-order filters typically used in post-transduction systems are usually passive filters formed from resistors and capacitors. It is not economical to construct an active first-order filter since it does not produce enough attenuation outside the passband to justify the circuit complexity involved. For a modest increase in cost and circuit complexity, an active second-order (or higher-order) filter can be easily constructed.

Second-order (and higher-order) low-pass filters may be optimized for various signal input characteristics. Second-order filters have a final theoretical attenuation rate of -12 dB/octave (40 dB/decade) or twice that of a first-order filter. Note that this means that at 10 times the cutoff frequency, ($f/f_c = 10$), the attenuation is 10 times greater than that of a first-order filter (0.01 instead of 0.1; see Figs. 23a and 24a). Unfortunately, a second-order filter also produces a much larger phase shift (-90° at f_c) and the phase shift approaches -180° at high frequency (see Fig. 24 b). The transfer function of a second-order all-pole filter is

$$H(s) = (e_0/e_1)(s) = A_0 [u_c / (s^2 + d u_c s + u_c^2)] \quad (19)$$

$$G(\omega) = | (e_0/e_1)(j\omega) | = A_0 / \sqrt{(\omega/u_c)^4 + (\omega/u_c)^2 (d^2 - 2) + 1} \quad (20)$$

Where

A_0 = circuit gain at $\omega = 0$

$G(\omega)$ = steady-state sinusoidal gain at ω

d = filter damping factor

$H(s)$ = transform of the transfer function

$\omega = 2\pi f$, rad/sec

$u_c = 2\pi f_c$, where f_c is the filter cutoff frequency

$\omega/u_c = f/f_c$

$s = j\omega$ for determining $G(\omega)$ (if the circuit has no elements with stored energy)

The Laplace transform of Eq. (19) is reduced to a transfer function that is a complex function of the angular frequency. The absolute value of this complex equation is shown in Eq. (20) and is the amplitude response of the filter to a sinusoidal input voltage of fixed amplitude and frequency. The phase response of the filter is derived in Appendix I.

Figure 24a displays the amplitude equation of Eq. (20) for a few values of filter damping. Notice in this figure that only one curve intercepts the cutoff frequency at -3 dB, the curve for $d = \sqrt{2}$. All of the curves in Fig. 24a asymptotically approach the same final attenuation rate. When this final slope is extrapolated backward, it intercepts the 0-dB normalized amplitude response line at $f/f_c = 1$. In this text, unless otherwise specified, this will be the definition of the filter cutoff frequency, f_c .

The values of f_c , A_0 , and d in Eqs. (19) and (20) are derived in Appendix I for various circuit configurations in terms of resistances and capacitances that are used in conjunction with an operational amplifier or amplifiers to form active filters. It is important here to know only that if f_c , A_0 , and d can be derived in the format of Eq. (19), and therefore as in Eq. (20), considerable insight into many classic types of filters can be derived from these parameters alone. When f_c has been selected and A_0 defined, the filter damping factor d can be optimized for various signal waveforms. For example, when d in Eq. (20) is $\sqrt{3}$, the equation describes the Bessel filter; when d equals $\sqrt{2}$, the equation describes the Butterworth filter; and when the damping d is decreased further ($d < \sqrt{2}$), then a resonant peak results and the equation describes a Chebyshev filter. Figure 24 shows the amplitude response and phase shift for the Bessel, Butterworth, and the 3-dB, peak-to-peak Chebyshev filters. Chebyshev filters have ripple or peaks in the passband and are usually specified in terms of this ripple amplitude.

When the engineer first encounters filters, confusion often results because there are so many types, each with its claimed advantages. To make it even more difficult, many identical filters are called by more than one name. In flight-test data-acquisition signal conditioning, the most popular filters are the Bessel, Butterworth, Chebyshev, and the compromise filters. These filters are all described by Eq. (19). Fortunately, this equation is relatively easy to analyze mathematically (see Appendix I).

The second-order lowpass Butterworth filter, which corresponds to a filter with a damping factor of $d = \sqrt{2}$, has a "maximally flat" amplitude response to sinusoidal inputs. It is called a maximally flat filter since any less damping produces a peak in the passband. It is a very popular flight-test signal-

conditioning filter in that many data channels have sinusoidal signal output. Comparing first- and second-order filter characteristics for example, the first order filter described earlier had a 30% amplitude attenuation at $f/f_c = 1$, as does the second-order Butterworth filter; however, at $f/f_c = 0.5$ (half bandwidth), the first-order filter has about 10% amplitude attenuation and the second-order Butterworth filter has an attenuation of only 3%, a considerable improvement.

The second-order Bessel filter results when $d = \sqrt{3}$ and produces a "maximally flat" group-delay response. The group delay is equal to the derivative with respect to angular frequency of the phase response:

$$\text{Group delay} = \tau = d(\phi)/d\omega \quad (21)$$

This type of filter is optimum for transient data inputs. For a step input, the Bessel filter produces less distortion and reaches the final values faster than the second-order Butterworth and Chebyshev filters. However, its midband ($f/f_c = 0.5$) amplitude attenuation, is 13%, and at cutoff frequency f_c the amplitude response is down 42%. The compromise filter is a compromise between the Butterworth and Bessel filters characteristics, ($\sqrt{3} > d > \sqrt{2}$), which makes it better than the Butterworth filter for transient data and better than the Bessel filter for sinusoidal inputs. The compromise filter is often recommended when the data will contain both transient and sinusoidal information.

The Chebyshev filter, such as shown in Fig. 24a has a ripple or peak in the passband. With a second-order low-pass filter there will be one peak near the band-edge. Higher-order Chebyshev filters may have a number of peaks in the passband; however, the peak-to-peak amplitude of the ripple is usually specified for 1, 2, and 3 dB. These levels of passband ripple are not usually suitable for flight-test data-acquisition purposes. For example, a 3-dB peak-to-peak amplitude error involves an error of over 30%. A peak-to-peak ripple of 0.2 dB ($\approx 2\%$) is a more reasonable level. Chebyshev filters, since they have even less damping than the Butterworth filter, are not desirable filters for use with transient data.

It must be remembered that at any point in the amplitude response where there is a rapid change in the rate of attenuation, there will also be a correspondingly large change in the phase shift. This produces a group delay τ which is not constant. If the group delay were constant everywhere inside and outside the filter passband, there would be a linear relationship between frequency and phase shift.

A transmission function that has smooth roll-off and has a constant group delay is the well-known Gaussian function for which a real-filter implementation is impossible. The reasons for this are developed in Ref. 12. The Bessel filter is one of the simplest, maximally flat group-delay approximations.

When the advantages of the above low-pass filters are being explained, one often hears statements like "The Bessel filter is good for transient data but cuts off too slowly outside its passband; the Butterworth filter has the flattest amplitude response and an acceptable cutoff outside the passband; the Chebyshev filter is primarily desirable because its roll-off outside the passband is fast." Referring to Fig. 24, these claims for various roll-offs do not seem to be justified since the final asymptotic roll-off of all the filters is identical at $f/f_c = 10$. To understand the rationale behind the above quoted statement, it is necessary to replot the filter characteristic such that the cutoff frequency f_c can be defined as the point at which the filter final roll-off crosses the -3-dB point. Figure 25 shows the curves of Fig. 24a replotted according to this alternative definition.

Note that the Butterworth filter ($d = \sqrt{2}$) does not have to be replotted since it already passes through -3 dB at $f/f_c = 1.0$. When the curves are plotted as in Fig. 25, the claims about different roll-offs outside the bandwidth become apparent.

The Chebyshev filter in this figure seems at first glance to offer considerable advantages outside the passband; however, the distinct difference shown in Fig. 25 is for a 3-dB, peak-to-peak, ripple Chebyshev filter. This improvement would be less striking for a 0.2-dB, peak-to-peak, Chebyshev filter, since the improvement increases with increasing passband ripple amplitudes (the 0.2-dB peak-to-peak ripple is recommended as a maximum permissible ripple for general-purpose, data-acquisition filters).

When the engineer has sinusoidal data and must have rapid attenuation outside the filter passband, the Cauer filter (also called the elliptic filter) is probably a better alternative than the Chebyshev filter. The Cauer has a very steep roll-off outside the passband for the number of components involved; however, its transient response (overshoot performance on transient data) is less desirable than that of even the Chebyshev filter. It also has ripple in both the passband and the stop-band, and filter mechanization involves substantial matching and selecting of components. These filters are usually implemented from computer-derived tables (see Appendix I). Figure 26 compares various types of fifth-order filters to a similar fifth-order Cauer filter. Note that the Chebyshev and Cauer filters both have been selected to have equal peak-to-peak passband ripple.

As can be seen from Fig. 26, the Cauer filter approaches the ideal-filter amplitude response in the region of cutoff; however, it also has ripple in the passband and stop-band, and a final attenuation which is less than the all pole filters (Bessel, Butterworth, and Chebyshev). When the engineer must contend with transient data and needs a sharper attenuation than available with the Bessel or compromise filters, the equi-ripple time-delay filter (Ref. 12) is another option.

The standard low-pass active filter reflects operational amplifier low-frequency drift and output offset voltage in the output signal. When low-level signals that contain very-low-frequency information must be filtered, this drift and offset voltage may overwhelm the signal itself. A very valuable zero-offset low-pass-filter circuit is developed in Table 13 of Appendix I in the Butterworth, Bessel, compromise, and Chebyshev formats.

Practical high-pass filter. — It was mentioned earlier that high-pass filters are not generally desirable flight-test signal conditioners; however, when combined in a proper manner with a low-pass filter, a broadband bandpass filter is formed. The broadband bandpass filter is a very effective and often-used signal-conditioning filter. It is normally desirable to specifically limit the high-frequency cutoff in all applications.

Practical bandpass filter. — For purposes of this discussion, bandpass filters will be divided into two classes: (1) the broadband bandpass filter, and (2) the narrow-band bandpass filter (see Fig. 27).

The broadband bandpass filter is very useful when the engineer wishes to discriminate against frequencies below the filter low-frequency cutoff f_{CL} and still reject noise above the highest data frequency of interest, f_{CH} . This type of filter is often used to reject steady-state offset and low-frequency drift and still limit high-frequency noise.

The broadband bandpass filter can be made by combining overlapping high-pass and low-pass filters. As already discussed, the low-pass filter could be a Bessel-, Butterworth-, or Chebyshev-type filter. Corresponding types of high-pass filters also exist such as the Bessel, Butterworth, and Chebyshev. Since the criteria for selecting the type of low-pass filter will also apply to the selection of the high-pass-filter characteristics, the high-pass and low-pass characteristics are usually matched and thus could be Bessel-, Butterworth-, or Chebyshev-type broadband bandpass filters.

The narrow-band bandpass filter characteristics shown in Fig. 27b are not commonly used in airborne flight-test data-acquisition signal conditioning for reasons that will be discussed under narrow-band band-reject filters.

Practical band-reject filter. — Like the bandpass filter, the band-reject filter will be discussed in two broad categories: (1) the broadband band-reject filter, and (2) the narrow-band "notch" band-reject filter (Fig. 28). The narrow-band, band-reject-filter center-frequency is f_C . The band-reject filters are not frequently encountered in airborne flight-test data acquisition and signal conditioning; however, they are sometimes used to solve special problems.

From Fig. 28 it is apparent that both broadband band-reject filters and the notch filters as shown here have similar characteristic response curves; that is, the attenuation curves intersect eventually, and the curves of Figs. 28a and 28b will generally have the same shapes. The differences, however, are significant in that the broadband band-rejection filter is designed with well-defined lower and upper cutoff frequencies f_{CL} and f_{CH} , respectively. The point of maximum attenuation is usually not defined. In the case of the narrow-band or notch filter, the frequency of maximum attenuation f_C and the sharpness of the notch are the main design parameters.

The broadband band-reject filter is herein implemented by using high-pass and low-pass filters connected in parallel, as shown in Fig. 29. Since the high-pass and low-pass filters can be composed of Bessel, Butterworth, Chebyshev, or any other appropriate high- and low-pass filters, the band-reject filter can also be a Bessel or Butterworth filter.

Fixed-frequency, narrow-band band-reject filters, sometimes called high-Q filters (see Appendix I for an explanation and definition of Q), or notch filters, are most commonly used to reject a strong, single-frequency, noise-spike input such as the vehicle electrical power frequency. This solution should be applied only when efforts have failed to remove the offending noise input by improved signal conditioning and by better wiring and grounding techniques. Reference 3 presents a discussion of grounding and shielding techniques. When these efforts fail to sufficiently reduce the single-frequency-noise spike and the spike is substantially outside the desired frequency spectrum of the data, three solutions are available: (1) use a higher-order filter (faster attenuation outside the bandpass (see Appendix I for a description of these types of filters); (2) use a Cauer filter; or (3) use a notch filter. Since all of these techniques are frequency-rejection techniques, they are discussed below.

Solution (1) involves the use of a low-pass or bandpass filter which passes all the frequencies of interest while attenuating the noise input that is outside the filter bandpass. For example, if a second-order (40-dB/decade) low-pass filter is used to pass the data of interest and the external noise inputs are still too large, a fifth-order (100-dB/decade) low-pass filter could be used.

Solution (2) involves the use of certain special filters, such as the Cauer filter, which have transmission zeros in the band-reject portion of their spectrum. Refer to the Cauer filter amplitude response shown in Fig. 26. These zeros are inherent in notch filters and with proper circuit-parameter selection the notches can theoretically be made to coincide with the frequency of the noise input. Since the notches are theoretical points of infinite attenuation, an exact match would in theory completely attenuate this single-frequency-noise portion of the signal. The problem with this approach will be discussed under notch filters.

Solution (3) uses a fixed-frequency notch filter to remove a single-frequency-noise spike. When used inside the data spectrum, these real non-ideal notch filters will introduce significant phase and amplitude distortions around the notch frequency. All fixed-frequency high-Q filters used in flight-test signal conditioning suffer from two major limitations. The first limitation is that most noise sources in the aircraft, such as the aircraft 400-Hz power, are not rigidly controlled. Secondly, aircraft temperature variations and the stability of the filter components make it difficult to maintain the rejection notch at a given frequency. Figures 30a and 30b illustrate two notch filters which are different only in that the one shown in Fig. 30b has a much narrower (higher-Q) notch than the one in Fig. 30a. The filter characteristic illustrated in Figs. 30a and 30b is intended to have infinite attenuation at f_C (that is, a parallel-tee filter); however, because of component mismatch and circuit input-to-output

coupling, this is never achieved, and the filter characteristic of Fig. 30b will look more like that of Fig. 30c. The high-Q filter of Fig. 30b is usually desirable because it produces very little amplitude attenuation to steady-state sinusoids adjacent to its notch frequency f_c . Low-Q notch filters can produce significant amplitude distortions at relatively low frequencies. The same precautions that apply to notch filters also apply to high-Q bandpass filters, and considerable judgment should be exercised for each application.

Tunable filter. — Tunable bandpass and band-reject filters can be very useful signal-conditioning tools. The high-Q, tunable bandpass filter is used in airborne spectrum analyzers. A tunable band-reject filter could conceivably be synchronized to the noise source (aircraft ac power for example), and thus track the noise frequency with a very sharp frequency-rejection notch. A filter of this type is discussed in Appendix I.

3.2.4 Disadvantages of Filters

After reviewing the effects associated with the introduction of filters into the signal-conditioning system, it is reasonable that many engineers might say, "Wouldn't it be wonderful if data-acquisition systems did not require filters?" But such a statement is based on an erroneous understanding of the nature of a data-acquisition system. The data-acquisition system is a chain of elements all of which cause amplitude and phase changes.

As an illustrative example, consider an accelerometer which has been located in an air-data nose boom in such a way that the sensitive axis is linked directly to the position of the angle-of-attack vane. Since the boom is flexible and in fact has a resonant frequency of its own, the accelerometer's position is a function of various vehicle and aerodynamic inputs such as aircraft normal acceleration. Thus, a positional transfer function must be derived that allows corrections even for oscillatory motions of the boom. The angle-of-attack vane responds to the aerodynamic inputs, and its response is a very complex function. In many ways, its input/output transfer function is a function of many variables, such as air density and air velocity. The common small force-balance accelerometer often used in this application has an input/output transfer function that behaves exactly as a second-order filter with a low cutoff frequency. To compare or combine these data with other data on the aircraft, all pertinent component transfer functions in the entire data-acquisition chain must be known and defined. Any one of the above input/output transfer functions may exert more influence than an anti-aliasing filter.

The important point is that the frequency response of every link in the entire data-acquisition chain from the measurand detection process to the data recorder or transmitter should be known so that if necessary, the data can be corrected.

3.3 DIGITAL SIGNAL CONDITIONING

Computers are becoming significant data sources on flight vehicles mainly because of their widespread use in avionics subsystems — flight-control systems, inertial navigation systems (INS), and air-data computer systems (ADCS). These computerized avionics subsystems are advanced and sophisticated sources of information that the vehicle requires to perform its function. On the more modern commercial and military vehicles, these systems exchange information with each other, as required, by means of a data bus that links all the systems together. In many cases, the bus is used to handle the data from computers and digital transducers.

Digital signal conditioning, the subject of a future AGARDograph, is becoming quite common in many aircraft data-acquisition systems. Because of the versatility and unique capabilities of digital computers, it is also becoming more common to convert analog data to digital data and to manipulate those data by means of airborne computers which then become sophisticated signal conditioners.

In modern aircraft, digital logic, microprocessors, microcomputers, and minicomputers are commonly found in signal-conditioning equipment. The use of microprocessors in flight-test applications will be covered extensively in a future AGARDograph; however, the following discussions should give the engineer a preview of digital signal-conditioning techniques.

3.3.1 Analog-to-Digital Converter

The analog-to-digital converter (ADC) serves as the critical interface between the analog voltage signal and the downstream digital systems. This converter is in large measure the determining factor in the quality of data obtained from a system. It determines the limits of data accuracy, resolution, and sample rate from an acquisition system. For high-quality data, the conversion should be done as close as physically possible to the analog-to-digital converter. Digital data are highly resistant to noise contamination and usually suffer no degradation until additive noise levels reach a substantial fraction of the signal level. Early digital conversion therefore limits the chance for noise introduction before digital conversion.

Placing an ADC in each transducer channel would not only be expensive but inappropriate. The practical way to digitize a large number of data channels is to place an electronic switching system (multiplexer) before the ADC and sample each data channel at an appropriate time, this is called a PCM system (see Sec. 5).

Since the analog multiplexer must sequentially connect the desired data input channels to the ADC for processing, it is important that minimal additive noise be introduced by the multiplexer. For this reason, a high-quality multiplexer with capability commensurate with the ADC is an absolute necessity if the highest quality data possible are to be obtained from a given system. Appropriate pre-sample filters are required upstream of the analog multiplexer to avoid data damage owing to aliasing (see Sec. 5).

Occasionally, a special transducer will require that a dedicated ADC be installed at the transducer location. An example of this situation is a high-accuracy total or static pressure transducer that provides high-resolution data to the aircraft systems. The PCM system is not usually capable of providing the accuracy or resolution commensurate with the high-quality transducer; as a result, a special ADC unit is required. When the dedicated ADC is used, the interface to the PCM system is fully digital, and the high-resolution data require special processing to be included in the normal data system process.

3.3.2 Digital Filter

The digital filter is a powerful signal-conditioning technique. Digital filters are presently used extensively in computerized ground-station data reduction. They are being used more frequently in airborne applications as filter requirements exceed those possible with analog filters. Digital filters are not commonly used in analog data channels because an analog aliasing filter is required before the digital filter, and an analog interpolation filter is required after the digital filter. The engineer must have a particularly difficult requirement to justify this complexity.

As mentioned earlier, when specific requirements become crucial, it is often best to consult a filter specialist. Digital filters are used in analog data systems when producing a precise, stable transfer function is too difficult for an analog filter. Further reading on digital filters can be found in Refs. 13 and 14.

A commonly used digital filter is the finite impulse response (FIR) digital filter. Symmetric FIR filters exhibit purely linear phase characteristics. This feature alone would make them very desirable filters; however, a filter expert may be required to make sure that these advantages are realized, since the analog filters at the digital filter input and output produce nonlinear phase characteristics.

If the data have been digitized and are to remain digitized, such as in a PCM or computer system, digital filters become much more attractive. Even under these conditions, unless the data are being used in a real-time on-board application, it is probably easier to perform the digital filtering in the ground station or on a ground-based main frame computer.

3.3.3 Extracting Data from a Digital Data Bus

Acquiring data from an avionics subsystem computer for a general-purpose flight data-acquisition system is often very difficult since these computers are not designed for ease of data-acquisition interfacing, and flight safety requirements dictate that such access not produce avionics subsystem failures. Presently, avionics subsystems are linked together by a data bus, and it usually is quite easy to passively monitor the data on the bus. A research engineer will usually be permitted to do no more than monitor the data bus. Considerable data are available to the engineer on bus techniques and the acceptable methods for tapping this information.

By definition, these avionics systems are aircraft control systems, which are not part of the data-acquisition system. Two considerations, however, have caused them to heavily affect the engineer who is responsible for the data-acquisition signal conditioning. The first consideration is that these systems have become extremely complex; therefore, the avionics engineers, especially in the first stages of flight test, often want to study all the information on the data bus to aid in problem analysis. The second consideration is that systems (for example, the INS, ADS) have become highly advanced and the data bus contains many data that are useful to the engineer.

Figure 31 shows how an actual flight-test system can meet both types of demands with formatting-type signal conditioners. The "avionics bus interface I" satisfies the requirements of the avionics design group to record all the information available at buses A and B. The data bus used on this aircraft is the Military Standard (MIL-STD) 1553B data bus (Ref. 15). Three types of 20-bit words are permissible on data buses A and B: command words, data words, and status words. A word on one bus can overlap a word on the other bus, and there are many times when no words exist on either bus. The avionics bus interface I is a simple formatting-type signal-conditioning system that generates 20-bit pseudodata words for insertion onto the tape channel until a data bus word is available. When a data bus word arrives, it is inserted into the data stream as soon as a 20-bit pseudodata word is completed. If a word on the second bus should overlap another word, it is delayed until the end of the first word and then it also is inserted into the data stream: Thus all words on both buses are recorded with only minor time shifts.

The avionics bus interface II is considerably more sophisticated. In this system, the data bus, which generates words asynchronously, has to be matched to a continuously repetitive PCM data stream functioning at a different bit rate. Figure 32 is a block diagram of this system. The bus receiver takes the 20-bit words off the two buses and forwards one bit in order to identify from which bus the word was derived. The decoder changes the code format from Manchester II bi-phase level to a non-return-to-zero (NRZ) format, removes the synchronization word which involves three bit-times, and also removes the parity bit. The resulting 16-bit serial word is passed on to the buffer register. The buffer register takes the 16-bit serial word and constructs a new 20-bit parallel word which contains a parity bit, one bit to denote the bus from which the word originated, and two bits which identify the type of word involved, that is, command, data, or status. Also, this register sends the command word to the word selector logic. The word selector logic can be set to recognize requests for up to 256 words and selects which words will be entered into the PCM data stream. The buffer register passes all data words on to the data register which takes the words in at one rate and clocks them out at a much slower rate, since the word is now a 20-bit parallel word. All words are sent to the random access memory but only the words of interest are written into memory. From the random access memory the data words are selected in the order they are to appear in the PCM data stream and sent to the buffer memory, which synchronizes the word rate to that of the PCM system. The parity bit is replaced in the random access memory by a bit

that notifies the data user if the word in the random access memory has been refreshed since it was last inserted in the data stream. This total bus interface takes up one printed circuit card and is a sophisticated example of formatting-type signal conditioning.

3.3.4 Signal Conditioning with Microcomputers

In the two previous examples there were no requirements for on-board, real-time data reduction and thus no real need for the computational capabilities of a microcomputer. However, one flight-test instrumentation group has used a microcomputer to accomplish the same bus interface, except that the outputs were presented in engineering units and scaled to be displayed and recorded on airborne strip-chart recorders. In this case, where actual data reduction was required, the computational power and flexibility of the microcomputer were essential.

A visitor to the various flight-test facilities cannot escape the conclusion that the major trend at present in signal conditioning is the rapid increase in the application of microcomputers. Microcomputers are being used, for example, to control a small 32-cell pressure manometer which electronically scans and repetitively calibrates each pressure module during flight. In addition, these devices are used to implement a scanning spectrum analyzer and to change raw data to engineering units for aircraft real-time use.

When should computers be used for airborne signal conditioning? The answer is simply that they should be used when they can do the task more effectively and faster than other means. The authors' position is that computerized systems should be used when real-time, on-board data reduction is required and two-way telemetry (that is, raw data on the telemetry down-link and reduced data on the telemetry up-link), is not desirable. An example is discussed below, which illustrates how this type of airborne signal conditioning can be used to good advantage.

A commercial aircraft company uses microcomputers to provide real-time, on-board computation of flight-test gross weight (GW) and longitudinal center-of-gravity (c.g.). A block diagram of this system is shown in Fig. 33. The real-time GW/c.g. computing system (Ref. 16), was developed to solve two similar problems. On-board flight-test engineers were required to compute the aircraft GW or c.g. from the volumetric flow data and other raw data, a difficult and time-consuming process involving complex graphic solutions. The present system performs this computation and in so doing significantly reduces actual flight hours. The second situation required that GW/c.g. profiles be available before follow-on data reduction. Microcomputers are now used to accumulate flow data and compute the profiles in real time to avoid the previous lengthy flight tape playback process. This system has made an appreciable reduction in the ground-based computer data-reduction time.

A complete system uses 10 microcomputers. Each of the five fuel weight flow encoders and the two discrete data-acquisition units has its dedicated microcomputer; the GW/c.g. processor uses three microcomputers. In the GW/c.g. processor, one microcomputer controls the keyboard interface, video display, message processing, and the computing; the two subordinate microcomputers transmit and receive messages via the communications network. The microcomputer in each fuel weight flow encoder unit is programmed with several diagnostic parameters and a set of very complete calibration equations, including fuel temperature, fuel pressure, fuel flow rate (pounds per hour), and fuel used (pounds). Calibration equations are programmed into the microcomputer for the transducers, the fuel encoder unit, a turbine flowmeter, a platinum temperature sensor, and a pressure sensor. The GW/c.g. processor provides the fuel encoder unit with an initialization factor which is derived from a preflight fuel density and temperature measurement. The discrete data-acquisition unit accepts inputs as shown in Fig. 33 and outputs information such as the moment changes caused by a change in the position of the landing gear and flaps; the composite weight and moment of the aircraft water ballast; and the fuel-system configuration.

3.3.5 Signal Conditioning with Minicomputers

The Boeing Commercial Airplane Company (BCAC) saved considerable flight time by using a microcomputer during the flight-certification program of the 747 SP aircraft (Ref. 17). Figure 34 is a simplified representation of the BCAC computerized flight-test data-acquisition system. The BCAC standard flight-test data-acquisition system is shown in Fig. 34 above the dashed line. The portion of the system below the dashed line represents a very limited version of the BCAC ground-monitoring station. This lower portion provides preflight and postflight instrumentation analysis capabilities. Since BCAC was testing a large commercial passenger aircraft which had no stringent space or weight restrictions, it was logical to use the minicomputer capabilities to monitor and accomplish near-real-time analysis of the data in flight. BCAC estimates that the on-board computerized monitoring system used on the 747 SP program cut the flight load survey flight time by about 20% and reduced the airplane performance testing by 15%-20%. This change was facilitated since BCAC does not use telemetry except for critical flight-safety testing, such as flutter flight tests. Their reasoning is summarized as follows: first, BCAC test aircraft are large enough to carry analysis and instrumentation engineers; second, the Seattle, Washington, area, because of surrounding mountains and the prevailing weather patterns, is one of poor telemetry reception; and third, BCAC wishes to be flexible in scheduling flight tests at many different locations, some of which may not have telemetry facilities. BCAC has found this flight testing technique very useful, is using it on all their present test programs, and plans to use this same approach on its future flight-test programs. If other flight-test facilities agree with the BCAC telemetry approaches, then placing this amount of ground-station-type computing capabilities in large test aircraft constitutes a desirable alternative to the air-to-ground telemetry.

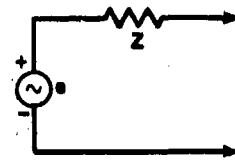
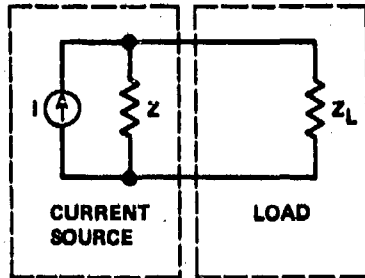
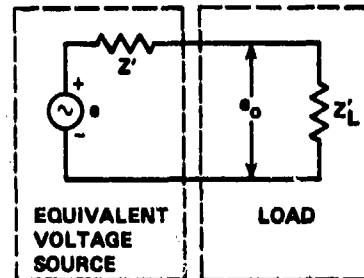


Figure 4. Thévenin equivalent circuit

- $e = IZ$
- $e_o =$ VOLTAGE SOURCE OUTPUT ACROSS THE LOAD IMPEDANCE, Z_L
- $I =$ CURRENT GENERATOR OUTPUT
- $Z = Z' =$ INTERNAL SOURCE IMPEDANCE
- $Z_L = Z'_L =$ LOAD IMPEDANCE



(a) Current-source circuit



(b) Equivalent voltage-source circuit

Figure 5. Current-source circuit and equivalent voltage-source circuit

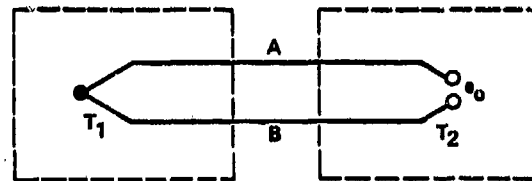


Figure 6. Simple thermocouple circuit

- A = AMPLIFIER GAIN
- $e =$ VOLTAGE GENERATOR OUTPUT
- $e_i =$ AMPLIFIER INPUT VOLTAGE
- $e_o =$ AMPLIFIER OUTPUT VOLTAGE ACROSS R_L
- R = VOLTAGE SOURCE INTERNAL IMPEDANCE
- $R_i =$ AMPLIFIER INPUT IMPEDANCE
- $R_L =$ AMPLIFIER LOAD RESISTANCE
- $R_o =$ AMPLIFIER OUTPUT IMPEDANCE

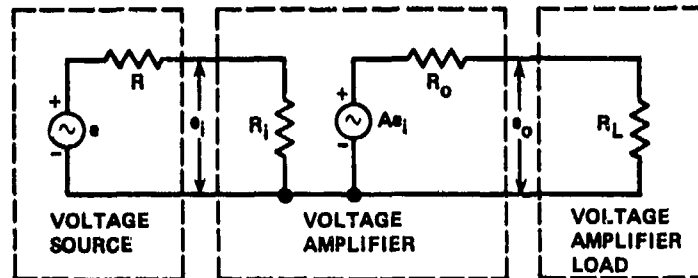


Figure 7. Voltage-amplifier system

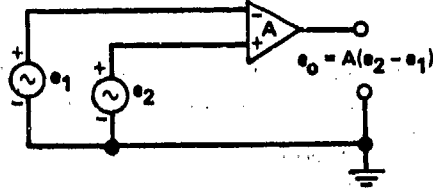


Figure 8. Differential instrumentation amplifier model

- e_B = BRIDGE OUTPUT = $e_1 - e_2$
- e_{CM} = COMMON-MODE VOLTAGE
 $\approx (e_1 + e_2)/2 \approx E_B/2$
- e_0 = $Ae_B = \pm AE_B \Delta R/2R$
- e_1 = $E_B(R \pm \Delta R)/(2R \pm \Delta R)$
- e_2 = $E_B R/(2R \pm \Delta R)$
- $R \gg \Delta R$

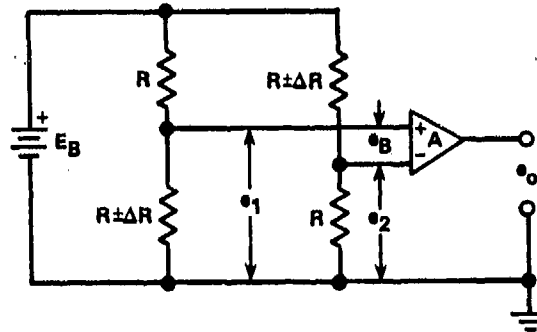
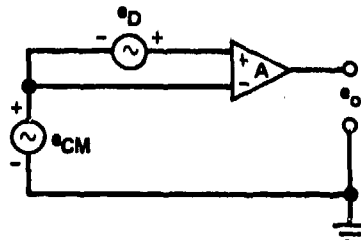
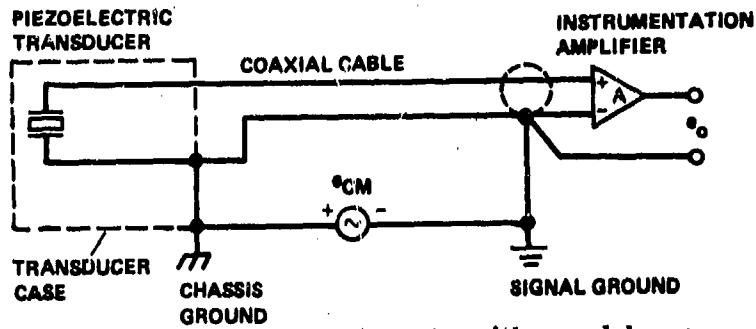


Figure 9. Simplified strain-gauge bridge amplifier system

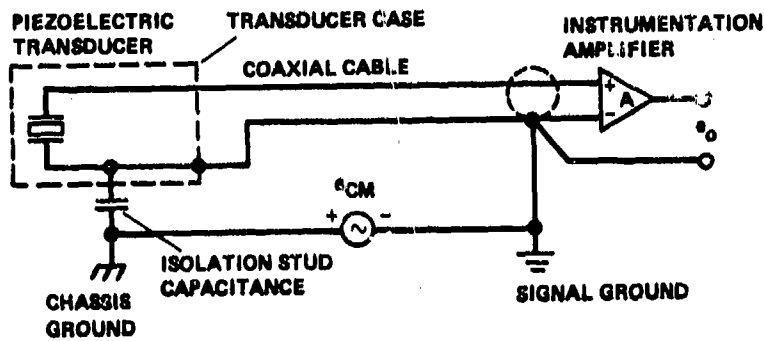


- A = AMPLIFIER GAIN
- e_{CM} = AMPLIFIER COMMON-MODE INPUT VOLTAGE
- e_D = AMPLIFIER DIFFERENTIAL INPUT VOLTAGE
- e_0 = AMPLIFIER OUTPUT VOLTAGE

Figure 10. Common-mode rejection instrumentation amplifier model



(a) Piezoelectric accelerometer with grounded case



(b) Piezoelectric accelerometer with isolation stud

Figure 11. Transducer common-mode voltage coupling modes



(a) Isolation operational amplifier symbol



(b) Isolation instrumentation amplifier symbol

Figure 12. Isolation amplifier circuit symbols

$I_s = KX$
 $X = \text{INPUT MEASURAND}$
 $Z_L \rightarrow 0$
 $Z_S \rightarrow \infty$

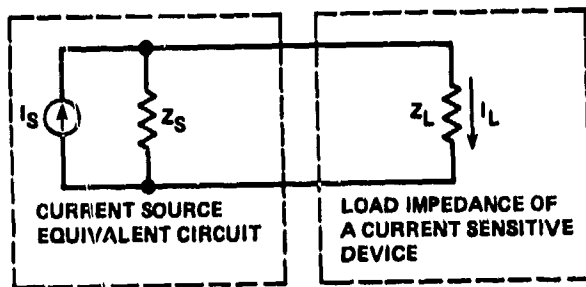
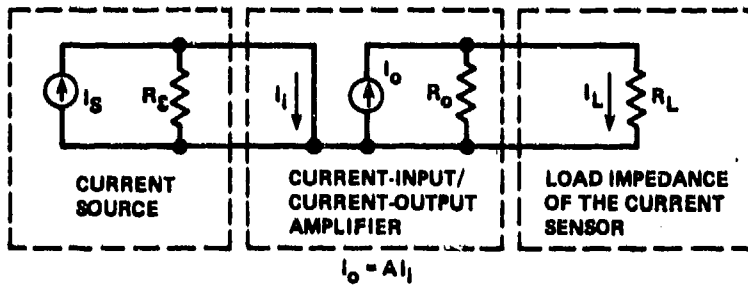
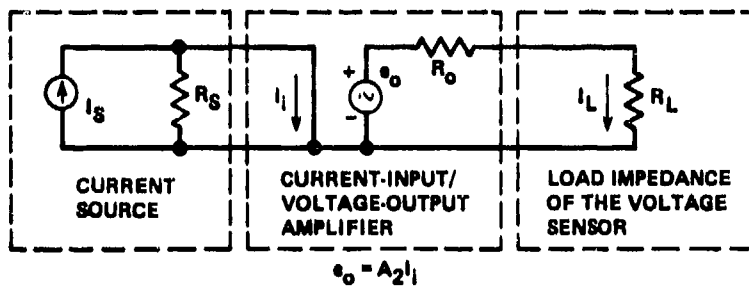


Figure 13. Current-source equivalent circuit and load impedance

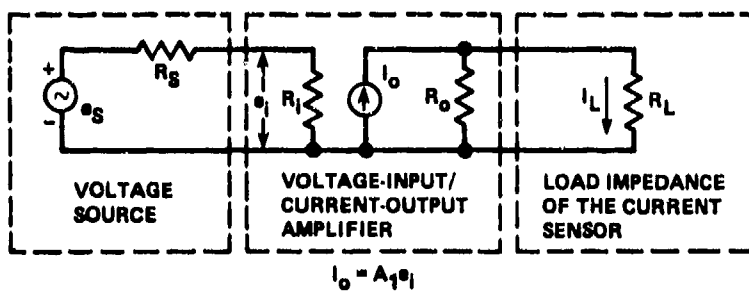
- A = GAIN OF THE CURRENT-INPUT/CURRENT-OUTPUT AMPLIFIER
- A₁ = GAIN OF THE VOLTAGE-INPUT/CURRENT-OUTPUT AMPLIFIER
- A₂ = GAIN OF THE CURRENT-INPUT/VOLTAGE-OUTPUT AMPLIFIER
- e_i = INPUT VOLTAGE TO THE AMPLIFIER
- e_o = VOLTAGE GENERATOR OUTPUT OF VOLTAGE-OUTPUT AMPLIFIER
- e_s = VOLTAGE GENERATOR OUTPUT
- i_i = CURRENT INPUT TO AMPLIFIER
- i_L = CURRENT THROUGH AMPLIFIER EXTERNAL LOAD RESISTANCE
- i_o = AMPLIFIER CURRENT OUTPUT
- i_s = CURRENT GENERATOR OUTPUT
- R_i = INPUT IMPEDANCE OF AMPLIFIER
- R_L = OUTPUT LOAD RESISTANCE TO THE AMPLIFIER
- R_o = OUTPUT RESISTANCE OF THE AMPLIFIER
- R_s = SOURCE RESISTANCE AT THE AMPLIFIER INPUT



(a) Current-input/current-output amplifier



(b) Current-input/voltage-output amplifier



(c) Voltage-input/current-output amplifier

Figure 14. Three types of current amplifiers

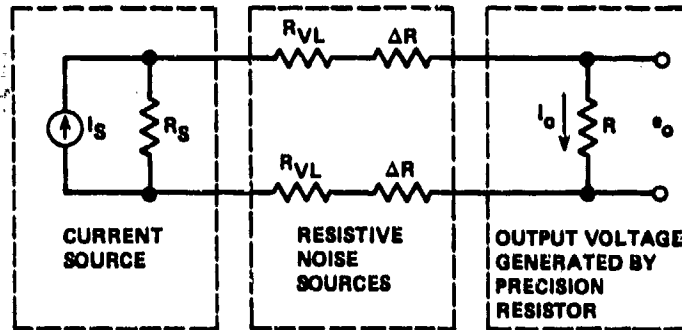


Figure 15. Resistive noise reduction with a current source

C = TRANSDUCER CAPACITANCE
 K = PIEZOELECTRIC CHARGE SENSITIVITY
 Q = CHARGE GENERATED BY DISTORTING THE PIEZOELECTRIC CRYSTAL
 R = TRANSDUCER LEAKAGE RESISTANCE
 X = INPUT DISTORTION

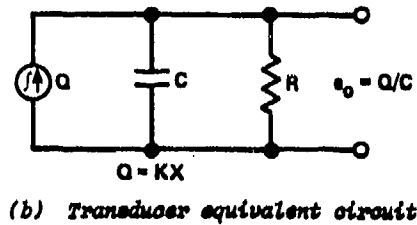
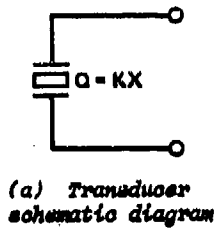
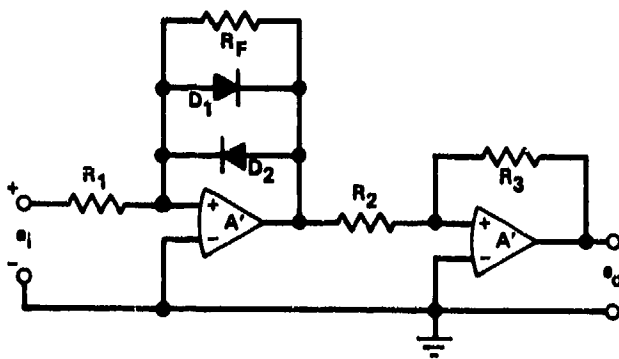
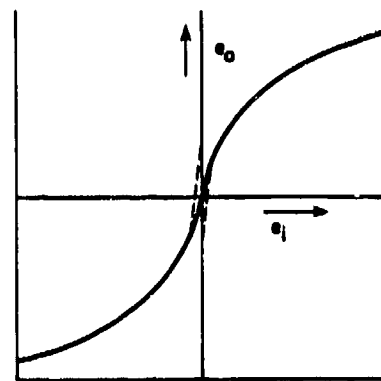


Figure 16. Electrical model of a piezoelectric transducer



(a) Compression amplifier



(b) Pseudo-logarithmic compression characteristic

Figure 17. Compression amplifier and characteristic curve

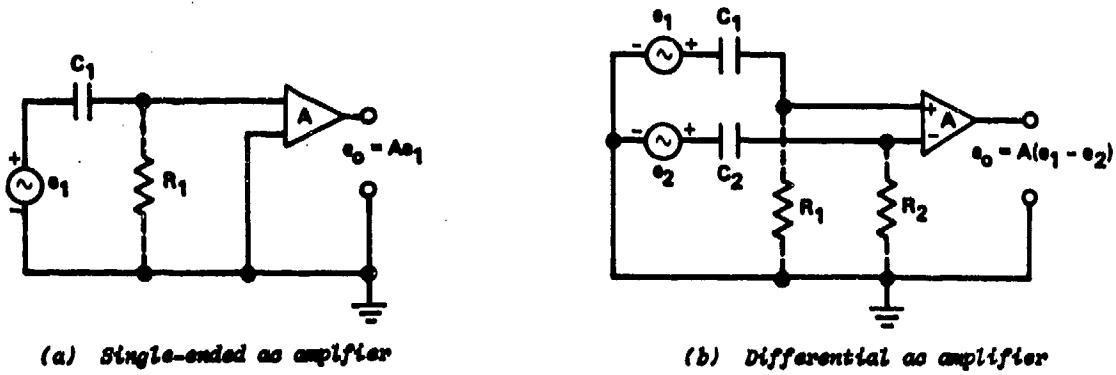


Figure 18. Capacitively coupled amplifiers

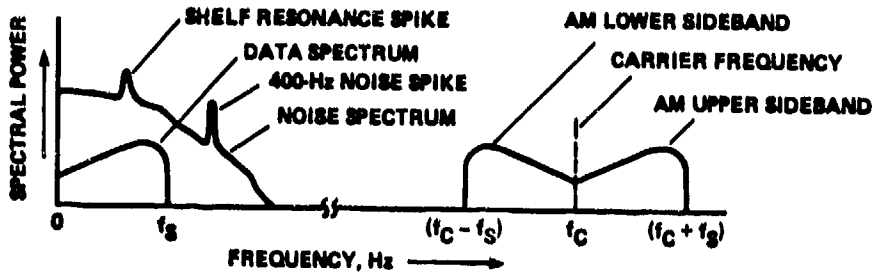
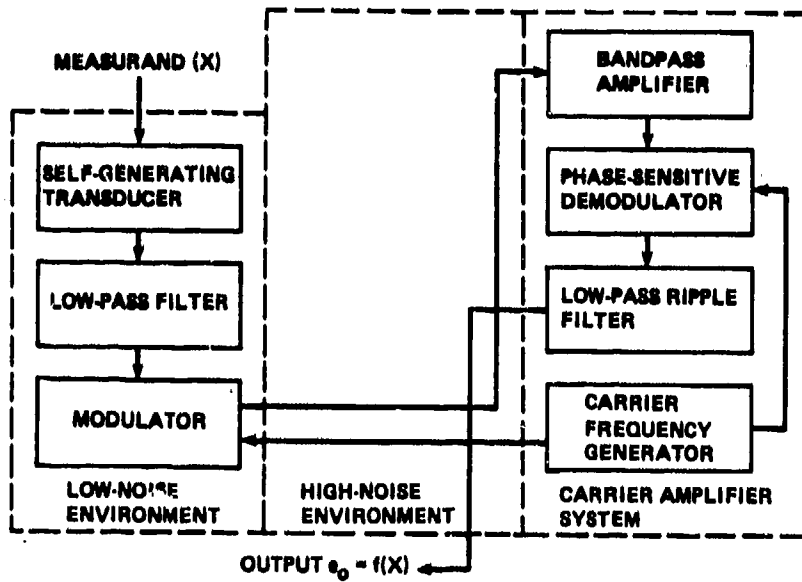
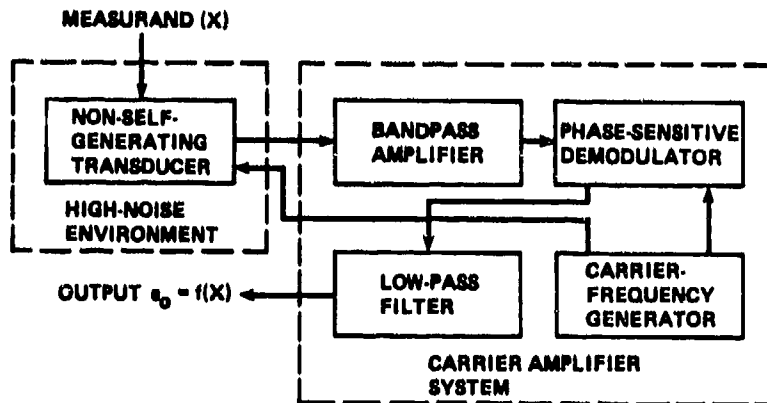


Figure 19. Using AM techniques to shift a signal spectrum



(a) Self-generating transducer carrier system



(b) Non-self-generating transducer carrier system

Figure 20. Carrier-amplifier systems

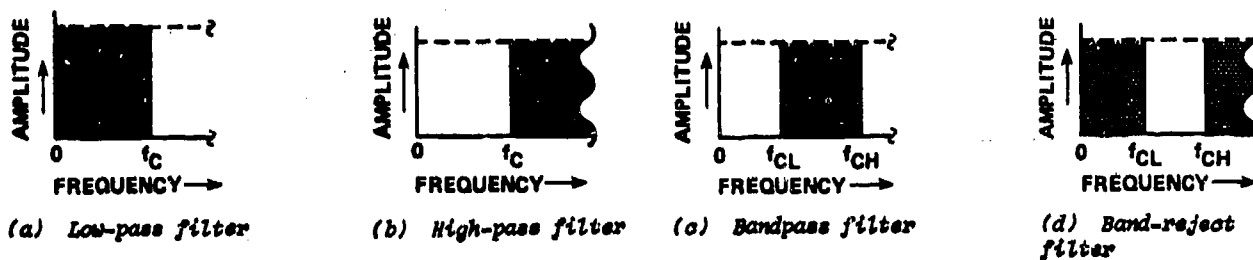


Figure 21. Amplitude response of ideal filters (Shaded areas are pass-bands).

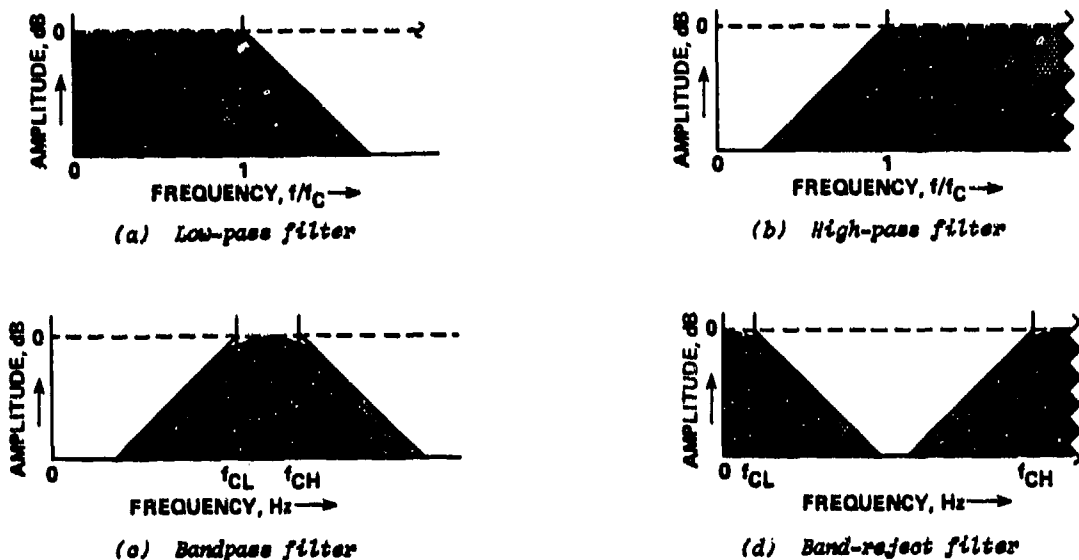


Figure 22. Amplitude responses of practical filters (All frequency axes are plotted on a log scale.)

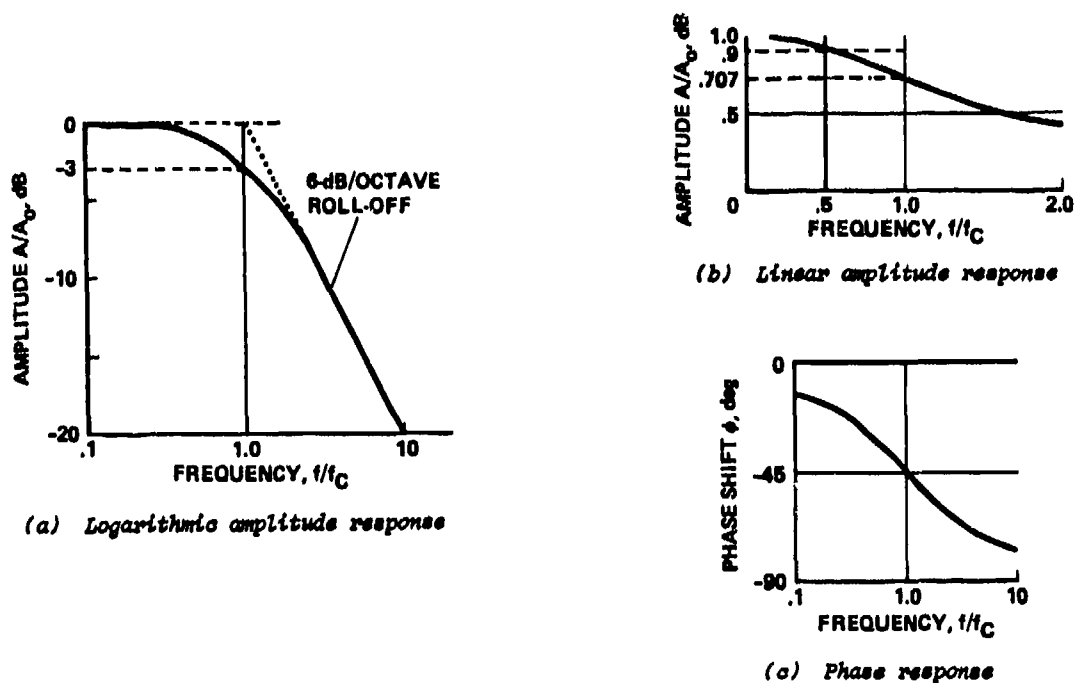
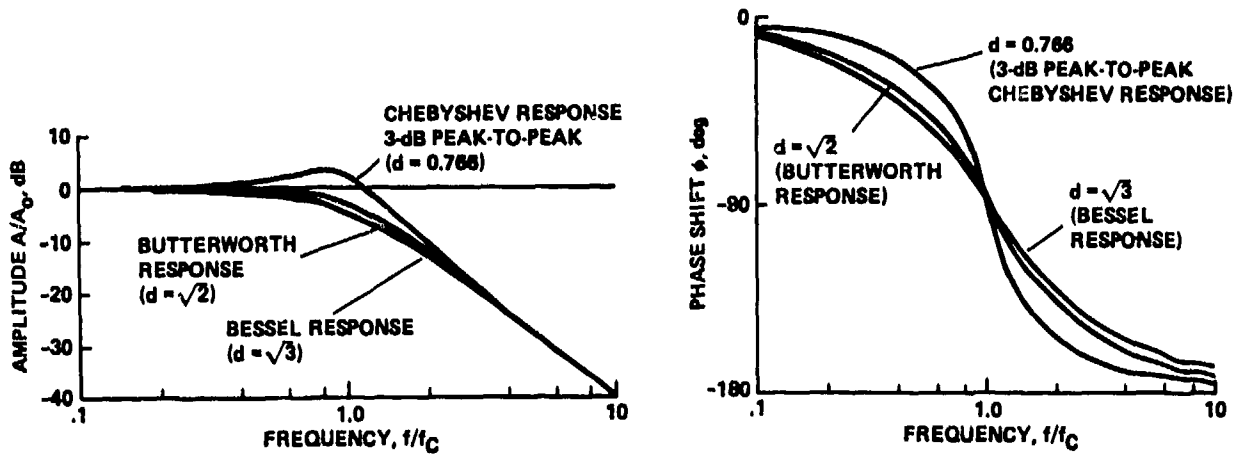


Figure 23. Amplitude and phase response of a first-order low-pass filter



(a) Amplitude response

(b) Phase response

Figure 24. Amplitude and phase response of a second-order low-pass filter

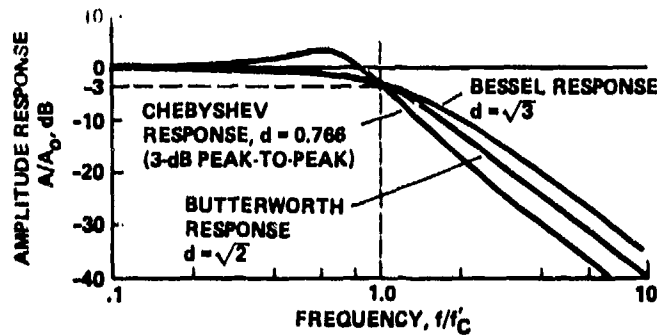


Figure 25. Normalized cutoff frequency response of second-order filters

- ① IDEAL LOW-PASS FILTER RESPONSE
- ② FIFTH-ORDER CAUER RESPONSE
- ③ FIFTH-ORDER CHEBYSHEV RESPONSE
- ④ FIFTH-ORDER BUTTERWORTH RESPONSE

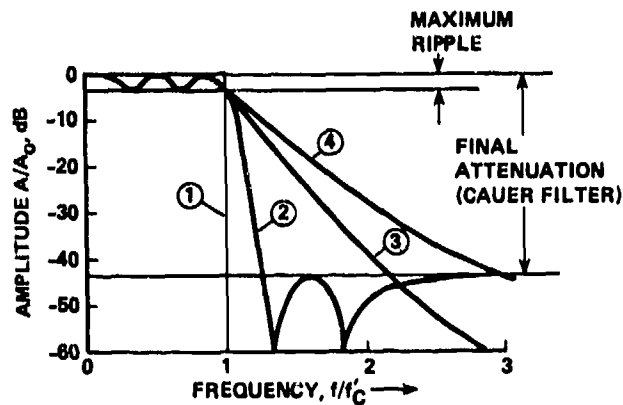
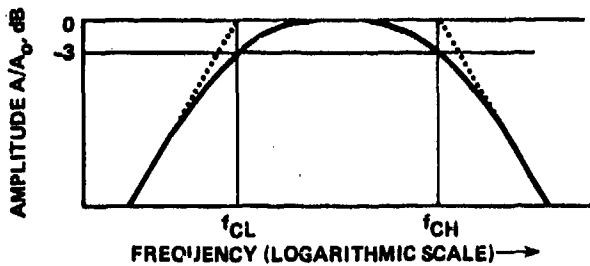
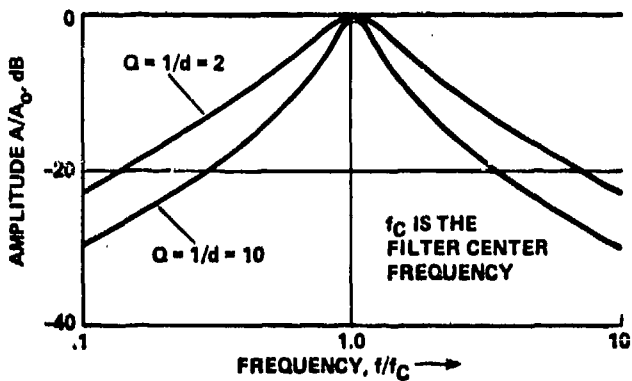


Figure 26. Ideal, Butterworth, Chebyshev, and Cauer filter responses

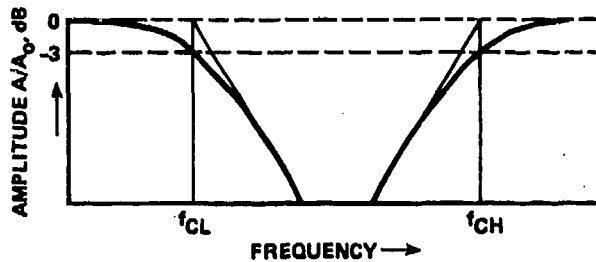


(a) Broadband bandpass filter

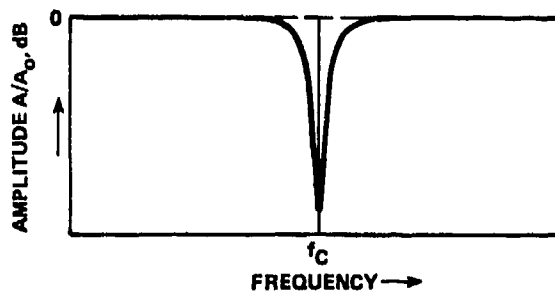


(b) Narrow-band bandpass filter

Figure 27. Bandpass filter response



(a) Broadband band-reject filter



(b) Narrow-band (notch) band-reject filter

Figure 28. Band-reject filter response

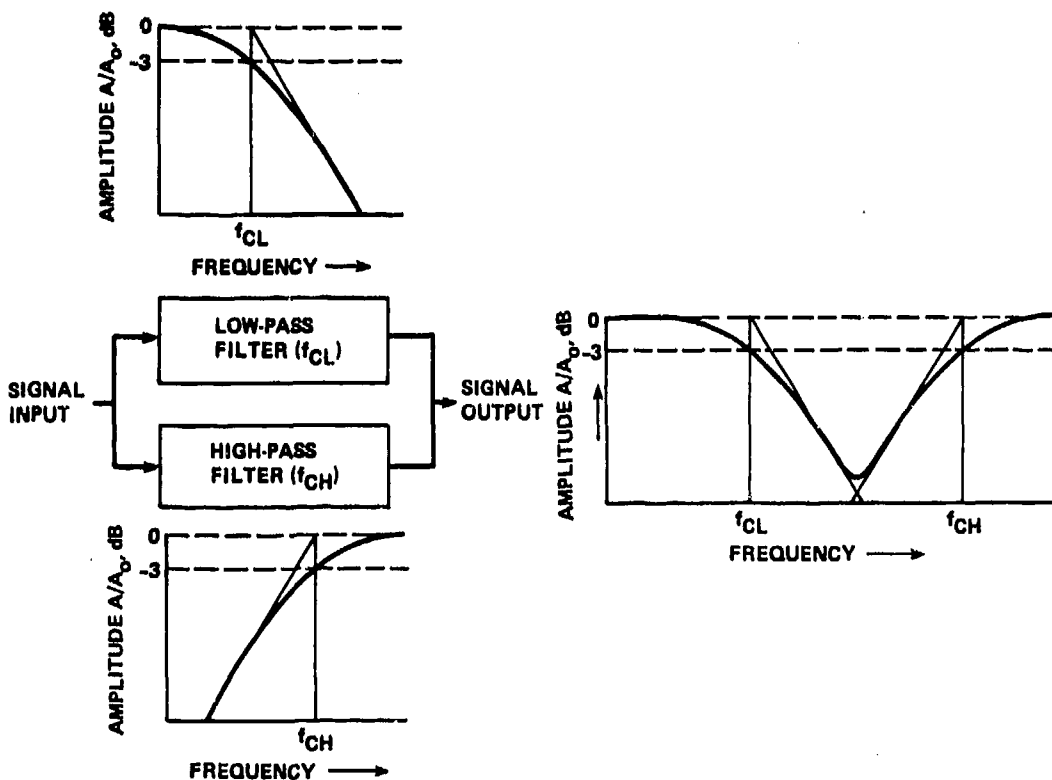


Figure 29. Broadband band-reject filter amplitude response

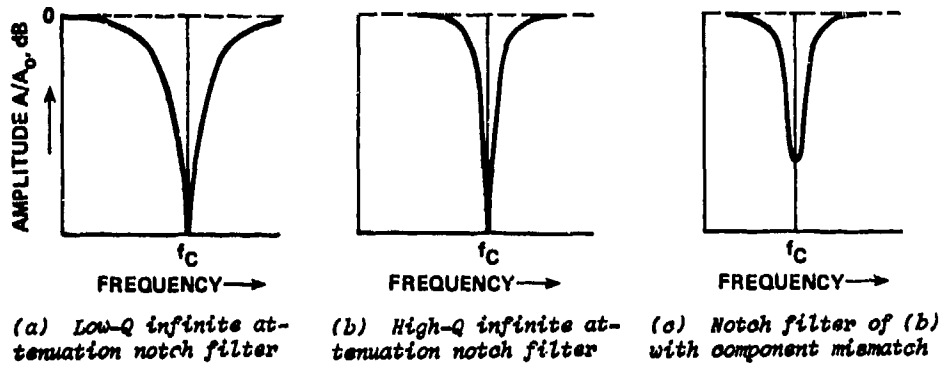


Figure 30. Notch filter amplitude response

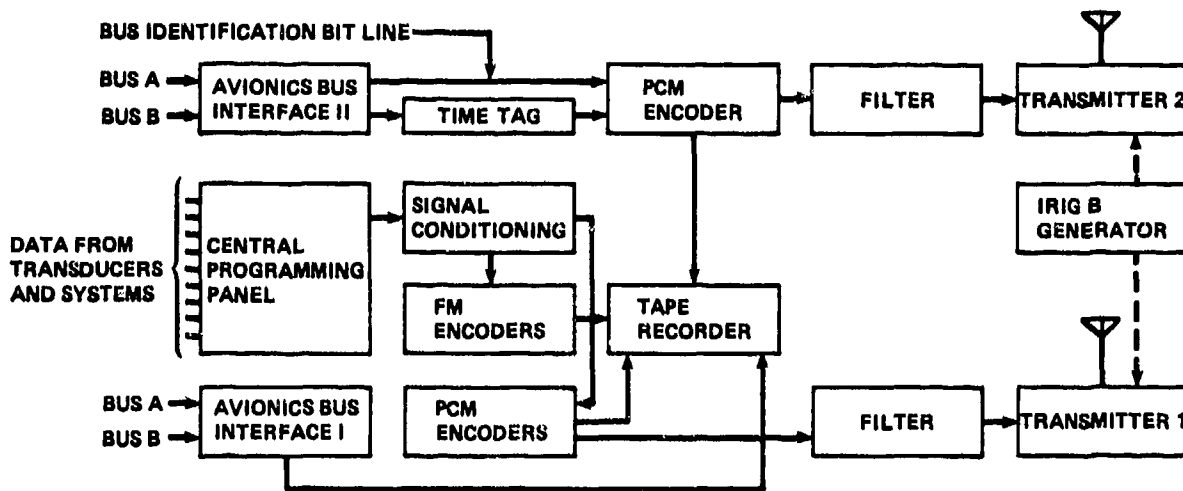


Figure 31. Block diagram showing avionics interface buses

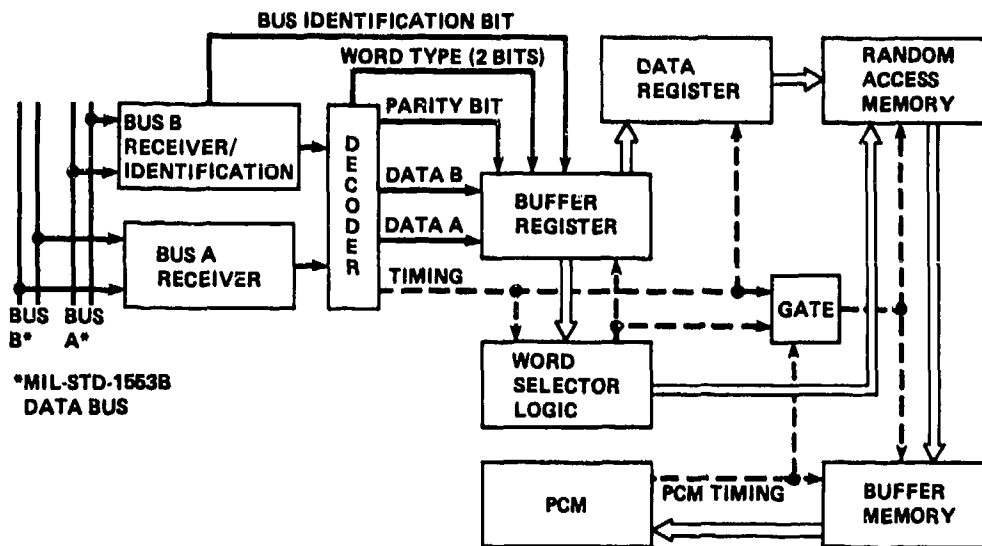


Figure 32. Avionics bus interface II block diagram

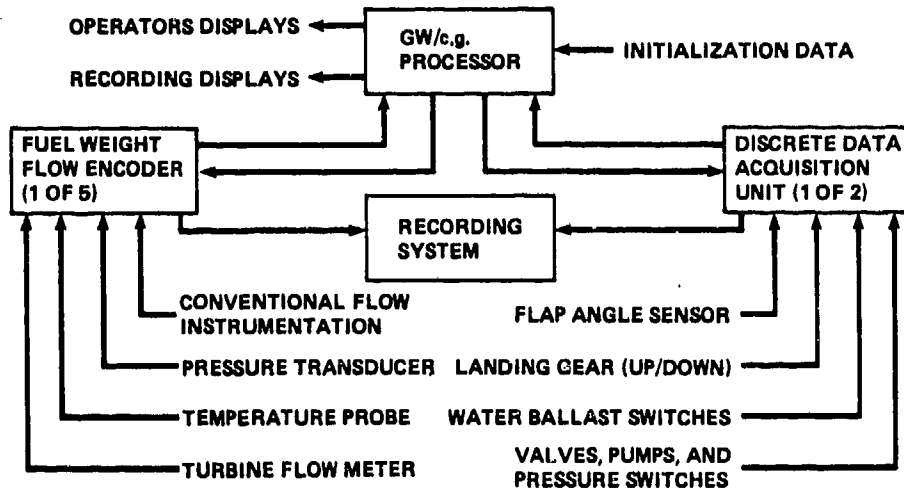


Figure 33. A flight-test real-time GW/o.g. computing system

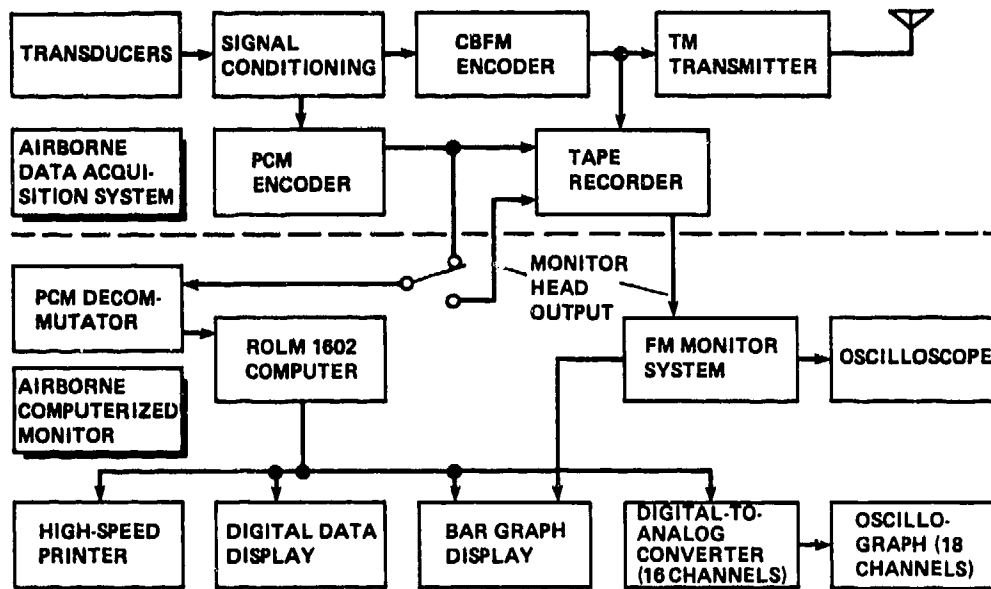


Figure 34. Airborne computerized data-acquisition system

4. SIGNAL CONDITIONING OPTIMIZED FOR SPECIFIC TRANSDUCTION TECHNIQUES

The purpose of this section is to acquaint the engineer with signal-conditioning techniques that are optimized for use with popular transduction techniques. Most of the signal-conditioning techniques discussed here are general in that they can be applied to other appropriate types of transducers. Transduction principles are discussed only to the extent required to make the selection of the signal-conditioning technique understandable. No attempt has been made to list all the possible transduction principles. Reference 18 lists 392 "laws" and "effects" which can be used as the basis for transduction techniques; however only a few are used in current instrumentation practice. The transduction techniques addressed in this section cover only the most popular transducers used for airborne flight-test purposes.

Self-generating and non-self-generating transducers form the basis for dividing the signal-conditioning discussions in this section. A further division of signal conditioning uses the associated transduction principle. In many cases, more than one type of signal-conditioning technique is discussed for the same transduction principle. When more than one example of signal-conditioning technique is discussed for a single transduction principle, the rationale for the technique selection is presented.

4.1 SELF-GENERATING TRANSDUCER SIGNAL CONDITIONING

The self-generating transducer uses energy from the measurand itself to produce output energy and thus does not require an external power source. Examples of self-generating transducers include the Seebeck effect transducers (heat energy produces voltage output), the piezoelectric effect transducers (strain generates an electrical charge output), and the photovoltaic-cell (incident light photons produce a current output). Any transducer in which the measurand-input energy causes an impedance change will require a supplementary power source and thus is a non-self-generating transducer (addressed later in this section). Some confusion can result when two transducer elements are combined. For example, the Bourdon-tube-type transducer produces a mechanical motion which can drive a pilot's instrument and is a self-generating transducer. Quite often, a Bourdon tube will be used to drive a potentiometer, and the potentiometer is a non-self-generating transducer which requires an external power source to produce a usable output.

4.1.1 Piezoelectric Transducer Signal Conditioning

Signal conditioning for piezoelectric transducers is from one of three major categories: (1) remote high-impedance voltage amplifier; (2) remote charge amplifier; or (3) internal amplifier. These types of transducers and their signal conditioning are covered in Ref. 19.

Piezoelectric-effect transducer. - Certain crystalline materials (quartz, tourmaline, Rochelle salt, and lithium sulfate) and certain specially polarized ceramics (barium titanate) when deformed generate an electrical charge within the material. This is a reversible effect: when a charge is generated in the material a deformation is likewise produced. This is called the piezoelectric effect. Transducers that use the piezoelectric effect are commonly used to measure dynamic acceleration, mechanical force, and pressure. These transducers have a basic limitation in that they cannot be used to measure a true static input.

Piezoelectric transducers are popular for many reasons: they are compact, operate over a wide range of temperatures (-260°C to 700°C), have a wide frequency response, and are economical.

The piezoelectric materials used for these transducers are very good insulators, and when two plate-type electrodes are placed on the appropriate opposing faces of the material a capacitor is formed. When an electrical charge is generated between the electrodes of the capacitor a voltage is created according to

$$e_0 = Q/C \quad (22)$$

where e_0 = transducer open-circuit voltage, Q = transducer generated charge, and C = transducer capacitance.

When a deformation is produced along the sensitive axis of the crystal and then held constant, the electrical charge that has been generated is dissipated through leakage resistance paths both internal and external to the crystal. This characteristic limits the transducer low-frequency response; it will be discussed under each type of signal conditioner.

The typical piezoelectric transducer element is essentially undamped, the result of the mechanical characteristics of the piezoelectric materials. These materials are very stiff, and only minute deflections are required to produce a usable output voltage. These small deflections make damping the transduction element very difficult by such standard techniques as immersing the transduction element in a high viscosity fluid. Any significant input near the transducer resonant frequency f_n can cause transducer failure through resonance-related overstrain. As can be seen in Fig. 35, the frequency response of such a transducer becomes very nonlinear as the natural frequency of the transducer is approached.

Manufacturers usually specify that transducers should only be used to measure frequencies that are limited to some fraction of the transducer natural resonant frequency. For example, a 0.2 f_n frequency limitation will cause a maximum amplitude response change A/A_0 of 4%. The relative amplitude response

A/A_0 , expressed as a function of the transducer natural resonant frequency f_n , the forcing frequency f , and the damping factor d is

$$A/A_0 = 1/\sqrt{[1-(f/f_n)^2]^2 + 2d(f/f_n)^2} \quad (23)$$

where A_0 is the amplitude of the output when the transducer is driven by a sinusoidal measurand of a constant peak-to-peak amplitude at a frequency f_0 that is very much lower than the transducer natural frequency f_n . Since most piezoelectric devices are essentially undamped ($d = 0$), the relative amplitude response can be represented by

$$A/A_0 = |1/[1-(f/f_n)^2]| \quad (24)$$

Equation (24) is shown graphically in Fig. 35.

The amplitude error caused by the resonant peaking is approximately 1% at $0.1f_n$, 4% at $0.2f_n$, 10% at $0.3f_n$, and 19% at $0.4f_n$; it approaches infinity at f_n . Transducer manufacturers often promote the fact that in such an undamped device the phase shift is essentially zero out to the maximum frequency for which the transducer is to be used (for example, $0.2f_n$) as an advantage. The value $0.2f_n$ is often chosen since it limits the resonant preemphasis to 4%. For piezoelectric accelerometers on a laboratory sinusoidal vibration table, the near-zero phase shift and only 4% amplitude error at $0.2f_n$ may seem desirable, but on an aircraft, this limitation is unrealistic, because the maximum driving frequency cannot be controlled. Explosive squibs, which are sometimes used for flutter excitation, may well introduce frequencies up to f_n at which the transducer can be damaged. It is difficult to use pre-transduction filtering because any such filtering device modifies the structural resonance characteristics of the system. If frequencies exist above $0.2f_n$ and pre-transduction filtering is undesirable, a post-transduction filter is often required. This post-transduction filter introduces significant amounts of attenuation above $0.2f_n$ to keep such higher frequencies from obscuring the data; it also adds large phase shifts into the system and provides no physical protection for the transducer itself.

Remote high-impedance voltage amplifier. — The remote high-impedance voltage amplifier was the signal conditioner used originally with piezoelectric transducers. Today, it has been largely supplanted by the remote-charge amplifier and the transducer with an internal amplifier, although the remote high-impedance voltage amplifier is still used in some applications. Even though the piezoelectric transducer is a true charge generator, a voltage amplifier is an appropriate signal-conditioning amplifier under certain conditions. Equation (22) shows the relationship between the electrical charge generated by the transducer and the voltage produced across the transducer capacitance. In a remote voltage-amplifier application, other circuit parameters, as shown in Fig. 36, must be considered. The voltage available to the amplifier at mid-frequencies is

$$e_0 = Q/(C_T + C_A + C_C) \quad (25)$$

The major drawback to using the remote voltage amplifier as a piezoelectric transducer signal conditioner is that the system gain is a function of the total distributed capacitances. The capacitance of the transducer, the voltage amplifier, and the connecting cable (usually a coaxial cable) must all be calibrated as a unit to achieve acceptable accuracy. In airborne applications where long cable runs are usually laced together with other wiring and passed through many vehicle structural members, a calibration of this cable is either very difficult or unfeasible. Furthermore, since these cables are usually passed through the structure in the wire bundles and then terminated at the signal conditioning, the original cable assembly may never have been available as a unit, thus making even the initial calibration difficult. Another disadvantage is that temperature-related changes in leakage resistance cause the low-frequency response of this signal conditioning to vary drastically, particularly when the transducer is subjected to large temperature variations at engine-test locations. An advantage of the remote voltage amplifier over the charge amplifier is its quick recovery from transient overloads.

Equation (25) illustrates that the voltage available to the amplifier, e_0 , is a function of the system-distributed capacitance. For example, when a piezoelectric transducer with a capacitance of 300 pF is connected by 10 ft of 30-pF/ft coaxial cable to a voltage amplifier with an input capacitance of 3 pF, the voltage available to the amplifier is

$$e_0 = \frac{Q}{C_T + C_C + C_A} = \frac{Q}{300 + 300 + 3} = Q/603 \quad (26)$$

This represents less than one-half the voltage output of the transducer itself, as shown by

$$e_0 = Q/C_T = Q/300 \quad (27)$$

At frequencies below the transducer mid-frequency, the voltage available to the amplifier is limited by an equivalent high-pass filter whose -3-dB point occurs at the frequency shown by

$$f_{CL} = \frac{1}{2\pi R_0 C_0} \quad (28)$$

where R_0 and C_0 are defined in Fig. 36. In addition, the transducer has a resonant response as previously described in Eq. (24) and illustrated in Fig. 35. The combined high-pass-filter effect and the transducer resonance are shown in Fig. 37.

To maintain the low-frequency cutoff as low as is possible, both the cable leakage and amplifier input resistance should be much larger than the transducer leakage resistance. At room temperature, the transducer leakage resistance R_{TL} can be very high; for instance, the Endevco Model 2252 quartz accelerometer is specified as having a minimum R_{TL} of 20,000 M Ω minimum at 24°C, and a capacitance of 100 pF. This transducer, without any added external capacitances or resistive loads, has a cutoff frequency f_{CL} of

$$f_{CL} = 1/(2\pi C_T R_{TL}) = 0.08 \text{ Hz} \quad (29)$$

In normal use, the coaxial cable leakage R_{CL} is maintained very high by using the highest quality dielectrics in the cable construction. For normal ambient cable temperatures, high-quality polyethylene is popular with virgin Teflon being used for higher temperatures. For very high ambient cable temperatures, many less desirable dielectrics are used. For long cable lengths or high cable ambient temperatures or both, the cable leakage R_{CL} is often the limiting factor in determining low-frequency response.

Fortunately, with the advent of the field-effect transistor (FET), the amplifier input impedance can be suitably high (see Voltage Amplifier in Sec. 3. and Appendix C). The FET instrumentation amplifier has typically $10^9\text{-}\Omega$ differential input impedance and $10^{10}\text{-}\Omega$ common-mode input impedance. The input capacitances are also relatively small (2 pF differential and 3 pF common mode). Although $10^9 \Omega$ is not large when compared to the 20,000-M Ω ($2 \times 10^{10}\text{-}\Omega$) impedance of the quartz accelerometer mentioned earlier, it is more than adequate for most applications. Certain FET amplifiers are available that have input impedances as high as $10^{13} \Omega$.

The transducer low-frequency cutoff is strongly affected by the temperature dependence of the leakage resistance. To illustrate this effect, an actual high-temperature piezoelectric accelerometer will be analyzed, one that has a leakage resistance of 100 M Ω at 24°C, 25 M Ω at 260°C, and 10 M Ω at 400°C. The nominal transducer capacitance is 100 pF at 24°C. The mounted natural resonant frequency f_n is 30,000 Hz; therefore, the highest recommended drive frequency is 6,000 Hz ($0.2 f_n$). Figure 38 illustrates some typical frequency-response curves for this transducer with no additional shunt elements. The -3-dB knee frequency was determined by using Eq. (28).

At a total shunt resistance R_0 of 100 M Ω , f_{CL} is 16 Hz; for R_0 of 25 M Ω , f_{CL} is 64 Hz, and for R_0 of 10 M Ω , f_{CL} is 160 Hz. It must be noted that -3 dB is equivalent to a voltage attenuation of 30%. As can be seen from the last example, increases in leakages can considerably reduce available bandwidths when using the remote voltage amplifier. This increased leakage can be caused by high cable temperature, contaminated connectors, or numerous other leakage paths, and the results can be very detrimental to system performance. When working with impedances in the range of 10^9 to $10^{13} \Omega$, it must be realized that almost any oversight can completely destroy this level of insulation. In particular, the connectors are susceptible to contamination and moisture-related leakage. In many flight-test situations, it is difficult to prevent moisture and other contaminants from reaching high-impedance cable connectors. In these cases, the connectors should be the so-called hermetically sealed connectors, but even then additional protection may be required.

The charge sensitivity of the transducer, that is, the charge output per unit measurand input, is temperature-sensitive. A typical plot of the variation of the charge sensitivity versus temperature is shown in Fig. 39. The solid line in Fig. 39 represents the nominal change in charge sensitivity versus temperature, and the dashed lines show the voltage-sensitivity change versus temperature (with the indicated external capacitors). For voltage-amplifier signal conditioning, external capacitance can often be used, as illustrated in Fig. 39, to compensate for the temperature-related change in charge sensitivity; however, if this means adding capacitance to the external circuit to produce the optimization, the additional capacitance also reduces the voltage output and thus decreases the system signal-to-noise ratio. The selection of the coaxial cable is particularly important for the remote voltage-amplifier application to maintain negligible leakage resistance.

A low-noise coaxial cable must often be used for transducer connection. In a vibration environment (which is the standard aircraft environment) even these low-noise coaxial cables can generate significant amounts of noise if the cable movement is not suitably restrained. These noise voltages are generated by several mechanisms: (1) the motion of a conductor in a magnetic field generates noise voltages; (2) the cable movement also produces small changes in the internal capacitance and capacitance changes in relation to other objects (since the charge on these capacitances cannot be changed instantly a noise voltage results); and (3) the movement of the shield over the insulation material generates a charge that is sensed as noise voltage. These problems should emphasize the necessity of restraining the cable motion and using a high-quality, low-noise coaxial cable. Some piezoelectric accelerometer manufacturers test all cable sold for use with their transducers for its low-noise performance. They do this, in addition to buying premium grade low-noise coaxial cable, because their experience has shown that this precaution is necessary.

In summary, the remote voltage amplifier can be used with piezoelectric transducers when the constraints already discussed are acceptable. When extreme input overdriving is expected, the quick recovery time of the voltage amplifier makes it a desirable alternative.

Remote charge-amplifier. — The charge amplifier (in practice, a charge-to-voltage converting amplifier) is the most popular signal conditioner for piezoelectric transducers. The advantages include a well-defined system gain and low-frequency response. The main disadvantage is that subtle application restrictions exist which, if ignored, can produce substantial system errors. When the limitations of the charge amplifier are taken into consideration, the charge amplifier is the most desirable signal conditioner for piezoelectric transducers.

A charge amplifier as discussed in this text is an operational amplifier (see Appendixes A and F) that uses a feedback capacitor to produce an integrator module (Fig. 40). The amplifier output e_o is the integral of the input current, that is,

$$Q = \int i dt \quad (30)$$

and therefore the amplifier voltage output is proportional to the charge input.

One main advantage of this circuit is that the output voltage is only a function of the value of the feedback capacitor C_f and of the charge input Q . This contrasts sharply with the same application using a voltage amplifier where the output voltage is a function of all of the input capacitances.

The low-frequency response of the charge amplifier is limited to the cutoff frequency, which is given by

$$f_{CL} = 1/(2\pi R_f C_f) \quad (31)$$

As Eq. (31) shows, the cutoff frequency is dependent only on the resistive and capacitive feedback circuit components. This is very desirable, since unlike the voltage amplifier, the low-frequency response is not dependent on the highly variable leakage resistances. The leakage resistances in voltage amplifier circuits change by many orders of magnitude in high-temperature or contaminated environments. The shunt feedback resistor R_f is required to provide a path for amplifier input bias currents and pyroelectrically generated charges, which cause amplifier drift and saturation.

Grounding considerations are very important in rejecting electrical noise inputs resulting from ground loops. In many piezoelectric transducers, particularly accelerometers, one side of the transduction element is often made common to the transducer case. When this type of transducer must be mounted directly to the vehicle structure, a differential type of charge amplifier should be used to avoid a ground loop and the resulting electrical noise inputs. A simple way of avoiding the more complex differential charge amplifier is to electrically isolate the piezoelectric transducer from the vehicle structure and to ground the system at the charge amplifier. As shown in Fig. 41, ground-loop noise is still coupled into the system through the case-to-ground capacitance (and other stray capacitances), but this technique is acceptable for most situations. Note that using a vibrational accelerometer with an insulated stud can reduce the accelerometer resonant frequency by as much as 30% (see Ref. 19).

Transducers are available with transduction elements that are isolated and shielded from the case for applications in which ground-loop noise is severe. These units, used with triaxial cable and differential charge amplifiers which can drive the guard shield, have outstanding noise-voltage rejection capabilities (see Ref. 20).

As explained in Appendix F, the charge-amplifier noise gain A_N and stability are functions of external capacitance and leakage resistance. For example, the amplifier noise gain A_N above the low-frequency cutoff is approximated by

$$A_N = (C_s + C_f)/C_f \quad (32)$$

where

- A_N = amplifier noise gain
- C_s = total amplifier shunt capacitance
- C_f = feedback capacitance

Therefore, the amplifier external shunt capacitance should not be allowed to increase indiscriminately. Also, as the amplifier external shunt resistance (leakage resistance) decreases, the low-frequency noise gain increases (see Appendix F), and, if the external resistance continues to decrease, the reduced impedance will eventually cause the charge amplifier to become unstable. Charge amplifiers are available that will remain stable with input impedance as low as 1 k Ω , however, this condition should be avoided, since low-frequency noise amplification is greatly increased with low input impedance.

The charge amplifier is a very desirable remote signal conditioner for piezoelectric transducers, having some very useful characteristics and very few restrictions. When its limitations are understood and respected, it is the best remote signal-conditioning technique for piezoelectric transducers.

Internal signal conditioning. — The development of integrated-circuit technology has made it possible to produce very complicated circuits that require very little space. As small as the average piezoelectric transducer is, the inclusion of a signal-conditioning amplifier inside the transducer increases the total size (and weight) very little. A major advantage of such an integrated unit is that it has a low-impedance output which can readily be matched to the next link in the data-acquisition process. This type of system is often smaller and less expensive than a separate transducer and a remote signal-conditioning amplifier. Cable requirements are also much less stringent. A major disadvantage is

that the internal electronics impose strict environmental temperature limits on the transducer (the high temperature extreme is usually limited to no more than 120°C). Scaling the amplifier output voltage is also more difficult with internal signal conditioning.

The signal-conditioning circuit inside the transducer case is one of three types: (1) voltage amplifier, (2) charge amplifier (charge-to-voltage converter amplifier), or (3) impedance converter. (One company markets a charge amplifier that is a charge-to-current converter amplifier, an advantage when driving long lines.) The close coupling of an internal voltage amplifier minimizes the distributed capacitance of the system. Now that the gain is independent of the distributed capacitance, the fast recovery time of the voltage amplifier is an advantage. Since the maximum temperature is restricted, the temperature sensitivity of the low-frequency cutoff f_{CL} is normally not a factor. An internal-charge amplifier offers no particular advantage (or disadvantage) as an internal signal conditioner, except that many piezoelectric materials have linearized charge-sensitivity-versus-temperature curves for use with charge amplifiers.

The impedance converter (a voltage amplifier with a gain of 1) is attractive because of its basic simplicity; it is used as the illustrative example in this section. Figure 42 shows a transducer coupled to an internal, metal-oxide-semiconductor field-effect transistor (MOSFET) amplifier T_1 , a shunt resistor, and an optional capacitor (see Ref. 21).

The input requirements on the MOSFET amplifier are the same as those discussed earlier in this section (Remote High-Impedance Voltage Amplifier), since the MOSFET amplifier is operated in a source-follower mode, that is, as a voltage amplifier with a gain of 1. A current-limiter, a decoupling capacitor C , and a well-regulated voltage supply E_B , make up the remote power supply for the amplifier. The current-regulating diode is used to power the P-channel MOSFET since the high dynamic resistance of the diode yields a source-follower gain which is very close to unity. This circuit has the advantages of simplicity, two-wire input, and low output impedance (less than 100 Ω). A disadvantage is that the decoupling capacitor C is usually quite large (for example, 10 μF), and when the system is first turned on, it must be charged by the current-regulating diode. This charging time can be as long as 1 min and requires that the instrumentation system be turned on well before data are to be acquired. A system of this type cannot be turned "on" and "off" without time being allowed for capacitor charging. The internal shunt resistance R_S is usually required to prevent drifts resulting from charge buildup at low frequencies from such sources as pyroelectric effects (electrical charge generated as a result of temperature changes and gradients). The shunt capacitor C_S can be increased to reduce the sensitivity (see Eq. (25)), or can be used to reduce the voltage sensitivity change with temperature (see Fig. 39).

Piezoelectric transducers with internal signal conditioning are very desirable when the temperature limitations are compatible with the application environment. They are easy to calibrate, easy to match to the subsequent stages, and are usually more economical than separate transducers and signal-conditioning units.

4.1.2 Thermocouple Transducer Signal Conditioning

Seebeck-effect transducers, or as they are more commonly called, thermocouple transducers, are the most often used sensor for acquiring in-flight temperature data. With proper selection of materials, thermocouples can be used to measure almost any temperature from very high (1,650°C) to very low (-185°C). In addition to being small, thermocouples are readily available, inexpensive, reliable, and accurate. Their disadvantages include low-voltage output (typically below 80 mV and often less than 30 mV) and an apparent simplicity which can lead even the experienced engineer into designing systems with significant inherent errors.

A thermocouple transducer is no more than two thermoelectrically dissimilar materials joined together at one end. Traditional thermocouple signal conditioning includes lead wires, junction temperature references (such as ice baths, reference ovens, and zone boxes), junction compensators, and various types of voltage amplifiers. Since signal levels are so small, almost every portion of the circuit is a potential source of significant error. Appendix J provides an analytical technique that is useful for analyzing complex thermocouple circuits; called the pattern-circuit technique, it will be used in the appendixes to evaluate some of the most commonly encountered airborne circuit problems. The engineer will then be able to employ the technique to analyze specific problems that are not covered.

Ordinarily, it is not necessary to understand the transduction principle in order to design a signal-conditioning system; however, this is not the case with thermocouple transducers. Such knowledge is required when thermocouple transducers are used because inside all thermocouple signal-conditioning systems there is at least one and in most cases several thermocouple junctions. Appendixes J-O present a practical technique for analyzing any thermocouple signal-conditioning circuit problem and provide examples of using this technique to analyze the most common flight-test thermocouple signal-conditioning situations. In general, only the results of the detailed analysis in the appendixes will be reported in this discussion.

Thermocouple transducer. — The Seebeck effect is the sum of the Thompson and Peltier effects, (Ref. 22). Thermocouple theory is discussed in this text only to the extent necessary for an intelligent analysis of the errors introduced by the signal-condition circuits. For simplicity, each individual type of conductor is considered to be homogeneous everywhere along its length. Inhomogeneities will be discussed where appropriate and in a subsequent subsection (Error Voltage).

According to the Thompson effect, an internal voltage is generated if a temperature gradient exists between the two ends of the same (homogeneous) conductor. This voltage can be expressed as

$$e_T = \int_{T_1}^{T_2} \sigma dT \quad (33)$$

where

$$\begin{aligned} e_T &= \text{Thompson voltage} \\ \sigma &= \text{Thompson coefficient} \\ T_1, T_2 &= \text{wire end temperatures} \end{aligned}$$

It should be noted that when this single conductor is made into a closed loop there is no net voltage regardless of the temperature gradients introduced around the loop, because when the ends are joined, T_1 equals T_2 .

An additional source of voltage called the Peltier electromotive force is generated at the junction where two thermoelectrically dissimilar conductors are joined together. The Peltier voltage depends only on the two metals and on the temperature of the intervening junction. For two conductors A and B, whose junction is at a temperature T , the Peltier voltage, e_p , can be represented as

$$e_p = T \Pi_{AB} \quad (34)$$

where Π_{AB} is the Peltier coefficient of materials A and B at the junction temperature T .

When two conductors, A and B, are joined at both ends, as shown in Fig. 43, the net voltage e_{AB} around the loop is expressed as the sum of the Thompson and Peltier voltages:

$$e_{AB} = T_1 \Pi_{AB} + \int_{T_1}^{T_2} \sigma_A dT + T_2 \Pi_{AB} + \int_{T_2}^{T_1} \sigma_B dT \quad (35)$$

$$e_{AB} = \int_{T_1}^{T_2} [(T_1 \Pi_{AB} + \sigma_A) - (T_2 \Pi_{AB} + \sigma_B)] dT \quad (36)$$

Basic thermocouple circuit. — Two unbroken lengths of wire (A and B), joined at both ends and subjected to a temperature difference form a simple thermocouple circuit. This circuit is shown in Fig. 43. A current will flow in such a circuit as a function of the generated voltage and the circuit internal resistance. The voltage generated by the thermocouple circuit is a function of the temperature difference between the two ends of the loop and the thermoelectric characteristics of the two wires. A current-measuring instrument, such as a galvanometer, could be used to determine the temperature; however, since the Seebeck effect generates a voltage, the current measurement must be calibrated for circuit resistance.

Thermocouple pattern circuit. — The pattern-circuit technique for analyzing complex thermocouple circuits is the best one known to the author for thermocouple circuit analysis. It was devised by Dr. Robert J. Moffat, chairman of the Thermosciences Division and professor of mechanical engineering at Stanford University, Stanford, California. Dr. Moffat's technique was first described in Ref. 23 and later in Ref. 24. The following discussion draws extensively on Dr. Moffat's work, and his technique is used in the appendixes to analyze various flight-test signal-conditioning techniques.

A thermocouple circuit is shown in Fig. 44a, where the thermocouple circuit is the same as that of Fig. 43 except that the junction at T_1 has been opened and is now maintained at a known reference temperature, T_R . Temperature T_2 is the temperature to be determined by the thermocouple, which is made up of the two thermoelectrically dissimilar metals A and B. The voltage e_0 at the open junction is the Seebeck voltage. The circuit of Fig. 44b is called the pattern circuit and is used to represent the "ideal" thermocouple circuit.

The instrument used in Fig. 44a is a null-balance millivoltmeter. When the null-balance millivoltmeter output voltage exactly counters the Seebeck voltage, no current flows in the thermocouple circuit. The circuit can now be represented by Fig. 44b, the pattern circuit (described in Appendix J). When a complex thermocouple circuit is made equivalent to the pattern circuit, the calibration tables provided for the thermocouple materials may be used to establish the overall circuit calibration.

Thermocouple wires often have high resistivity and usually have resistivity that is a strong function of temperature. Thus, when these wires pass through areas of unknown ambient temperatures, the wire resistance is unknown. Therefore, even when a small current flows in the thermocouple circuit, voltage drops can be generated which produce appreciable errors when measuring the small Seebeck output voltage. Since the circuit of Fig. 44 is a null-balance circuit, no current flows when a measurement is being made and circuit resistance does not affect the measurement.

In most applications, the input impedance of voltage-measuring systems is so high that no measurable errors are introduced by the current that does flow. However, this is not always true, particularly if the thermocouples are being used with a galvanometric recorder. In all the following discussions, except for the section on galvanometric applications, it will be assumed that there is only insignificant current flow in the thermocouple wires.

In Fig. 44c, the null-balance millivoltmeter is shown in an isothermal temperature environment, T_R . In few laboratory and in no airborne applications is this a realistic situation. The environment of the airborne temperature-measuring instrument is far from stable, and a stable isothermal thermocouple reference temperature is therefore required. A reference temperature for thermocouples can be provided in many ways, some of the most popular of which will be discussed in latter sections.

Converting output voltage to temperature. — To derive the temperature difference in a thermocouple circuit, an algorithm is required which relates the voltage output e_0 of Fig. 44b to the temperatures T_2 and T_R . For accurate conversion of voltage to temperature, thermocouple users have traditionally used reference tables such as that shown in Table 1. In the United States, the National Bureau of Standards (NBS) publishes reference tables for many popular combinations of thermocouple materials (Ref. 25). Manufacturers produce thermocouple materials that are guaranteed to conform to NBS tables or manufacturer tables within certain tolerances. An example of a reference table used in manufacturer literature for a Type J (iron/Constantan) thermocouple is shown in Table 1. For example, to find the thermoelectric voltage at a temperature of 340°C, read down the first column to 300°C, then across to the column headed 40°C; the voltage is seen to be 18.537 mV. The manufacturer tolerances for the standard thermocouple have been included with this same table. Note that the table accuracy far exceeds the specified tolerances.

TABLE 1. — TYPE J THERMOCOUPLE (IRON/CONSTANTAN)^a

Temp. °C	Thermoelectric voltage, ^b mV					
	0	20	40	60	80	100
-200	-7.890	-8.096				
-100	-4.632	-0.995	-6.159	-6.821	-7.402	-7.890
(-10)	0.000	-0.995	-1.960	-2.892	-3.785	-4.632
(+10)	0.000	1.019	2.058	3.115	4.186	5.268
100	5.268	6.359	7.457	8.560	9.667	10.777
200	10.777	11.887	12.998	14.108	15.217	16.325
300	16.325	17.432	18.537	19.640	20.743	21.846
400	21.846	22.949	24.054	25.161	26.272	27.388
500	27.388	28.511	29.642	30.782	31.933	33.096
600	33.096	34.273	35.464	36.671	37.893	39.130
700	39.130	40.382	41.647	42.922		

^aStandard thermocouple tolerances: $\pm 2.22^\circ\text{C}$, 0°C to 427°C ; $\pm 0.5\%$, 428°C to 760°C .

^bBased on 1968 International Practical Temperature Scale, reference junction at 0°C .

When the conversion process is being performed by computer data-reduction techniques, storing extensive tables is not usually desirable because of the extensive time required to generate and set up the tables. Various groups have described these tables with power series polynomials which are more compatible with computer operations. Power series polynomials are derived in Ref. 25 for all the standard types of thermocouples (Types E, J, K, S, and T). Table 2 explains these thermocouple letter designations. Reference 26 contains polynomials that characterize a Type J (iron vs Constantan) thermocouple within $\pm 0.1^\circ\text{C}$ over a conversion range of 0°C to 760°C using a fifth order polynomial. In this same

TABLE 2. — THERMOCOUPLE TYPE DESCRIPTIONS
(from Ref. 25)

Type designations ^a	Temperature range, ^b °C
E	- 270 to 1,000
J	- 210 to 1,200
K	- 270 to 1,372
S	- 50 to 1,767
T	- 270 to 400
Single-leg material	
.... N:	Negative wire in a combination
.... P:	Positive wire in a combination
EN or TN:	Nominally 55% Cu, 45% Ni; often referred to as an Adam's Constantan. (Tradenames: Cupron, Advance, Thermo Kanthal JN)
EP or KP:	Nominally 90% Ni, 10% Cr (Tradenames: Chromel, Tophel, T-1, Thermo Kanthal KP)
JN:	A copper-nickel alloy similar to, but not always interchangeable with, EN and TN; often referred to as SAMA Constantan
JP:	Nominally 99.5% Fe (Tradename: Thermo Kanthal JP)
KN:	Nominally 95% Ni, 2% Al, 2% Mn, 1% Si (Tradenames: Alumel, Nial, T-2, Thermo Kanthal KN)
SP:	90% platinum and 10% rhodium by weight
TP:	Copper, usually electrolytic tough pitch

^aThe letter designations used in this section follow the recommendations of Committee E-20 of the American Society for Testing and Materials.

^bSee Ref. 25 for specific limitations and restrictions on these temperature ranges.

reference, the platinum/13% rhodium versus platinum thermocouple is characterized to within $\pm 0.5\%$ of the NBS values over the conversion range of 0°C to $1,750^{\circ}\text{C}$ with a ninth order polynomial. The graphic presentation of standard thermocouple pairs is very useful in system design studies. The curves in Fig. 45 show the output and temperature range of various thermocouple wire pairs.

For analysis of nonstandard thermocouple wire pairs, the curves of Fig. 46 and the table from which they are derived can be very useful. In this figure, individual thermocouple-grade wires have been calibrated against platinum. When two wires have been calibrated against platinum, the output can be obtained by algebraically summing the outputs of both wires at each temperature. The pattern-circuit technique for analyzing complex thermocouple circuits in Appendices J-M and O also uses a linearized form of the curves shown in Fig. 46. From any one of the above type representations of thermocouple outputs, the engineer can determine the output of a given circuit.

Extension wire. — When the thermocouple junction is in an area remote from its signal-conditioning equipment, special extension wires are often used to reduce costs. These cost savings can be very significant if expensive thermocouple wires, such as platinum or tungsten, are being used. The use of thermocouple extension wire causes a slight sacrifice in accuracy and a reduction of the usable temperature range compared with the original thermocouple wire. Thermocouple extension wires are alloys that are thermoelectrically similar to the thermocouple wire over a limited temperature range. For base-metal thermocouples, the extension wires may be the same alloys prepared to less exacting standards. In all situations using extension wire, the manufacturer's recommendations should be rigorously followed.

Reference temperature. — In the previous discussions on thermocouples, the existence of a reference temperature has conveniently been assumed. In actual practice, the establishment of this reference temperature is a critical part of the thermocouple flight-test signal-conditioning task. Almost all tables and equations are formulated based on an ice-bath reference, that is, a reference temperature of 0°C (32°F); however, ice-bath references are not often used in actual flight-test work. If the reference temperature T_R is some temperature other than 0°C , a new table can be generated from the table specified for 0°C . This is accomplished by determining the voltage output e_R at T_R from the ice-bath reference table. This voltage, e_R , is then algebraically subtracted from all the tabulated values in the ice-bath tables. The resultant table is now based on the new reference temperature, T_R . Polynomial equations are even easier to adjust, since the voltage e_R is simply subtracted algebraically from the polynomial.

Ice-bath reference. — The ice bath is one of the most precise temperature references, being far more accurate than is usually necessary for thermocouple temperature measurements in flight-test aircraft. Usually, an ice bath made from water of potable quality will provide a reference temperature which is within a few hundredths of a degree of 0°C . The disadvantages include the time-consuming preparation of the ice bath, which must be made up before each flight, the reference temperature is held only as long as the ice lasts; the reference is available only in one temperature; and the bath is somewhat fragile.

An ice bath suitable for flight test is simple to construct. Distilled, de-ionized, or a good-quality drinking water should be used for the ice and water solution. A Dewar flask (about 0.5 liter or larger) is filled with ice crushed to a diameter of 0.5 to 1.5 cm, and the ice is covered with water. A cork stopper can be used to close the flask. Through the cork should pass two thin-wall tubes (roughly 0.5 cm in diameter sealed as shown in Fig. 47) to an immersed depth of two-thirds the depth of the Dewar flask. About 0.5 cm of mercury is placed in the bottom of both tubes. One of the thermocouple wires and a copper wire are immersed in the mercury in one tube, and the other thermocouple wire and a copper wire are immersed in the other tube (Fig. 47). The mercury and wires are sealed in the tube with a soft sealant (refined beeswax warmed and poured down the tube provides a satisfactory seal). The cork must be secure and the flask mechanically protected. A pattern-circuit analysis of an ice-bath reference is given in Appendix K.

Reference oven. — The reference oven uses a heating element to provide an isothermal zone of known temperature to which a thermocouple can be referenced. Reference ovens are commercially available that are designed for flight-test use. The circuit shown in Fig. 44b is also applicable to the reference oven, since T_R is now the oven temperature. Reference ovens used in flight tests are very practical as long as the heater power can be maintained and sufficient time is allocated for the oven to reach the reference temperature after the heater power is turned on. Reference ovens operate at temperatures above ambient and are not as accurate as an ice bath; however, they are suitable for almost all airborne applications.

The airborne reference-oven temperature is controlled in two ways: (1) bimetal "on-off" thermostat and (2) proportional control. The bimetal thermostatic oven control has limited accuracy and the on-off switching action can produce electrical transient signals in the low output voltages of the thermocouples; however, it is less expensive than the proportional control. The proportional control oven can be made quite accurate and, despite its complexity, can be very reliable. An electronic schematic for a proportional heater control circuit is shown in Appendix L.

A reference oven that could be used to reference many thermocouples is shown in Fig. 48. The main feature of such an oven is a well-insulated, high-thermal-conductance metallic "isothermal" bar (silver, copper, or aluminum), a heating element, and control electronics. Each thermocouple wire is joined to a copper wire in such a manner that the junction is thermally closely coupled to, and electrically isolated from, the isothermal bar. The copper wires and thermocouple wires are passed through the insulation by a circuitous route to maintain the isolation from ambient temperature.

The temperature of the isothermal bar should always be recorded on a data channel. A platinum resistive-temperature gauge is useful for this purpose. In this way, if the temperature is not as expected, the data can still be retrieved. When a computer data-reduction system is being used and

many thermocouple sensors are involved, corrective provisions for oven-temperature shifts in the initial computer software often saves much time later on.

Zone box. — The zone box is built just like a reference-oven box but without heating provisions. The zone box provides an interior isothermal zone or chamber which is allowed to drift slowly with the local ambient temperature. Zone boxes can be located in very harsh environments since they are basically simple and rugged devices. In the zone box, the temperature of the isothermal zone must be determined before the thermocouple data can be reduced. Fig. 49 illustrates a zone box in which a platinum resistance probe is used to measure the zone temperature. (Note that more than one type of thermocouple pair has been used in this design).

Reference-junction compensator. — The use of the thermocouple reference-junction compensator has become widespread because they are readily available from commercial sources and are accurate, economical, reliable, and easy to use. A compensator uses a bridge circuit to provide the equivalent of an ice-bath reference or a reference oven. A simplified schematic of such a device is shown in Fig. 50. Table 3 lists the characteristics of one commercially available unit. These and other units are made for almost all available standard thermocouple-wire combinations. Consult Appendix M for a description of the reference-junction unit.

Care must be exercised when using a reference-junction compensator to avoid thermal gradients within the compensator. Compensator design is based on the assumption that all components within the compensator are at the same temperature. For most situations, this is a valid assumption, but should a thermal transient occur during a test, a thermal gradient may be created, thereby voiding the isothermal design assumption.

TABLE 3. — SPECIFICATIONS FOR A THERMOCOUPLE JUNCTION COMPENSATOR

Reference temperature:	0°C (other references available)
Accuracy:	±0.25°C at +25°C ambient ±0.50°C from +15°C to +35°C ambient ±0.75°C from 0°C to +50°C ambient temperature
Output impedance:	Less than 250 Ω standard; other output impedances available on request
Storage temperature:	-25°C to +75°C
Operating life:	Up to 1,500 hr of continuous use; to 2 years of intermittent use
Size:	2 cm diam, 3 cm long, lead length of 30 cm

Low-impedance circuit. — The low-impedance circuit shown in Fig. 51 would seem at first glance to provide an ideal solution to thermocouple circuit problems. After transitioning to copper wire at the reference, the entire remaining circuit could be made of copper; thus, from the law of inserted materials, there should not be any error introduced into the copper portion of the circuit. Unfortunately, there is at least one connector at the galvanometric recorder, and it will have contacts which are often machined, plated, soldered, or oxide-coated. Temperature gradients at this point will still produce unwanted error voltages.

The limitations of low-impedance thermocouple circuits are illustrated in Fig. 51. Thermocouple materials A and B often have relatively high resistivity compared with that of copper wire, and in many cases this resistivity is strongly related to the wire temperature. In most flight-test aircraft, the ambient temperature in the vicinity of the wire as it passes through the aircraft structure is both unknown and highly variable. Because galvanometer displacement is directly proportional to circuit current and because the circuit current is inversely proportional to the total circuit resistance, the total circuit resistance can significantly influence the indicated temperature (galvanometer displacement). One solution is to use oscillographic recorders with very sensitive galvanometer elements that have enough excess current sensitivity so that a stable resistance can be added to the circuit. This approach reduces the fraction of the total circuit resistance that is temperature-sensitive and thereby reduces the overall circuit resistance variation. Another approach is to use thermocouple wire pairs, such as copper/Constantan, the resistivity of which is less temperature-sensitive than most other wire pairs.

Error voltage. — A major source of error voltage is inhomogeneities in the thermocouple circuit. An inhomogeneity is defined as a place where a temperature gradient along the wire produces a thermal voltage output. Connectors and switches are obvious sources of error; however, the inhomogeneity that never ceases to startle engineers is the one that appears in a single continuous run of wire. To make matters worse, even when all of the wire has been tested in the laboratory (by passing a sharp temperature gradient over the wire), the final aircraft installation may contain inhomogeneities as a result of kinking, bending, or twisting of wires when they are being installed. Type K thermocouples are particularly susceptible to developing inhomogeneities from cold working. To a lesser extent, Type J and T thermocouples show similar effects.

When thermocouples are used in very hot environments, the shunt resistance of many types of wire insulation (including refractory metal oxides such as magnesium oxide, aluminum oxide, and beryllium oxide, which are found in the modern armored cables) is low enough that the insulator becomes only a resistive connection between the two wires. Under these conditions, a series of distributed thermocouples is created along the wire and can produce significant errors in the output. A model of this situation was presented by Moffat in Ref. 24. This model is a distributed network model and not easily reducible by hand calculations.

Some thermocouple materials generate a voltage when a strain is applied. Dr. Moffat has observed that Type K materials in particular, and Type J and T materials to a lesser extent, exhibit a strain sensitivity, and during the act of straining can generate appreciable voltages. Temperature-measurement equipment that is subject to strong vibration may show apparent temperature fluctuations induced by the flexing of the lead wires. Moffat reports observing spurious signals equivalent to 100°F when using Type K materials.

Thermocouples necessarily involve pairs of dissimilar materials and hence are capable of generating galvanic voltages in the presence of electrolytes. Moffat notes that in tests conducted at Stanford University, neither Types K nor T materials showed significant effects; however, ordinary Fiberglass-insulated iron/Constantan material showed a vigorous action. This action took place even when the wire was immersed in distilled water! According to Moffat, an electrolyte was created when the color-coded dyes dissolved in the water. In the Stanford University iron/Constantan thermocouples tests, typical values for E_S and R_S of Fig. 52 were respectively 250 mV and 0.25 M Ω /foot (24 gauge duplex Fiberglass-insulated material, wet with distilled water). Caution is advised when conditions prevail that precipitate galvanic action, particularly when color-coded dyes are present.

Common-mode voltage. — Common-mode voltage in thermocouple circuits can be generated in many ways. The following list includes the more important causes:

1. Thermocouple sensors are often grounded directly to the aircraft metallic structure to achieve the best possible thermal contact.
2. The ordinary thermocouple wire, which uses Fiberglass or other nonmetallic insulation, does not meet the desired shielded, twisted-wire-pair criteria for good common-mode rejection.
3. Thermocouple wires typically have different lead impedances because the individual wire materials have different resistivity.

The low-output voltage typical of a thermocouple circuit makes even a small amount of noise significant. When unshielded or untwisted thermocouple wire pairs are used in long runs, common-mode-noise contaminated pickup is almost inevitable. A grounded thermocouple may have many volts of common-mode voltage difference with respect to other parts of the circuit. The relatively high resistivity of many thermocouple wire materials and the considerable difference in the resistivities of the two types of wire can easily change a common-mode voltage to a differential voltage through unknown leakages and capacitive coupling of grounding paths.

For reducing common-mode voltage, differential input instrumentation amplifiers can be used (see Voltage Amplifier in Sec. 3; also Appendix D). These amplifiers can reject common-mode voltages that are 1 million times as large as the input signal; however, a typical limitation of 10 Vdc exists on the absolute maximum voltage allowed for most amplifiers. If the common-mode voltage is larger than the maximum allowed for the ordinary instrumentation amplifier, an isolation amplifier may be required.

Electrical connector. — Early in NASA's space program, electrical connectors were identified as the single component most likely to produce a system malfunction. From a reliability standpoint, it is therefore desirable to eliminate connectors altogether in data-acquisition circuits; however, in flight-test instrumentation, such considerations as aircraft disassembly, panel replacement, and sensor replacement require that connectors be used in most wiring installations. Since connectors are a requirement, the unique problems associated with thermocouple circuits and connectors will be discussed.

Electrical connectors are available with contacts constructed from thermocouple materials. These connectors are prohibitively expensive for any but the most critical applications and seldom do they have those properties that are most desirable for making reliable disconnect pins. In addition, other factors such as oxide coatings, cold working, annealing, and soldering often cause thermally generated voltages, even when these special connectors are used. Such connectors are commercially available and are well designed; however, the reliability is not as good as for the typical flight-qualified connector. The use of flight-qualified connectors is discussed in the following subsection.

A common solution when a long thermocouple wire pair must be interrupted by a connector is to use a standard copper-contact, flight-qualified connector. This is not necessarily an undesirable solution when certain restrictions can be imposed on the system. Figure 53 illustrates the connector configuration.

In Appendix N, this particular problem is analyzed in more detail using the pattern-circuit technique. No circuit errors are introduced as long as T_1 equals T_2 and T_3 equals T_4 . When a connector is used in a high temperature gradient (along the direction of the wire) then it is more likely that this condition of equal connector temperature will be violated. This condition can introduce large apparent temperature errors; it is a result of one-half of the connector being at a higher temperature than the other, unfortunately a commonly encountered condition. In a bulkhead connector installation (separating one compartment from another), substantial temperature differences often exist between the two compartments. In one extreme case, a thermocouple connector was installed on a bulkhead dividing a compartment housing a rocket engine from a compartment containing a liquid oxygen tank. Connectors located near the thermocouple sensor can also have high-temperature gradients. Therefore, it is imperative that steps are taken to ensure that the contacts are isothermal, particularly when a connector using copper contacts must be placed in a length of thermocouple wire. Contact plating, soldering, contamination, and inhomogeneities make the situation even more complex and call for extreme care to ensure that the isothermal condition is achieved. The isothermal condition is accomplished by minimizing the heat paths into the connector and by providing good thermal conduction paths internally to prevent the buildup of thermal

gradients. Simple solutions, such as insulating the connector and some of the adjacent wiring, may not be adequate to prevent significant errors. Systems including connectors located in areas of high temperature gradients should always be carefully designed. Even when those connectors are used in which contacts are constructed from thermocouple materials, high temperature gradients can introduce error voltages since there is no way in which machined contacts that are soldered or crimped and continually flexed by connector separations and matings can be guaranteed to be homogeneous.

One way to reduce the number of dissimilar-metal connections in the thermocouple wiring is to place the reference oven or zone box close to the thermocouple sensor, thus permitting copper wire to be used between the oven and aircraft data-acquisition system. Positioning the oven or zone box near the sensors will also reduce the amount of thermocouple wire required.

Mechanical commutator. — Thermocouple commutation is sometimes accomplished with mechanical switches after transitioning from thermocouple wires to copper wires. Much research and effort have been expended to make the mechanical commutator an electrically low-noise device. Commutators used with millivolt-level signals such as are generated by the typical thermocouple are subject to several limitations, as Moffat explains:

"The principal requirement of a switch or a connector is that it not affect the signal it is passing; i.e., it should not produce voltages which would contaminate the temperature signal from the thermocouple. Switches and connectors, by their very nature, involve several materials connected together and are susceptible to generation of thermoelectric voltages. In particular, the thermoelectric power of an alloy is a function not only of its chemical composition but also its mechanical state (i.e., cold work) so there is no assurance that a cast and machined component of a switch will have exactly the same calibration as a drawn and annealed wire of the same nominal composition. Metallic oxides may have thermoelectric power values measured in volts per degree instead of millivolts per degree. Thin films of metals may have different thermoelectric properties from bulk material of the same name. Thus the probability is high that any switch or connector will be susceptible to generation of thermoelectric voltages if there are temperature gradients in the materials.

The principal defense against spurious voltages is to ensure an isothermal region, not only "on the whole" but "in detail." Switches and connectors should provide good conduction paths within their structure to equilibrate temperature inside the body. Outer surfaces should be insulators to impede heat transfer from the surroundings. Switch points, in particular, should provide good heat conduction paths. The mechanical energy dissipated as heat when the switch is moved appears first as a high temperature spot on the oxide films of the two contacts. It then relaxes through the structure of the switch, raising the average temperature. If the switch points are not good conductors, substantial temperature gradients may persist for several seconds after a switch movement: just when the data are being taken!" (Ref. 24)

If the above considerations are observed, satisfactory switch operation can be expected; however, maintaining a low-level commutator so as to generate no significant noise levels can prove difficult. In an actual case at the Dryden Flight Research Facility, one technician was used full time to maintain two mechanical commutators in flight status. When switching-noise voltages are minimized, using the commutator downstream of a reference oven is quite simple. When a commutating switch is used in conjunction with a single type of thermocouple and zone box, an interesting technique of adding a reference junction is possible. Appendix O illustrates two methods of adding a reference junction to commutated thermocouples of a single type. In these cases, the reference-junction voltage is successively added to each sampled thermocouple sensor. Appendix O also provides a pattern-circuit analysis of two commutator circuits.

4.1.3 Faraday-Law Transducer Signal Conditioning

Faraday-law transducers are implemented by causing a coil of wire to move relative to a magnetic field such that the wires in the coil pass through, or cut, the magnetic flux to generate a voltage. In a self-contained, self-generating transducer, the magnetic flux is generated by a permanent magnet. All the comments in this section on generated voltages would also be true if the magnetic flux were generated by an electromagnet; however, in this case the transducer would not be classified as a self-generating transducer. An exception is when a wire coil is used alone, as a detector of a varying magnetic field normally generated by electromagnetic equipment.

To visualize how a Faraday-law tachometer is constructed, consider the rectangular coil of Fig. 54. In this figure, a coil composed of N turns of wire and of a length b and radius a is rotated at an angular velocity, ω , in a magnetic field which has a flux density, B . In this example, the generated voltage e_0 is proportional to

$$e_0 = BNbaw \cos \theta \quad (37)$$

The term θ is the angle of the coil with respect to the magnetic flux lines; it is zero when the sides of the coil are cutting the maximum number of flux lines and the maximum voltage is produced.

At $\theta = 90^\circ$, the coil is not cutting flux lines and the output voltage is zero. The sign of the voltage reverses beyond $\theta = 90^\circ$ and a negative voltage maximum is reached at $\theta = 180^\circ$. The simple device described above can easily be used as a tachometer. In a given device the flux density B is fixed, as is the area of the coil (area = $2ba$). The term θ can be replaced with ωt to give

$$e_0 = K\omega \cos \omega t \quad (38)$$

Examination of Eq. (38) shows that both the amplitude and frequency of the output voltage e_o are directly proportional to the angular velocity, ω ; K is a constant of proportionality. In the simple device described here, the angular velocity is usually determined from the signal frequency information. Since on many devices the desired datum is an angular velocity that varies between two limits, neither of which is zero, the output voltage and frequency are never zero. If the angular displacement is limited in excursion to less than $\pm 15^\circ$, then $\cos \theta$ is approximately 1 and, therefore,

$$e_o = K\omega \quad (39)$$

In this case, the output is directly proportional to the angular velocity and the required signal conditioning is minimal.

Many tachometers use mechanical commutation to produce an output that is directly proportional to the angular rotation rate. This type of transducer can be easily understood if the engineer can visualize the coil of Fig. 54 repeated every 15° around a rotor for a total of 12 coils. Now, instead of using continuous slip rings to carry the voltage from the revolving rotor to the stationary transducer body the slip rings are each divided into a number of segments equal to the number of coils or, in this example, each of the two slip rings is divided into 12 contacts. The coils are individually connected to two of the commutator contacts. Two sliding-switch contacts (brushes) are arranged so that each successive coil is connected to the output as the sampled coil is cutting the maximum number of flux lines, that is, when θ of each individual coil approaches zero degrees. Since the output voltage of each coil is a cosine function of the angular relationship to the magnetic flux lines, the output voltage is not strongly affected by the small angular separation of the various coils at small angles. Usually the brushes slightly overlap each commutator contact to avoid open-circuit transients. The output voltage amplitude of such a generator is an excellent representation of the angular velocity with a small ripple caused by the commutation process.

The last example of a Faraday-law transducer is one in which a permanent magnet, such as might be located in the rotor of a vane-type volumetric flowmeter, periodically passes a small wire coil. Each time the magnet passes the coil a voltage pulse is generated at the coil output. The repetition rate of these pulses is directly proportional to the rotor angular velocity which in turn is proportional to the volumetric flow rate.

Frequency-output signal conditioning. — There are two common signal-conditioning techniques used with Faraday-law transducers in which the output voltage is a sinusoidal voltage whose frequency and amplitude are directly proportional to the input angular velocity. These are the conventional analog- and digital-type signal conditioners. Both of these techniques use the output voltage frequency component, $\cos \omega t$ (see Eq. (38)). Even though the output voltage amplitude and frequency are both direct functions of the input angular velocity, the voltage amplitude is more susceptible to noise inputs, and thus the frequency component is used to obtain higher quality data.

The analog signal-conditioning technique typically utilizes an integrated circuit frequency-to-voltage converter (FVC). In these devices, the variable amplitude and frequency are processed by a voltage comparator which functions as a zero-crossing detector. The FVC generates for each zero crossing a precision pulse which contains a precise amount of charge. These charges (pulses) are summed, and, when the pulse ripple frequency is filtered out, the resultant output voltage is proportional to the input pulse rate or input angular velocity.

The digital-type signal conditioner is very popular. One implementation of the digital-type conditioner is to use an FVC to produce an output series of pulses as discussed above. The pulses then are counted over a given time period and placed in a digital word. A popular application of this technique is to condition a volumetric flowmeter to produce a digital word value proportional to the total volume flow. A significant advantage of the digital technique is that these pulses can be totaled over a given time period, to give a value that represents the total flow volume for that period.

Amplitude-output signal conditioning. — The dc tachometer has a voltage output that is a direct function of the angular velocity of the tachometer shaft. The simple tachometer shown in Fig. 54 also provides a voltage that is a direct function of the angular velocity when the coil rotation is limited to $\pm 15^\circ$. An amplifier is usually the only signal conditioning required for these types of transducers.

4.2 NON-SELF-GENERATING TRANSDUCER SIGNAL CONDITIONING

Non-self-generating transducers do not use energy from the measurand to produce output energy; an external power source is necessary to provide output signals. All variable-impedance-type transducers are non-self-generating; even the variable coupling devices such as the linear-variable-differential-transformer and potentiometer are variable-impedance devices.

The non-self-generating transducer signal conditioners selected for discussion in the following sections represent the most commonly encountered transduction principles and the most popular or most desirable signal-conditioning techniques. When a non-self-generating transduction principle is not discussed, it is hoped that the following discussions will illustrate a signal-conditioning technique that is applicable. Although the emphasis of each discussion is on the signal conditioning and the issues associated with applying the signal conditioning to each transduction principle, a simplified discussion of the transduction principle will be included to place the signal-conditioning problems in perspective. The reader is cautioned that this discussion covers only the transducer basics and the characteristics that particularly affect the signal conditioning; it does not provide a complete understanding of the transduction principle or of how well the transducer output represents the desired measurand. There are numerous good transducer texts (for example, Refs. 1 and 27), and they should be consulted when more details are required.

4.2.1 Variable-Resistance-Transducer Signal Conditioning

Variable-resistance transducers are widely used and are available in many forms. Their simplicity, ruggedness, and relatively low cost contribute to their popularity. Examples include the potentiometric transducer, the strain gauge, the resistance temperature gauge, and the piezoresistive transducer. The characteristics of these transducers vary strongly with each type and are discussed in more detail in the sections that follow.

Potentiometric transducer signal conditioning. — Potentiometric transducers are often used to measure linear and angular displacements. The transducer transfer function may be linear or may have a variety of nonlinear characteristics. In general, it usually has a very limited frequency response (for example, 0 to 4 Hz) at a low amplitude displacement.

The potentiometer owes some of its popularity to the simplicity of the required signal conditioning. When the resistance of the potentiometer is reasonably high (1,000 to 10,000 Ω) and a 5-10-V power supply is used for excitation, direct connection can be made with most modern high-impedance signal encoders. The major difficulty encountered with potentiometric transducers is an effect called "loading." Figure 55a illustrates a typical potentiometric transducer which has a total resistance R_p and is loaded by a resistive load R_L ; R_L is the signal-conditioner impedance that is presented to the potentiometer. The output voltage e_o , shown for two values of R_L in Fig. 55b, is a function of the power-supply voltage E_b , R_L , and n . The term n is a number that varies between 0 and 1.0, and represents the position of the movable contact on the linear potentiometer. Figure 55c illustrates the nonlinear loading effects as a function of contact position and loading-resistance ratio. Loading also occurs for a nonlinear potentiometer and must be determined for each specific application. The resistive value of the potentiometer should be kept reasonably high to reduce the effects of the cable lead-wire resistance (if long wires are used to connect the potentiometer to the signal conditioning), reduce power-supply loading, and reduce power dissipation in the potentiometer.

When a very-low-impedance potentiometer, such as a slide-wire potentiometer is used, a constant-current power source is desirable. In the case of a low-impedance potentiometer that is remote from the signal conditioning, the signal outputs should be separate wires brought back to a high-impedance load, as shown in Fig. 56. The output of the circuit of Fig. 56 is independent of the lead-wire resistances R_w , but is dependent on the absolute magnitude of R_p .

Strain-gauge-transducer signal conditioning. — Strain gauges are encountered quite commonly in flight-test data-acquisition systems. A large vehicle undergoing loads research can be instrumented with a thousand or more strain gauges at one time. Not only can gauges be applied directly to aircraft structures for measuring strain, but they are also often used in transducers (for example, pressure transducers), to convert mechanical displacement into an electrical output.

The subject of strain-gauge measurements is addressed thoroughly and in excellent detail in Ref. 28, which covers a wide variety of strain-sensing techniques in addition to the metal and semiconductor-type strain sensors discussed here. In addition, it also covers the entire subject of strain measurement, including signal-conditioning techniques. This section will present a quick overview of strain gauges and associated signal conditioning.

The strain gauge is one of the most popular types of airborne transducers, and its main appeal is attributable to its good accuracy combined with its simplicity and low cost. Though strain gauges are usually associated with medium-accuracy applications, with proper care they exhibit errors from 1% to 3% of full scale. Unbonded strain-gauge pressure transducers are used in a very successful air-data computer. However, in that application, the transducers are carefully selected premium units that are well isolated from vibration and temperature variations.

A brief discussion of the principles and characteristics of metal and semiconductor gauges is presented at this point to provide a general understanding of how strain gauges function. As the name suggests, strain gauges are sensitive to strain. Strain can be visualized by considering a circular rod of cross-sectional area A . If a tensional force F is applied to this rod at its ends, the original length L of the rod will change by an amount of ΔL . The longitudinal strain, ϵ_L , is defined as

$$\epsilon_L = \Delta L/L \quad (40)$$

(It should be noted that the diameter of the rod also decreases at the same time by some amount which is about 0.3 ϵ_L for metals). The longitudinal strain ϵ_L is related to the deforming force by Young's modulus E . The two relationships are

$$E = \sigma_L/\epsilon_L = \text{Young's modulus} \quad (41)$$

where

$$\sigma_L = F/A = \text{stress} \quad (42)$$

Structural materials for aircraft flight tests are intended to be operated in the elastic (Hooke's law) region, and these relationships then hold for the given material.

The materials handbooks (and Table 2.1-1 in Ref. 28) list the maximum elastic stress for many common aircraft structural materials. Using this as the maximum stress and the given value of Young's modulus,

the maximum elastic strain can be calculated. Using values from Table 2.1-1 in Ref. 28, which covers aluminum, an aluminum alloy, titanium, a titanium alloy, carbon steel, and a chromium-nickel steel alloy, the maximum elastic strain, that is, $(\Delta L/L)_m$, ranges from a low of 0.0007 to a high of 0.0075. Since aircraft flight-loads stress limits are set well below the elastic limit, the actual strain available to drive the bonded strain gauge will be much less than the maximum strain for the material.

Scale factor must be considered when designing signal conditioning for stiff structural members when the strain gauges have been installed to determine the maximum design loads in the loads laboratory. Actual flight loads are often much lower than these structural design loads. The output of these gauges under normal flight conditions may then be very small and thus place an excessive burden on the signal conditioning. With flight-loads test aircraft, the strain gauges are usually installed during aircraft fabrication and it may be difficult to install new gauges in the best location. The best way to avoid this problem is to have the flight-loads requirements included in the initial design.

A strain gauge has an initial resistance R , which changes under strain by an amount ΔR . The relationship governing $\Delta R/R$ as a function of strain is

$$\Delta R/R = k(\Delta L/L) = k\epsilon = (\text{gauge factor}) (\text{strain}) \quad (43)$$

In this equation, the term k is called the gauge factor. The gauge factor for metallic strain gauges is typically about 2. Semiconductor (piezoresistive) strain gauges can be fabricated with gauge factors ranging from -100 to +200. Despite the advantages of its large gauge factor, the semiconductor strain gauge is seldom used in flight-test data-acquisition systems; this is because of its many disadvantages, including nonlinearity, highly temperature-sensitive gauge resistance, and highly temperature-sensitive gauge factor. Because they are so small, semiconductor strain gauges are used in transducers that are very small or that are used to measure very-high-frequency inputs. Semiconductor strain gauges are used on aircraft structural members to measure high-frequency, low-level strain. In these cases it is often desirable to use a bandpass filter to eliminate low-frequency offsets and drift.

Bonded strain gauges, that is, strain gauges that measure the strain in the material to which they are bonded, are often used to determine the load or force on a structural member. Other factors in addition to the applied force can cause a $\Delta L/L$ (Ref. 3, pp. 133,134). For example, temperature changes produce dimensional changes. These temperature-induced structural changes also affect in a number of ways the strain gauge that is directly bonded to the structure. By judicious selection of strain-gauge materials, strain-gauge manufacturers have produced gauges that can compensate over a limited temperature range for the temperature effects in most of the important structural materials. Figure 57 illustrates the results of a multiple-temperature cycle test involving four strain gauges mounted on a titanium alloy. If these gauges had been used to form a two-active-arm or four-active-arm bridge then much of the apparent strain would have been canceled. The one-active-arm strain-gauge bridge can be temperature-compensated by placing a "dummy" strain gauge mounted on the same material in the same thermal environment as the active strain gauge. The "dummy" gauge signal-conditioning technique will be discussed later in this subsection.

Strain gauges are most often used in bridges such as that shown in Fig. 58. In this figure, all arm resistances are equal to basic gauge resistance R . In Fig. 58, the output voltage is sensed by a very-high-impedance voltmeter. (When the bridge is used to drive a low-impedance device, for example, a current sensor such as a galvanometer, the output equations are more complex.) Inspection of the equations given in Fig. 58 shows that the outputs of the bridges are functions of the bridge-supply voltage E_b , the term $\Delta R/R$, and the number of active arms in the bridge.

In Fig. 58, it has been assumed for the two-active-arm and four-active-arm bridges that it is possible to position individual strain gauges at locations where there are equal and opposite stresses. This is often possible, for example, when measuring bending moments. This would not usually be possible when a structure responds only in pure tensile stress, unless special provisions, such as force rings, were designed into the system initially or could be added later. (The two-active-arm bridge can function with two similarly strained gauges if the gauges are located diametrically opposite each other in the bridge.)

Figure 59 displays the relative output of the bridges with one, two, and four active arms. Note that for the higher values of $\Delta R/R$, the one-active-arm bridge is very nonlinear. What is not shown is that in actual practice, the one-, two-, and four-arm bridges are even more nonlinear at large values of $\Delta R/R$. This is due to the nonlinearity of the gauge factor. In the equations for the two-active-arm and four-active-arm strain-gauge bridges, the assumption has been made that the resistive increase in one arm exactly equals the resistive decrease in the other arm. This obviously cannot be valid when ΔR is greater than $-R$, since this would require that the resistance in that arm be a negative resistance, which is impossible since it means the strain gauge would become a power source. The physical implication of this is that no gauge factor can be linear in the region where the strain-gauge resistance approaches zero Ω . With metal strain gauges, the maximum elastic strain limits the value of ΔR to much less than R . Semiconductor gauges with large gauge factors can encounter this limitation. This explanation is required since the equations of Fig. 59 for two-active-arm and four-active-arm strain gauges seem to imply that the bridge-output voltage can exceed the bridge-input voltage. This is impossible for the reasons mentioned above. The one-active-arm bridge is reasonably linear for $\Delta R/R \ll 2$, which is an acceptable assumption for most applications involving metal strain gauges.

In general, the strain-gauge sensing element or elements are located remotely from the signal conditioning. This means the sensing element is connected to the signal-conditioning system by lead wires. These lead wires can be quite long and can pass through unknown temperature environments. This means that a lead-wire resistance R_w is introduced into the bridge circuit. This lead-wire resistance can vary in an unknown manner as a function of the unknown temperature environment through which it passes. Figure 60 illustrates some of the most common wiring techniques used to reduce these lead-wire resistance

effects. For best electrical noise rejection, the lead wires are usually twisted together inside a shield. The shield is isolated from ground and normally grounded only at the signal encoder.

All the wiring schemes shown in Fig. 60 have two principles in common: (1) when some lead-wire resistance R_L must be included in the arms of a bridge, it is placed in two arms of the bridge such that its effects tend to cancel; and (2) when returning a wire to the high-impedance signal detector, a lead wire is used that is not carrying bridge-power currents, for this wire will produce a voltage error owing to the current through R_L . Note however that in all cases, the lead-wire resistance that carries bridge power to the bridge causes a voltage drop which reduces the effective E_p across the sensor and thus reduces the output voltage.

Since the bridge output is a function of $\Delta R/R$, which is independent of the magnitude of R , it is usually desirable in a voltage-sensing signal-conditioning system to use the highest resistive value of strain gauge available. With the metal-type strain gauge, it is often hard to find gauge resistances that exceed 1,000 Ω . High gauge resistances in metal gauges are also sometimes associated with low gauge reliabilities so care must be exercised in this regard. This large value of basic gauge resistance R reduces the effects of R_L to a smaller fraction of R . The large value of basic gauge resistance also reduces the current through R_L , thus reducing voltage drops. Other advantages of using strain gauges with higher resistances are that for the same supply voltage, the power-supply loading is reduced as is the strain-gauge self-heating.

Figure 60 illustrates a shunt-calibrate resistance R_C , and a calibrate switch S . When the calibrate switch is closed, the shunt-calibrate resistor is placed in parallel with one arm of the bridge and decreases the arm's resistance by an amount ΔR_C , which is equal to the difference between R and the parallel combination of R_C and R . This produces a $\Delta R_C/R$, which corresponds to a one-active-arm bridge with an effective input $\Delta R_C/R$ and produces an output voltage that is algebraically added to existing strain-induced outputs. Note that in Figs. 60a-60c, the calibrate resistor is placed across a fixed-bridge completion resistance in the signal-conditioning system. In Fig. 60d, the calibrate resistor is shown connected to wires that do not carry bridge currents. If the lead resistances are small enough, when the extra wire for the calibrate resistor of Fig. 60d is not required.

The shunt-calibrate technique was originally used when strain-gauge bridges were powered by batteries. Switch S was closed for short periods during a flight, thereby producing a signal step-output which could be used to calculate the actual battery voltage throughout the flight. A decrease in the battery voltage (as it discharges during flight) directly affects the bridge output.

The advent of the modern, highly regulated power supply has removed the main reasons for using a calibrate technique, whether the shunt-calibrate technique shown here or the series-calibrate technique discussed in Ref. 28. The main justification for using a calibrate resistor in conjunction with modern regulated power supplies is that a calibrate can be used during preflight and postflight record checks to provide a crude and limited indication of the system electrical wiring integrity.

Use of the dummy gauge (R^*) shown in Fig. 60b is a very useful way of reducing the temperature effects produced when the strain sensor in a one-active-arm strain-gauge bridge is exposed to large temperature fluctuations. Figure 57 illustrates some strain gauges which would exhibit an apparent variation of 110 micro-strain over the temperature range of 27°C to 277°C, when mounted on titanium. In the one-active-arm-bridge configuration of Fig. 60a, the accuracy would be limited to this value. (Note that a temperature measurement at the bridge could also be used to correct the reading, but this requires another data channel or a complicated signal-conditioning compensator.) If a dummy gauge could be mounted in the same temperature environment and on the same material as the active strain sensor, but remain unstrained by loads, then the apparent strain owing to temperature for the example shown in Fig. 57 would be less than the shaded area, a considerable improvement. For best results, the dummy gauge should be matched to the active gauge. This matching process usually means matching the resistance of the gauges that have been constructed from the same batch of strain gauge wire or strain-gauge material. The required isolation of the dummy gauge from the structural loads can be accomplished by mounting a tab of the structural material at the active gauge site such that it is subjected to the same temperatures while being isolated from the structural loads.

If the bridge power supply is a nongrounded power supply, it would be possible to use a single-ended amplifier to amplify the strain-gauge bridge output. However, because of the low-level signals associated with strain-gauge bridge circuits, a differential amplifier such as an instrumentation amplifier (see Sec. 3). is desirable to reduce common-mode noise signal contamination.

When the power supply is grounded, a differential amplifier will be required; however, a grounded power supply should be avoided, because the signal circuit should be grounded at one point only. That ground point is usually at the signal terminus, such as the PCM encoder (see Fig. 61). With a grounded power supply, considerable amounts of steady-state, common-mode voltage can be introduced into a typical direct-coupled bridge circuit. In addition, if the circuit is grounded anywhere else, such as at the signal encoder, common-mode voltages can be introduced owing to the multiple grounds. If the gauge is located where the ground reference voltage is at a much higher level than that of the signal-conditioning system, it may be desirable to use an isolation amplifier instead of the instrumentation amplifier. Single-ended and differential voltage amplifiers and isolation amplifiers are covered in Sec. 3. When electrical noise is particularly troublesome, a carrier amplifier (also described in Sec. 3) may be used to reduce noise contamination.

Strain gauges are capable of a frequency response that is quite high. A typical strain gauge mounted on a wing panel can reproduce structural input frequencies as high as 800 Hz for standard sensing elements. Figure 61 is a schematic diagram of a one-active-arm-bridge circuit using an instrumentation

amplifier of gain A , a floating power supply, a PCM encoder signal terminal device, and shielded wires which are single-point grounded at the signal terminal device.

When the highest frequency of interest to the engineer is 10 Hz and the bridge output is directly connected into a 50-sample/sec PCM encoder, there is considerable possibility for aliasing (see Sec. 5 and Ref. 1). To control aliasing, it is mandatory to filter the signal before it is sampled. This filter would typically have a cutoff frequency of 10 Hz.

Strain-gauge bridges have characteristics that establish filter requirements that are particularly difficult to satisfy. A strain-gauge bridge typically has a low-level output voltage and quite often requires a low-pass filter, especially when used with a low-sampling-rate PCM channel. When neither of the bridge output signal wires is grounded, the output has considerable common-mode voltage. Even if one of the bridge output leads can be grounded, substantial common-mode voltage may remain. None of the filters illustrated in Appendix I is of the differential-type input filter, which is necessary to reject common-mode voltages. Active filters with differential inputs are available but they require more components and additional component matching. When excessive common-mode voltage is present, a differential input instrumentation amplifier can be used followed by a single-ended filter. Filters are discussed in Sec. 3 (under Filters) and Appendix I. A filter that circumvents the active filter dc drift is the zero-offset filter described in Appendix I. This filter is particularly effective when used with a transducer having a low output voltage and requiring a filter with steady-state response.

The maximum power-supply voltage is normally limited by the maximum allowable power dissipation of the strain gauge. For a given gauge resistance, the power dissipation increases as the square of the power-supply voltage, whereas the signal output of the bridge is directly proportional to the input voltage. Therefore, doubling the input voltage doubles the output voltage, but it quadruples the power dissipated in the gauge. To overcome this limitation, a pulse power source is sometimes used. For example, when a 350- Ω , four-active-arm bridge is used with a 10-Vdc supply, 286 mW are dissipated in the bridge. A power supply that pulses this bridge with a 1-msec, 50-V pulse every second produces an average power of 7 mW, which is 40 times lower than that produced with the 10-Vdc supply. Now if the output of the bridge is sampled only when the bridge is pulsed, the output of the pulsed bridge is 5 times higher than produced with the steady-state 10-Vdc power supply. Obviously, when this pulsed power supply is synchronized with a sampling-type data encoder, a very efficient system is produced.

In practice, implementation of such a pulse-excitation system is very difficult because of aliasing (see Sec. 5). In the above example, the sampling rate was 1 sample/sec which corresponded to the power supply pulses to the bridge of 1 pulse/sec. In this case any strain input or electrical noise pickup with a frequency component above 0.5 Hz will be irretrievably aliased into the data bandwidth 0 - 0.5 Hz.

In conclusion, even though pulsed power supplies seem to offer great advantages, applications of pulsed power supplies must be well analyzed and the power supplies carefully designed to ensure quality data.

Even though it would not seem to be in the province of signal conditioning, all installed strain-gauge bridges should be quality-tested with a high-voltage, megohm tester before use. A minimum of 1,000 M Ω should be registered between each sensor and structure, particularly when large temperature excursions are anticipated. Low values of insulation resistance are just one indication of improper gauge installation and low sensor-to-structure resistance is highly correlated with later system difficulties.

Figure 62 illustrates one channel in a typical signal-conditioning box for a four-active-arm bridge. The channel includes provision for initial balance of the bridge output by means of the potentiometer R_p and for insuring a shunt-calibrate resistance R_C by means of relay contact S. By judicious use of the terminals A through G, the signal conditioning can also accommodate one-active-arm and two-active-arm bridges.

To ensure reliable data recovery, one data channel is often used for monitoring the bridge supply voltage. This is done even if a calibrate-resistance system is used, since any error in the bridge input voltage is directly reproduced as a scale-factor error in the output signal. Thus, although it is not highly probable that a reliable, regulated power supply will change voltage, it is very important to know if it does change.

Although potentiometers are often included in the bridge-signal conditioning, their presence often contributes to data degradation, and good practice dictates that they not be used. The resistor R_B in the bridge channel shown should be replaced with fixed, precision resistors which will zero balance the bridge to within 5% of full scale. This is done to (1) Eliminate between-flight adjustments; (2) Improve reliability without potentiometers; (3) Eliminate potentiometer step resolution; and (4) Eliminate vibration sensitivity. The most important reason for eliminating the potentiometer is so that the bridge cannot be re-zeroed after each flight. Bridge output voltage drift is an important indicator of diminished bridge integrity, and repeated re-zeroing eliminates this measure of bridge quality. The appropriate place to correct the data for offset or drift is during the data-reduction process, not in the signal conditioning. A potentiometer can be used to determine the approximate values of the fixed-resistor divider. Though the bridge balancing must be done at the aircraft, the potentiometers can be replaced in the flight laboratory, particularly when the signal-conditioning circuitry is designed with this in mind.

The output of a one-active-arm bridge is very nonlinear with large changes in gauge resistances, such as occur with semiconductor strain gauges. A circuit that is linear for large variations of the sensor resistance is discussed below.

Thermoresistive-transducer signal conditioning. - In this subsection, the signal conditioning for the thermoresistive-effect transducers, the RTD (metal-type resistive temperature gauge) and the thermistor, will be discussed. (Thermocouple signal conditioning was discussed previously in this section.)

The metal resistive-temperature detector (RTD), and the thermistor are two of the most common airborne resistive temperature sensors. The RTD is very accurate and stable, but the best units are somewhat expensive. The thermistor produces very large resistive changes for a given temperature change; however, in its basic form it is highly nonlinear. Other resistive-temperature sensors exist, but they are not commonly used in airborne applications.

Figure 63 illustrates the temperature-related resistance variations of some of the more common RTD materials. Platinum is the most desirable temperature gauge material because it has excellent repeatability and stability. Nickel is an economical material, and its nonlinear temperature properties can be compensated with bridge circuits over a limited temperature range. Copper, whose response is not illustrated, has a very linear variation of resistivity versus temperature, but is not normally used because its low resistivity makes it very difficult to achieve practical values of total gauge resistances. Most RTD materials have positive temperature coefficients (resistance increases as temperature increases.)

Figure 64 illustrates the resistance versus the temperature response of a thermistor and shows the typical shape expected of a thermistor characteristic curve. Thermistors are formulated from many semiconductor materials (for example, oxides of nickel, manganese, magnesium, iron, cobalt, and titanium) and, thus, the absolute value of resistance can vary considerably.

In general, a thermistor resistance as a function of temperature can be approximated by

$$R = R_0 \exp \{ \beta [(1/T) - (1/T_0)] \} \quad (44)$$

where

- R = resistance at absolute temperature T
- R_0 = resistance at absolute reference temperature T_0
- β = thermistor material determined constant
- T = thermistor temperature, K
- T_0 = reference temperature, K

Manufacturers sometimes supply more complex equations which give better approximations over large temperature ranges, or provide tables listing the thermistor resistance at various temperatures. When the data are to be reduced by a computer, an equation is often desirable. The important feature to notice in the above equation is that it is an exponential function, which means that the thermistor resistance changes dramatically over most of the usable temperature range. Another important characteristic is that the thermistor has a negative temperature coefficient (resistance decreases as temperature increases).

The RTD is usually used in one-active-arm-bridge circuits. This is essentially the same bridge circuit as the one-active-arm bridge discussed above. As can be seen from Fig. 63, even platinum (curve D), which has a lower sensitivity resistance versus temperature than the other illustrated gauge materials, produces large resistance changes over its temperature range. (Note that both tungsten and platinum can be used at much higher temperatures than other materials shown, depending on the mounting technique and the atmosphere in which the sensor is immersed.) Even though the resistance sensitivity versus temperature characteristic of a platinum RTD is nearly linear over its usable temperature range, the output of the one-active-arm bridge with equal-resistance arms is far from linear.

Figure 65 illustrates some common bridge configurations used with the RTD. Figure 65a is used when the lead-wire resistance in the cable to the gauge is negligible or when accuracy is not critical. Note that when the lead-wire resistance is known and stable it can easily be incorporated in the calibration equations as a simple increase in the absolute value of the gauge resistance. When the lead-wire resistance is significant and undergoes unknown changes because the cable passes through unknown temperature environments, the configurations of Figs. 65b and 65c are desirable. The three-wire configuration of Fig. 65b is particularly useful in the equal-arm bridge configuration. In this case, R_0 is the resistance of the resistive gauge at the temperature where the bridge has zero output voltage, and R_1 , R_2 , and R_3 are all equal to R_0 . Since the lead-wire resistance is split into two bridge arms, the bridge loses some sensitivity, but variations in R_W cancel out.

For the equal-arm bridge configuration, where R_1 , R_2 , and R_3 are equal, the configuration shown in Fig. 65c has no advantage over that in Fig. 65b; however, when R_2 and R_3 are equal and significantly greater than R_1 , then the advantages of the configuration in Fig. 65c are important. In this case the lead-wire resistance value ($2R_W$) is split into the arms containing R_1 and R_G . The configuration in Fig. 65b does not provide compensation for lead-wire resistance changes when R_2 and R_3 are equal and much greater than R_1 .

Why should the engineer wish to use $R_2 = R_3 \gg R_1$? To help visualize the situation, a hypothetical RTD is postulated which is absolutely linear in the temperature range 0°C to 800°C , where its resistance varies from 100Ω at 0°C to 500Ω , at 800°C . This temperature characteristic roughly approximates that of a platinum RTD. Assume further that it is desired to have zero bridge output voltage at 400°C at which point $R_G = 300 \Omega$. If $R_1 = R_2 = R_3 = 300 \Omega$, and the lead-wire resistance is negligible, then with a supply voltage of 1 V, the bridge output would be as shown in Fig. 66, curve A. This is a very nonlinear curve but acceptable for some applications. Much better linearity can be achieved using the same hypothetical gauge in a modified bridge. This is accomplished by making R_2 and R_3 much larger than R_G ,

for example, let $R_2 = R_3 = 5,000 \Omega$. If the supply voltage is increased to 6.8 V and R_1 is still 300Ω (the bridge still nulls at 400°C), then curve B in Fig. 66 is the resultant output voltage relationship. Figure 66 shows the benefits of increased linearity resulting from optimized bridge-arm resistances. In the second of the two circuit examples, a significant increase in linearity is achieved in addition to the reduction in the power dissipated in the resistive temperature sensor. At bridge balance, the apparent impedance seen by the voltage detector is only increased from 300Ω to 566Ω , an amount that is insignificant for the modern voltage detector.

The bridge nonlinearity can be used to partially compensate for the nonlinearity present in the nickel RTD characteristic. As can be seen in Fig. 63, curve A, the nickel temperature sensitivity increases with increasing temperature. By judicious choice of bridge components, the bridge nonlinearity can be selected to partially complement the type of nonlinearity displayed by the nickel (and Balco) RTD.

The active circuit shown in Fig. 67 is often recommended when the gauge resistance varies over a wide range and when an output is desired that is directly proportional to gauge resistance. The null point for this active bridge circuit is easily set by varying R_2 . However, setting the system gain involves simultaneously trimming the two R_1 resistances by the same amount, since a mismatch in the two R_1 values will produce a bridge null error.

The resistance of a simple thermistor varies so dramatically with temperature (see Fig. 64), that most applications are usually limited to measuring small variations of a temperature from a reference level. Fortunately, modern thermistors are very stable and for some applications manufacturers sell thermistors that are interchangeable. When used to measure small variations of temperature, for example, monitoring the temperature of a thermocouple oven, a thermistor bridge can provide large voltage swings for even small temperature changes and the bridges shown in the previous section for RTD are suitable for this application.

The exponential nature of the thermistor tends to make data acquisition difficult over a large temperature range. Thermistor assemblies are available that provide either a voltage or resistive output that is nearly linear with temperature. These assemblies are often very complex. For example, one linearized assembly uses three different thermistors and three different fixed resistors.

The engineer can linearize any simple thermistor to a considerable extent by combining a thermistor with a fixed resistor. Figure 68 illustrates how the thermistor of Fig. 64 could be linearized around a temperature of 112°C . The composite curve resistance, R_C , varies from 100Ω at 0°C , to 10Ω at 250°C . The usable temperature range extends from 25°C to 200°C . Obviously, by using another value of fixed resistor, R_f , or another thermistor, R_T , other linearized resistance-versus-temperature curves can be drawn.

The strain-gage bridge (particularly a metal-type strain-gage bridge) usually needs more amplification than an RTD or thermistor bridge. This is because RTD and thermistor bridges have high output voltage levels. When amplification is required, the same comments that applied to the strain-gage bridge apply here. Quite often the RTD and the thermistor are mounted to aircraft structures where the temperature data have no high-frequency components. Since these bridges usually have low impedance, careful shielding and good grounding practices may make filtering unnecessary. When filtering is required, it is used primarily to limit the data-channel noise bandwidth.

Carrier amplifiers have capabilities for high gains while rejecting electrical noise. This can be an advantage when it is desirable to use very low supply voltages to reduce heat generation in the gauge itself, a condition which has the potential of introducing substantial errors into the temperature measurement system. Pulsed power supplies are one solution to reducing temperature-gauge self-heating while retaining high output levels. Since temperature gauges are low-frequency devices, pulsed power supplies offer considerable promise.

4.2.2 Variable-Capacitance-Transducer Signal Conditioning

The capacitive transducer used in airborne applications, is usually a high-quality and expensive device. The change in transducer capacitance is produced by changing the spacing of the capacitor plates or by changing the dielectric material between the plates. The capacitive microphone is an example of varying the capacitance by changing the plate separation. The airborne capacitive fuel-level detector is an example of varying the amount of dielectric between fixed capacitor plates.

Capacitive transducer. — The parallel-plate transducers shown in Fig. 69 are used to illustrate some features of the capacitive transducer. The parallel-plate-type transducer is used because it is easy to demonstrate some of the inherent characteristics that must be considered in producing these devices.

From Fig. 69a, x is the effective or average plate separation. This is because the diaphragm deflection under the pressure forces forms a curved surface. As also shown in Fig. 69b, the fixed electrodes are sometimes curved to avoid contact when the diaphragm deflects.

In most transducers the plate area A is so large relative to the plate separation x that the edge effect is usually negligible, and the transducer capacitance is described by

$$C = \epsilon\epsilon_0 A/x \quad (45)$$

Where

- A = effective capacitor plate area, m²
- C = transducer parallel-plate capacitance
- ϵ_0 = permittivity of free space, 8.85×10^{-12} F/m
- ϵ = relative permittivity ($\epsilon = 1.0006$ for air at standard conditions)
- x = plate separation, m

To minimize size, it is usually desirable to keep the transducer diameter relatively small, for example, 5 cm or less. The smallness of the transducer limits the area term A (see Eq. (45)). Assuming the dielectric material is air, the relative permittivity ϵ is 1. The combination of small size and a low dielectric-constant material (like air), means that the plate separation x must be very small in order to achieve a usable capacitance change as the result of plate deflection. This spacing is 0.05 mm or less in some applications. These close tolerances require meticulous attention to detail when designing and fabricating these transducers. Transducer dimensional stability under changing temperatures is critical since it can affect both the plate spacing and the diaphragm tension. Diaphragm tension is particularly important because tension changes affect the sensor scale factor.

From Eq. (45), the capacitance is inversely proportional to the plate separation x. It is also apparent that the capacitance increases dramatically as x approaches zero. The sensitivity of the capacitance to a change in plate separation is given by

$$dC/dx = -\epsilon\epsilon_0A/x^2 \quad (46)$$

It can be demonstrated that the percentage change in capacitance is directly proportional to the percentage change in plate separation for small changes in plate separation around a neutral position. The following equation is directly derived from combining Eqs. (45) and (46).

$$dC/C = -dx/x \quad (47)$$

Capacitive sensors have some outstanding characteristics. Capacitive pressure transducers commonly have an accuracy of $\pm 0.1\%$ with an accuracy 3 times better than this in the higher pressure range transducers. Repeatability can be $\pm 0.005\%$ over restricted temperature ranges. The better capacitive pressure transducers are often used as secondary standards for calibration of other pressure gauges. The disadvantages of capacitive sensors are expense (which is related to construction) and the complex signal conditioning that is required.

Basic signal-conditioning techniques. — In the following paragraph three basic types of signal-conditioning techniques will be examined: (1) high-impedance voltage amplifier used with a dc bias supply; (2) charge amplifier used with an ac power supply; and (3) transformer-bridge signal conditioner.

Capacitive transducers have inspired numerous signal-conditioning techniques. Techniques (1) and (2) above are simple and adequate for many applications. Technique (3) is somewhat complex, but for critical applications where high accuracy is required it provides outstanding results.

The high-input impedance voltage amplifier is one of the simplest signal-conditioning circuits. It is used extensively with capacitive microphones and other dynamic pressure sensors. The main weakness of this technique is that it is impossible to achieve a static detection capability. Another weakness is that it works best when the amplifier is physically closely coupled to the sensor, but this can limit the system temperature tolerances. The reason for this required proximity limitation is that cable capacitances reduce the system sensitivity in the same manner as discussed earlier in this section. Figure 70 illustrates how this circuit can be implemented. Where there are no significant circuit capacitances other than the sensor capacitance C, and the amplifier input impedance is much greater than the bias supply resistor R, then the sensor output voltage response is that of an RC high-pass filter. This circuit response would be down 3 dB at a frequency (in Hertz) of $1/(2\pi RC)$. A detailed discussion of this type of frequency response is covered in Sec. 3 (under Filters).

The charge-amplifier circuit is shown in Fig. 71. When it is used with a capacitive sensor, the output voltage is directly proportional to the plate separation x rather than inversely proportional to x, as it was in the discussion of the previous section. This is particularly an advantage when the plate separation varies by a large amount as it does in a capacitive proximity gauge. This circuit can be used to measure static displacements.

This relationship can be demonstrated by the following analysis using an ideal operational amplifier

$$(1/C_R) \int I_R dt = e_g \quad (48)$$

$$(1/C) \int I_C dt = -e_o \quad (49)$$

$$I_R = I_C \quad (50)$$

$$e_o = -(C_R/C)e_g \quad (51)$$

When the sensor is a parallel-plate capacitor such as that described by Eq. (45), then it follows that

$$e_0 = -(e_g C_R x) / (\epsilon \epsilon_0 A) \quad (52)$$

The output voltage is an amplitude-modulated signal, and it must be demodulated as discussed in Sec. 3.

The transformer-bridge signal conditioner is one of the most useful techniques for measuring small changes in capacity. It can be used to measure slowly varying large changes in capacity if it is made into a self-balancing, that is, a nulling-type signal conditioner. The transformer ratio-arm bridge was introduced almost 100 years ago. The development of high-permeability nickel-iron alloys and ferrites has been responsible for the recent popularity of this type of bridge network.

Figure 72 illustrates a simple equal-arm transformer bridge. A constant-amplitude and constant-frequency oscillator supplies the bridge excitation voltage e_x . A transformer T, usually toroidal, has N_1 turns in the primary and $2N_2$ turns on the center-tapped secondary winding. The bridge nulling accuracy, the ratio of C_x/C_R , is related to the turns-ratio accuracy. The turns ratio is unaffected by age, temperature, and voltage. The detector which senses e_0 is a phase-sensitive detector (these are discussed in Sec. 3 and in Appendix H). In this figure, C_R is a reference capacitor which is adjusted so that the bridge nulls at the desired value of C_x , which is the nominal capacitance of the transducer. As will be shown later, this bridge is readily adaptable to the differential capacitance transducer of Fig. 69b.

A particular advantage of this circuit is its ability to tolerate cable capacitances that are several orders of magnitude larger than the sensor capacitances. This immunity to distributed cable and stray capacitances can be deduced by inspection of Fig. 72b. The capacitance C_1 appears across the low-impedance transformer winding (between points a and d) where its effect is negligible. The capacitance C_2 appears across the detector (across points a and b) where it does not enter into the balance equations.

The two cases most commonly encountered are the following:

1. C_x is the transducer capacitance whose nominal value is C and changes value by a small amount $\pm \Delta C$; C_R is a fixed capacitor which is adjusted to be equal to the nominal sensor capacitance C (see Fig. 73a).
2. The transducer is a differential capacitance-type transducer where C_R and C_x are both nominally equal to C and are both part of the differential capacitance (see Fig. 73b).

The single-capacitor transducer has an output

$$e_0 = (e_1/2)\Delta C / (2C \pm \Delta C) \quad (53)$$

If, as is quite common, $\Delta C \ll C$, then this equation simplifies to

$$e_0 = (e_1/4)(\Delta C/C) \quad (54)$$

Although the single capacitance is approximately linear when $C \gg \Delta C$, the differential capacitance transducer is linear over much larger excursions of ΔC . The output of the differential capacitance transducer in a transformer bridge can be shown to be

$$e_0 = (e_1/2)(\Delta C/C) \quad (55)$$

The most common excitation frequency lies between 100 Hz and 10 kHz.

4.2.3 Variable-Inductance-Transducer Signal Conditioning

There are many types of popular variable-inductance and variable-mutual-inductance transducers. These types of transducers can be constructed with very desirable characteristics — for example, excellent resolution, ruggedness, and stability. When special care is used in construction, some of these units can provide useful outputs at ambient temperatures approaching the Curie point (or Curie temperature) of the core material. The Curie point is the temperature at which ferromagnetism abruptly starts to vanish. A detailed explanation of this effect is given in Ref. 29. Disadvantages of variable-inductance transducers include complicated signal conditioning, and a special, separate ac excitation source.

This section will cover signal conditioning for the synchro family of transducers, the linear variable differential transformer (LVDT), the rotary variable differential transformer (RVDT), the variable-inductance transducer, the inductance potentiometer, the variable-reluctance transducer, and the Microsyn. There are many other transducer variations; however, these examples illustrate the most desirable signal-conditioning techniques. Simpler examples of signal-conditioning techniques abound in the literature for the various transducers; however, these simplified techniques often place severe restrictions on the system applications, and the economies are not that significant when modern integrated circuitry is used. The synchro family of transducers is covered first, since many of the signal-conditioning techniques for obtaining refined accuracy for these devices are also applicable to the other devices.

Synchro transducer signal conditioning. — The synchro transducers have long been used as accurate angular position sensors. Of the shaft-angle sensors capable of high accuracy, the optical (or brush) encoders and the synchros are the most popular. Both types of sensors are very accurate but the synchro is popular for airborne applications because of its durability in harsh environments. The advent of high-accuracy electronic converters (decoders) has also contributed to the continued popularity of synchro devices.

Synchro transducer family includes a large number of members. The family is divided into two main groups. The first group produces power outputs that are used to generate directly usable torques. The second group produces a voltage output; its members are called control devices. The names and codes that identify the various devices are torque transmitters (TX), control transmitters (CX), torque receivers (TR), control receivers (CR or CT), torque differential transmitters (TDX), torque differential receivers (TDR), control differential transmitters (CDX), resolvers (RS), and transolvers (TY). Although it is not a rotary device, the Scott-T transformer is used quite frequently in synchro circuitry, because it can be used to convert a synchro output into a resolver output and vice versa. Figure 74 illustrates some of the more common members of synchro hardware.

The multiplicity of synchro hardware can be best understood if the engineer considers the chronological development of synchro systems, which here is roughly divided into three phases: (1) torque-type synchro systems, (2) synchro systems that use servomechanisms to close the system loop, and (3) synchro transducers that use strictly electronic signal conversion.

The early synchro systems were power devices in that the torque transmitter actually generated enough power to force a lightly loaded torque receiver to track the transmitter angular position. A flight-test data-acquisition system might have been constructed as shown in Fig. 75. In such a system the remote transducer might be linked to an angle-of-attack vane on a flight-test air-data head and the torque receiver connected to the indicator on the pilot's cockpit panel display. (In a more complex system, the TDR could provide a means of combining two data input shaft angles.) If the TX stator were set so that its electromechanical zero were equal to the angle of attack and, further, if the TDR shaft were locked, then the lightly loaded output shaft of the TR would attempt to track the vane position. The TR was mechanically damped internally to reduce the tendency for the output to overshoot and oscillate. The advantage of the TDR in the signal-conditioning chain (only the TX can be called a transducer in this example), is that it is possible to easily adjust the system zero. The TDR can be set up with a mechanical friction lock and can be used to zero the TR.

The static-output of the system of Fig. 75 is

$$\theta_3 = \theta_2 + \theta_1 \quad (56)$$

By proper sizing of the TX, additional parallel TDR and TR sensors can be driven as required. For example, the pilot indicator and a data recorder may be driven from a single TX.

The torque synchro systems are not used extensively at the present time because (1) the smaller units produce low torque output; (2) in multiple receiver units, if one receiver is in error then the error is propagated to all other receivers; and (3) the receiver internal damping is mechanical and thus cannot be changed to optimize the receiver response for a specific application. Perhaps the most important limitation of the torque synchros is that the design considerations required to provide torque outputs also limit ultimate accuracy.

By constructing the synchro so that it is not a source of torque, greater accuracy can be designed into the system; however, the synchro receiver is no longer capable of tracking the synchro transmitter without an external torquing device. The natural development in synchro systems has been to use an electromechanical servo system to provide this nulling torque to the synchro receiver. Such a system is illustrated in Fig. 76. In this type of system, aircraft ac power is often used as the synchro excitation voltage e_x . In this case, a 400-Hz, two-phase servomotor is used. The rotor output voltage of the CR is either in phase or 180° out of phase with the aircraft power, depending on which side of the null the CR shaft is located. The servomotor reference voltage e_R , a fixed voltage derived from the aircraft power, is either ±90° out of phase with e_x . The servomotor is geared to the CR rotor so that the servomotor drives the CR rotor shaft until $\theta_2 = \theta_1$. At this point, the error voltage e_e from the amplifier is equal to zero. The gear train is also used to drive a mechanical load such as a potentiometer or an instrument panel indicator. The gear train used in an accurate synchro system must be of high quality to minimize backlash.

The two-speed synchro system can position shaft angles with high accuracy. For example, a system such as that shown in Fig. 76 is capable of an accuracy of ±0.1°. A two-speed servo system such as that illustrated in Fig. 77 can be used to increase the accuracy approximately by a factor of n , where n is the gear ratio between the coarse and fine synchros. The fine synchro is geared to rotate as some whole number integer n faster than the coarse synchro. The overall system accuracy approaches $1/n$ times the basic accuracy of the coarse systems. In Fig. 77, e_x and e_R are the same voltages as were defined for Fig. 76. The gear trains for these systems must be of the highest quality. Critical gears should be antibacklash gears.

In synchro systems, the CT rotor has two angles with respect to the CX rotor at which the output is zero: 0° and 180°. In the single-speed system of Fig. 76, the false null at 180° is an unstable null, and the slightest system perturbation will cause the system to search out the stable correct null. In the two-speed servo system of Fig. 77, the level sensor detects the amplitude of the coarse CT rotor output and, when it is within 90° of null on the fine CT and almost at null on the coarse CT the level sensor switches the servo system error detector from the coarse CT rotor output to the fine CT rotor output.

Under certain conditions in a two-speed system, it is possible to have a stable false null at 180°. The voltage e_s in Fig. 77 can be used to correct this condition.

The null offset voltage e_s is only required when the gear train produces an even value of n . When n is an even integer, the voltage e_s can be used to avoid a stable false fine null at 180°; e_s is not required if n is an odd integer (e_s is of the same frequency as e_x and e_r). The voltage e_s is also phased to agree with the coarse CT rotor output for rotor angles of essentially 0° to 180° and, therefore, to be 180° out of phase with this output for rotor angles of 180° to 360°. The amplitude of e_s is adjusted to shift the output of the coarse CT rotor with respect to that of the fine CT rotor by 90°. The coarse rotor is then adjusted by 90° to bring the input shaft-angle null back to 0°. These two operations cancel each other and produce a null at 0°, but the effects at 180° are additive and produce a 180° phase shift with respect to the fine frequency, thus, an unstable null.

Figure 78 illustrates why the two-speed system can achieve a stable null when the coarse CX and CT rotors are misaligned by 180°. When the gear ratio n produces an odd number of fine CT rotations (see the lower curve in Fig. 78) with respect to the coarse CT motion, the level-sensor switch operating at 180° maintains the proper phasing, and the 180° null becomes even more unstable. However, if n is an even integer (see the upper curve in Fig. 78) then when the level-sensor switches the error voltage to fine CT rotor output, the normal phase relationships for 180° are reversed, and small perturbations cause the system to lock in on a false 180° null. The addition of an appropriate voltage e_s removes this ambiguity. In the two-speed, servo-loop synchro system, the gearing is critical, expensive, complex, and increases the frictional and inertial loading of the input shaft.

An "electrical" two-speed synchro does not require a mechanical gear train to achieve what is effectively two-speed performance. The electrical two-speed synchros are constructed on a common shaft (Ref. 30, pp. 14,15). These synchros have two isolated rotors and stators. The two-speed rotation is accomplished by placing many more poles on the fine synchro. Although the coarse and fine synchros have a common shaft, the two synchros are electrically independent.

The electrical two-speed synchro is more reliable than the mechanical two-speed synchro since it has fewer moving parts. In addition, it is smaller, has less inertia, and eliminates gear limitations such as backlash, wear, and friction. Electrical two-speed synchros are expensive, but when all factors are considered they will often be the most desirable solution if the transducer, that is, the control transmitter (CX), can be changed. The electrical two-speed synchro is typically available in binary ratios (for example, 8 to 1, 16 to 1 and 32 to 1). Binary ratios are even integers, that is, since n is even, the use of the null offset voltage e_s of Fig. 77 would be required.

In this section on synchro-type transducers, the emphasis has been on accuracy. Reliability and ruggedness also justify synchro use in many applications; however, it is the accuracy that makes synchros desirable in most applications.

In the previous examples, the synchro systems were all nulling systems. Other applications require an analog or digital format for the shaft position. Electronic signal conditioners convert electrical outputs of the transducer, such as a control transmitter or resolver into an analog or digital representation of the shaft angle.

The output voltages that define the stator angle θ , are all derived from the excitation voltage, which is

$$e_x = K_1 \cos \omega t \quad (57)$$

This excitation voltage e_x is often aircraft power and as such may introduce extraneous factors owing to its variable amplitude K_1 , variable frequency ω , noise, and harmonics. The output voltage relationships for a synchro are (see Fig. 74)

$$e_{1-3} = K_1 \sin \theta \sin (\omega t + \alpha_1) \quad (58)$$

$$e_{3-2} = K_2 \sin (\theta + 120^\circ) \sin (\omega t + \alpha_2) \quad (59)$$

$$e_{2-1} = K_3 \sin (\theta - 120^\circ) \sin (\omega t + \alpha_3) \quad (60)$$

Almost all high-accuracy electronic synchro resolver decoders convert the synchro three-wire, three-voltage output to the four-wire, two-voltage resolver format. This transformation can be accomplished by means of a Scott-T transformer. The output voltage relationships for a resolver (Fig. 74c) are

$$e_A = K_A \sin \phi \sin (\omega t + \alpha_A) \quad (61)$$

$$e_B = K_B \cos \phi \sin (\omega t + \alpha_B) \quad (62)$$

In these equations, K_1 , K_2 , and K_3 are approximately equal to each other and are directly proportional to K_1 . The same is true of K_A and K_B . The angle ϕ represents the stator shaft angle. The frequency ω is that of the excitation voltage. The terms α_1 , α_2 , and α_3 are the time-phase shifts of the rotor-

stator system with respect to the excitation voltage. The terms α_A and α_B are the time phase shifts for a resolver. In an ideal system, all the α 's would be zero, and the K 's would be equal. In a real system, the time-phase shifts can be a source of significant errors, especially when the maximum accuracy is required.

Using the resolver output voltages to form a ratio produces a ratio voltage e_M ,

$$e_M = e_A/e_B = K_A \sin \phi \sin (\omega t + \alpha_A)/K_B \cos \phi \sin (\omega t + \alpha_B) \quad (63)$$

when $K_A = K_B$ (even if $K_A \neq K_B$, then K_A should be nearly equal to K_B and the ratio becomes a stable value near one) and α_A is equal to α_B ; then

$$e_M = \sin \phi / \cos \phi = \tan \phi \quad (64)$$

Thus, the ratio of e_A to e_B produces a ratio voltage e_M that is independent of amplitude variations of the excitation voltage, the carrier frequency, and the time-phase shifts! In high-accuracy systems, that is, in systems requiring accuracy greater than 1 min of arc, the signal conditioning references the output signals against the excitation voltage, and the time-phase shifts α_A and α_B limit the accuracy to less than about 1 min of arc. To achieve higher accuracy, a reference voltage e_R must be synthesized from e_A and e_B . Reference 30 illustrates one technique that can be used to generate a synthesized reference voltage that has the following characteristics:

$$e_R = K_R \cos (\omega t + \alpha) \quad (65)$$

where

$$\alpha_A = \alpha_B \text{ and } \alpha = (\alpha_A + \alpha_B)/2$$

This synthesized reference frequency now includes a time-phase shift term, α , which is the average of α_A and α_B . A phase-shift network is not desirable because the time phase-shift term varies from one resolver to another (also from synchro to synchro), and is also sensitive to temperature variations. Quadrature voltage-rejection capability is greatly increased when the reference voltage is maintained in phase with the output signals. Quadrature voltage is voltage at the same frequency as the carrier frequency but $\pm 90^\circ$ out of phase with the carrier. One of the most common sources of quadrature voltage is the speed voltage which is a function of $d\theta/dt$ (Ref. 30).

The error sources discussed account for most of the system error. Section VI of Ref. 30 includes an extensive list of error sources — over two pages of internal, external, and interface errors. When reliable production signal conditioners are used, most of these error sources will have been minimized.

Electronic signal conditioners are characterized as continuous or sampling types and have digital or analog outputs. The digital output signal conditioners are very popular; a typical signal conditioner resolves a signal to 14 binary bits (± 1.3 min of arc). This is very difficult to accomplish with an analog output signal.

A continuous signal conditioner tracks the input signal by means of real-time, trigonometric-function generators. The output of this device can be a digital or analog signal depending on the implementation technique. The tracking signal conditioner exhibits high resolution with excellent frequency response, but it is expensive. Production units are available for single- and double-speed synchro systems. Typical single-speed signal conditioner resolution is ± 1 min of arc for a 16-bit conditioner, ± 2.5 min of arc for a 14-bit conditioner, and ± 21 min of arc for a 10-bit conditioner. Dual-speed synchro systems, using a 36-to-1 speed ratio, currently achieve a resolution of ± 20 sec of arc for a 16-bit signal conditioner.

Sampling-type synchro signal conditioners have nearly the same resolution as the continuous-tracking signal conditioners discussed above and are more economical. The main limitation is that the output is sampled only once every cycle of the reference frequency; for this reason the frequency response is less than that of the tracking-type signal conditioner. This is not a limiting consideration in many applications.

The circuit of Fig. 79 is useful when angle accuracy no better than $\pm 0.5^\circ$ is required. The circuit of Fig. 79 is easily constructed and although it has limited accuracy, it has the following advantages: (1) insensitivity to minor carrier-frequency shifts (major changes can produce significant errors), and (2) it is independent of time phase shift. Its disadvantages include (1) a sample data technique subject to frequency limitations; (2) it is susceptible to errors from quadrature voltages, harmonics, and noise; (3) single frequency operation; (4) false zero at 180° ; and (5) special circuitry is required to avoid lock-up.

The digital output is taken from an n -bit counter in Fig. 79. This counter starts counting clock pulses when the Gate On signal arrives and continues until the Gate Off signal appears. After the Gate Off signal has been received, the counter data can be stored in a digital register until they are required or updated. A technique for merging these digital data into a data stream is covered later in this section.

An analog, airborne data-acquisition data encoder with an overall accuracy of 0.1% is rare. The usual technique for recording at this accuracy (at the appropriate resolution) with analog signal recorders or encoders is illustrated in Fig. 80. In this figure, channel 1 represents the transducer full scale, such as 360° for a synchro transmitter, and channel 2 represents a 10 times expansion of channel 1. In this case, each full-scale excursion of channel 2 represents 36° . Channel 1 must be recorded to identify the segment of channel 2 under consideration. A third channel could be added, again at a 10-to-1 ratio, and this third channel would be a 100 times expansion of channel 1. In practice, when the data of channel 1 are changing rapidly, it will be impossible to reduce the data on channel 3. The reduction of channel 2 data is difficult except when the measurand is essentially static. (Data reduction difficulties make this approach undesirable.) As a result, data of very high accuracy are usually recorded in a digital format.

Variable-differential transformer signal conditioning. — Figure 81 illustrates the operating principle of the variable differential transformer (VDT). The linear and rotary variable differential transformers (LVDT and RVDT) are similar in operation. The RVDT can be implemented in several ways, but the principle is identical to that of the LVDT. As can be seen in Fig. 81, an output null occurs when the movable core couples equal and opposite amounts of voltage into the two secondaries. Ideally, the sum of e_{o1} and e_{o2} at null is zero. Any displacement of the core from the null position causes more coupling of flux into one secondary and less into the other secondary, producing a net output voltage.

The output-voltage frequency is, of course, the same frequency as the excitation voltage; however, every transformer has an associated phase shift that is a function of frequency. An LVDT is typically manufactured to be used with excitation frequencies from 50 to 20,000 Hz. Normally, a VDT is designed and purchased for the specific frequency of application where the excitation and output voltage are in phase. It is important that these voltages be in phase, because the preferred signal conditioning is a phase-sensitive demodulator (PSD) and the excitation voltage is used to drive the demodulator. Figure 82 illustrates some techniques for adjusting the phase angle for LVDT and RVDT devices that are used at frequencies other than the design frequency.

The PSD is discussed in Sec. 3 (under Amplification, Attenuation, and Zero Shifting). Appendix H provides a more detailed analysis of the PSD and shows one technique for implementing a PSD, using operational amplifiers and an analog multiplier. The advantages of the PSD include excellent noise rejection and a negative polarity output for a "negative" core position. A negative core position is defined here as the core direction from null that produces an output voltage that is 180° out of phase with the excitation voltage (Fig. 81) when e_o is compared to e_x . The null voltage may not be quite equal to zero owing to transformer-generated harmonics and capacitive coupling between primary and secondary windings. This error is usually quite small, but it can be significantly reduced in most cases by the circuitry of Fig. 83. By using a center-tapped voltage reduction transformer, this null error-voltage reduction technique can easily be implemented.

Although aircraft ac power is a convenient option, several substantial limitations arise when this source is used for excitation. Aircraft power is seldom maintained at constant amplitude, and the VDT excitation must be constant to maintain a constant scale factor. Also, the aircraft power is often noisy and can contain significant harmonics. Fortunately, a PSD has good noise-rejection characteristics and has the ability to discriminate against some harmonics and quadrature components. An elusive problem occurs when an aircraft has two unsynchronized ac power sources with a common ground. With this power configuration, beat frequencies can be introduced into the signal.

The basic carrier frequency, in this case 400 Hz, limits the maximum measurand frequency. A general rule is that the carrier frequency should be 10 times larger than the highest desired data frequency. This would mean that a 400-Hz excitation frequency would allow data inputs up to 40 Hz. Even with this 10-to-one rule of thumb, a second-order, low-pass output filter (see Fig. 139 in Appendix H) is required for a good signal-to-noise ratio (in this case the noise is the ripple frequency in the demodulated waveform and is twice the excitation frequency). The type of filter response (see the discussion under Filter in Sec. 3) depends on the permissible amplitude errors and phase shifts at 40 Hz. The 10-to-1 ratio of excitation frequency to highest data frequency of interest is a general guideline, and smaller ratios may be used if greater ripple can be tolerated.

The linearity of a typical VDT is excellent over the design range, but deteriorates rapidly above this range. For example, an RVDT is typically linear to about $\pm 1\%$ of full scale over the range of $\pm 40^\circ$, and $\pm 3\%$ of full scale over the range of $\pm 60^\circ$. Above $\pm 60^\circ$, the linearity drops dramatically.

Variable-reluctance transducer. — The variable-reluctance transducer (or variable-inductance transformer) is made in many forms, including both linear and rotary position detectors and is similar to the VDT. Figure 84 illustrates four of the many variations of this type transducer. Figure 84a shows a variable-inductance linear position transducer which uses a center-tapped transformer to provide the excitation voltage and form a bridge circuit with the variable-inductance transducer. In this transducer, the movement of the ferromagnetic core from its null position increases the inductance of one arm as it decreases the inductance of the other bridge arm. This unbalances the bridge in such a way that the output of the phase-sensitive demodulator is a function of the input.

The configuration of Fig. 84b uses two "E-cores." The two E-cores and the pressure diaphragm are all ferromagnetic materials. The windings on the two E-cores are constructed such that when the iron diaphragm is centered, the magnetic reluctance of the two systems is balanced, and the output to the PSD is zero. Most of the magnetic reluctance of the circuits is the air gap between an E-core and the diaphragm. When pressure causes the diaphragm to move in one direction, it decreases the reluctance in one E-coil and increases the reluctance in the other E-coil. The signal voltage from the PSD will be proportional to the diaphragm position, and the signal will either be in phase or 180° out of phase with the excitation frequency, depending on the direction of the diaphragm displacement from null.

The Microsyn of Fig. 84c is another example of a variable-reluctance transducer. The advantage of the Microsyn is that it is capable of very low null voltages (equivalent to an angular rotation of 45 sec of arc) and can, therefore, detect very small angular displacements. The output is also very linear over a limited angular displacement (0.5% over $\pm 7^\circ$). A PSD is required to determine the direction of displacement.

The simple variable-reluctance transducer of Fig. 84d is not often used in quality airborne transducer systems. Unlike the other transducers discussed in this section, it is not a symmetrical transducer. In symmetrical transducers, when the ambient temperature changes, the corresponding inductance changes tend to be self-compensating in the bridge circuit. The inductance of the transducer in Fig. 84d does not exhibit this symmetry, and there is no inherent compensation. This transducer is quite often connected in parallel with a capacitor and an operational amplifier to create an oscillator whose output frequency f is a function of the inductance L and of the capacitance C , as shown by the following equation:

$$f = 1/(2\pi\sqrt{LC}) \quad (66)$$

A frequency-to-voltage converter can be used to convert the oscillator frequency into a dc output voltage. It should be noted that a frequency output produces the potential for very high resolution, but the associated absolute accuracy may be far less.

4.2.4 Mechano-Optical Effect Transducer Signal Conditioning

Many engineers argue that there is no "true" digital transducer. They maintain that there are only analog transducers which function as analog-to-digital converters. The digital optical shaft encoder is certainly one of the most easily visualized "digital" transducers, and it can be used to illustrate many of the typical digital transducer characteristics. In some texts, transducers with a variable frequency output are defined as digital transducers. In this text, these devices are defined as variable-frequency transducers (see the above subsection for an example of a basic variable-frequency transducer).

Mechano-optical effect transducer. - Figure 85 illustrates the mechanization of a shaft angle encoder disk. The coding format shown in Fig. 85 is generated by lights that are coupled and decoupled from their detectors by transparent and opaque segments on the coded disk. In this example, there are five coded segments on the disk. The outer segment contains 16 transparent segments (that is, 1's), and 16 non-transparent segments, (that is, 0's). In this segment the data bit, that is, a one or zero, is the least significant bit (LSB) since if an error occurs in interpreting this data bit it introduces less error than for any other bit in the data word. In Table 4 the LSB is the 1 or 0 on the right-hand side of the column titled "Straight Binary." The most significant bit (MSB) is the inner, or fifth segment. If an error is made in this segment, the shaft-angle readout is in error by 180° .

The binary (base 2) system is used to simplify interfacing to the digital-computer-based systems that play an increasingly important role in data reduction. Table 4 illustrates the conversion between decimal (base 10) and binary (base 2) number systems. A binary word which has n bits has a resolution of 2^n . The decimal number 20 in binary notation is 10100, that is,

$$20 = [(2^4) \times 1] + [(2^3) \times 0] + [(2^2) \times 1] + [(2^1) \times 0] + [(2^0) \times 0]$$

$$20 = (16 \times 1) + (8 \times 0) + (4 \times 1) + (2 \times 0) + (1 \times 0) = 16 + 4 = 20$$

$$20 \text{ (decimal)} = 10100 \text{ (binary)}$$

TABLE 4. - EXAMPLES OF DECIMAL AND BINARY NUMBERS

Decimal	Straight binary	Binary-coded decimal (Giannini's Datrex) ^a	
		Tens/digit	Units/digit
0	00000	1000	1000
1	00001	1000	1100
2	00010	1000	0100
3	00011	1000	0110
4	00100	1000	0010
5	00101	1000	0011
6	00110	1000	0111
7	00111	1000	0101
8	01000	1000	1101
9	01001	1000	1001
10	01010	1100	1000
11	01011	1100	1100
12	01100	1100	0100
13	01101	1100	0110
14	01110	1100	0010
15	01111	1100	0011
16	10000	1100	0111
17	10001	1100	0101
18	10010	1100	1101
19	10011	1100	1001

^aFrom Ref. 31.

TABLE 4. — Concluded

Decimal	Straight binary	Binary-coded decimal (Giannini's Datrex) ^a	
		Tens/digit	Units/digit
20	10100	0100	1000
21	10101	0100	1100
22	10110	0100	0100
23	10111	0100	0110
24	11000	0100	0010
25	11001	0100	0011
26	11010	0100	0111
27	11011	0100	0101
28	11100	0100	1101
29	11101	0100	1001
30	11110	0110	1000
31	11111	0110	1100
	MSB LSB		

^aFrom Ref. 31.

From Table 4 it can be seen that the 5-bit straight binary code uniquely defines 32 positions (that is, zero through 31, where zero is a position). A 10-segment shaft encoder defines 1,024 positions (that is, $2^{10} = 1024$).

Figure 86 illustrates a 5-bit optical shaft encoder with associated circuitry. This figure will be used to illustrate the digital-transducer interface characteristics. When data must be transferred at a high rate, the parallel format is used. The parallel format requires the equivalent of one channel for each bit and is therefore costly to implement. The serial format is more economical when data may be transferred at slower rates. The serial format requires but a single channel to transmit the information.

In actual practice, an optical shaft encoder would not use a straight binary code. Multiple-bit state changes at transitions from one increment to another offer the risk of incorrect transition values. Special codes are used which change only one bit in moving from one increment to another. The BCD code of Table 4 and the Gray code are examples of these types of codes.

Data encoding. — Digital data must often be sequenced into a serial train of pulses, such as the transmitter output of a PCM system. Some PCM systems have registers that can be filled for delayed output at a selected rate. When the PCM does not have this capability, such a register must be provided external to the PCM. The register must sample and hold (freeze) the transducer data at a known time.

It is not unusual to have digital transducers that have 14-to 16-bit resolution outputs. An airborne PCM system typically encodes analog signals into 9-bit digital words (roughly $\pm 0.2\%$ of full-scale resolution). To place a 14-bit digital word into a 9-bit PCM system requires that the transducer word take up two PCM word slots (that is, 18 bits), a process known as concatenation. These required interface processes are easy to implement for an experienced logic-circuit designer. The widespread use of integrated circuit functional logic modules normally makes these interfaces easier to build than the traditional analog interfaces. A further benefit is that the digital interface circuits do not require adjustment or "calibration."

4.2.5 Force-Balance-Transducer Signal Conditioning

The force-balance transducer was probably a natural evolution of the laboratory null-balance voltmeter (described in Sec. 3) and the deadweight pressure gauge. Modern high-quality transducers often incorporate electromechanical null-balance techniques into the transducer itself. These transducers are often called force-balance transducers, since the measurand generates a force that is countered servometrically by an equal and opposite electromechanical force.

In a force-balance transducer, a deflecting element is servometrically constrained to very small movements about a null position. By careful selection of the deflecting element, the force required to restrain the movement is directly proportional to the input measurand. In a pressure transducer, the deflecting element is often a bellows-type pressure sensor; in an accelerometer, the deflecting element is a pendulous mass.

Some of the advantages of the force-balance technique can be inferred from Fig. 87a. The position detector need not be calibrated as long as it has a stable zero and a large output for small deflections. (In a deflection-type system, the deflection sensor must be accurate over full scale.) The pendulous mass is restrained both electrically and mechanically (mechanically by the position detectors themselves) to very small deflections. In a deflection-type accelerometer, the deflection is dependent on the accuracy of the spring associated with the pendulous mass. In the case of the force-balance accelerometer of Fig. 87a, the system sensitivity is dependent on the pendulous mass, its radius arm, the precision of the output resistor (R), and the characteristics of the torquing coil. Reference 27 presents a concise analysis of this type of system. All of these parameters can be precisely controlled. The magnetic field strength to which the torquing coil is subjected is the most difficult parameter to stabilize over the environmental temperature range; however, the accuracy of existing systems proves that it can be done. Nonlinearities in the magnetic field and spatial non-uniformities are not important since the coil nulls at the same position each time.

Inspection of Fig. 87a reveals that when the pendulous mass is absolutely nulled, there is no error output voltage. However, with very-high-gain amplifiers, even minute mass displacements produce sizable currents. Amplifier gain must be traded off against system stability.

The force-balance transducer output is a well-buffered, high-level output signal from the internal electronics. Because of the output signal characteristics, no external signal conditioning is usually required. Figure 87a illustrates one technique that is used to implement an analog force-balance transducer. Figure 87b illustrates how the accelerometer of Fig. 87a is modified to be a 12-bit binary output transducer. Another common technique for nulling transducers is the pulse-balance technique. In this type of force-balance transducer, pulses of equal energy but of varying repetition rates are used to null the transducer. Since the pulse rate is proportional to the acceleration, this pulse-balance technique lends itself well to simple-pulse summation (integration) for measuring velocity.

Transducers constructed using force-balance techniques can be extremely accurate. What is possibly even more important is that they can be smaller and almost as economical as non-force-rebalance transducers. The accuracy of available analog accelerometers varies from $\pm 1\%$ for standard-grade accelerometers to micro-g's for inertial-grade accelerometers (Ref. 32). Most units are quite small and economical.

Analog output force-balance transducers do not ordinarily require signal conditioning. Because of extensive internal electronics, transducers are available (or can be constructed) so as to be compatible with any standard flight data-acquisition system. Since the ultimate accuracy often exceeds that of the flight-test data-acquisition system, vernier range extenders can be used (Ref. 33). When the basic channel has a high-frequency response or considerable noise on its output, this vernier channel may be very difficult to read. Details of interfacing these transducers to a flight-test data-acquisition system were discussed earlier in this section.

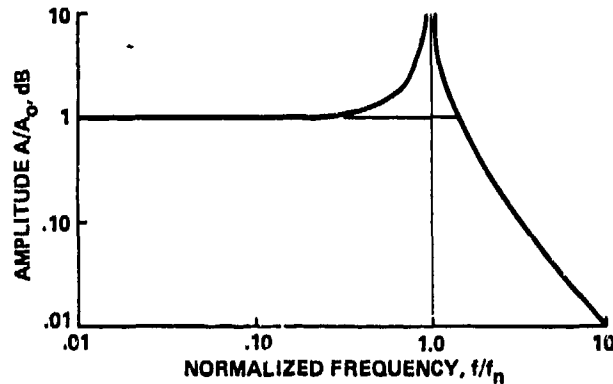


Figure 35. Undamped piezoelectric transducer amplitude response

- C_A = AMPLIFIER INPUT CAPACITANCE
- C_C = COAXIAL CABLE CAPACITANCE
- $C_o = C_T + C_C + C_A$ = TOTAL CIRCUIT SHUNT CAPACITANCE
- C_T = TRANSDUCER CAPACITANCE
- e_o = AMPLIFIER INPUT VOLTAGE
- Q = TRANSDUCER CHARGE
- R_A = AMPLIFIER INPUT RESISTANCE
- R_{CL} = COAXIAL CABLE AND CONNECTOR LEAKAGE RESISTANCE
- $1/R_o = (1/R_{TL}) + (1/R_{CL}) + (1/R_A)$
- R_{TL} = TRANSDUCER LEAKAGE RESISTANCE

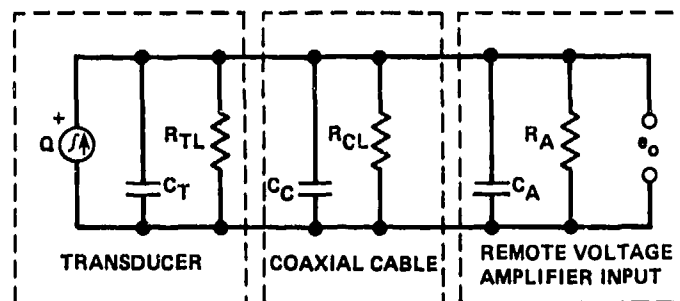


Figure 36. Piezoelectric transducer system model

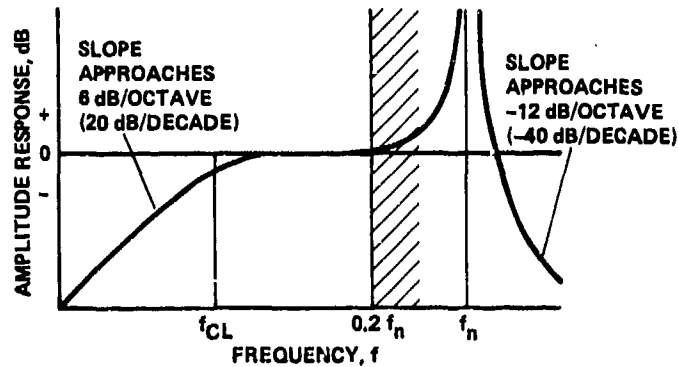


Figure 37. Combined piezoelectric transducer and voltage-amplifier response

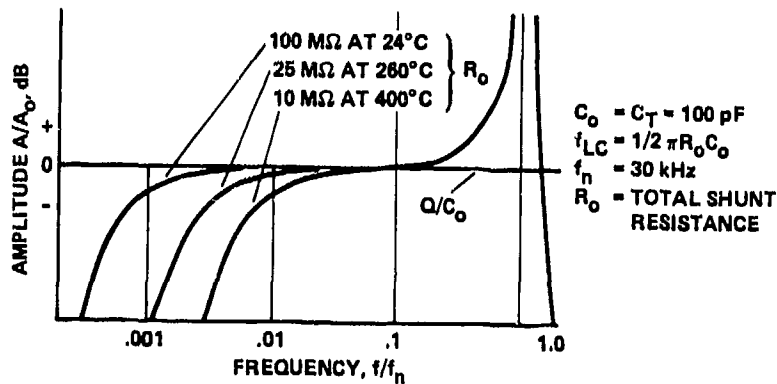


Figure 38. Temperature-related piezoelectric accelerometer frequency response

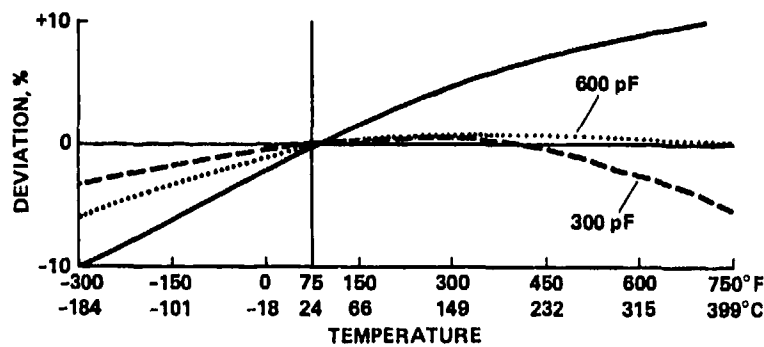


Figure 39. Piezoelectric accelerometer charge-temperature sensitivity (Solid line represents nominal change in charge sensitivity compared with temperature, and dashed lines show change in voltage sensitivity compared with temperature, for Endevco model 2273A accelerometer.)

- A' = OPERATIONAL AMPLIFIER OPEN-LOOP GAIN
- C_C = COAXIAL CABLE CAPACITANCE
- C_F = OPERATIONAL AMPLIFIER FEEDBACK CAPACITANCE
- C_T = TRANSDUCER CAPACITANCE
- e_o = AMPLIFIER OUTPUT VOLTAGE
- Q = PIEZOELECTRIC TRANSDUCER CHARGE
- R_{CL} = COAXIAL CABLE LEAKAGE RESISTANCE
- R_F = SHUNT RESISTANCE ACROSS C_F
- R_{TL} = TRANSDUCER LEAKAGE RESISTANCE

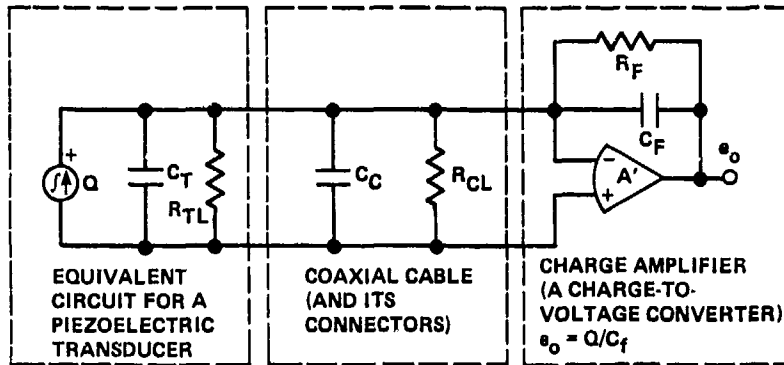


Figure 40. Transducer charge-amplifier equivalent circuit

- C_1 = ISOLATION STUD CASE-TO-GROUND CAPACITANCE
- e_N = GROUND-LOOP NOISE VOLTAGE

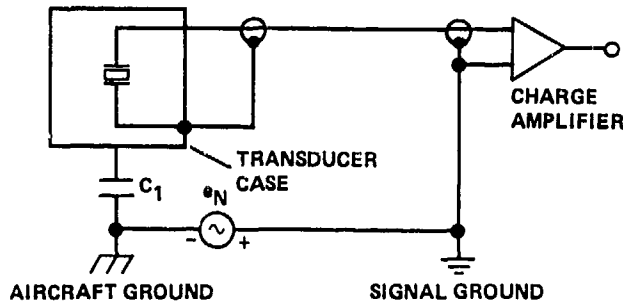


Figure 41. Transducer grounding connection

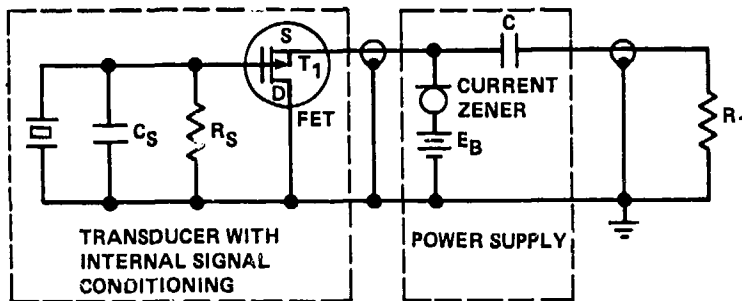


Figure 42. Piezoelectric transducer with internal impedance converter

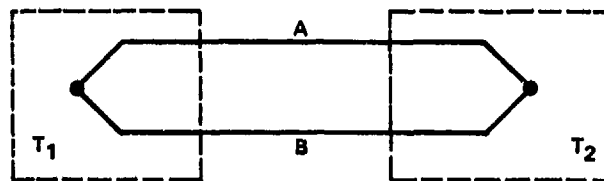
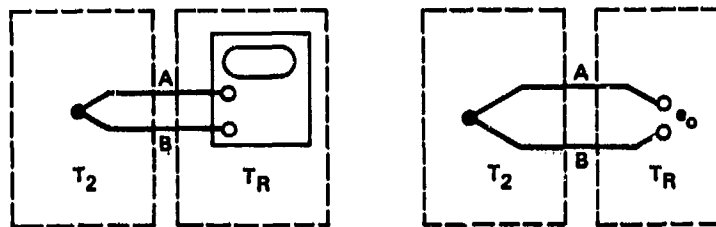


Figure 43. Simple thermocouple circuit



(a) Thermocouple temperature-measuring circuit

(b) Equivalent circuit at null-balance

Figure 44. Null-balance thermocouple temperature-measuring system

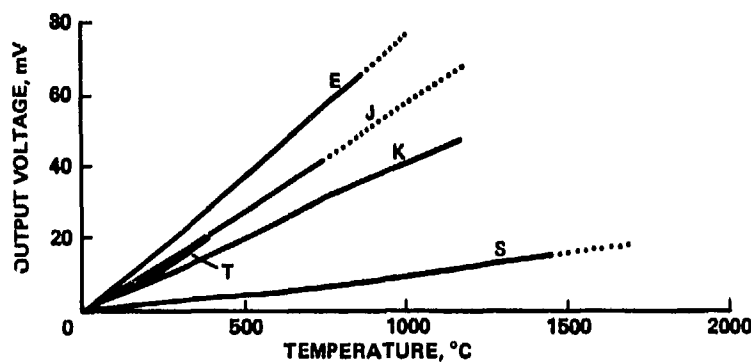


Figure 45. Thermocouple voltage-temperature characteristics

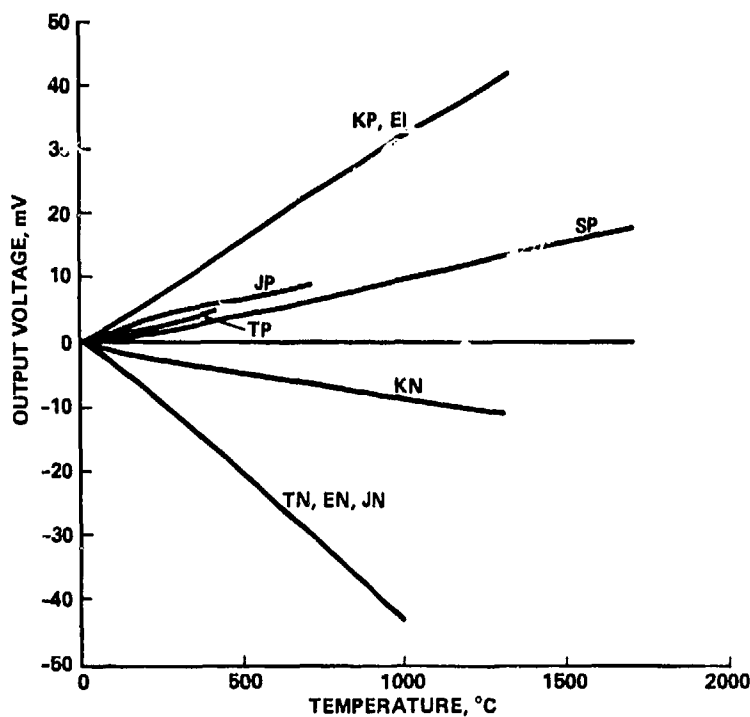
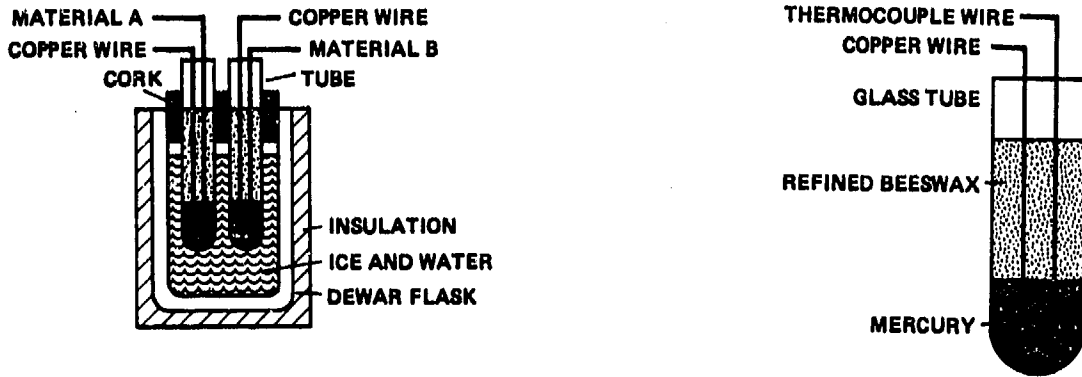


Figure 46. Thermocouple pattern-circuit temperature-voltage characteristics (Refer to Table 2. JN has slightly lower output than TN and EN and is limited to maximum temperature of 780°C.)



(a) Reference detail

(b) Tube detail

Figure 47. Ice-bath reference

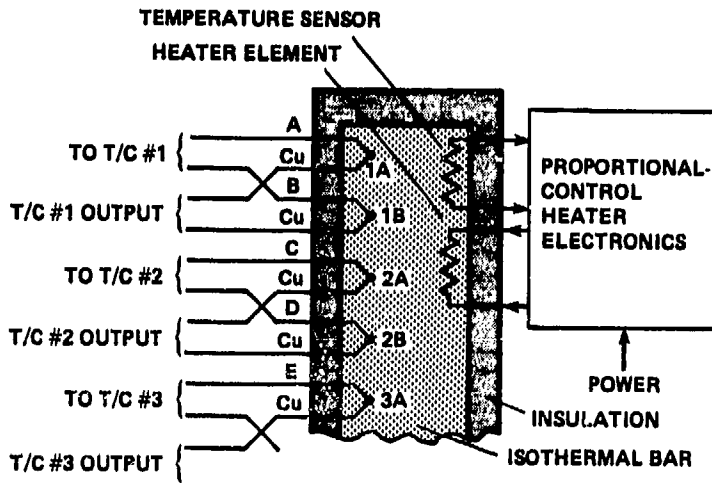


Figure 48. Reference oven for multiple thermocouples

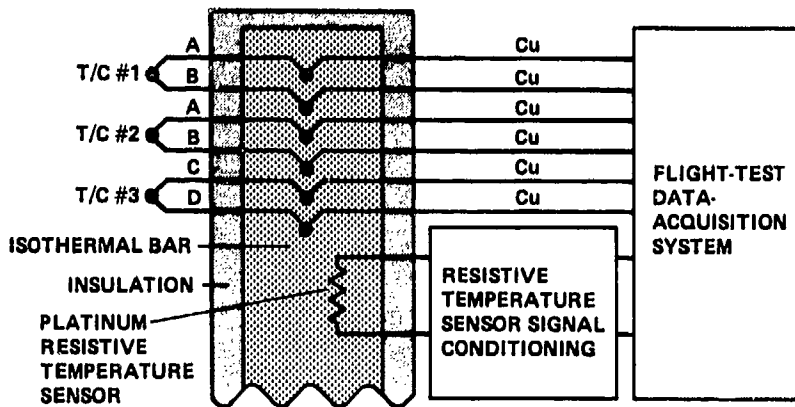


Figure 49. Zone box temperature reference system

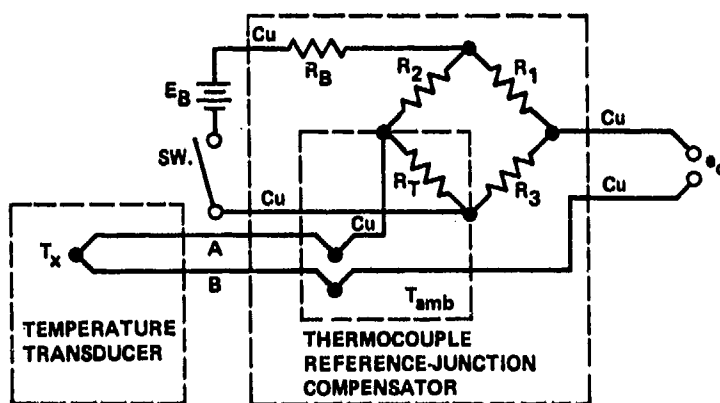
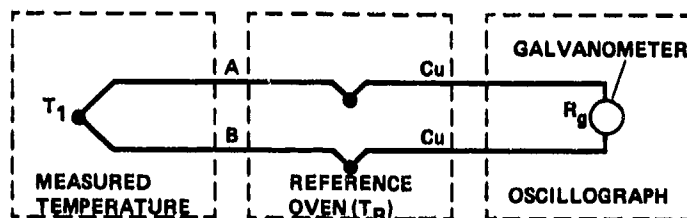
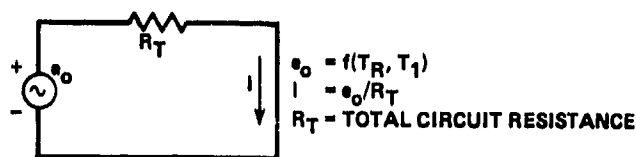


Figure 50. Thermocouple reference-junction compensator schematic



(a) Thermocouple in a galvanometric circuit



(b) Equivalent circuit of (a)

Figure 51. Galvanometric temperature-measurement circuit

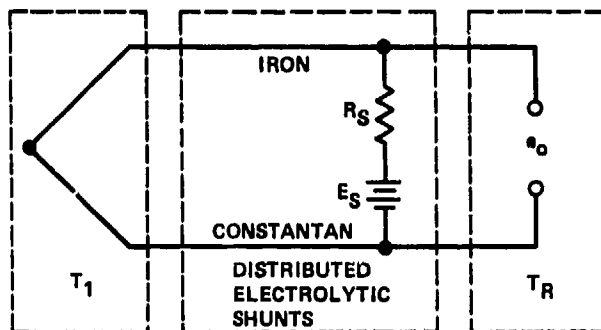


Figure 52. Galvanometric voltage electrical network model

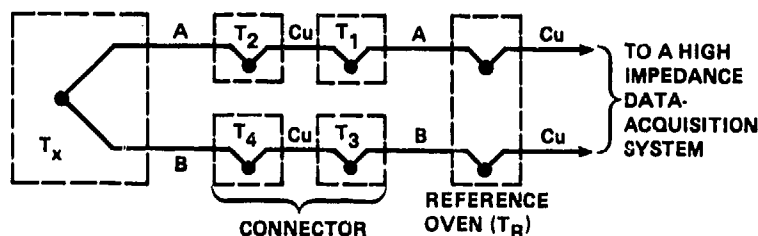


Figure 53. Thermocouple circuit including copper contacts

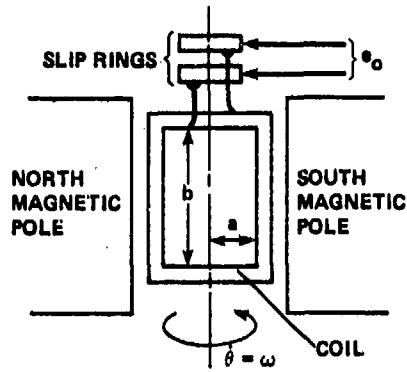
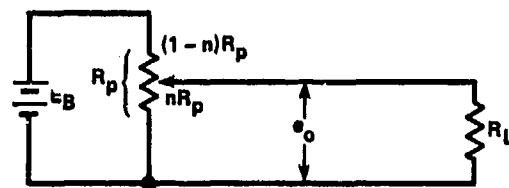
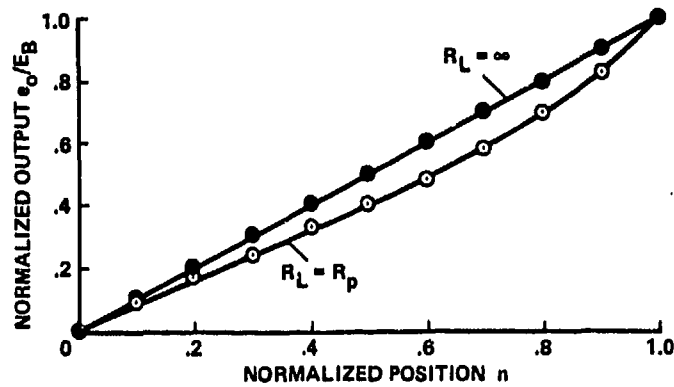


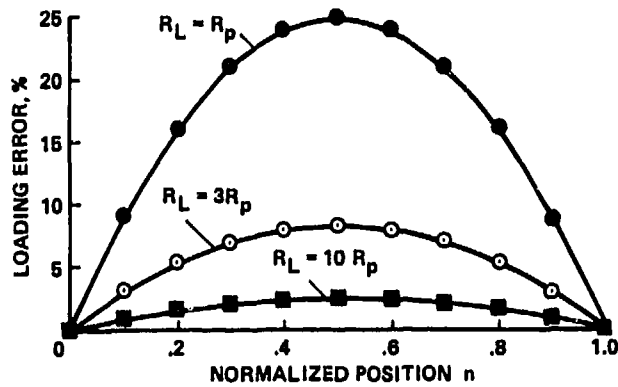
Figure 54. Self-generating tachometer



(a) Resistively loaded linear potentiometer



(b) Potentiometer loading nonlinearity



(c) Loaded potentiometer output deviation

Figure 55. Potentiometric transducer loading effects

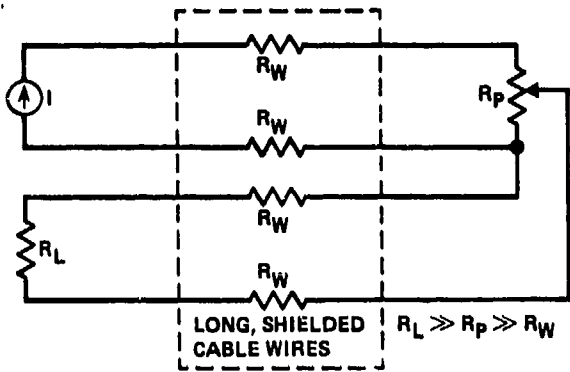


Figure 56. Low-impedance (slide wire) potentiometer sensing technique

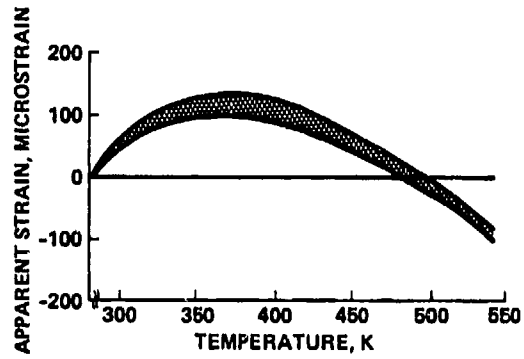
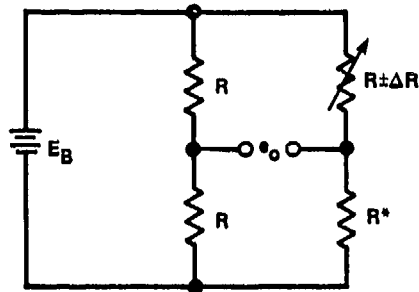


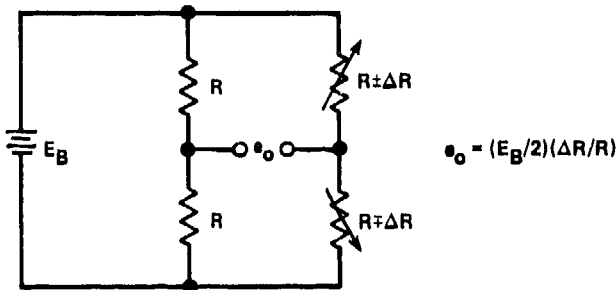
Figure 57. Apparent strain of four Karma-type strain gauges mounted on titanium alloy



$$e_o = E_B (\Delta R/R) / 2 [2 + (\Delta R/R)]$$

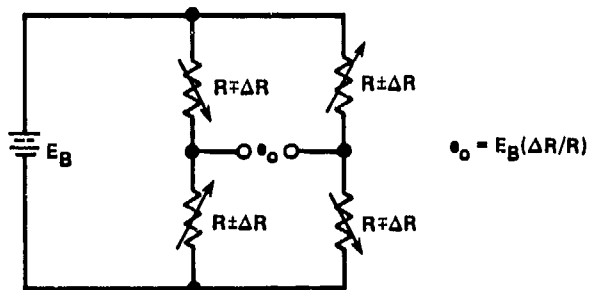
WHEN $2 \gg \Delta R/R$
 THEN $e_o = (E_B/4)(\Delta R/R)$

(a) One-active-arm bridge



$$e_o = (E_B/2)(\Delta R/R)$$

(b) Two-active-arm bridge



$$e_o = E_B(\Delta R/R)$$

(c) Four-active-arm bridge

Figure 58. Common strain-gauge bridge configurations (For high-temperature application for one-active-arm bridge, this is usually a dummy gauge-R*.)

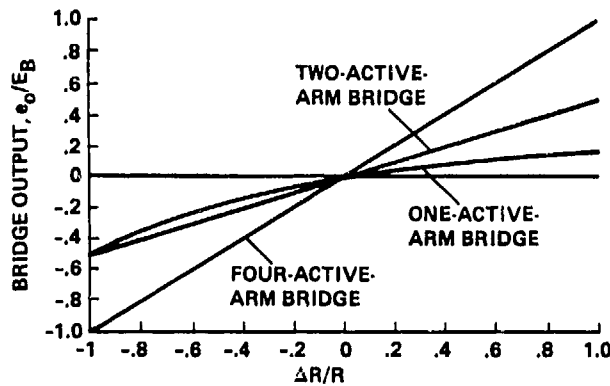
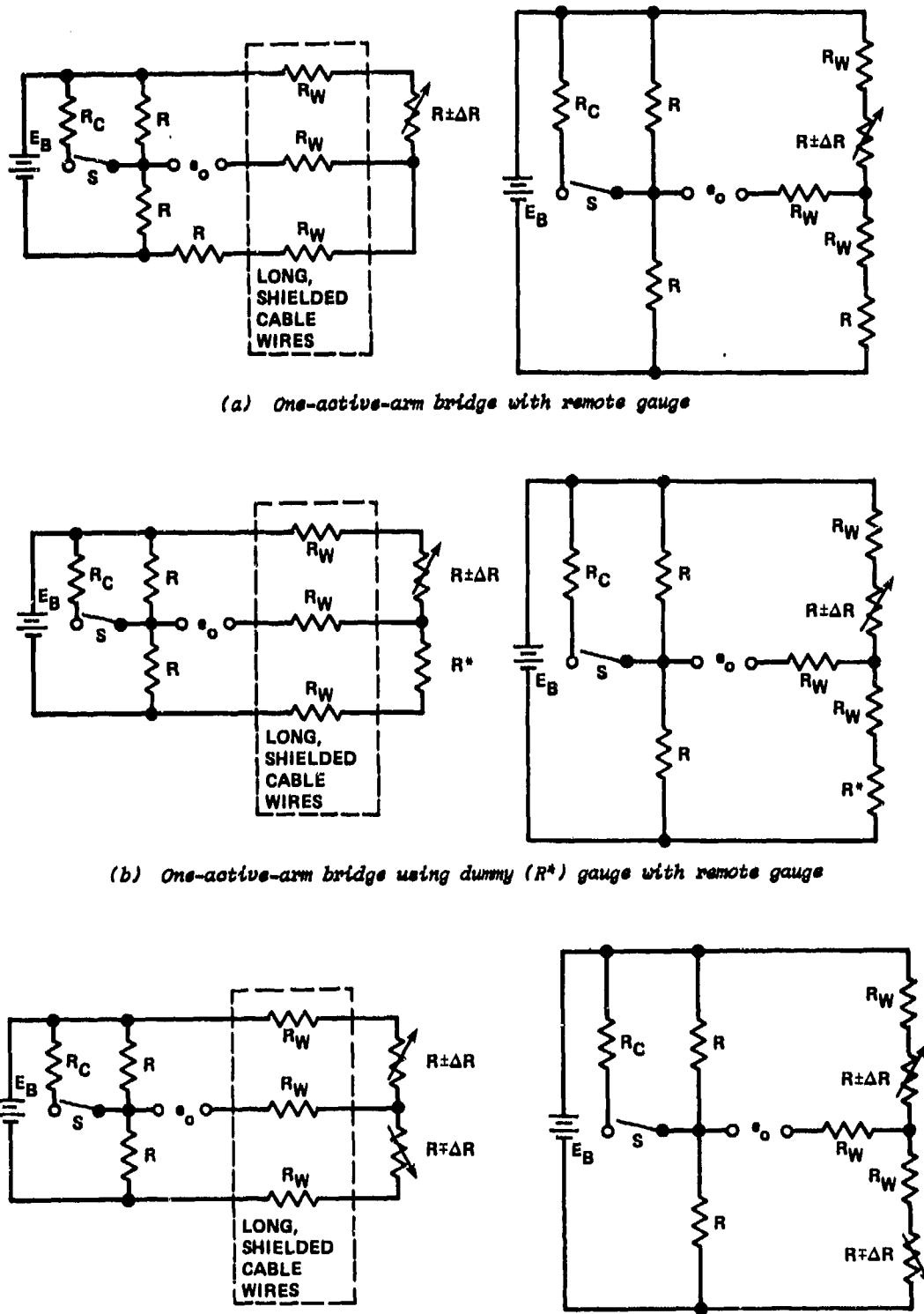


Figure 59. Idealized bridge characteristics

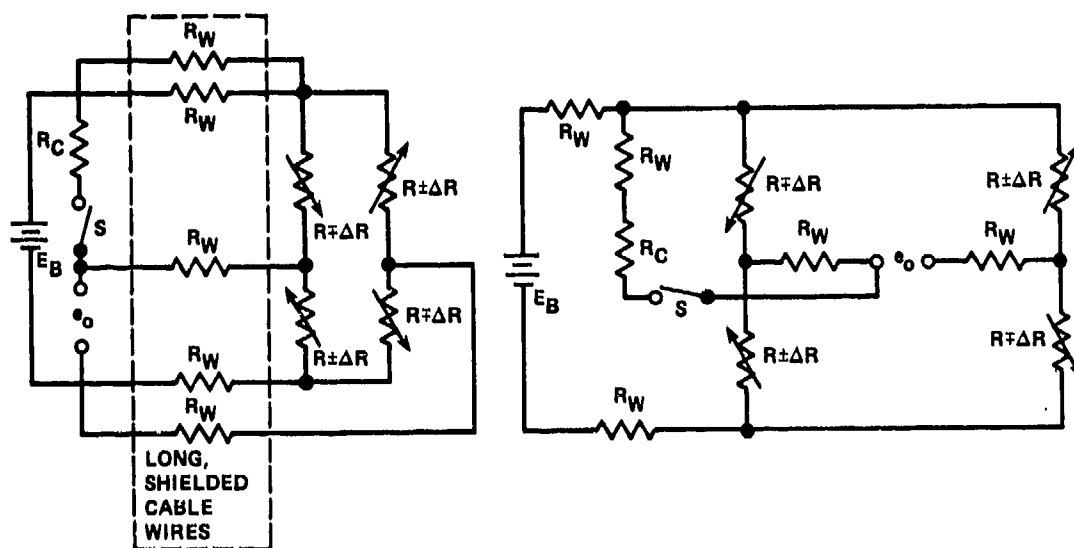


(a) One-active-arm bridge with remote gauge

(b) One-active-arm bridge using dummy (R^*) gauge with remote gauge

(c) Two-active-arm bridge with remote gauge

Figure 60. Lead-wire compensation techniques



(d) Four-active-arm bridge with remote gauge

Figure 80. Concluded

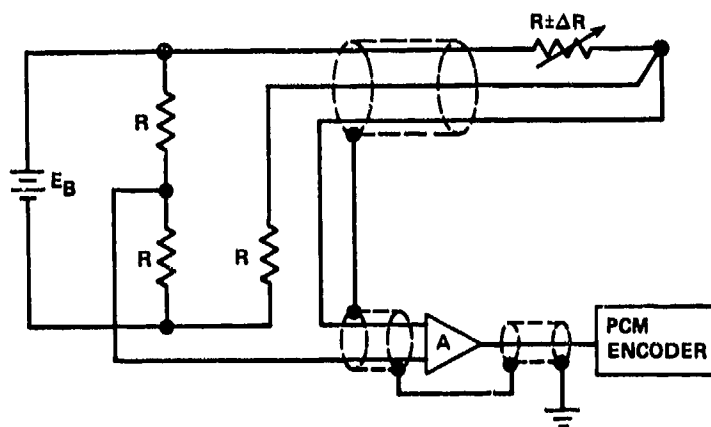


Figure 81. Typical one-active-arm strain-gauge bridge circuit

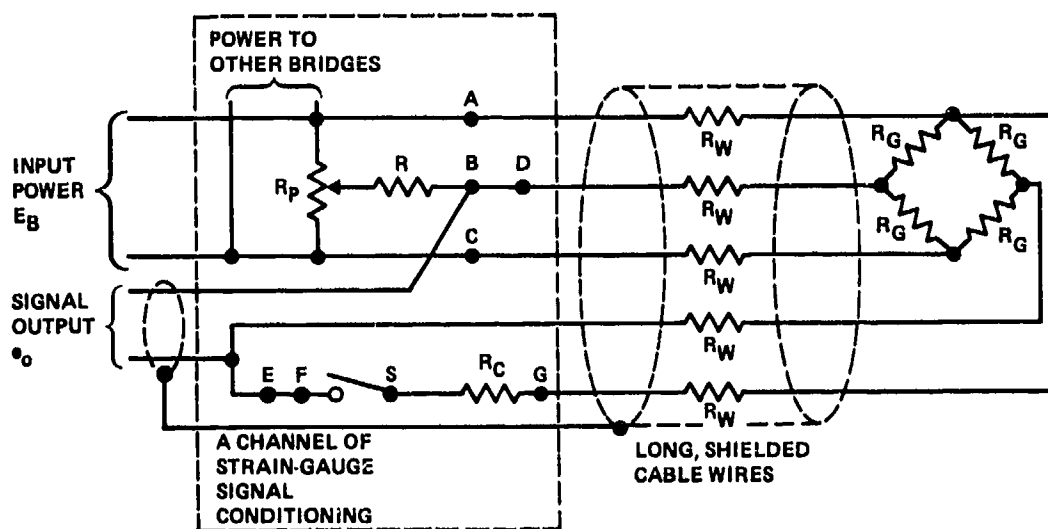


Figure 82. Typical signal-conditioning channel

- A - NICKEL
- B - BALCO
- C - TUNGSTEN
- D - PLATINUM
- E - MANGANIN (0-400°C) USED AS A NONTEMPERATURE-SENSITIVE RESISTANCE WIRE

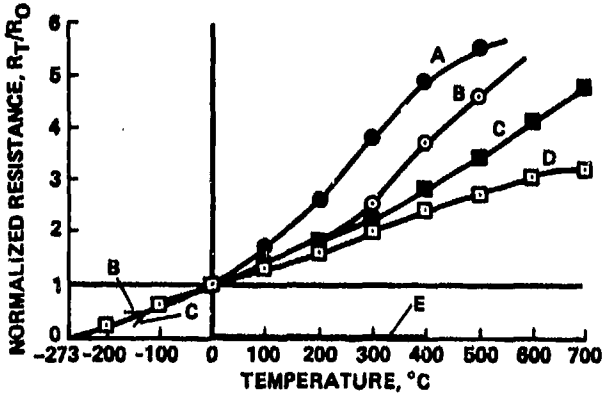
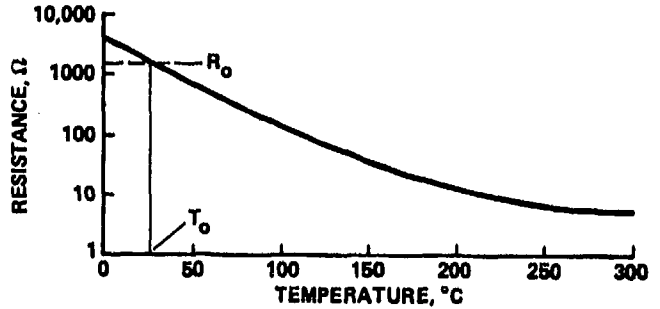
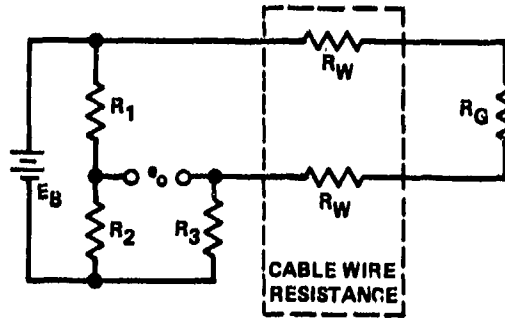


Figure 63. Normalized gauge resistance as a function of temperature

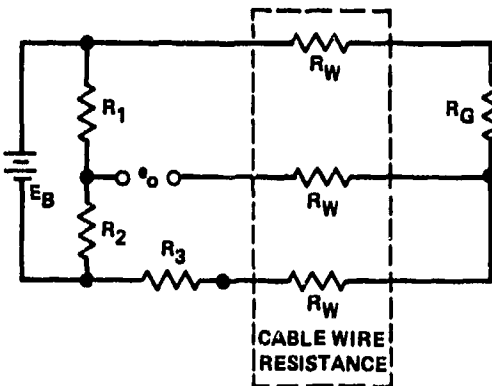


$R_0 = 2000 \Omega$
 $T_0 = 298 \text{ K (} 25^\circ\text{C)}$
 $\beta = 3495 \text{ K}$

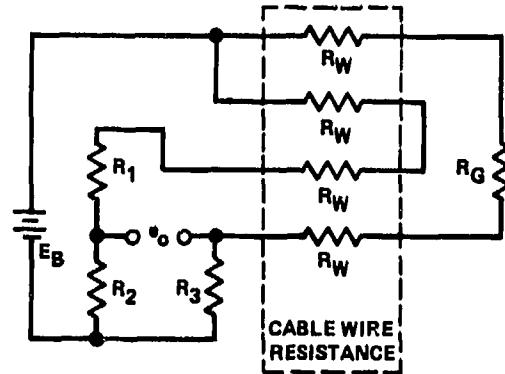
Figure 64. Thermistor resistance-temperature characteristic



(a) Two-wire format for remote temperature gauge



(b) Three-wire format for remote temperature gauge



(c) Four-wire format for remote temperature gauge

Figure 65. Bridge wiring formats for resistive temperature gauges

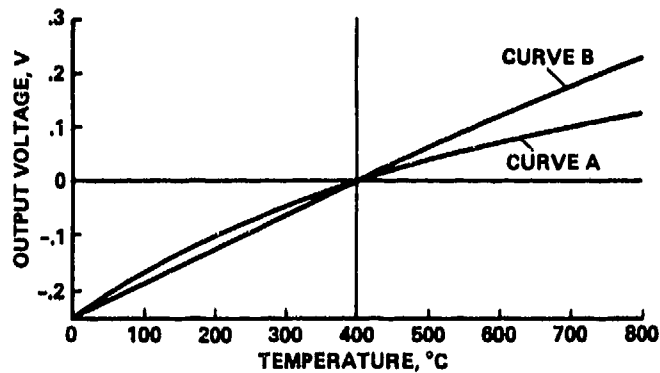
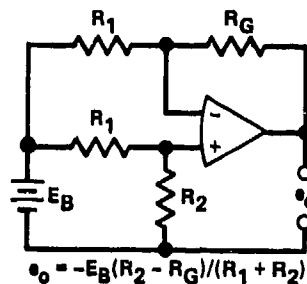
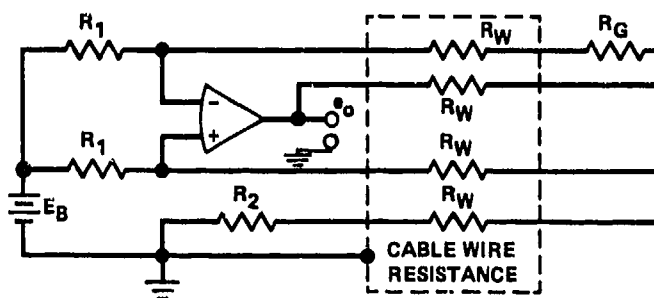


Figure 66. Linearised bridge output



(a) Linear gauge amplifier



(b) Circuit of (a) compensated for lead-wire effects

Figure 67. Amplifier used to eliminate bridge nonlinearity

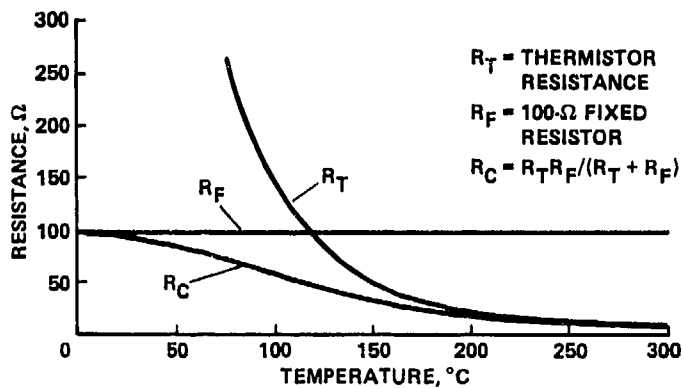
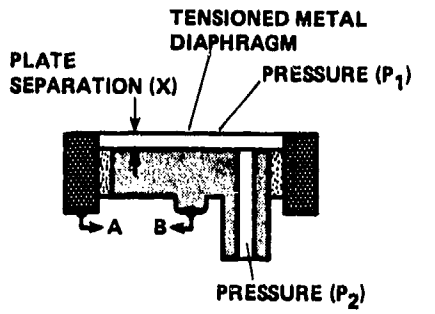
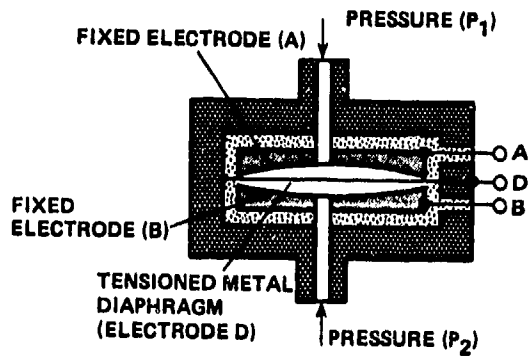


Figure 68. Linearisation of thermistor characteristic with parallel resistor



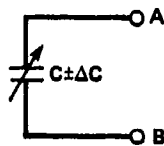
- METAL SENSOR CASE ELECTRODE A
- INSULATION
- METAL FIXED ELECTRODE B

(a) Flush-diaphragm capacitive pressure transducer

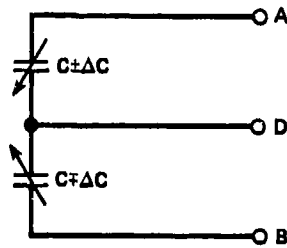


- METAL SENSOR CASE ELECTRODE D
- INSULATION
- METAL FIXED ELECTRODES (A AND B)

(b) Differential capacitive pressure transducer



(c) Flush-diaphragm transducer schematic



(d) Differential transducer schematic

Figure 69. Two capacitive pressure transducers

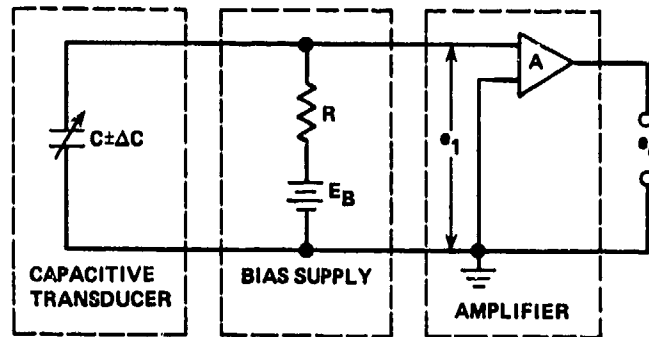


Figure 70. High-impedance amplifier used with biased capacitive transducer

- C = NOMINAL SENSOR CAPACITANCE
- C_R = REFERENCE CAPACITOR
- e_o = OUTPUT VOLTAGE
- e_x = FIXED FREQUENCY AND AMPLITUDE VOLTAGE GENERATOR
- $e_1 \rightarrow 0$
- I_C = FEEDBACK CAPACITOR CURRENT
- I_R = CURRENT GENERATED BY THE VOLTAGE GENERATOR e_x

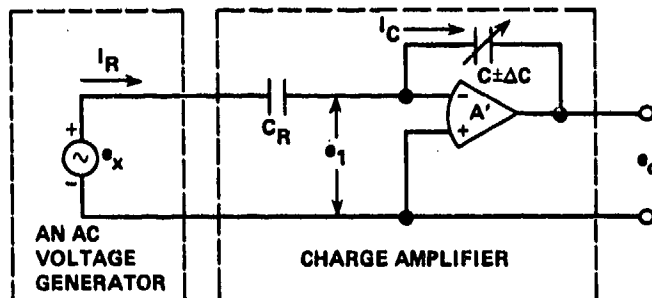
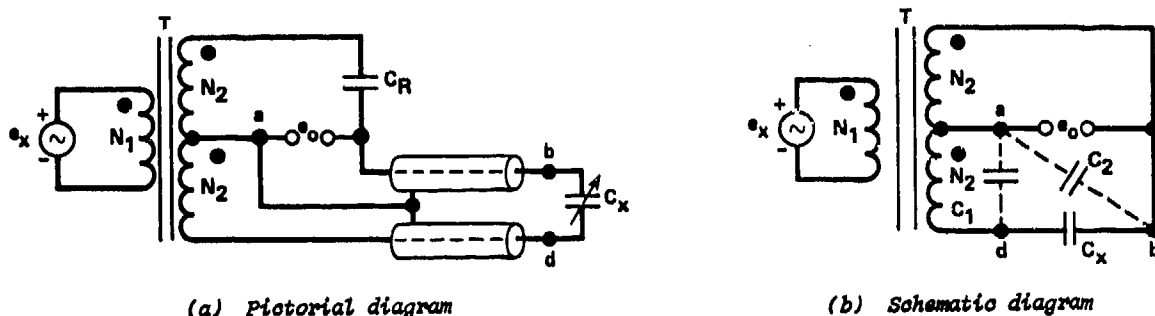


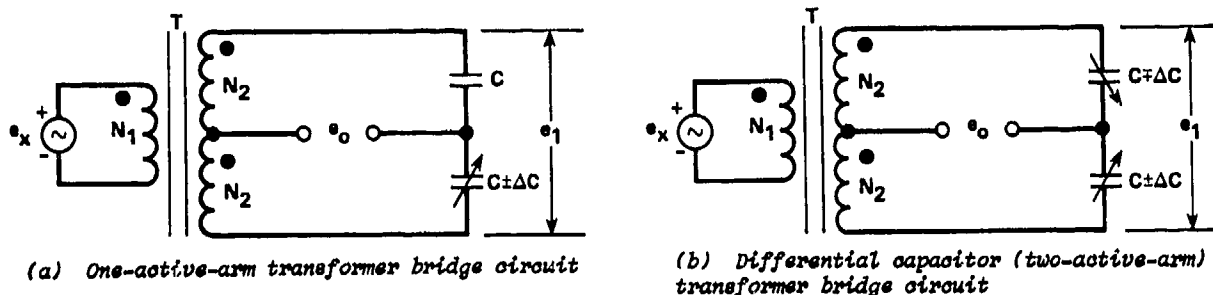
Figure 71. Charge-amplifier circuit



(a) Pictorial diagram

(b) Schematic diagram

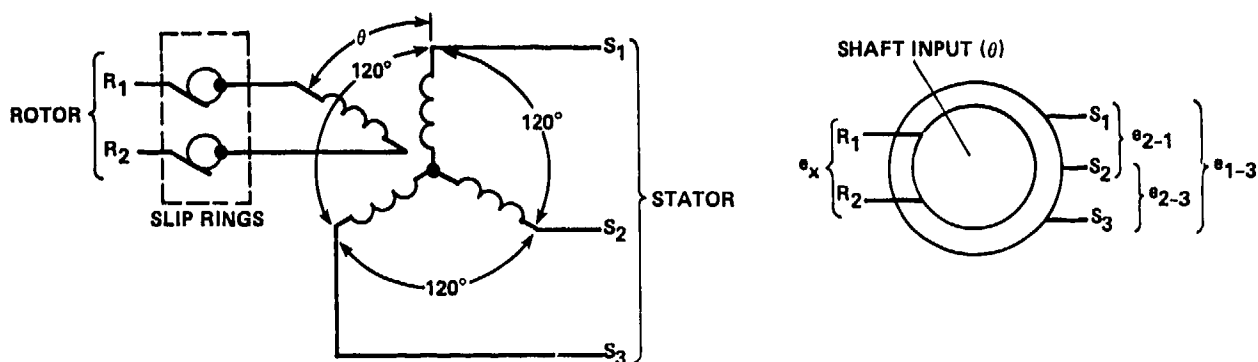
Figure 72. Equal-arm transformer bridge circuit



(a) One-active-arm transformer bridge circuit

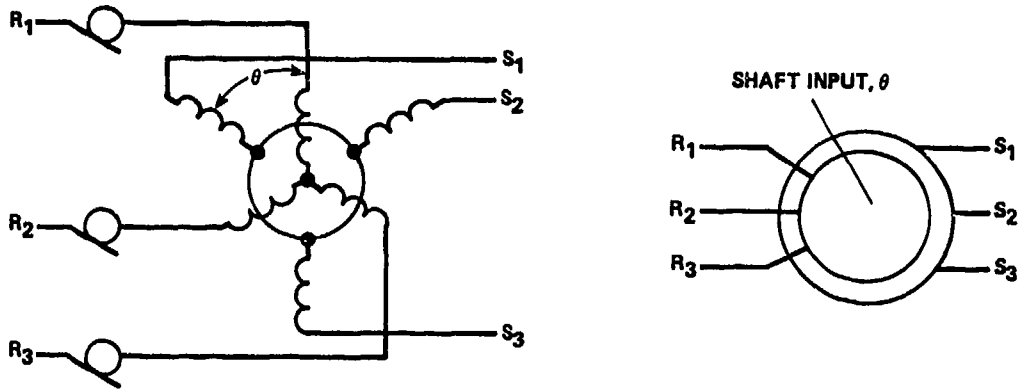
(b) Differential capacitor (two-active-arm) transformer bridge circuit

Figure 73. Transformer bridge circuits used with capacitive transducers

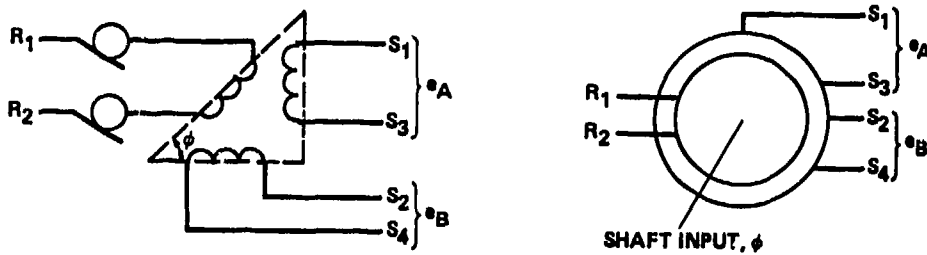


(a) Schematic diagram and symbol for torque transmitter (TX), torque receiver (TR), control transmitter (CX), and control receiver (CR)

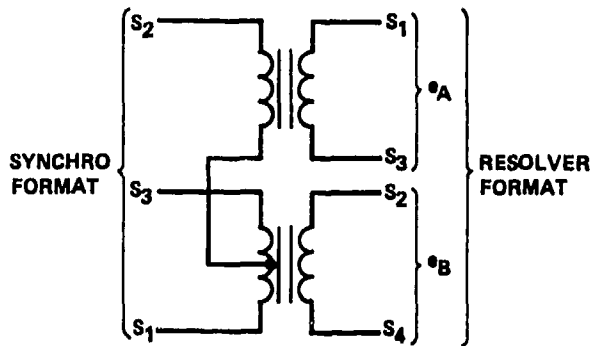
Figure 74. Common synchro hardware



(b) Schematic diagram and symbol for torque differential transmitter (TDX), torque differential receiver (TDR), and control differential transmitter (CDX)



(c) Schematic diagram and symbol for resolver (RS)



(d) Scott-T transformer

Figure 74. Concluded

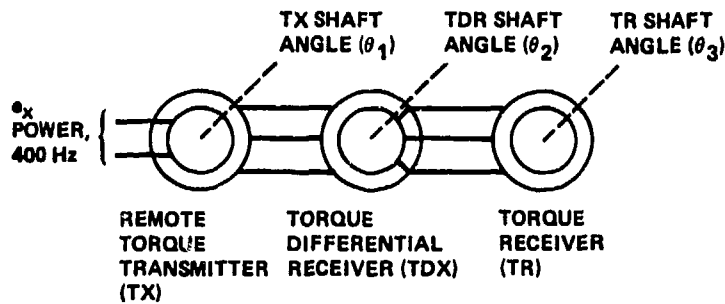


Figure 75. Torque synchro system

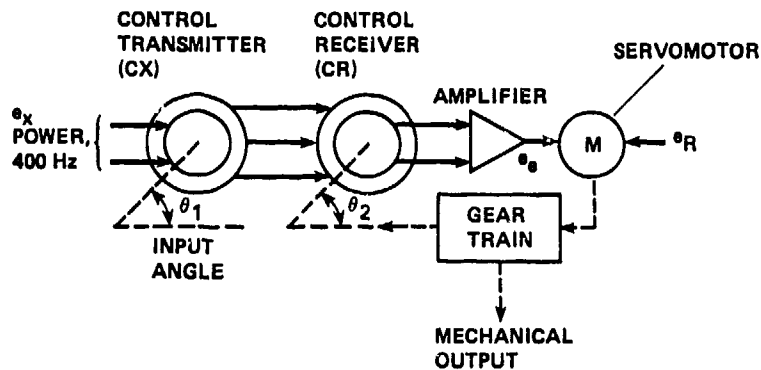


Figure 76. Servometric synchro system

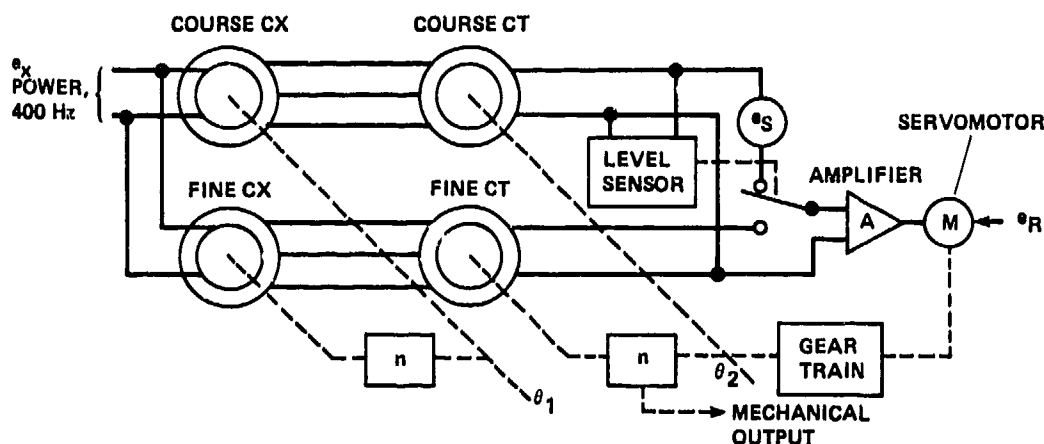
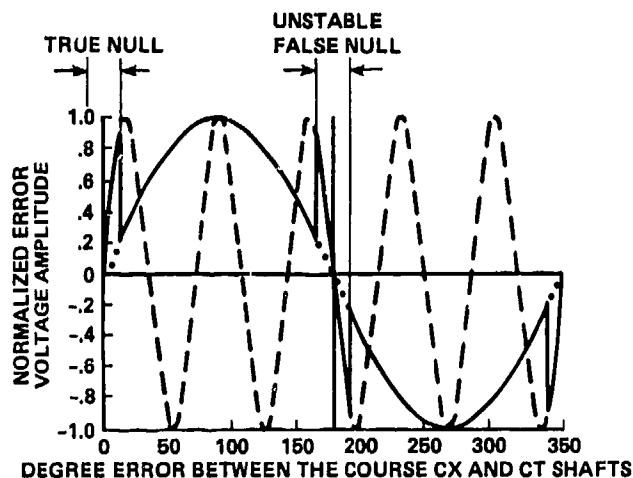
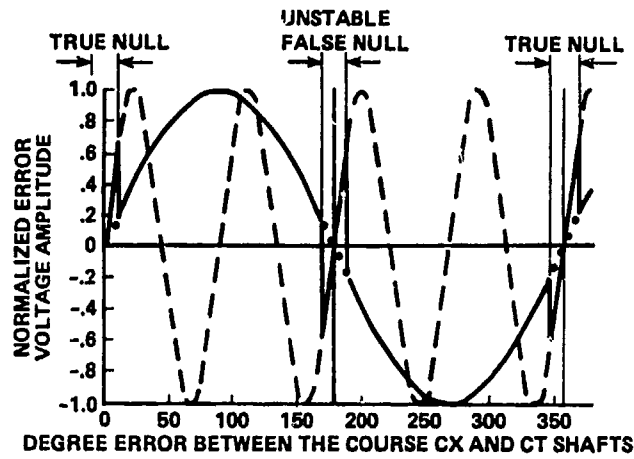


Figure 77. Two-speed servo-loop synchro system (Voltage e_s is only required if n is an even integer.)



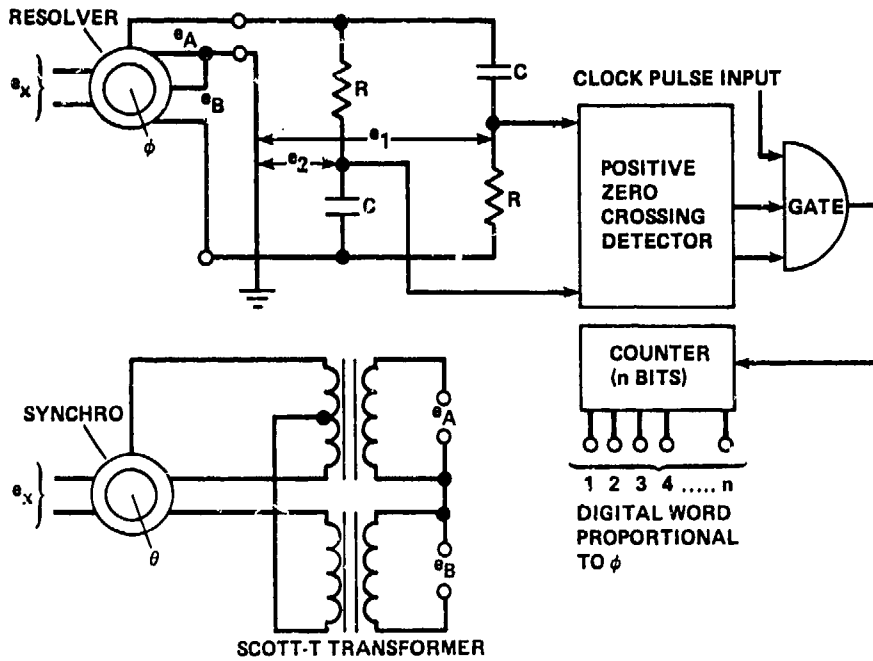
(a) Example of n equal to an odd integer ($n = 5$)

Figure 78. Error voltages in two-speed synchro system (Solid portion of two sinusoids is error voltage presented to servo error detector. Discontinuities are caused by level-sensor switch. Higher frequency sinusoid represents shaft angle of fine CT that rotates n times faster than coarse CT shaft. The low-frequency sinusoid represents shaft angle of coarse CT.)

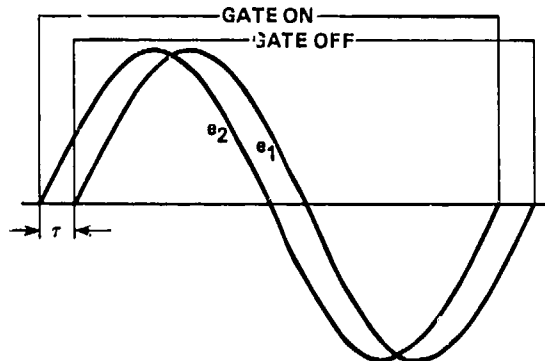


(b) Example of n equal to an even integer ($n = 4$)

Figure 78. Concluded



(a) Synchro resolver (or synchro) used with dual time-constant electronic signal conditioner



(b) Gating relationship between e_2 and e_1

Figure 79. Dual time-constant synchro electronic signal conditioner

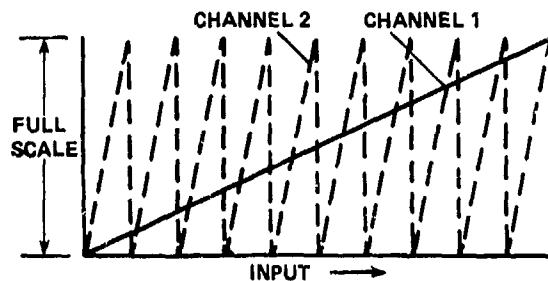
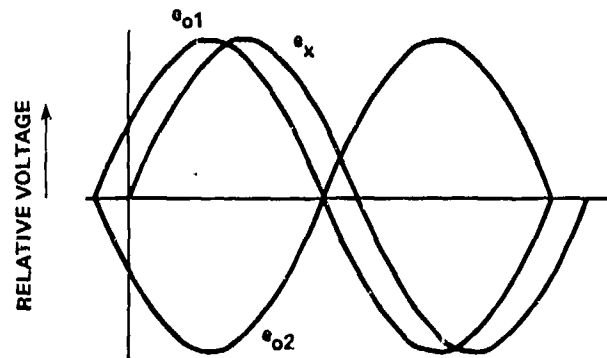
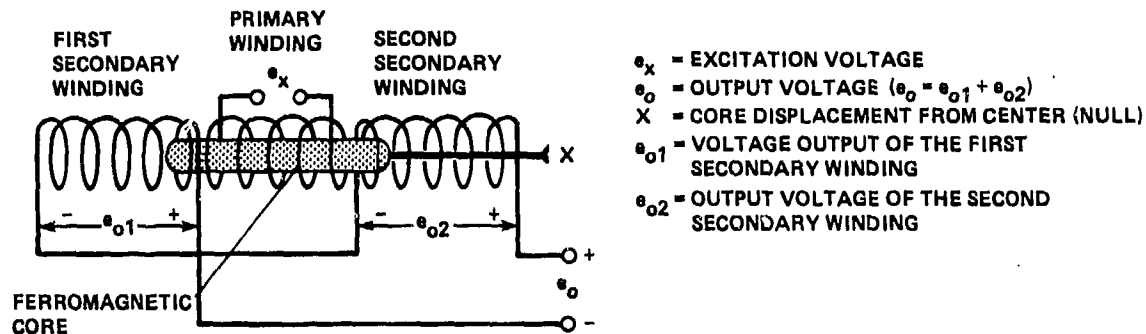
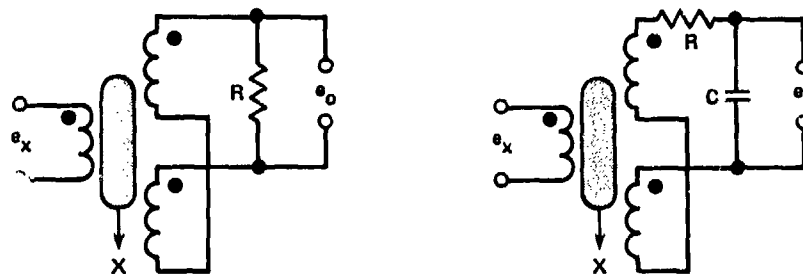


Figure 80. Two-channel, extended resolution data system

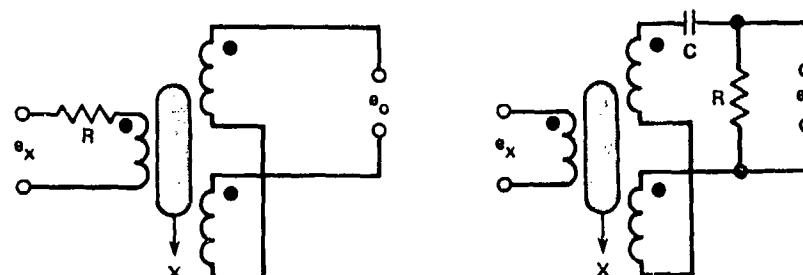


AT NULL: $e_o = e_{o1} + e_{o2} = 0$

Figure 81. Linear variable-differential transformer and waveforms



(a) Two methods of compensating for leading phase angle



(b) Two methods of compensating for lagging phase angle

Figure 82. Compensating for phase-angle errors

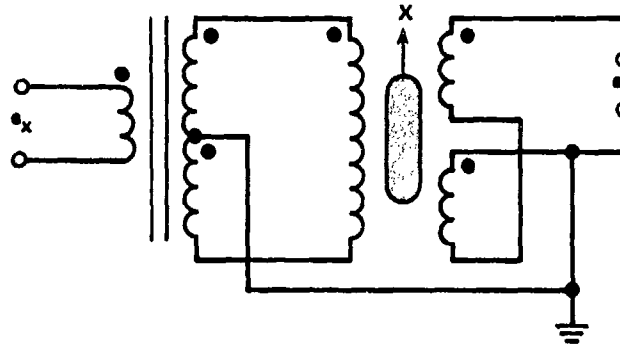
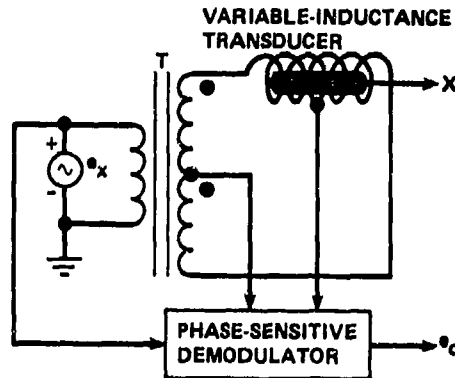
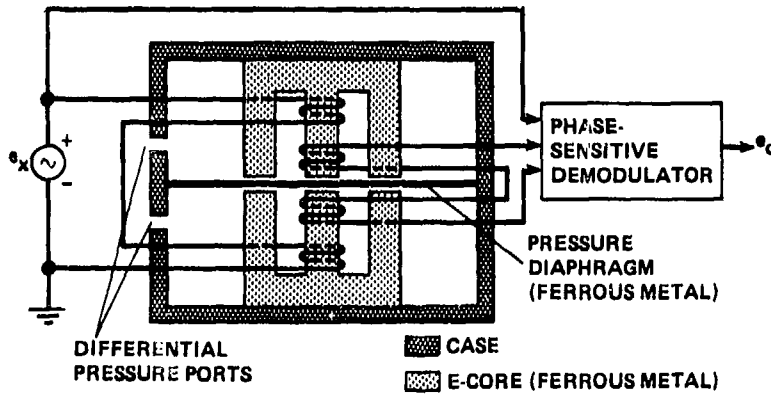


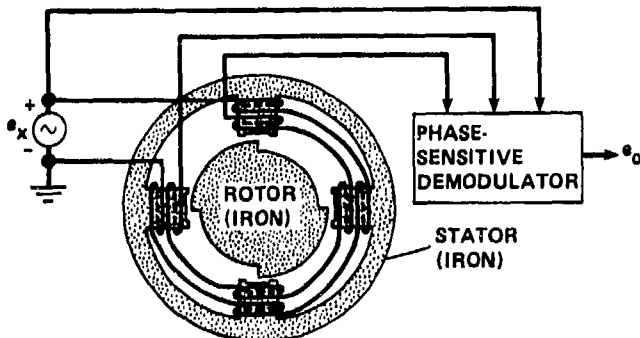
Figure 83. Null error-voltage reduction technique



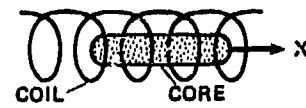
(a) Variable-reluctance position transducer



(b) Variable-reluctance pressure transducer



(c) Variable-reluctance angular position transducer



(d) Variable-inductance linear position transducer

Figure 84. Variable-reluctance and variable-inductance transducers

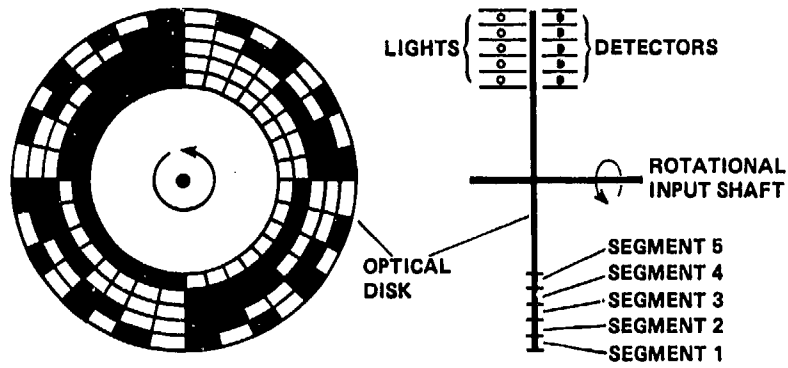


Figure 85. Straight binary code shaft-angle encoder

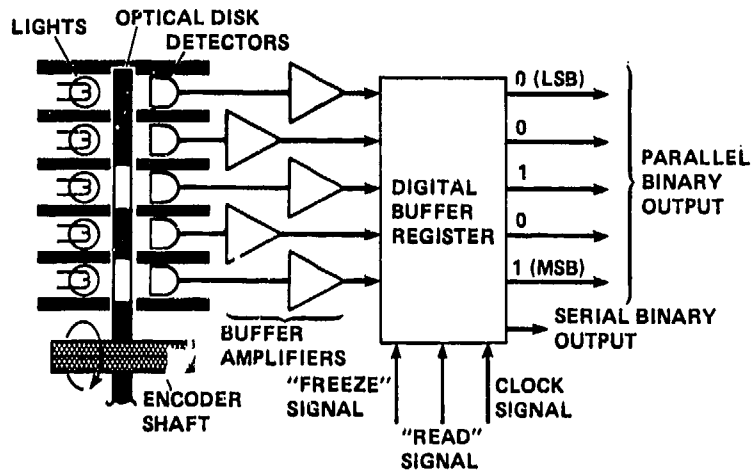
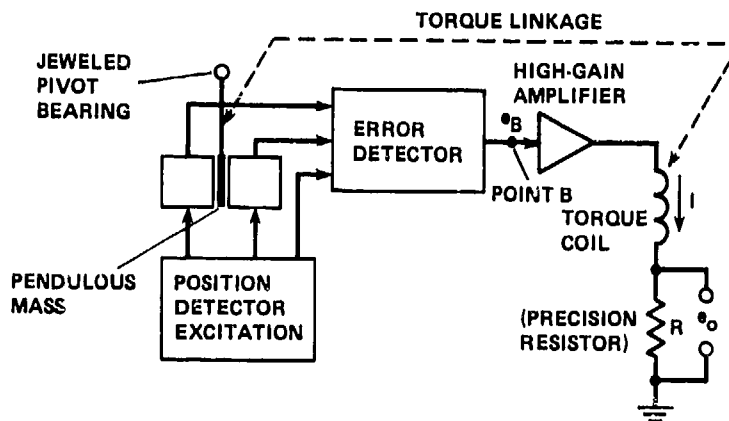
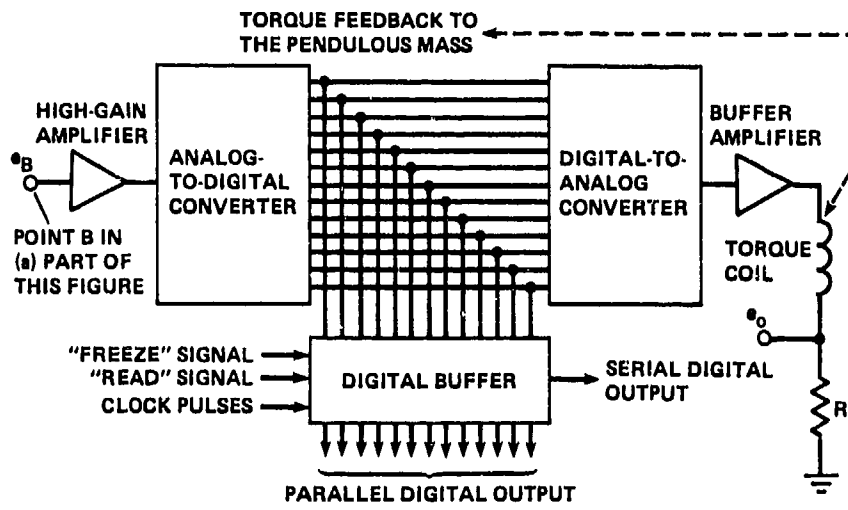


Figure 86. Optical shaft-angle encoder



(a) Analog output force-balance accelerometer

Figure 87. Force-balance accelerometers



(b) Digital output force-balance accelerometer

Figure 87. Concluded

5. MULTIPLEXERS AS SIGNAL CONDITIONERS

In the discussions of the previous sections, signal conditioning was generally used to condition a single input measurand. In actual practice, a flight-research vehicle often has instrumentation for 500 to 1,500 or even more data measurements. This same vehicle might have only one 14- or 28-channel magnetic tape recorder for on-board recording and one telemetry transmitter as a real-time aircraft-to-ground link. Obviously, a means is required to combine the many channels into a few, or even one, channel.

This is accomplished with multiplexing. There are two major types of multiplexing: frequency-division multiplexing (FDM) and time-division multiplexing (TDM). There are many ways to implement both FDM and TDM. For example FDM can be implemented using amplitude modulation (AM) techniques (such as double-sideband AM, double-sideband suppressed-carrier AM, and single-sideband suppressed-carrier AM), frequency-modulation (FM) techniques, and phase-modulation (PM) techniques. TDM can be implemented using pulse-amplitude modulation (PAM), pulse-duration modulation (PDM), and pulse-code modulation (PCM).

Of all the possible multiplexing techniques only a few are commonly used, a result of the certain demonstrated clear advantages they have over the others. Another equally important reason, is that groups such as the Telemetry Group of the Inter-Range Instrumentation Group (IRIG) of the U.S. military test and evaluation ranges have investigated the technical limits of the more useful techniques and have established standards for these systems. Reference 34 lists IRIG standards for range users and includes standards for frequency-division multiplexing (both for proportional- and constant-bandwidth FM multiplexing), PCM, and PAM. These standards are the results of considerable effort to develop workable and documented systems. For example, the test leading to the IRIG FM standards is extensively documented in Ref. 35. Once these standards are established, all the U.S. military ranges adopt the standards. All U.S. Government agencies, such as NASA, and aircraft companies who use these ranges employ equipment that meet these standards. Other test groups often adopt equipment conforming to these IRIG standards because it is readily available, economical, and its various characteristics are well documented. Thus, equipment manufacturers meeting these standards have a wide market for their equipment and this may lower prices.

Although the IRIG standards may not provide the best solution for each specific problem, they do provide economical answers to the general problems, known and well-documented system characteristics, and systems that can be used without major modifications on a wide variety of flight-test ranges. The main disadvantage is the limiting of competitive techniques; however, most range users and operators realize that standardization has many more advantages than disadvantages.

Although not widely known, FDM techniques exhibit aliasing effects under certain conditions. Most FDM systems are designed with the carrier-frequency deviation much greater than the highest data frequency. When this condition is violated, aliasing effects can damage the reconstructed data. Although FDM offers a theoretically infinite resolution capability, when sound design practice is not observed, it may exhibit the same aliasing effects that are usually associated only with TDM techniques.

5.1 TIME-SAMPLED DATA AND ALIASING

All time-division multiplexing (TDM) systems are subject to aliasing. This discussion will concentrate on a practical approach to the solution of aliasing problems. For an in-depth analysis of aliasing, the reader should refer to Ref. 10. This reference also provides an excellent, concise coverage of the airborne pre-sampling filters and interpolation filters.

Before delving into the techniques of reducing aliasing error, a short explanation of aliasing is appropriate. In TDM systems, a data channel is sampled at specific intervals. In a typical flight-test data-acquisition system, these samples are normally taken at equal intervals. Unless the engineer places some restrictions on the frequency spectrum of the input data channel, he has no information about what happened between the time the data was sampled. These restrictions on the input-data-channel frequency effectively limit the rate of change of data between data samples. Typically, this is accomplished by means of pre-sampling filters.

Figure 88 illustrates how aliasing can affect various sinusoidal data inputs. Curves 1a, 1b, and 1c illustrate how a sinusoidal input signal (1a) sampled five times per cycle (1b) would be reconstructed (1c). Curve 2, a composite, shows how a sinusoidal signal sampled two times per cycle could be reconstructed; however, curve 3 illustrates the loss of amplitude information which can occur when the two-sample-per-cycle limit is reached. Curve 4 is particularly interesting since at 1.25 samples per cycle, the reconstructed data frequency is identical to that of curve 1, even though the sinusoidal data frequency is 4 times higher than that of curve 1.

Without further information, once the data of curve 4 in Fig. 88 have been sampled, they are irretrievably lost. For example, if the sampling rate was 10 samples/sec and the input frequency was 8 Hz, the data would be reconstructed as a -2 Hz signal. This effect is called aliasing.

The graph in Fig. 89 is included to help visualize the effect. As can be observed from this graph, in a TDM system no output frequency f_0 can exist higher than one-half the sampling rate; that is, $f_s/2$. This frequency, $f_s/2$, is called the Nyquist frequency, or folding frequency. Any input frequency f_i higher than the folding frequency $f_s/2$, appears in the data output as a frequency of zero to $f_s/2$, as shown in the graph. A point worth noting is that any frequency that is exactly an even multiple of the sampling frequency, that is, $f_i = nf_s$ (where n is an integer) will always produce a steady-state output.

To help illustrate Fig. 89 assume f_s is 10 samples/sec; then, for example, the output frequency is 1 Hz for input frequencies of 1, 9, 11, 19, 21, 29, 31, 39, 41, and so on until the sampling system can no longer respond.

How does one avoid aliasing problems? There are several general approaches;

1. Use bandwidth-limited transducers that restrict the highest data frequency
2. Use established wiring and signal-conditioning techniques (Ref. 3) to reduce noise inputs
3. Avoid inputs above the folding (Nyquist) frequency, such as aircraft ac power pickup, and shelf resonances for accelerometers
4. Use pre-sampling filters to restrict high-frequency data

All of the above are recommended instrumentation practices.

One way of reducing aliasing involves increasing the sampling rate, usually in conjunction with pre-sampling filters. Figure 90 is used to illustrate how this technique is applied. In Fig. 90, a frequency spectrum is presented of an accelerometer mounted on an instrumentation shelf. The accelerometer has a frequency response of 0 to 40 Hz and is mounted on a shelf that has a 37-Hz resonance. The accelerometer is a force-rebalance accelerometer and is used to detect gross aircraft body motions. The engineer expects the highest frequency of interest (f_m) to be no more than 4 Hz. In theory, a sampling frequency slightly greater than 8 Hz, that is, $2f_m$, could define the data. In practice, engineers usually specify some sampling rate 4 to 10 times the highest frequency of interest, f_m . A commonly used number is a sampling rate of $5f_m$. The difference between the theoretical $2f_m$ and the often quoted $5f_m$ is the penalty paid for filters that are less than ideal. In this example, a $5f_m$ sampling rate would be 20 Hz. Any input frequency greater than 10 Hz, that is, $f_s/2$, would be folded back into the spectrum of 0 to 10 Hz. For example, without filtering, the 400-Hz power pickup would appear as a dc offset in the signal and the 37-Hz shelf resonance would appear as a 3-Hz data signal. After sampling has been performed, it is impossible to distinguish the desired data from the aliased data.

By using a second-order filter with a cutoff frequency of 5 Hz, a signal at 10 Hz will be attenuated by 12 dB, and a signal at 20 Hz will be attenuated by 24 dB. The advantages of filtering have to be weighed against the amplitude and phase errors introduced (see Ref. 34). In this example, if the accelerometer was located in a vibrationally noisy environment (for example, near a jet engine, as sometimes happens when trying to get measurements near the vehicle c.g.) then it would be desirable to increase the sampling rate to 40 samples/sec and to use a fourth-order filter with a cutoff frequency of 5 Hz.

In practice, many well-behaved data channels may not require any sophisticated anti-aliasing filters. A simple first-order passive filter is often sufficient to reject mild aircraft electrical power pickup. One precaution is worth noting. Engineers tend to set sampling frequencies at convenient numbers such as 2, 4, 10, 20, 40, or 100, samples/sec. Unfortunately, the aircraft power frequency of 400 Hz is an even multiple of these frequencies. Even a filtered channel will sometimes have enough residual noise at this frequency to produce appreciable aliasing errors. Since 400 Hz is an even multiple of these sampling frequencies, the aliasing error will appear as a steady-state offset signal. If the basic sampling frequency can be offset some prescribed small amount, the aliased image of the 400-Hz input will be a distinctive frequency and easier to detect by visual inspection.

5.2 FREQUENCY-DIVISION MULTIPLEXING

Proportional-bandwidth FM and constant-bandwidth FM (PBFM and CBFM) systems are the most widely used frequency-division multiplexing (FDM) techniques. Table 5 lists the IRIG-recommended proportional-bandwidth FM subcarrier frequencies. Table 6 lists the IRIG-recommended constant-bandwidth FM subcarrier frequencies. Figure 91a and 91b illustrate partial frequency spectrums for these two FDM techniques. These are obviously not the only combinations; however, the characteristics are well known, and hardware that meets these standards is readily available.

As can be seen from Fig. 91c one way to implement an IRIG CBFM system is to connect each data channel to a subcarrier oscillator (SCO). The SCO is a voltage-controlled oscillator (VCO), with a center frequency corresponding to the center frequencies of Table 5 or 6. By appropriate selection of VCOs, a frequency spectrum such as those shown in Figs. 91a and 91b and described in Tables 5 and 6 can be developed. Any given channel can be located within its assigned frequency bandwidth. Proportional bandwidth and constant bandwidth are the dominant FDM formats. A discussion follows of the salient characteristics.

5.2.1 Proportional-Bandwidth FM-Type FDM Systems

If the engineer has a research vehicle that requires multiplexing 25 data channels into a single channel and input data frequency spectrums that range uniformly from a narrow bandwidth (that is, 0 to 6 Hz) to a wide bandwidth of about 0 to 8.4 kHz, the IRIG PBFM system with its $\pm 7.5\%$ deviation may be the desirable system. When a multitrack magnetic tape recorder is available, more than one group of 25-channel proportional-bandwidth arrays can be recorded, assuming the tape frequency bandwidth can accommodate them.

TABLE 5. — PROPORTIONAL-BANDWIDTH FM SUBCARRIER CHANNELS

Channel	Center frequency, Hz	Lower deviation limit, ^a Hz	Upper deviation limit, ^a Hz	Nominal frequency response, Hz	Nominal rise time, msec	Maximum frequency response, ^{a,b} Hz	Minimum rise time, ^b msec
±7.5% Subcarrier deviation channels							
1	400	370	430	6	58	30	11.7
2	560	518	602	8	44	42	8.33
3	730	675	785	11	32	55	6.40
4	960	888	1,032	14	25	72	4.86
5	1,300	1,202	1,398	20	18	98	3.60
6	1,700	1,572	1,828	25	14	128	2.74
7	2,300	2,127	2,473	35	10	173	2.03
8	3,000	2,775	3,225	45	7.8	225	1.56
9	3,900	3,607	4,193	59	6.0	293	1.20
10	5,400	4,995	5,805	81	4.3	405	0.864
11	7,350	6,799	7,901	110	3.2	551	0.635
12	10,500	9,712	11,288	160	2.2	788	0.444
13	14,500	13,412	15,588	220	1.6	1,088	0.322
14	22,000	20,350	23,650	330	1.1	1,650	0.212
15	30,000	27,750	32,250	450	0.78	2,250	0.156
16	40,000	37,000	43,000	600	0.58	3,000	0.117
17	52,500	48,562	56,438	790	0.44	3,938	0.089
18	70,000	64,750	75,250	1,050	0.33	5,250	0.067
19	93,000	86,025	99,975	1,395	0.25	6,975	0.050
20	124,000	114,700	133,300	1,860	0.19	9,300	0.038
21	165,000	152,624	177,375	2,475	0.14	12,375	0.029
22	225,000	208,125	241,875	3,375	0.10	16,875	0.021
23	300,000	277,500	322,500	4,500	0.08	22,500	0.016
24	400,000	370,000	430,000	6,000	0.06	30,000	0.012
25	560,000	518,000	602,000	8,400	0.04	42,000	0.008
±15% Subcarrier deviation channels ^c							
A	22,000	18,700	25,300	660	0.53	3,300	0.106
B	30,000	25,500	34,500	900	0.39	4,500	0.078
C	40,000	34,000	46,000	1,200	0.29	6,000	0.058
D	52,500	44,625	60,375	1,575	0.22	7,875	0.044
E	70,000	59,500	80,500	2,100	0.17	10,500	0.033
F	93,000	79,050	106,950	2,790	0.13	13,950	0.025
G	124,000	105,400	142,600	3,720	0.09	18,600	0.018
H	165,000	140,240	189,750	4,950	0.07	24,750	0.014
I	225,000	191,250	258,750	6,750	0.05	33,750	0.010
J	300,000	255,000	345,000	9,000	0.04	45,000	0.008
K	400,000	340,000	460,000	12,000	0.03	60,000	0.006
L	560,000	476,000	644,000	16,800	0.02	84,000	0.004
±30% Subcarrier deviation channels ^d							
AA	22,000	15,400	28,600	1,320	0.265	6,600	0.053
BB	30,000	21,000	39,000	1,800	0.194	9,000	0.038
CC	40,000	28,000	52,000	2,400	0.146	12,000	0.029
DD	52,500	36,750	68,250	3,150	0.111	15,750	0.022
EE	70,000	49,000	91,000	4,200	0.083	21,000	0.016
FF	93,000	65,100	120,900	5,580	0.063	27,900	0.012
GG	124,000	86,800	161,200	7,440	0.047	37,200	0.009
HH	165,000	115,500	214,500	9,900	0.035	49,500	0.007
II	225,000	157,500	292,500	13,500	0.026	67,500	0.005
JJ	300,000	210,000	390,000	18,000	0.019	90,000	0.004
KK	400,000	280,000	520,000	24,000	0.015	120,000	0.003
LL	560,000	392,000	728,000	33,600	0.010	168,000	0.002

^aRounded off to the nearest Hz.

^bThe indicated maximum data frequency response and minimum rise time is based on the maximum theoretical response that can be obtained in a bandwidth between the upper and lower frequency limits specified for the channels. (See Appendix B of Ref. 34 for determining possible accuracy-versus-response trade-offs).

^cChannels A through L may be used by omitting adjacent lettered and numbered channels. Channels 13 and A may be used together with some increase in adjacent channel interference.

^dChannels AA through LL may be used by omitting every four adjacent double-lettered and lettered channels and every three adjacent numbered channels. Channels AA through LL may be used by omitting every three adjacent double-lettered and lettered channels and every two adjacent numbered channels with some increase in adjacent channel interference.

TABLE 6. — CONSTANT-BANDWIDTH FM SUBCARRIER CHANNELS

A Channels ^a		B Channels ^a		C Channels ^a	
Deviation limits = ± 2 kHz		Deviation limits = ± 4 kHz		Deviation limits = ± 8 kHz	
Nominal frequency response = 0.4 kHz		Nominal frequency response = 0.8 kHz		Nominal frequency response = 1.6 kHz	
Maximum frequency response = 2 kHz		Maximum frequency response = 4 kHz		Maximum frequency response = 8 kHz	
Channel	Center Frequency, kHz	Channel	Center Frequency, kHz	Channel	Center Frequency, kHz
1A	16				
2A	24				
3A	32	3B	32	3C	32
4A	40				
5A	48	5B	48		
6A	56				
7A	64	7B	64	7C	64
8A	72				
9A	80	9B	80		
10A	88				
11A	96	11B	96	11C	96
12A	104				
13A	112	13B	112		
14A	120				
15A	128	15B	128	15C	128
16A	136				
17A	144	17B	144		
18A	152				
19A	160	19B	160	19C	160
20A	168				
21A	176	21B	176		

^aThe indicated maximum frequency is based on the maximum theoretical response that can be obtained in a bandwidth between deviation limits specified for the channel. (See discussion in Appendix B of Ref. 34 for determining practical accuracy-versus-response trade-offs.)

Because the engineer seldom encounters a data system with a proportional spread of frequency responses, the application of the PBFM system is difficult. A typical flight-research vehicle will have quite a large number of low-frequency channels (for example, 0-20 Hz), a much smaller number of medium frequency channels (for example, 0-400 Hz) and a small number of reasonably high-frequency channels (for example, 0-2,000 Hz). This channel distribution will vary, depending on the nature of the research program, but it is certainly true that few vehicles have channel frequency response requirements that are distributed like the PBFM system channels. In a dynamic sense, PBFM data from one channel of the group can not be time-corrected to data on another channel of the same array unless the low-pass output filters for the two channels are matched. This follows, since otherwise each channel has a different filter time-delay.

The limitations associated with PBFM systems have caused many of these systems to be replaced with PCM systems for low- and medium-frequency data and CBFM-type FDM systems for high-frequency data. Frequency response higher than 0 to 8 kHz of the IRIG nominal constant-bandwidth FM "C" channels of Table 6 are usually handled by other means (for example, see Sec. 6 for information on magnetic tape recorders).

Table 5 has both "Nominal frequency response" and "Maximum frequency response" columns. The nominal frequency response corresponds to a deviation ratio of 5. The deviation ratio of a channel is defined as one-half of the VCO deviation frequency divided by the cutoff frequency of the discriminator output filter. The maximum frequency response corresponds to a deviation ratio of 1. In general, the rms signal-to-noise (S/N) ratio of a given channel varies as the 3/2 power of the deviation ratio used with that channel. Some of the IRIG studies indicated that subcarrier deviation ratios of 4 produced data channel S/N ratios of about 2% rms; deviation ratios of 2 produced S/N ratios of about 5% rms; and at a deviation ratio of 1, some channels showed peak-to-peak errors as high as 30%. Reference 34 warns that these S/N ratios were evolved from specific test conditions and may not be representative of a particular test or particular equipment; however, they demonstrate the desirability of keeping the deviation ratio high, say near 5. An engineer who must understand the various ways to optimize the IRIG FM systems should read Refs. 34 and 35.

5.2.2 Constant-Bandwidth FM-Type FDM Systems

It has already been mentioned that constant-bandwidth FM systems have become popular because they complement the PCM-type data-acquisition system for high-frequency channels. The IRIG standards for constant-bandwidth FM (CBFM) subcarrier channels are listed in Table 6. As can be seen, there are three groups of standard channels: A, B, and C. In the CBFM specifications, the three types of channels can be mixed if an appropriate separation of channels is maintained. PBFM and CBFM subcarrier oscillator modules can also be intermixed under the same conditions.

The nominal and maximum frequency responses have the same meaning as for PBFM: nominal corresponds to a deviation ratio of 5 and maximum corresponds to a deviation ratio of 1. All comments in the preceding PBFM section on deviation ratio apply to this section on CBFM. It is not true that all the CBFM (or PBFM) channels can be used in a particular application. The telemetry transmitter or magnetic tape recorder frequency response may not permit the use of some of the higher-frequency subcarriers. Also, various control frequencies are often inserted into the frequency spectrum and limit the use of adjacent channels.

5.3 TIME-DIVISION MULTIPLEXING

Table 10.1 in Ref. 1 lists three time-division multiplexing (TDM) techniques approved by IRIG standards: pulse-amplitude modulation (PAM), pulse-duration modulation (PDM), and pulse-code modulation (PCM). Since Ref. 1 was published, PDM has been deleted from the IRIG standards (Ref. 34), a result of its low utilization. PAM and PCM will thus be the two TDM systems discussed in this text.

In TDM, data from many channels are sampled at specific times and stored sequentially in time slots of period T , as shown in Fig. 92. Obviously, some method must be incorporated into the stream of data to permit the data user to identify the location of an individual channel. This is accomplished by means of a frame-synchronization technique. Some frame-synchronization techniques use data strings that are not permitted in a normal data-stream sequence. An example of this type of frame-synchronization word will be discussed later in this section for the case of return-to-zero PAM.

Another means of generating a frame-synchronization word is to generate a series of words that could actually occur in the data sequence. This type of synchronization code will be illustrated for the 100% duty cycle PAM system and for PCM systems. This last type of synchronization technique usually requires more time-slot periods to avoid erroneous synchronizations. It must be noted in this case that it is possible for actual data to form such a sequence; however, it is not probable that the data will hold this sequence for any length of time.

The frame synchronizer initially searches for a pattern that corresponds to the frame-synchronization pattern, synchronizes itself to this sequence, and uses this frame synchronization location to reference each given data channel and to reconstruct the original data. If the frame synchronizer should initially "lock" onto a data pulse sequence that has the same characteristics as the synchronization word, erroneous data-channel labeling would result until the data changes and the frame synchronizer were forced to search further for the synchronization word. Once the frame synchronizer has acquired true synchronization, it can hold synchronization even though an occasional synchronization word is damaged by noise. The longer the frame synchronization word, the less likely it is that a data word sequence will match the frame synchronization word; however, the longer synchronization word obviously uses up available system bandwidth.

Referring to Fig. 92, if n (the number of data slots, each of duration T) were 95 and the frame synchronization word utilized 5 additional time slots T and if 95 different data channels were sampled each and every frame, the maximum data frequency (assuming 5 samples per highest input data frequency) of each input channel would be calculated as in the following examples: If the period of each data channel were T and equal to 10^{-4} sec, the time to complete the frame (95 data word periods plus five synchronization periods) would be $100T$ or 10^{-2} sec. It has been stated that 5 samples/cycle are desired to accurately reconstruct the highest frequency in the input data; therefore, in this case five frames are required for each cycle of the input frequency. This corresponds to a maximum data input frequency of 20 Hz.

Supercommutation can be used to achieve higher frequency bandwidths. Supercommutation involves sampling a data channel more than once in each frame. A supercommutated channel should be sampled symmetrically throughout the frame. To illustrate, as in the previous example, when the first five time-periods are devoted to the frame synchronization and it is desired to have a channel with a 200-Hz frequency response, the data channel could be supercommutated by sampling it at time periods 6, 16, 26, 36, 46, 56, 66, 76, 86, and 96. In this case, the data are sampled 10 times/frame, and using the same sampling rule the input channel now has a frequency response of 0 to 200 Hz. Note that increasing the basic bandwidth of a single channel by 10 used up 10% of the time-slot available in each frame.

Subcommutation can be used to sample low-frequency channels from one or more of the basic frame time-periods. To illustrate, if time-slot 7 in the above example were connected by means of additional switches to 10 data-input channels, which in turn were sequentially sampled over 10 frames, the frequency response of the subcommutated would be 1/10 the basic frame capability of 0 to 20 Hz or 0 to 2 Hz. Unlike supercommutation, subcommutation requires some form of a subframe synchronization to identify when the subframe sequence started. The most popular subframe synchronization technique is the subframe counter, which maintains the subframe identification through a counter in one of the main frame data slots.

5.3.1 Pulse-Amplitude Modulation TDM Systems

Figures 93a and 93b illustrate two pulse-amplitude modulation (PAM) formats. These formats are taken from the IRIG standards. The PAM format shown in Fig. 93a provides additional timing information which can be used to create a system clock. The data are available for half the period, and during the other half are clamped at a position corresponding to 0% of full-scale (F.S.) pulse swing. This type of system is self-clocking because clock frequency, $1/T$, is generated at every data channel position. In this case, the frame-synchronization word is recommended to be $2T$ -sec long, that is, 1.5 periods at full-scale followed by a half-period pulse at 0% of full-scale output.

This frame synchronization is a unique word and it has no possible equivalent, legitimate duplicate in the data word sequence. All data time-periods are composed of a pulse height which is proportional to the data amplitude at a given time for one half the data period, and a 0% of full-scale pulse amplitude for the other half of the data period T . However, the frame-synchronization word has three consecutive time periods T that are full-scale, an unallowed sequence for any other portion of the frame.

The format for Fig. 93a is called a return-to-zero PAM format (RZ PAM); because it has a low dc spectral content, RZ PAM is mainly used for direct recording on magnetic tape recorders (see Signal Conditioning for Magnetic Tape Recorders in Sec. 6). For a given recording period T , this format requires about twice the frequency bandwidth of the format shown in Fig. 93b. Thus, if the special features of the RZ PAM format are not required, for example, when the output is directed to a telemetry transmitter, then the format of Fig. 93b would usually be used.

In Fig. 93b, the frame synchronization has been selected to be 5 time-periods long (5 T sec). First, a time-period T at an equivalent of zero input, then 3 time-periods of 100% of full-scale input, and then a time-period of 50% of full-scale input. This kind of frame synchronization is not unique in that an actual data sequence can produce the same pattern. Usually, this is only important on starting the synchronization process, since it is unlikely that the data would hold this sequence very long; however, non-unique frame-synchronization sequences are usually longer in order to reduce the probability of this happening.

As mentioned in Ref. 1, PAM is a good system when moderate accuracy is required. Since the data are stored as amplitude information, they are sensitive to electrical noise. If the PAM is used to drive, for example, an FM telemetry transmitter or an FM subcarrier such that high deviation ratios are achieved in the transmitter or subcarrier, the result is called PAM/FM, and from that point on has good noise immunity. PAM systems suffer from aliasing, just as do all TDM systems (and FDM systems).

5.3.2 Pulse-Code Modulation TDM Systems

Pulse-code modulation (PCM) has become very popular since economical, digital integrated circuitry became available. Two of the major reasons for its popularity are (1) the digitized data words are highly resistant to noise contamination, and (2) a PCM format can easily be interfaced with a digital computer. Another reason for its popularity is that it is one of the few multiplexing techniques that can efficiently handle data with a wide range of accuracy. For example, two-position data, such as switch positions, and very-high-accuracy data can both be accommodated by most modern PCM systems. Deep-space vehicles usually use PCM because of its excellent noise immunity characteristics. Ordinary flight-test vehicles gain from the fact that unlike PAM, which deteriorates directly as a function of the noise added to the channel, PCM is relatively immune to noise until the noise approaches a level that can alter the states of the serial bit sequence.

All PCM systems can be interpreted as being initially PAM systems in which the amplitude modulated data are later digitally encoded. A straight binary code is usually used to encode the analog signal (see Force-Balance Transducer Signal Conditioning in Sec. 4; also Table 4). A "zero" in Table 4 could indicate the maximum negative input to be a telemetry transmitter, and a "one," a maximum positive input.

A PCM system typically has two or more different digital code outputs. The IRIG standard of Ref. 34 recognizes eight different digital code formats (Fig. 94). The first three code formats are usually used with telemetry transmitters. The remaining five codes are mainly used with direct-record magnetic tape channels. Therefore, in actual practice a PCM system might have a serial NRZ-L code (also called straight binary) for the transmitter, a serial DM-M code for the tape recorder input, and a parallel output code for a low-speed tape recorder. The advantage of a parallel output for a tape recorder is that for example, a 10-bit PCM can have the digital code read out on 10 different tape channels, that is, space multiplexed, and thus be able to use a tape speed that is 10 times slower than required for the same PCM serial output. Head-alignment precision limits this technique in practice to less than the factor of 10 theoretical improvement.

Optimum PCM frame-synchronization patterns can be constructed by referring to various articles on the subject, for example, Ref. 36. Table 7 was reproduced from the IRIG standards (Table C-1 of Ref. 34); it lists synchronization pattern lengths from 7 to 30 bits in length. These patterns were derived from the techniques of Ref. 36: "These patterns were determined by examining all 2^n binary patterns of a given length n for that pattern with the smallest total probability of false synchronization over the entire pattern overlap portion of the ground-station frame synchronization." (Ref. 34). As an example, a frame-synchronization pattern with 30 bits, or $n = 30$, would have roughly 10^9 possible patterns. To design such patterns by intuition will hardly produce optimum results.

TABLE 7. — OPTIMUM FRAME SYNCHRONIZATION PATTERNS FOR PCM TELEMETRY

Pattern length	Patterns
7	101 100 0
8	101 110 00
9	101 110 000
10	110 111 000 0
11	101 101 110 00
12	110 101 100 000
13	111 010 110 000 0
14	111 001 101 000 00
15	111 011 001 010 000
16	111 010 111 001 000 0
17	111 100 110 101 000 00
18	111 100 110 101 000 000
19	111 110 011 001 010 000 0
20	111 011 011 110 001 000 00
21	111 011 101 001 011 000 000
22	111 100 110 110 101 000 000 0
23	111 101 011 100 110 100 000 00
24	111 110 101 111 001 100 100 000
25	111 110 010 110 111 000 100 000 0
26	111 110 100 110 101 100 010 000 00
27	111 110 101 101 001 100 110 000 000
28	111 101 011 110 010 110 011 000 000 0
29	111 101 011 110 011 001 101 000 000 00
30	111 110 101 111 001 100 110 100 000 000

5.4 TIME CORRELATION OF MULTIPLEXED DATA

As was noted earlier, rigorous time-correlation of data in PBFM systems requires compensation for the different output filter time delays. This also affects CBFM channels when different bandwidth options are used to record data that must be tightly time-correlated.

TDM, as usually implemented, also requires special consideration when close time-correlation is required between channels. From Fig. 92, it can be seen that the typical TDM system samples the data channels sequentially between each synchronization word. Data reconstruction is usually performed assuming that all data were sampled simultaneously at either the beginning or the end of each frame of data. This means that a time-correlation error sequentially accumulates from either the first or the last channel in the frame.

When TDM systems require very precise time-correlation, the engineer must be aware of this limitation and compensate for its effect. The most popular approach is to modify the data reconstruction technique to account for the time-skew between samples. In some cases, it is necessary to "create" pseudosample data values between the actual samples to give the effect of simultaneous sampling. The intermediate sample values are created using interpolation. The most accurate compensation technique is to add a hardware module to the PCM system which performs a "sample-and-hold" operation to simultaneously sample all the critical data and sequentially place the data in the frame in the usual way.

The important point to recognize is that the signal-conditioning process introduces an interchannel, variable time-delay which affects both the relative and absolute timing of the reconstructed data. Various time-compensation techniques are available to correct this timing error.

5.5 REMOTE MULTIPLEXING

Traditionally, the signal conditioning for flight-test data-acquisition systems has been located in one central, easily accessible location. Much of the other instrumentation equipment, such as power supplies, tape recorders, transmitters, and junction panels, is usually in the same area. The transducers are located throughout the aircraft where required and the associated wiring is routed from them through the aircraft to this central location for the multiplexing operation, that is, central multiplexing. When flight-test programs are changed, a frequent occurrence on most flight-test vehicles, many persons require simultaneous access to this central area; thus gaining physical access to the signal-conditioning equipment often becomes a limiting factor in flight schedules.

Another restriction with the central-multiplexing approach is associated with the signal wiring. On large vehicles, signal wiring runs of up to 50 m are not uncommon. Analog signal wiring is prone to noise contamination, and long wiring runs are particularly susceptible to the introduction of unwanted noise. It is therefore desirable to design an instrumentation system with analog signal wiring runs no longer than absolutely necessary. Shorter wiring interconnections will substantially improve the data quality from a data-acquisition system. On vehicles instrumented with a large number of data channels, the massive wire bundle at each junction panel makes these junction panels difficult to modify or repair. In many situations, the modification or repair of a connector will cause damage to adjacent connector junctions that goes undetected until a failure occurs during a preflight check or during an actual flight. Needless to say, this situation should be avoided.

Remote multiplexing is an approach to data-acquisition-system design that minimizes the above difficulties. In this approach, the multiplexing or encoding function is distributed among several sites in the vehicle. The remote sites are then connected to the central location by serial communication links, which supply the multiplexed data to a system controller and exchange control and sequencing information. The distributed remote-multiplexing sites afford ease of access compared with the central multiplexing approach. In addition, the wiring of the aircraft is substantially simplified. Far fewer signal wires are terminated at each remote site than in the central multiplexing approach. Fewer terminations translate to smaller junction panels and to simpler termination with smaller wire bundles. The serial communication wiring between each remote site and the central controller requires only a few conductors for its operation. Thus, the wiring is minimal between the remote sites and the central controller.

When remote multiplexing is used, spare capability can be included to accommodate both the planned and unknown changes that will be made to the program during its lifetime. As the needs of the program change, different multiplexing sequences (formats) are developed to optimize the data acquisition for each program phase. In modern systems, these format changes are accomplished largely through system software modifications. This approach greatly reduces the need for access to the multiplexing system and fosters rapid response to new program requirements.

For most types of multiplexing, the multiplexed or encoded data are protected from the introduction of the common kinds of noise contamination. Therefore, the communication links between the remote sites and the central location are protected from noise contamination. Thus, the remote-site arrangement minimizes the analog-data signal wiring length and, in turn, the noise contamination. The remote multiplexers serve as multiple data acquisition sites and therefore reduce the number of signal connections required at each site, thereby minimizing the difficulty with the junction panels.

Remote PCM multiplexers are the most common, and they have demonstrated significant advantages. In one case, the McDonnell-Douglas Aircraft Company reported savings of 88% in the wiring of a large commercial transport data-acquisition system (Ref. 37). With this reduction in wiring length go the associated reductions in installation costs, wiring costs, and wiring weight. Substantial payoff from the remote multiplexing approach is realized on systems with more than 150 parameters.

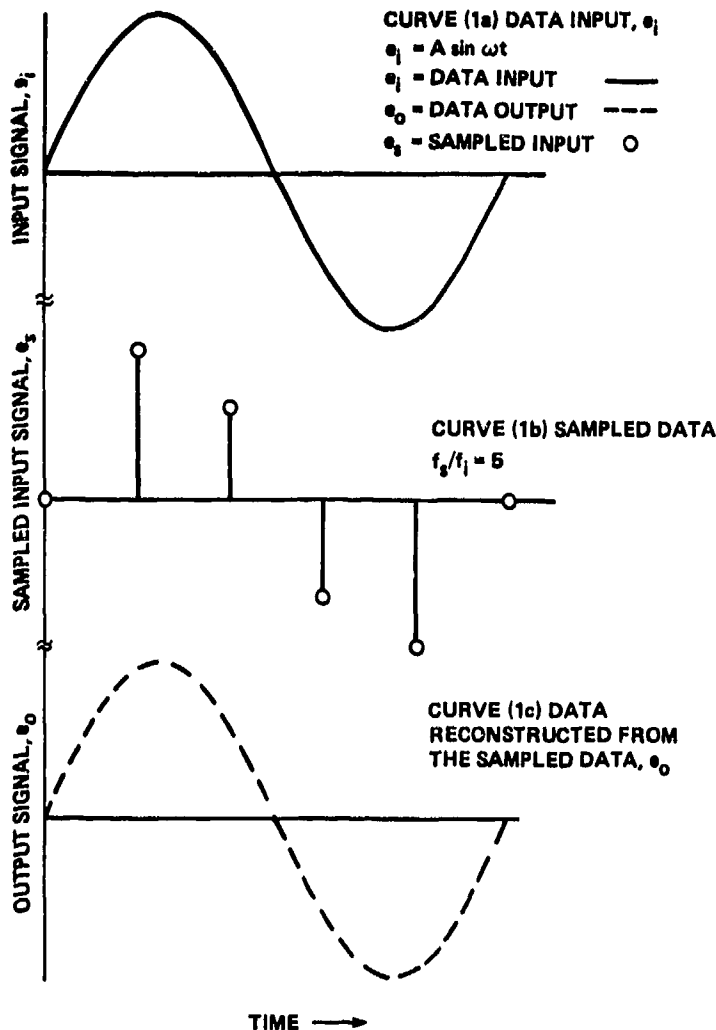


Figure 88. Effects of sampling on sinusoidal data signals

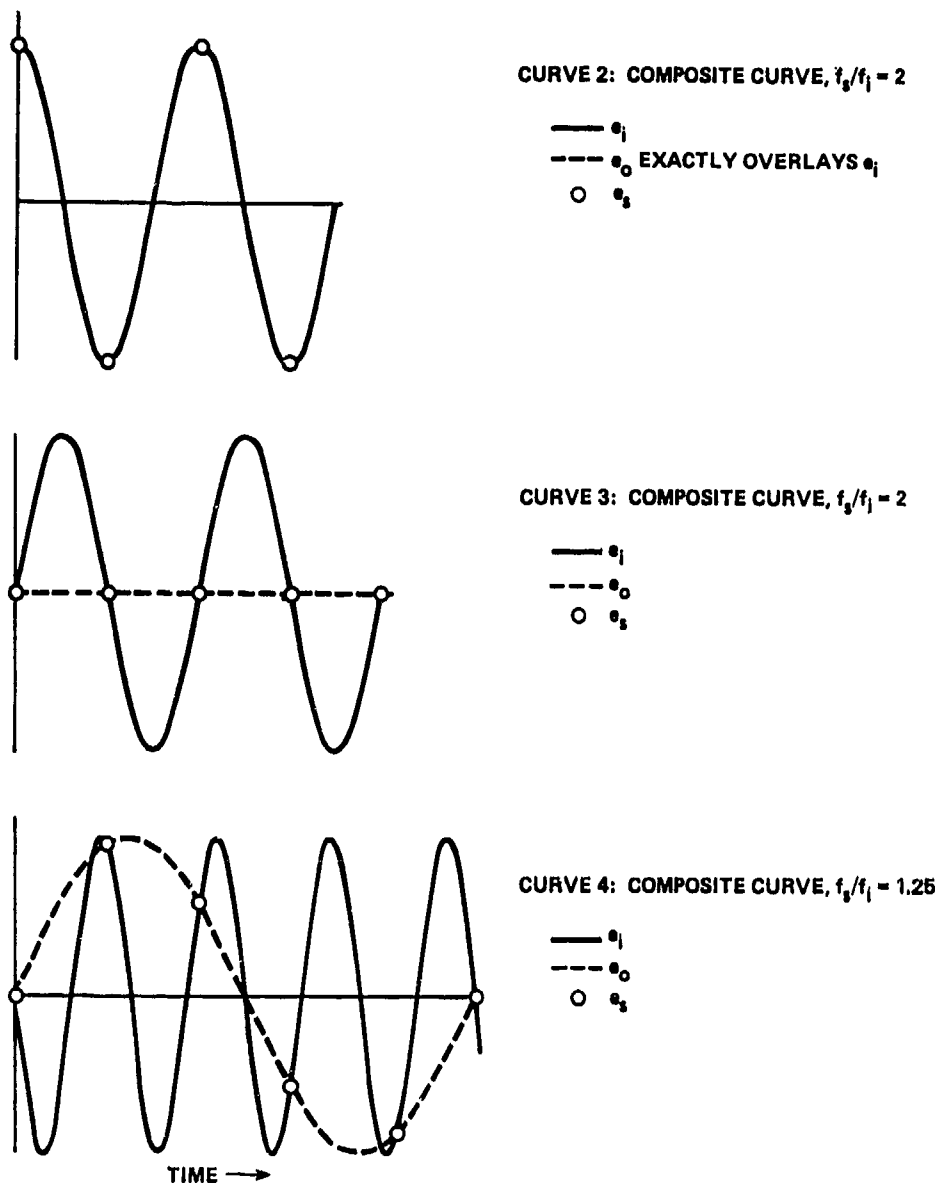
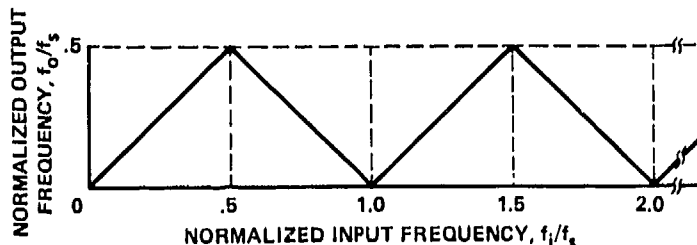


Figure 88. Concluded

f_1 = FREQUENCY OF THE INPUT SIGNAL
 f_0 = FREQUENCY OF RECONSTRUCTED OUTPUT SIGNAL
 f_s = SAMPLING RATE (SAMPLES/SEC)
 $f_s/2$ = NYQUIST, OR FOLDING, FREQUENCY



(a) Time-division multiplexing system



(b) Graphic representation of aliasing effect

Figure 89. Time-division multiplexed systems and aliasing effect

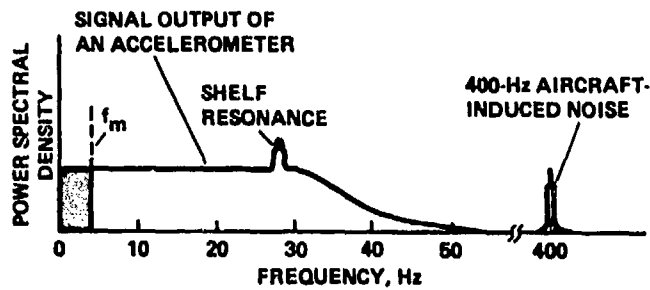
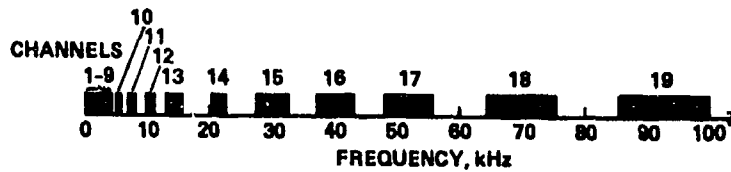
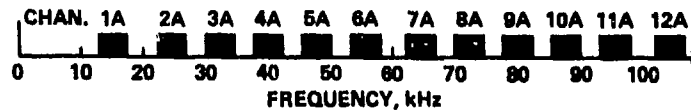


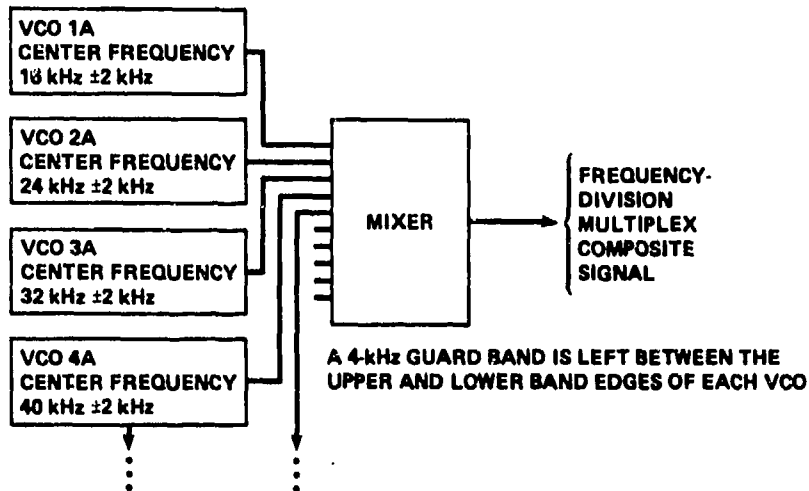
Figure 80. Hypothetical frequency spectrum of a signal



(a) IRIG proportional-bandwidth FM subcarrier channels ($\pm 7.5\%$)

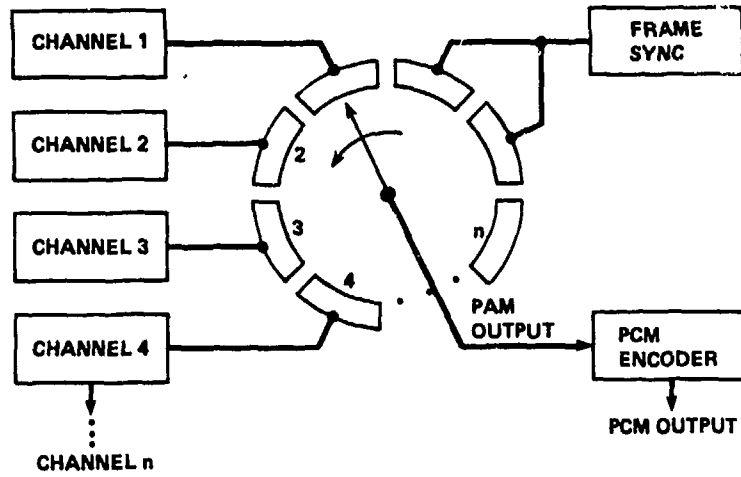


(b) IRIG constant-bandwidth FM subcarrier A channels, 2-kHz frequency deviation (Refer to Table 6.)

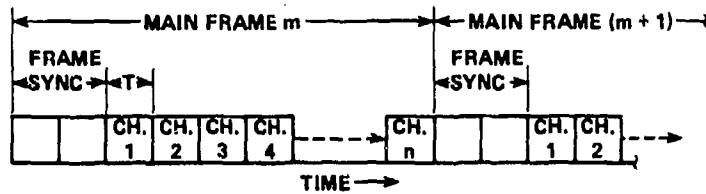


(c) System for producing constant-bandwidth FM frequency-division multiplexing

Figure 91. FM frequency-division multiplexing spectra and system

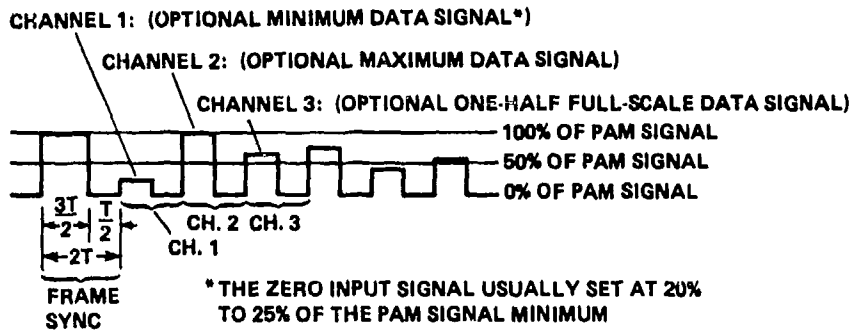


(a) Mechanical implementation of time-division multiplexer system

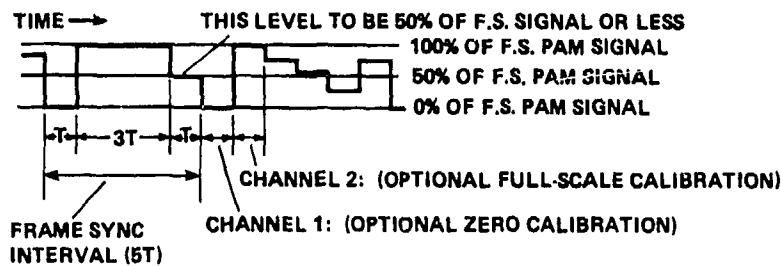


(b) Illustration of time-sequential nature of time-division multiplexer

Figure 92. Mechanical time-division multiplexing system with frame synchronization



(a) Pulse-amplitude modulation, 50% duty cycle



(b) Pulse-amplitude modulation, 100% duty cycle

Figure 93. IRIG standard pulse-amplitude modulation formats

CODE DESIGNATIONS	LOGIC WAVEFORM LEVELS	CODE WAVEFORMS	CODE DEFINITIONS
NRZ-L	"1"		<u>NON-RETURN-TO-ZERO-LEVEL</u>
	"0"		"ONE" IS REPRESENTED BY ONE LEVEL "ZERO" IS REPRESENTED BY THE OTHER LEVEL
NRZ-M	"1"		<u>NON-RETURN-TO-ZERO-MARK</u>
	"0"		"ONE" IS REPRESENTED BY A CHANGE IN LEVEL "ZERO" IS REPRESENTED BY NO CHANGE IN LEVEL
NRZ-S	"1"		<u>NON-RETURN-TO-ZERO-SPACE</u>
	"0"		"ONE" PRODUCES NO CHANGE IN LEVEL "ZERO" PRODUCES A CHANGE IN LEVEL
Biφ-L	"1"		<u>BI-PHASE LEVEL (SPLIT PHASE)</u>
	"0"		LEVEL CHANGE OCCURS AT CENTER OF EVERY BIT PERIOD "ONE" IS REPRESENTED BY A "ONE" LEVEL WITH A TRANSITION TO THE "ZERO" LEVEL "ZERO" IS REPRESENTED BY A "ZERO" LEVEL WITH A TRANSITION TO A "ONE" LEVEL
Biφ-M	"1"		<u>BI-PHASE-MARK</u>
	"0"		LEVEL CHANGE OCCURS AT BEGINNING OF EVERY BIT PERIOD "ONE" PRODUCES A MIDBIT LEVEL CHANGE "ZERO" PRODUCES NO MIDBIT LEVEL CHANGE
Biφ-S	"1"	<u>BI-PHASE-SPACE</u>	
	"0"	LEVEL CHANGE OCCURS AT BEGINNING OF EVERY BIT PERIOD "ONE" PRODUCES NO MIDBIT LEVEL CHANGE "ZERO" PRODUCES A MIDBIT LEVEL CHANGE	
DM-M	"1"	<u>DELAY MODULATION-MARK (MILLER CODE)</u>	
	"0"	"ONE" PRODUCES A LEVEL CHANGE AT MIDBIT TIME. "ZERO" FOLLOWED BY A "ZERO" PRODUCES A LEVEL CHANGE AT THE END OF THE FIRST "ZERO" BIT. NO LEVEL CHANGE OCCURS WHEN A "ZERO" IS PRECEDED BY A "ONE"	
DM-S	"1"	<u>DELAY MODULATION-SPACE (MILLER CODE)</u>	
	"0"	"ZERO" PRODUCES A LEVEL CHANGE AT MIDBIT TIME. "ONE" FOLLOWED BY A "ONE" PRODUCES A TRANSITION AT THE END OF THE FIRST "ONE" BIT. NO LEVEL CHANGE OCCURS WHEN A "ONE" IS PRECEDED BY A "ZERO"	

Figure 94. Code definitions for pulse-code modulation, recognized by IRIG standards (Ref. 34)

6. SIGNAL CONDITIONING FOR AIRBORNE SIGNAL TERMINAL DEVICES

The definition of signal conditioning taken from Ref. 1 and used in Sec. 1 of this text excludes signal-terminal devices; however, specific signal-terminal devices often require special signal conditioning to interface effectively with the airborne data-acquisition system. This section covers those interfacing requirements to the extent required to provide insight into why the special interface is needed.

Chapter 9 in Ref. 1 provides an overview of all the data terminal devices discussed here (except the telemetry transmitter); it also lists the characteristics of these data terminal devices.

6.1 SIGNAL CONDITIONING FOR MAGNETIC TAPE RECORDERS

Most of the major flight-test programs use an airborne instrumentation magnetic tape recorder as the prime flight-test data recording device. Even if the data are also telemetered, the quality and continuity of the on-board tape recorder data are normally the best available. In some cases, however, weight, size, or cost considerations preclude using a tape recorder.

A thorough review of tape recorder characteristics is undertaken in Ref. 38. A more recent review of the state of the art of magnetic tape recording and of anticipated improvements is presented in Ref. 39.

Magnetic tape recorders have three recording modes: (1) direct recording, (2) wideband-FM recording, and (3) digital recording. These techniques and their special input signal-conditioning requirements will be covered in the following sections. In the subsequent discussion, IRIG tape recording standards are used in the examples. In addition to the IRIG standards, the German DIN recording standards are internationally recognized. The DIN 66 210 standard, for example, addresses direct and FM recording on instrumentation magnetic tape. The DIN 66 224 standard covers PCM recording on instrumentation magnetic tape recorders. Other DIN standards exist and are widely recognized.

6.1.1 Direct-Recording Signal Conditioning

Figure 95 taken from Ref. 38, shows the major contributors to the basic direct-record/playback frequency response. The important part of this figure is curve E, which is the summation of curves A-D and is therefore the overall reproduce-head-output curve produced by an equal-amplitude sinusoidal input to the record head. The frequency-response characteristic of the direct-record mode is overwhelmingly influenced by the tape recorder head-gap loss (curve B) and the reproduce-head response (curve A).

Curve A of Fig. 95 reflects the nature of the reproduce head, which can detect only the time rate of change of the magnetic flux recorded on the tape. Thus, it is apparent that a steady-state magnetization cannot be detected by the reproduce head. The record head does magnetize the tape to a flat frequency response limited at high frequency by the head-gap separation.

The magnetization process has inherent nonlinearity and hysteresis. These are suppressed by the addition of an ac bias current superimposed on the data. This bias current is typically at a frequency 3 to 10 times higher than the channel bandwidth. This process for linearizing response through the use of ac bias is complex and not well understood.

Where the input frequency spectrum is not known, as is the case for most flight data channels, the correction for curve E of Fig. 95 is obtained by using a reproduction amplifier that compensates such that the resultant output is flat to within ± 3 dB, as tabulated in Table 8. These are the IRIG direct-record specifications (Ref. 34). Note that in no case is a steady-state signal output possible. This direct mode of recording has the lowest signal-to-noise ratio of the three recording techniques, typically 25 dB on wideband recorders and 40 dB on intermediate band recorders. However, this mode also has the highest recording densities of the three recording techniques. As long as the lack of a steady-state response and the low signal-to-noise ratio can be tolerated, the direct-record mode is a good choice.

TABLE 8. — IRIG DIRECT-RECORD BANDWIDTHS

Tape speed		Pass Band ± 3 dB	
mm/sec	in./sec	Intermediate band, Hz	Wideband, Hz
47.6 ^a	(1 7/8)	100-9,380	400-31,250
95.2	(3 3/4)	100-18,750	400-62,500
190.5	(7 1/2)	100-37,500	400-125,000
381.0	(15)	100-75,000	400-250,000
762.0	(30)	200-150,000	400-500,000
1,524.0	(60)	300-300,000	400-1,000,000
3,048.0	(120)	300-600,000	400-2,000,000
6,096.0 ^a	(240)	- - - - -	800-4,000,000

^aThese speeds are an extended range of operation for wideband systems which may be supported at the option of individual flight test ranges. This information was taken from Ref. 34.

Proportional-bandwidth and constant-bandwidth FM (PBFM and CBFM) subcarrier oscillators (SCO) with center frequencies such as those shown in Tables 5 and 6 can be recorded on these direct-record channels, with each subcarrier set at equal amplitude. If each SCO has a deviation ratio of 5, the individual

channels are relatively immune to the noise on the direct-record channels. As can be seen from Table 8 the use of various tape speeds and one of the intermediate or wideband-type tape recorders allows a considerable choice of IRIG FM channels to be recorded.

Since the IRIG direct-record specifications permit seven track heads for 12.7-mm (0.5-in.) tape and 14 or 28 tracks for 25.4-mm (1-in.) tape, quite a number of FM channels can be recorded on one tape recorder. Appendix E of Ref. 34, lists tape head formats approved by the International Standards Organization which permit 28 and 42 tracks on a 25.4-mm (1-in.) tape and 14 or 21 tracks on 12.7-mm (0.5-in.) tape.

6.1.2 Wideband-FM Recording Signal Conditioning

Wideband-FM recording uses a single FM SCO, as shown in Fig. 96. In this type of tape recorder, as can be seen from Table 9, the input data have a steady-state response. The wideband-FM recording technique also has the best signal-to-noise ratio of the three recording modes, typically 50 dB on IRIG intermediate band and 35 dB on wideband recorders. The IRIG specifications list the response at band limits as ± 1 dB on intermediate and wideband Group I recorders. This improved linearity, immunity to noise, and frequency response down to steady state has been achieved by sacrificing bandwidth.

When tape imperfections produce what is termed a dropout, the reproduced data signal amplitude drops to zero in the wideband FM recording mode. Unless the ground-station discriminator can compensate for this effect, wide excursions can take place in the data output.

TABLE 9. — IRIG-INTERMEDIATE AND WIDEBAND FM RECORD PARAMETERS

Tape speed, mm/sec (in./sec)		Carrier			Modulation frequency kHz
Intermediate-band FM	Wideband FM	Center frequency, kHz	Deviation limits		
			Plus deviation, kHz	Minus deviation, kHz	
Group I					
47.6 (1 7/8)		3.375	4.725	2.025	0 to 0.625
95.2 (3 3/4)	47.6 (1 7/8)	6.750	9.450	4.050	0 to 1.250
190.5 (7 1/2)	95.2 (3 3/4)	13.500	18.900	8.100	0 to 2.500
381.0 (15)	190.5 (7 1/2)	27.000	37.800	16.200	0 to 5.000
762.0 (30)	381.0 (15)	54.000	75.600	32.400	0 to 10.000
1,524.0 (60)	762.0 (30)	108.000	151.200	64.800	0 to 20.000
3,048.0 (120)	1,524.0 (60)	216.000	302.400	129.600	0 to 40.000
	3,048.0 (120)	432.000	604.800	259.200	0 to 80.000
Group II					
	47.6 (1 7/8)	14.062	18.281	9.844	0 to 7.810
	95.2 (3 3/4)	28.125	36.562	19.688	0 to 15.620
	190.5 (7 1/2)	56.250	73.125	39.375	0 to 31.250
	381.0 (15)	112.500	46.250	78.750	0 to 62.500
	762.0 (30)	225.000	192.500	157.500	0 to 125.000
	1,524.0 (60)	450.000	585.000	315.000	0 to 250.000
	3,048.0 (120)	900.000	1,170.000	630.000	0 to 500.000
	6,096.0 (240)	1,800.000	2,340.000	1,260.000	0 to 1,000.000

When frequency responses higher than those available on CBFM channels are required, wideband-FM recording techniques would be applicable. The wideband-FM tape recorder requires no specific signal conditioning for typical inputs. In some cases the FM SCO records in the saturation mode instead of the bias signal mode. In general, the bias signal mode provides better performance but may cost more initially owing to its more complex airborne hardware.

6.1.3 PCM-Recording Signal Conditioning

As discussed in Sec. 5, both frequency-division and time-division multiplexing (FDM and TDM) can be used to place many channels on a limited number of terminal device channels. Obviously, FDM can be used with both the previous tape recording techniques. What is not so obvious is that the TDM technique can be used with both of the previous recording modes. TDM system outputs can be recorded using any of the recording modes.

When PCM data are recorded on an FM subcarrier, they are identified as PCM/FM. The IRIG standards (Ref. 34) specify that the subcarrier channel shall be chosen such that the maximum frequency response of the channel, as shown in Tables 8 and 9, is greater than the reciprocal of twice the shortest period between transitions in the PCM waveform. When recording PCM data on an FM subcarrier, the subcarrier has steady-state response, so PCM code formats such as NRZ-L shown in Fig. 94 may be accommodated.

Signal conditioning for PCM data in the direct-record mode requires optimizing the coded data spectrum to curve E shown in Fig. 95. This means tailoring the bandwidth and frequency response. Tailoring the PCM data perfectly to the curve of Fig. 97 is not feasible since general scientific data conforms to no fixed spectrum. However, it is possible to match the characteristics in a statistical way. When PCM formats are recorded in the direct-record mode using bias current or in a head-saturation mode, that is, with no bias current, the lack of a steady-state response in these modes must be taken

into consideration. Figure 97 is the much publicized figure that illustrates normalized power densities for three different PCM code types as a function of normalized frequency. As can be seen from this figure, the power spectral density of the NRZ code contains a significant amount of steady-state information which makes it unsuitable for direct recording on magnetic tape. The B1-L (Manchester) code has an ideal steady-state response — zero frequency components at zero frequency — but requires a much wider bandwidth than the NRZ code. The delay modulation (Miller) code has very little of its power spectral density at dc and very little information beyond the normalized frequency of 1, which makes it the code of choice from a frequency spectrum standpoint.

Three advanced high-density digital recording codes, which optimize the code-to-the-tape recorder direct-record characteristics and simultaneously conserve bandwidth, are described in Ref. 39. These techniques can achieve bit-packing densities of the order of 13,000 bits/cm (33,000 bits/in.). Those listed are the Miller squared (M^2) code by Ampex, Enhanced NRZ by Bell and Howell, and Randomized NRZ by Sangamo/Weston-Schlumberger. Reference 39 also describes a new coding technique that shapes the spectrum and provides forward error correction with little additional bandwidth (less than 10%). This technique claims a bit-packing density of 26,000 bits/cm (23,500 information bits/cm). None of these last four encoding techniques is standard, and all require special electronic processing to implement. One of these advanced coding techniques may become a standard of the future.

The art of high-density digital recording is presently advancing rapidly. Fortunately, most flight-test data-acquisition systems do not presently require techniques more advanced than the IRIG standards. For most flight-test programs, the main advantages of the better packing densities is longer recording time, but a reduction in overall recording system volume is an added anticipated future benefit.

The IRIG standards have special specifications if it is desired to perform parallel PCM recording. Parallel recorders use 25.4-mm (1-in.) tape and have record heads with 14 or 28 tracks. Parallel PCM recording cannot achieve the high bit-packing densities of serial-direct-record techniques, but it can significantly reduce tape speeds. Parallel recorders require precise tape head alignment, and at high bit-packing densities data decoding often proves to be extremely difficult. Since airborne parallel PCM magnetic tape recorders are not presently in common use, they are quite expensive.

Many engineers new to flight testing wonder why the on-board tapes are not made truly computer compatible for optimum data compatibility. The ground-based and the airborne systems are quite different, and they are optimized for different purposes. Flight-test magnetic tape recorders move the tape through the machine at a constant velocity, record the data in a continuous stream, and have bit error rates of about 1 in 10^6 . Ground-based computer tapes are typically recorded in blocks, starting and stopping the tape as required, and exhibit bit error rates of the order of 1 in 10^{11} . To achieve this low error rate, ground-based computer tapes are recorded at substantially lower bit-packing densities. The highest computer-compatible-type tape packing densities are well below those encountered on airborne machines, thus requiring more tape for a given application. Tape weight, tape cost, and recording time are very important for airborne applications; as a result the use of airborne computer-compatible tape recorders in flight-test applications is severely limited.

6.2 SIGNAL CONDITIONING FOR TELEMETRY TRANSMITTERS

Transmission of flight-test data to the ground by means of telemetry transmitters is a very important flight-test technique. Telemetry transmitters cost less, weigh less, and are smaller than on-board tape recorders; therefore, they are often used as the prime source of flight-test data. In the aircraft environment, available power, and allowable weight may dictate the use of a transmitter. On scale-model, unmanned flight-test vehicles, telemetry may be the only realistic method of flying the vehicle and acquiring data. Telemetry transmitters are frequently used as a backup to on-board recording. Major telemetry applications include real-time flight-test monitoring, control of hazardous flight-test programs (such as flutter clearance testing), data up-links (such as used for pilot displays), and feedback for closed-loop flight-control systems. As a result of their many applications, telemetry transmitters are one of the most frequently encountered airborne data-terminal devices.

Available telemetry transmission frequencies are much sought after by various testing organizations. This demand often forces the available channels to be shared with other vehicles, which precludes simultaneous flights and requires close coordination of flight schedules. All frequencies must be justified, and bandwidth requirements necessary to transmit video pictures may require extensive justification. The frequency deviation must be restricted to avoid interference with the adjacent channels. Input amplitude-limiting and frequency bandwidth-limiting for FM transmitters are the most common conditioning technique used to avoid interference.

Frequency modulation is the most often used of the many possible modulation techniques. Amplitude-modulation and PM transmitters have some distinct advantages in many applications (see Chap. 11 of Ref. 40) but FM is almost universally used because of its widespread availability. Unless otherwise specified, it will be assumed that an FM transmitter is being used in all applications described in this volume. Frequency modulation and PM transmitters are the only types of standard transmitters recognized in the IRIG standards. Most applications require the data to be multiplexed at the transmitter input by either an FDM or a TDM system.

The frequency bandwidth of an FM system is a function not only of the input frequency bandwidth but also of the signal amplitude. A spectrum analysis of the transmitter output should be used to ensure that the input-signal amplitude is adjusted correctly; otherwise, adjacent channels will be distorted.

6.2.1 FM/PM Pre-Emphasis

There is considerable emphasis in the literature on how to achieve an optimum pre-emphasis of sub-carrier oscillators. Pre-emphasis is desirable because as the received signal available to the ground station is reduced, the information on certain subcarriers can be damaged or even destroyed by noise while the information on the other subcarriers in the same transmission is still acceptable. Optimum pre-emphasis is defined as a grouping of subcarriers such that the rms voltages of the undeflected carrier frequencies have been adjusted so that as the received signal is reduced, all subcarrier channels are simultaneously extinguished by noise.

It is the authors' opinion that many engineers involved in flight testing atmospheric research vehicles place undue emphasis on receiver threshold. In a situation in which the vehicle antenna and the ground-station antenna (particularly a high-gain ground-station antenna) are essentially in line-of-sight contact, the standard telemetry transmitter customarily achieves good receiver quieting even with relatively low transmitted power. When there are obscurations between the two antennas — the horizon, a mountain, or the metal structure of the vehicle — the signal at the receiver is usually below the receiver threshold no matter how much power the vehicle transmitter is radiating. Most low-signal inputs to the ground-station receiver are not indicative of an extended gradual weakening of the signal, but instead are indications of a rapid approach to signal extinction. (This is not true in deep-space applications, where the signal can become very weak, and where optimized subcarrier pre-emphasis is desirable.) When the signal path is direct line of sight, the effort required to adjust the various oscillator levels to the proper levels for optimum pre-emphasis may not be worthwhile. On the other hand, when one expects to be working with marginal receiver signals for a considerable portion of the flight-test program, pre-emphasis may be required. Even when pre-emphasis is required, various alternatives may make the task easier, as will be explained.

The IRIG specifications (Ref. 34), apply to both PBFM and CBFM types of FDM systems, as well as to FM and PM transmitters, which creates the four basic combinations of FDM transmissions (PBFM/FM, PBFM/PM, CBFM/FM, and CBFM/PM). In addition, there are many combinations that intermix the various PBFM and CBFM subcarriers. Reference 40 covers the preemphasis of these combinations in detail. The relationships governing the modulated amplitudes for four basic combinations are given below.

1. Proportional-bandwidth FM/FM:

$$A_j = (f_j/f_0)^{3/2} A_0 \quad (67)$$

2. Proportional-bandwidth FM/PM:

$$A_j = (f_j/f_0)^{1/2} A_0 \quad (68)$$

3. Constant-bandwidth FM/FM:

$$A_j = (f_j/f_0) A_0 \quad (69)$$

4. Constant-bandwidth FM/PM:

$$A_j = A_0 \quad (70)$$

In these equations, A_j is the amplitude of the unmodulated subcarrier center frequency of channel j , and f_j is the center frequency of this same channel j ; A_0 and f_0 are the amplitude and frequency, respectively, of the base channel in the subcarrier array. As can be seen from these equations and from Fig. 98, the optimum pre-emphasis schedule varies markedly for the four examples given. The easiest to implement is the constant-bandwidth FM combined with a PM transmitter (CBFM/PM). In this case, all the subcarrier oscillator output voltages are set to the same amplitude (see the appropriate curve in Fig. 98c). In the IRIG CBFM/FM combination, the pre-emphasis varies directly as the frequency, and an IRIG CBFM "A" channel amplitude would vary directly as the ratio of the frequencies. For example, if the subcarrier output of channel 1A were 10 mV, then channel 21A would be set to 110 mV. Likewise, if a 25-channel PBFM/PM system were implemented with channel 1 set at 10 mV, then channel 25 would be optimum at 375 mV (Fig. 98b). The optimum pre-emphasis is limited by system dynamic range for a 25-channel PBFM/FM system. In this case, when the subcarrier oscillator output of channel 1 is set to 10 mV rms, the "optimum" theoretical pre-emphasis schedule requires that channel 25 be set to 524 V, a preposterous level.

In theory, SCO center-frequency amplitudes for an optimum pre-emphasis schedule for an IRIG PBFM/FM transmission system are related by a 3/2 power relationship. Unfortunately, when this is implemented for more than seven or eight consecutive subcarriers, distortion becomes intolerable in the lower-frequency subcarrier channels. This distortion is caused by the pre-emphasized higher frequency SCOs and appears as intermodulation products and crosstalk. In results reported by Walter Hane of the Martin Company, Orlando, Florida, in a 17-channel PBFM system (using channels 2 through 18 of Table 5, the distortion in the lower channels is about 5%. By using the technique recommended by Mr. Hane, the distortion is reduced to less than 0.25%. Figure 99 illustrates the technique used by the Martin Company, in which each SCO is set up with an equal output amplitude. The high-pass filter removes low-band interference before the high-band and low-band are combined. The pre-emphasis filter then attenuates the array to the desired amplitude characteristics for low signal inputs to the receiver.

Reference 40 explains the technique to be used when a mixture of the various types of SCOs is used on one transmitter. The techniques of Ref. 40 could be extended to optimize a group of SCOs to any noise spectrum.

One of the best ways of avoiding these pre-emphasis problems, especially for PBFM/FM, is by preserving the best possible linearity in the telemetry link and by using the minimum pre-emphasis. Low amounts of pre-emphasis can be used, provided the receiver input signal is sufficient to provide good receiver quieting.

When input signals to the SCO have much wider variations of input frequencies and amplitudes than the expected nominal values, then one SCO can produce considerable crosstalk in the neighboring SCO. This crosstalk can be reduced in several ways. The use of sharp cutoff bandpass filters in the output of the SCO is not recommended since such filters introduce large time delays and time-delay variations. A better solution when the signal input has frequency components beyond the rated capacity of the channel is to use a low-pass filter at the input to the SCO. When the input signal amplitude is expected to exceed nominal levels, interchannel interference can be reduced by means of input limiting (that is, clipping circuits). The use of a high-pass filter or of a frequency-sensitive mixing network can also appreciably reduce crosstalk between channels.

6.2.2 PCM/FM Systems

PCM systems use an output format such as NRZ-L (see Fig. 94) which drives the transmitter frequency to the maximum desired positive deviation for a logical "one" and to the maximum negative deviation for the logical "zero." Note that there is no legitimate undeflected carrier mode for PCM systems. Of the codes defined by IRIG Standards and illustrated in Fig. 94, the first three codes, NRZ-L, NRZ-M, and NRZ-S, are quite suitable for input to a telemetry transmitter. The three biphasic codes could be used, but they require almost double the bandwidth, and the lack of dc response is no advantage for use with an FM transmitter. The two delay-modulation (DM) code formats would seem by visual inspection to present some advantages for FM transmission; however, RF transmission of DM is not considered because of a 3.5-dB signal-to-noise ratio penalty relative to NRZ (see Ref. 34).

6.2.3 Pre-Modulation Filter

In theory, an FM waveform maintains a constant amplitude while deviating about its center frequency f_C in a manner that is directly related to the amplitude and frequency of the modulating waveform. A carrier, $e = A \sin 2\pi f_C t$, when frequency-modulated by a sinusoidal signal waveform $e_s = A_s \sin 2\pi f_s t$, is expressed as

$$e = A \sin [2\pi(f_C + D \sin 2\pi f_s)t] \quad (71)$$

In this expression, D is the deviation ratio and is equal to f_C/f_s . The term f_C may be described as $f_C = K A_s$, where K is the modulator deviation sensitivity in Hertz per volt. The important point here is that f_C is a function of the amplitude of the modulating waveform.

When Eq. (71) is expanded, the following is obtained:

$$e = A J_0(D) \sin 2\pi f_C t + A \sum_{k=1}^{k=\infty} J_k(D) [\sin 2\pi t (f_C + k f_s) + (-1)^k \sin 2\pi t (f_C - k f_s)] \quad (72)$$

where J_k is a Bessel function of the first kind and is a function only of the deviation ratio D . Since k is summed from 1 to infinity, the number of sidebands is infinite and their amplitude depends on $J_k(D)$. This is a very difficult equation to grasp intuitively. Reference 40 contains a curve which shows at what point all sideband amplitudes are less than 1% of the unmodulated carrier. From that curve (shown in Fig. 100), one can calculate a bandwidth BW , which for most applications is adequate to provide a low-distortion demodulated waveshape. The engineer must control the maximum input frequency and the maximum signal amplitude. To limit the maximum input frequency information, engineers often use multipole Bessel-type filters. If the amplitude is unpredictable, the input may require limiting to prevent excessive amplitude excursions.

6.3 THE CAMERA

The airborne camera is frequently encountered in flight-test data-acquisition systems. In very small programs, the photo-panel camera can be an economical way to gather data. Cockpit cameras perform a multitude of tasks, such as documenting pilot instrument outputs and pilot actions. Externally focused cameras can record special events, such as positions of various aircraft surfaces, airflow patterns from tuft patterns, surface flexures, and landing-gear motions. Cameras allow others to "see" and preserve noteworthy events. Three main types of cameras are in general use: the pulse or cine low-frame-rate photographic camera, the high-speed photographic cine camera, and the television camera.

6.3.1 Photographic Camera

Photographic cameras allow the ground observer to "see" the desired data, but if a more complex data reduction is required, substantial data translation is necessary. For example, when a detailed documentation of the photo-panel data is required, a tedious and time-consuming data conversion is necessary.

Most applications require compensation for variable illumination. An exception would be the photo-panel instrumentation where the illumination is controlled and fixed. Most other vehicle camera applications encounter widely varying illumination. The illumination for the cockpit camera can vary from direct sunlight to shade, and unfortunately these conditions can coexist, thus causing high contrasts.

Fortunately, modern variable-aperture cameras can compensate for most simple illumination problems. Black-and-white film is often desirable because of its ability to record high-contrast subjects with high resolution.

Camera location and mounting positions are often difficult to determine. A pilot-instrumentation camera often must be placed where the pilot frequently blocks the view. The wing tuft camera can never be mounted directly above the wing. At desirable camera locations, there is often no mounting space available.

All framing-type motion picture cameras and video cameras are sampled data recorders and are subject to aliasing. When dynamic events are observed by a sampling device such as a motion picture camera or television camera, misleading information can be generated (see Time-Sampled Data and Aliasing in Sec. 5 or Ref. 1). An example is an aileron flutter of a few hertz bandwidth being observed with a one-frame-per-second camera. This camera will incorrectly describe aileron motions that occur faster than 0.5 Hz. Another example is an airflow tuft in a turbulent air current which appears relatively stationary at an incorrect angle owing to a slow-frame-rate camera.

6.3.2 Television Camera

The television camera is a very desirable airborne data-acquisition device. It provides flight-test personnel with a real-time visual perspective available with no other technique. With the normal data-acquisition process, emphasis is on the details of the process being monitored. The television camera as a data-acquisition system provides a valuable overview to complement the details of the standard system.

The bandwidth of a standard television camera is nominally 5 MHz but it can be much higher in certain high-resolution or high-speed cameras. To record these bandwidths on board the vehicle, a special rotating- or fixed-head video tape recorder is required. When a television camera is used, the data are often telemetered to the ground station to avoid the complications of on-board recording. A scarce wide-band channel (10-MHz spacing) is required for standard television camera transmissions.

6.4 CONTINUOUS-TRACE RECORDER

Continuous-trace recorders, such as the pen or hot-stylus strip-chart recorder, are sometimes used in the flight testing of commercial passenger-type aircraft. On these vehicles the environment is benign. However, it is desirable to use ruggedized equipment: when violent maneuvers do occur, the data are likely to be important, and errors introduced by such accelerations would be very undesirable. These recorders will not be discussed here, because they are not in general use and typically contain sophisticated internal signal conditioning, such as variable-gain amplifiers, zero offset, and deflection limiters, which allow most data channels to be easily matched. Oscillographs and other continuous-trace recorders are seldom used in modern, large-scale flight tests. The main reason is that there is no electronic technique for conversion and subsequent reduction of the data. Manual conversion of any major amounts of data can result in the expenditure of large amounts of manpower and usually involves long time-delays before the data are available.

Of all the continuous-trace recorders, only the light-beam type of oscillograph has achieved widespread acceptance for airborne flight-test data acquisition. Oscillographs have been perfected to the extent that they can be used effectively even in the harsh environment of high-performance aircraft.

An appropriate application for the oscillograph is the small program in which the data can be visually scanned for a significant, recognizable data event. Then the data for that event can be reduced by means of a ruler or some of the film reading aids available. When oscillographs are used in this manner, a small program can be accomplished with limited resources.

The light-beam oscillograph uses galvanometers; it is illustrated in Fig. 101a. The operation of a galvanometer is described as follows: A current I_G through the galvanometer coil, which is located in a magnetic field, causes the coil and the attached mirror to rotate, which moves a beam of light across the film. This film is moving at a known rate past a slot. The beam of light is focused as a bar of light perpendicular to the film slit, and this forms a trace on the film.

A typical oscillograph has 36 traces on one film strip. The film is nominally 20.3 cm (8 in.) wide. When the 36 active traces are placed on the 20.3-cm (8-in.) film, the traces often become scrambled and hard to separate. In a study conducted at the Dryden Flight Research Facility, real flight-test oscillographic data were re-submitted to an experienced and highly skilled film-reading group. The only significant errors they found occurred when the wrong trace was inadvertently tracked for short portions of active data, that is, when traces were crossing each other. These trace crossover errors occurred normally when two traces were merging at a slow rate (dramatic trace crossovers were usually detected). The errors involved were usually 10% or less, large enough to be significant but small enough, unfortunately, to pass as valid data. As far as could be determined, no data user had suspected that the data were in part erroneous. The problem of crossing over to another trace during data reduction can be alleviated to some extent by a device such as the trace interrupter shown in Fig. 101b. A trace interrupter interrupts the traces sequentially from channel 1 to the last channel; thus, when the trace identification is in doubt, the engineer can count interruptions to locate the correct trace. For subtle crossings of limited duration, such as those in the above study, the interruptions may be too infrequent to help. The trace interruptions in Fig. 101b are indicated by the a's on the film strip.

Recording the time on continuous-trace recorders is difficult. In Fig. 101b, the vertical lines are produced by a strobe light which illuminates the whole film slot at one instant. These vertical bars can be repeated at known intervals (0.1 sec is a common interval). In the example shown, every tenth line is missing to permit fast visual scanning for a particular time interval. It is often desirable to include further simple-time encoding, such as that shown by eliminating progressively one vertical bar in each sequence of nine bars, thus encoding each group of 10 timing lines into additional groups of 10. If all the relevant data to be reduced are on one oscillograph, no further time-coding may be required; however, when the data must be correlated to other instruments, pilots comments, or ground observations, then further time-coding and display may be required. Figure 101b (channel 1) is a channel used to record real range time. The time-reference starts at the leading edge of the first pulse.

A common way of increasing channel capacity is to time-multiplex the slowly varying data onto one of the oscillograph film traces. These data are usually presented as pulse-amplitude modulated (PAM) data. The structural-temperature thermocouple transducers are often used in PAM TDM systems because of a very low frequency-response requirement. Since PAM creates periodic step inputs to the data-recording device, the recorder step response must be controlled. Galvanometer-recorder response characteristics are illustrated in Fig. 102. Figures 102a and 102b illustrate the output response of a typical galvanometer element to a constant-amplitude sinusoid as a function of frequency. A sinusoidal signal at a 0.5 damping ratio can be electromechanically amplified by more than 15% at about 70% of its natural frequency f_n . At $d = 0.6$, the amplification is slightly less than 5% at about 54% of f_n . At $d = 0.64$, the amplification is about 2%. A damping of $1/\sqrt{2}$ is the lowest value of damping for which there is no amplification. A damping of $d = 1.0$ is called critical damping because it is the lowest value of damping for which a step input will produce no overshoot.

Galvanometers are usually damped at approximately $d = 0.64$. This produces a maximum amplification of 2%. More importantly this 0.64 value also produces the most linear phase shift with frequency in the passband 0 to f_n . This linear phase shift characteristic means that transient data are reproduced with minimum wave-shape distortion.

With a PAM waveform (step input), it is desirable that the final value be reached as quickly as possible. Too much damping results in the trace taking too long to reach its final value. Too little damping can result in excessive oscillations. Figure 102c illustrates a galvanometer response to a step input for various values of damping. A damping ratio of 0.64 is nearly optimum for both sinusoidal and transient data inputs. In Fig. 101b, the PAM trace channel 5 has $d = 0.64$ and reaches its final value before the next channel is sampled.

Table 10 lists some typical Honeywell galvanometer characteristics. Note that the sensitive galvanometers require that the external resistance, as seen by the galvanometer, be a specified value in order to achieve a given damping, for example $d = 0.64$. Figure 103 illustrates two techniques for accomplishing this task. This is called electromechanical damping. In general, galvanometers are divided into two types, those which achieve their desired damping by means of an external resistor (electromechanically damped galvanometers) and those which are fluid damped. The electromechanically damped galvanometers are usually sensitive units with low natural frequencies (for example, natural frequencies of 24 to 600 Hz; Table 10). The fluid-damped galvanometers depend on a viscous fluid to provide the damping and usually have high natural frequencies (Table 10), for example, 1,000 to 22,000 Hz, and low current sensitivities. The fluid-damped galvanometer can tolerate a wide range of input resistances.

TABLE 10. — MINIATURE GALVANOMETER CHARACTERISTICS
(from Ref. 40)

Galvanometer type, number	Undamped natural frequency, Hz	Frequency response, Hz $\pm 15\%$	External damping resistance	Current sensitivity, $\pm 5\%$	Maximum current
Miniature electromagnetically damped galvanometer characteristics					
M24-350	24	0 - 15	350	0.59 $\mu\text{A/cm}$	5
M100-120A	100	0 - 60	120	3.94 $\mu\text{A/cm}$	10
M200-350	200	0 - 180	350	10.00 $\mu\text{A/cm}$	10
M600-350	600	0 - 540	350	51.20 $\mu\text{A/cm}$	15
Miniature fluid-damped galvanometer characteristics					
M1000	1,000	0 - 600	---	1.04 mA/cm	70
M3300	3,300	0 - 2,000	---	7.87 mA/cm	70
M10000	10,000	0 - 6,000	---	15.70 mA/cm	70
M13000	13,000	0 - 13,000	---	32.10 mA/cm	70

By far the most popular airborne flight-test galvanometers are the high-sensitivity types. Quite commonly, the required external damping resistance will be 120 or 350 Ω , which corresponds to the two most common strain-gauge-bridge resistance values, thus providing optimum damping when the bridge is directly connected to the galvanometer. The galvanometer responds like a second-order low-pass filter. In this case the galvanometer natural frequency f_n corresponds to the second-order low-pass filter cut-off frequency f_{CH} . This can be a very useful characteristic since the galvanometer can then provide its own filtering.

Another desirable feature of galvanometers is the ground isolation. This can be an advantage when a low-output-voltage transducer, such as thermocouple, must be grounded at the sensor location. Ground isolation reduces multiple ground electrical noise contamination and simplifies instrumentation system design.

An unusual variation of the oscillograph is the fiber-optic, cathode-ray-tube (FO-CRT) oscillograph developed by Honeywell and used in the Model 1858 Visicorder. The galvanometers and the light source are replaced by a specially designed FO-CRT. The FO-CRT faceplate consists of about 10 million individual glass fiber-optic strands. These strands, each only a few microns in diameter, are fused together into a 5- by 200-mm (0.2- by 8-in.) area. Since the ultraviolet-emitting phosphor is deposited directly on one end of these fiber-optic strands, the light emitted by the phosphor is transmitted through the strands in an efficient manner to the photosensitive paper. The recording paper is in direct contact with the other end of the fiber optic strands and thus additional optical elements are not required. The photosensitive paper used in these recorders is self-developing so the film can be read like a strip-chart recorder for reasonable film speeds. In the FO-CRT oscillograph, the CRT electron beam is blanked except when a mark is desired on the film. The FO-CRT has a frequency response from 0 to 5 kHz. Since the FO-CRT trace is formed by an electron beam, it has no inertia; as a result, the damping problem associated with galvanometers is absent. This unit has plug-in modules that provide such desirable signal conditioning as differential amplifiers; strain-gauge modules with internal excitation voltage; thermocouple modules, including thermocouple junction compensators, for common types of thermocouples; and frequency-to-voltage converters.

In summary, the continuous-trace recorder is excellent for visually scanning data, but it is acceptable for data reduction only if certain visually identifiable events are to be read into reduced data. For computer processing of large amounts of flight-test data, continuous-trace recorders are operationally cumbersome.

6.5 PILOT AND AIRCREW DISPLAYS

In this section, airborne displays are divided into pilot displays and crew displays. The pilot displays refer to displays for use by the person controlling the flight-test vehicle; they are usually located in the vehicle cockpit, except for remotely piloted vehicles. The crew displays refer to displays for those persons on the flight-test vehicle whose function is to support the flight-test program. Since these displays are quite diverse and often unique, this section addresses the rationale for selecting the type of display that presents data parameters acquired from the flight-test data-acquisition system. Although it is not included in the original definition of signal conditioning, an interesting exception to the definition of Ref. 1 occurs in the case of pilot and aircrew displays. In this case, the signal conditioning problem could well be one of presenting the signal in a useful form to the terminal device, the pilot or crew member. This is the rationale used in the following discussions.

6.5.1 Pilot Displays

The task of piloting a flight-test vehicle is very demanding. Piloting a remotely piloted vehicle is in many ways (except for personal safety) even more demanding. During critical maneuvers, the active vision of the pilot narrows down to those instruments directly in front of him. Blinking red lights in the peripheral vision may warn of various emergency conditions, but the side panels are certainly not desirable sites for conveying critical flight-test information to the pilot. When a parameter is critical to meeting the flight-test objectives, it should be located directly in front of the pilot. Unfortunately, this area of the cockpit is usually already full of basic flight instrumentation and seldom is there room for an additional display. When there is no room available, two possibilities exist: preempt the space used by some other instrument or make one of the existing instruments serve two functions. The first alternative, taking over the space used by another instrument, is an easy but not too likely solution since only critical instruments are given these choice locations. The second alternative, using a multiple-mode instrument, is a very tempting one. For example, the three-axis ball is centrally located and the several display functions can be re-allocated. This approach has one major problem: if a serious flight emergency occurs, the pilot may, with disastrous results, revert to interpreting the instrument as if it were in the original mode. This type of confusion has actually happened, and the potentially adverse consequences of a dual-function display should be seriously considered.

Pilot displays should be kept as simple and straightforward as possible. Good results have been accomplished with a pilot display that indicated deviation from a desired condition. Even with simple displays, individual pilot preferences can produce complications. In one flight program, a vertically moving-pointer was used to display normal acceleration. Two pilots were involved in the program. One pilot wanted the pointer to move up as the stick was pushed forward and the other pilot preferred the reverse condition. A simple switch, preset before flight, solved this problem; but, this meant that a dual-function indicator had two possible modes in the flight-test application. This system functioned very well, but extra precautions were required in preflight setups.

What kinds of pilot presentations should be avoided? A good example is a large display panel that contained many binary switches to call up one of 512 data channels for a light-emitting diode (LED) display. The pilot would probably not use this kind of display when it requires mental computation during critical flight situations.

6.5.2 Crew Displays

The on-board crew members who need displays can include a copilot or a group of technical personnel. The crew can use more complex displays than the pilot, for example, the display described in the preceding paragraph as unacceptable. However, to use these crew members effectively, their only tasks should be to

make sure the flight-test objectives are achieved in an optimum manner. Examples of the use of microprocessors and minicomputers to expedite flight-test programs were cited in Sec. 4. To exploit the potential of the on-board personnel and to promote flight-test objectives, microprocessors and minicomputers deserve serious consideration. Computers can provide data in engineering units instead of in the raw form, and can perform complex calculations for derived parameters (gross weight and center of gravity) in near-real time. The output of these computers can be conveniently displayed on cathode-ray tubes where color graphics can increase intelligibility, limits can be marked, and special events highlighted. These displays can be used to provide crew members with the information they need to make realistic real-time contributions to the flight-test program; moreover, the displays can do so quickly and effectively. It does not make sense to include on-board crew members in a flight-test program to view displays unless they can increase flight test-efficiency, and well-designed displays can significantly increase that efficiency.

- A = IDEAL HEAD RESPONSE
- B = HEAD GAP LOSS
- C = HEAD/TAPE SEPARATION LOSS
(SHOWN FOR 0.1 GAP SPACING, g)
- D = MAGNETIC OXIDE THICKNESS, t ,
LOSS ($t = 0.5 g$)
- E = OVERALL HEAD RESPONSE
- g = REPRODUCE GAP SPACING
- λ = WAVELENGTH OF THE RECORDED
FREQUENCY

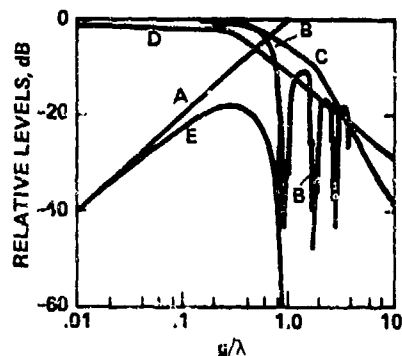


Figure 95. Frequency-response characteristic for magnetic record-reproduce process

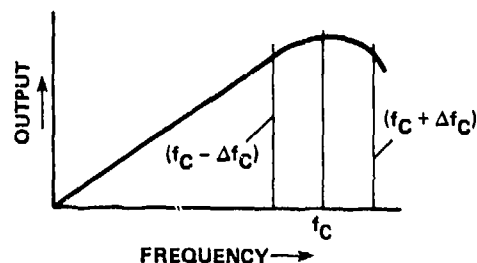


Figure 96. FM voltage controlled oscillator placement on wideband FM magnetic tape recorders

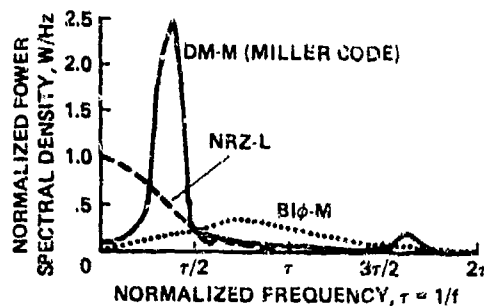
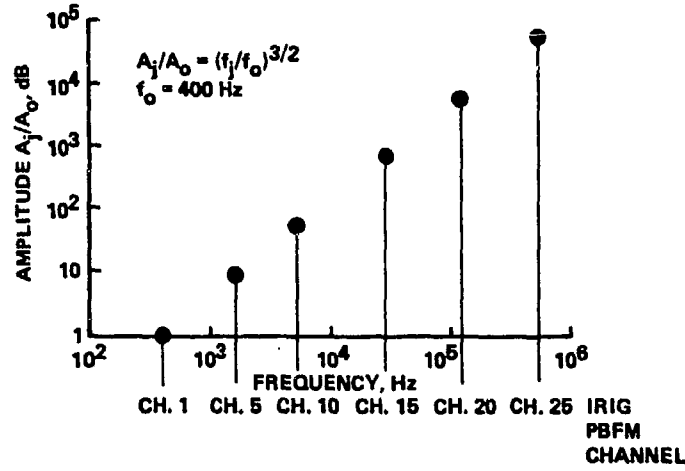
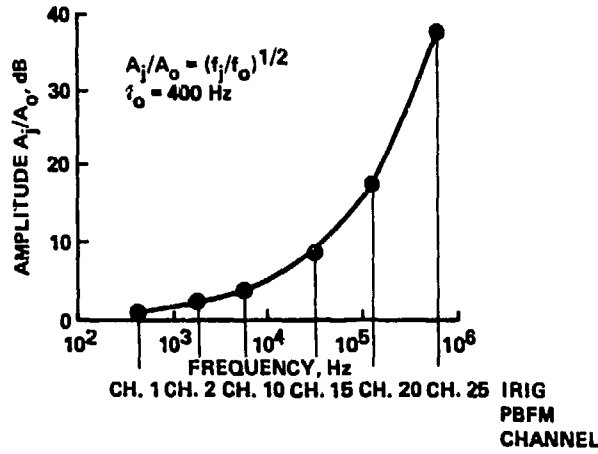


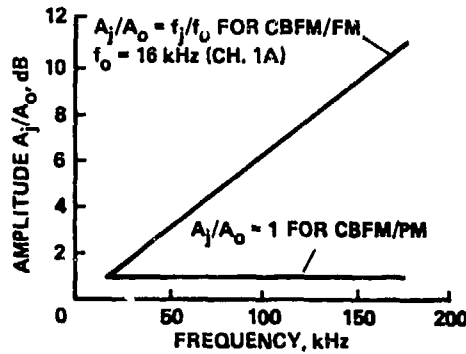
Figure 97. Power spectral density distribution for three digital codes



(a) Pre-emphasis schedule for PBFM/FM

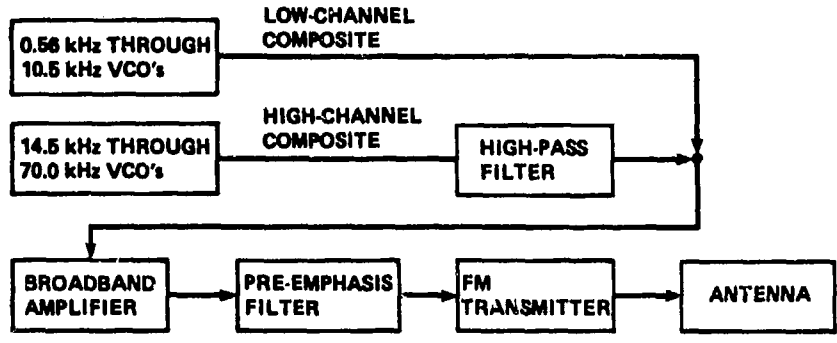


(b) Pre-emphasis schedule for PBFM/PM

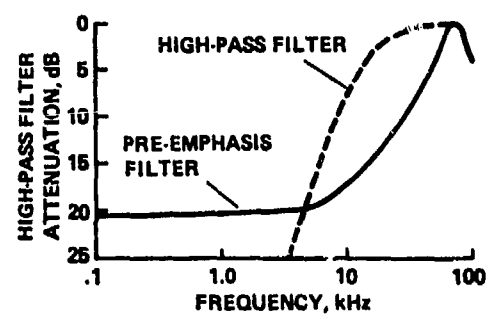


(c) Pre-emphasis schedule for CBFM

Figure 98. Pre-emphasis for IRIG frequency-division multiplexing transmission systems



(a) Noise reduction pre-emphasis technique



(b) Filter characteristics

Figure 99. PPM/FM telemetry pre-emphasis technique

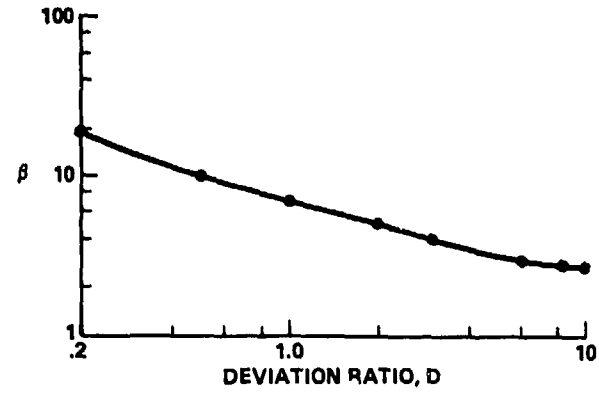
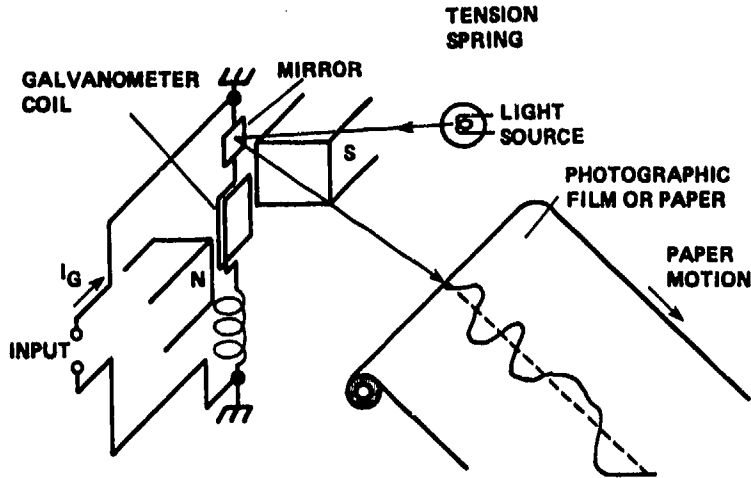
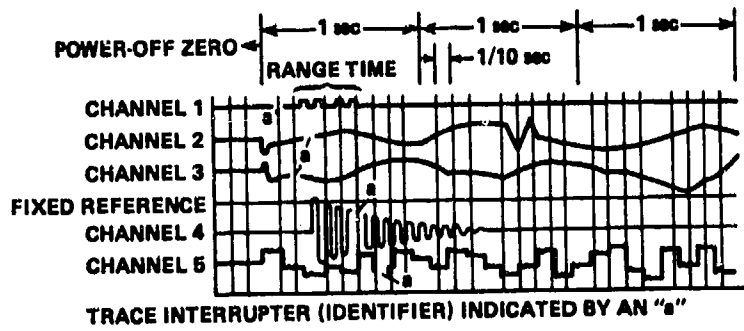


Figure 100. Bandwidth at which all sidebands have amplitudes less than 1% of unmodulated carrier (B is bandwidth factor.)



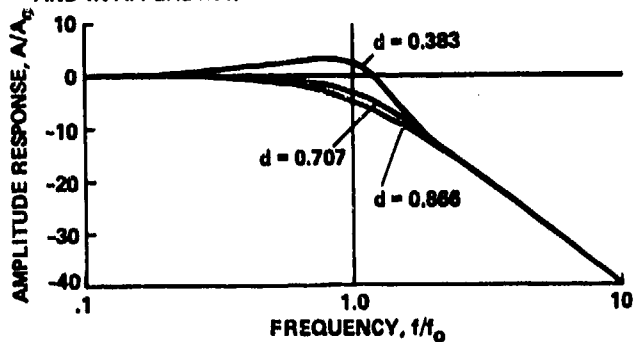
(a) Illustration of a D'Arsonval-type galvanometer recorder



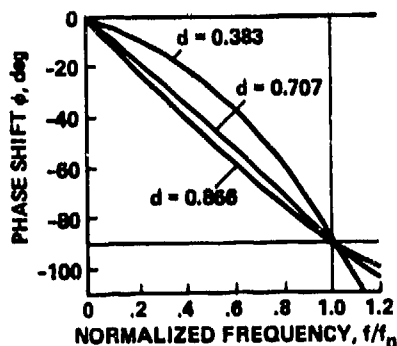
(b) Section of an oscillographic film strip (Trace interrupter indicated by an "a.")

Figure 101. Oscillograph and resultant film strip

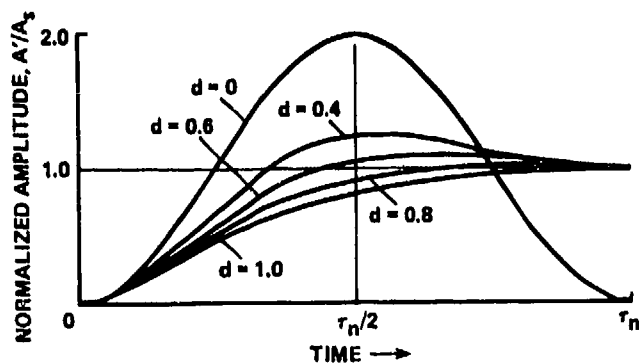
- A** - RECORDED AMPLITUDE OF THE SIGNAL AT ANY FREQUENCY f
A' - RECORDED AMPLITUDE AS A FUNCTION OF TIME OF A GALVANOMETER RESPONSE TO A STEP INPUT
 A_0 - RECORDED AMPLITUDE OF THE INPUT SIGNAL AT A FREQUENCY $f \ll f_n$
 A_s - AMPLITUDE OF A UNITY STEP FUNCTION
 d - GALVANOMETER DAMPING COEFFICIENT*
 f_n - NATURAL FREQUENCY OF THE GALVANOMETER ($f_n = 1/\tau_n$)
 INPUT SIGNAL = $A_0 \sin(2\pi ft)$
 ϕ - PHASE SHIFT OF THE OUTPUT WITH RESPECT TO THE INPUT
 τ_n - TIME TO COMPLETE ONE CYCLE AT f_n
 *THE GALVANOMETER DAMPING COEFFICIENT (d) IS HALF OF THAT OF THE FILTER DAMPING (ALSO d) DISCUSSED IN SEC. 3 AND IN APPENDIX I.



(a) Sinusoidal amplitude response as a function of damping coefficient



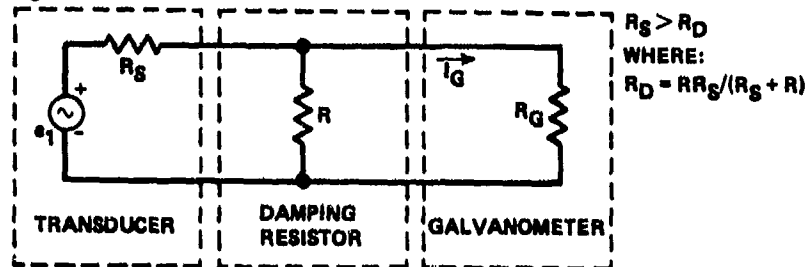
(b) Sinusoidal phase response as a function of damping coefficient



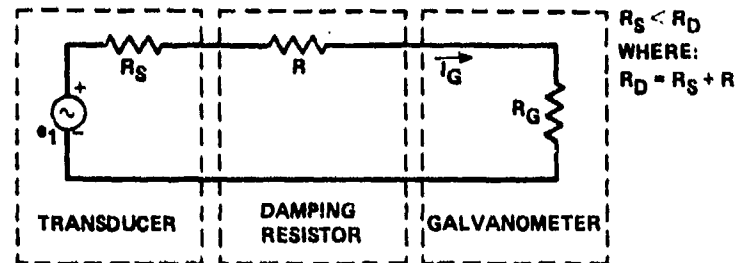
(c) Unit step response as a function of galvanometer damping coefficient

Figure 102. Galvanometer characteristics as a function of damping coefficient

- d = GALVANOMETER DAMPING
 e_1 = TRANSDUCER VOLTAGE
 I_G = GALVANOMETER DEFLECTION CURRENT
 R = RESISTANCE USED TO ADJUST GALVANOMETER DAMPING
 R_D = EFFECTIVE EXTERNAL RESISTANCE WHICH MUST SHUNT THE GALVANOMETER TO PROVIDE THE DESIRED DAMPING d
 R_G = GALVANOMETER COIL RESISTANCE
 R_S = INTERNAL TRANSDUCER RESISTANCE



(a) Damping network when source resistance R_S is higher than desired external damping resistance R_D



(b) Damping network when source resistance R_S is lower than desired external damping resistance R_D

Figure 103. Typical galvanometer damping techniques

APPENDIX A
OPERATIONAL AMPLIFIER

The name operational amplifier was originated by those who work with analog computers to designate the amplifiers that were used to perform various mathematical functions such as summation, subtraction, integration, and differentiation. One of the major applications for the modern operational amplifier is its use as a signal-conditioning element. Several operational-amplifier-circuit application books are readily available, Refs. 10 and 11.

The operational amplifier considered here is a direct-coupled, high-gain differential amplifier which uses feedback to obtain its unique operational characteristics. Figure 104 shows an operational amplifier with two drive voltages, e_1 and e_2 . The amplifier open-loop voltage gain is A' , and the input/output voltage relationships are represented by

$$e_o = A' (e_2 - e_1) \quad (A1)$$

From Eq. (A1) it is obvious why the input marked minus is called the inverting input and the input marked plus is the non-inverting input.

The characteristics of an "ideal" operational amplifier will first be examined, and then the practical deviations from the ideal case will be explored. The ideal operational amplifier has (1) infinite open-loop voltage gain (A'); (2) infinite input impedance; (3) zero output impedance; (4) infinite frequency bandwidth; and (5) no internally generated input voltages or currents.

Two important conclusions can be immediately drawn from characteristics (1) and (2) above: (1) since the amplifier gain is infinite, the voltage difference at the input terminals must always be equal to zero to avoid infinite output voltage ($e_2 - e_1 = 0$), and (2) since the amplifier has infinite input impedance, no current can flow into its input terminals. These two conditions lead directly to the idea of the "virtual short circuit." When one input terminal is grounded, the second input terminal must also be at ground potential; thus it is called a "virtual ground." Any input to this second input terminal is forced by feedback to function as a "virtual short circuit;" however, the two inputs can have no current flow between them.

Figure 105a illustrates an operational amplifier connected in what is known as the inverting mode, because the output polarity is opposite the input. The following equations can be derived from Fig. 105a:

$$I_1 = (e_1 - e_e)/(Z_1 + Z_S) \quad \text{where } e_e \approx 0 \text{ and } Z_S \ll Z_1$$

$$I_1 = e_1/Z_1 \quad (A2)$$

$$I_2 = (e_e - e_o)/Z_2 \quad \text{where } e_e \approx 0$$

$$I_2 = e_o/Z_2 \quad (A3)$$

In Eqs. (A2) and (A3), e_e is 0, since from Fig. 105 it can be seen that the non-inverting amplifier input is grounded and that the inverting input must be at a "virtual ground." In addition, since no current can flow into the amplifier terminal because of its infinite input impedance, then

$$I_1 = I_2 \quad (A4)$$

From Eqs. (A2)-(A4), the closed-loop gain A can be derived as

$$A = e_o/e_1 = (-I_2 Z_2)/(I_1 Z_1) = -Z_2/Z_1 \quad (A5)$$

It is important to note in Eq. (A5) that the closed-loop system gain A is a function only of the ratio of the impedance Z_1 and impedance Z_2 . The ratio of Z_1 to Z_2 can be tightly controlled through the use of precision components and, therefore, the amplifier gain can also be very well defined. It should be emphasized that even though the input impedance of the ideal operational amplifier is infinite, the input impedance of the inverted feedback operational amplifier circuit is Z_1 , which can be any value.

The non-inverting operational amplifier is illustrated in Fig. 105b. The voltage relationships of Fig. 105b are

$$e_1 = I_1 Z_1 = e_o Z_1/(Z_1 + Z_2) \quad (A6)$$

$$e_1 = e_2 \quad (A7)$$

Therefore, the closed-loop gain of the operational amplifier used in the non-inverting mode, as shown in Fig. 105b, is

$$A = e_o/e_2 = 1 + (Z_2/Z_1) \quad (A8)$$

From Eq. (A8), it should be observed that gain in the non-inverting mode is always greater than or equal to 1. One of the main uses of the non-inverting amplifier is as an impedance converter with a gain of 1. When Z_2 is 0 (a short), the voltage gain is exactly 1.

A.1 NON-IDEAL OPERATIONAL AMPLIFIER CHARACTERISTICS

Actual operational amplifiers do not have the ideal characteristics listed previously. The effects of these deviations from the ideal characteristics will be discussed in the following sections. Detailed mathematical derivations of these effects will not be covered in this text since they are very well detailed in Appendix A of Ref. 10. The following section will address the effects of deviations from the ideal. The emphasis will be on the limitations introduced by these non-ideal characteristics.

A.2 ERRORS CAUSED BY FINITE OPEN-LOOP AMPLIFIER GAIN

Actual operational amplifiers do not have infinite open-loop gain. Even the most economical of these amplifiers, however, usually have open-loop voltage gains of about 100,000 (100 dB) or more. Figure 106 illustrates the gain characteristics of an operational amplifier which has a finite open-loop voltage gain A' of 100,000 (100 dB) and a closed-loop voltage gain A of 100 (40 dB). A "feedback factor," β , is defined as the voltage feedback in the closed-loop network. The loop gain $A'\beta$, is approximately the ratio of the open-loop gain to the closed-loop gain, as shown by

$$\text{loop gain} = A'\beta \approx A'/A \quad (\text{A9})$$

In this example, the loop gain is 100 dB minus 40 dB or 60 dB; that is, a gain of 1,000. The loop gain $A'\beta$ is very important as a measure of the closed-loop circuit performance. In a real operational amplifier circuit, the gain instabilities and circuit nonlinearity are all reduced by increasing β (the amount of negative feedback). Usually $A'\beta$ will be much larger than unity so as to obtain a stable closed-loop gain. Where the relationship $A'\beta \gg 1$ is valid, the ideal closed-loop voltage gain closely approximates the actual amplifier voltage gain:

$$(\text{actual gain}) \approx (\text{ideal gain}) \{1 - [1/(A'\beta)]\} \quad (\text{A10})$$

As an example of an application of Eq. (A10), in an inverting-mode operational amplifier with an open-loop gain A' , of 100,000 and a closed-loop gain A of 100, the actual gain differs from the ideal gain by 0.1%:

$$\begin{aligned} (\text{actual gain}) &\approx 100[1 - (1/1000)] \\ &\approx 100(0.999) = 99.90 \end{aligned}$$

Now if the open-loop gain should vary by $\pm 25\%$, the actual gain would be

$$\begin{aligned} (\text{actual gain}) \Big|_{1.25A'} &= 100(1 - (1/1250)) = 99.92 \\ (\text{actual gain}) \Big|_{0.75A'} &= 100(1 - (1/750)) = 99.87 \end{aligned}$$

Therefore, a $\pm 25\%$ change in the open-loop gain produces less than $\pm 0.03\%$ change in the actual closed-loop gain.

The effective output impedance Z_{oe} of the non-ideal operational amplifier also is reduced by negative voltage feedback. (It should be noted that the effective output impedance of an operational amplifier can be increased by negative current (series) feedback). Using the feedback configurations as shown in Fig. 107, the effective output impedance Z_{oe} , when $A'\beta \gg 1$, is

$$Z_{oe} \approx Z_o / (A'\beta) \quad (\text{A11})$$

The overall system linearity also improves with the addition of negative feedback.

Thus, it can be seen that for stable gain, low-output impedance, and good linearity, it is very desirable to keep the loop gain very high — $A'\beta \gg 1$.

A.3 EFFECTS OF FINITE OPERATIONAL AMPLIFIER OUTPUT IMPEDANCE

It can also be deduced from Fig. 107 that the open-loop output impedance Z_o reduces the effective open-loop circuit gain because it interacts with the load and feedback network. The relationship between the expected open-loop gain A'_E , and the effective open-loop gain A' , caused by the inclusion of a finite output impedance Z_o , is

$$A'_E = A' \frac{1}{1 + (Z_o/Z_L) + Z_o/(Z_1 + Z_2)} \quad (\text{A12})$$

As can be seen from Eq. (A12), when $Z_L \gg Z_o$ and $Z_1 + Z_2 \gg Z_o$, then $A'_E \approx A'$. It is therefore desirable that Z_o be very small.

A.4 EFFECTS OF FINITE OPERATIONAL AMPLIFIER FREQUENCY RESPONSE

Real operational amplifiers have a non-infinite frequency response. Figure 108 illustrates an operational amplifier with an open-loop gain A' of 100,000 (100 dB), a closed-loop gain A of 100 (40 dB),

negligible output impedance, a unity gain frequency, f_1 , of 1 MHz, and an internally adjusted frequency roll-off of 6 dB/octave (20 dB/decade).

It is important to note in Fig. 108b that even though the unity gain bandwidth is 1 MHz, the open-loop gain starts decreasing at 10 Hz. At 10 Hz, the output is already down 3 dB (about 70.7% of its low-frequency value). This means that the loop gain $A\beta$ is dropping at 6 dB/octave above 10 Hz. It is this loop gain that stabilizes the amplifier gain, reduces the effective output impedance, and linearizes the output. For example, the loop gain is 60 dB at very low frequencies, 20 dB at 1 kHz, and 0 dB at 10 kHz. At and above 10 kHz, the closed-loop gain is the open-loop gain. Both the open-loop gain and the closed-loop gain are 0 dB at 1 MHz (f_1).

The relationship $A\beta \gg 1$ must be maintained to simplify many of the operational amplifier equations. Design equations including the effects of $A\beta$ are derived in Ref. 10; they are not included here because operation under conditions of $A\beta \approx 1$ should be avoided. Most flight-test data signals have low bandwidths; hence this loss of gain with increasing frequency does not degrade critical amplifier performance. When wide bandwidth is required, premium operational amplifiers, which have much greater bandwidths than those in the example, should be used.

Most internally compensated operational amplifiers have a roll-off of 6 dB/octave. The reason for selecting this roll-off is that such an amplifier is unconditionally stable when used with resistive loads and resistive feedback. According to Bode's criterion, the closed-loop stability of an amplifier is ensured when the rate of closure of the open-loop frequency response curve and the closed-loop gain curve is less than 12 dB/octave. Figure 109 illustrates some examples of stable and unstable amplifier frequency-response based on this criterion. The illustrated rate in Fig. 109a is 6 dB/octave; in Fig. 109b, 12 dB/octave; in Fig. 109c, 18 dB/octave, and in Fig. 109d, 6 dB/octave.

Some designers use operational amplifiers with a roll-off of 12 dB/octave to achieve larger open-loop gain at higher frequencies and to achieve higher frequency bandwidths for the same basic amplifier design (compare dotted line in Fig. 109b to solid curve). To provide adequate stability margins, these designers usually incorporate a capacitor in the feedback network to provide the characteristics shown in Fig. 109d.

A.5 EFFECTS OF OPERATIONAL AMPLIFIER FINITE INPUT IMPEDANCE

In the idealized open-loop operational amplifier, it was assumed that the input impedance was infinite. In practical operational amplifiers, two types of input impedance must be considered: differential mode Z_D and common mode Z_{CM} . In Fig. 110, an ideal operational amplifier is shown with the input impedances Z_D and Z_{CM} shown as external components. In this figure, e_1 is the inverting-mode input and e_2 is the non-inverting-mode input.

The relationship of the output voltage e_o as a function of the input voltages e_1 and e_2 in a closed-loop configuration, which includes the input impedances, is shown in the following equations:

$$e_o = \frac{e_2[1 + (Z_2/Z_1) - (Z_2/Z_{CM})]}{1 + 1/A\beta_1} - \frac{e_1(Z_2/Z_1)}{1 - 1/A\beta_1} \quad (A13)$$

where

$$\beta_1 = \frac{1}{1 + (Z_2/Z_1) + (Z_2/Z_D) + (Z_2/Z_{CM})} \quad (A14)$$

Note that the actual feedback factor β_1 approaches the ideal feedback factor when $Z_D \gg Z_2$ and $Z_{CM} \gg Z_2$. Under these same conditions, Eq. (A13) reduces to the ideal operational amplifier equation.

The closed-loop input impedance Z_i of an inverting amplifier for low frequencies and $A\beta \gg 1$ is essentially Z_1 . For the non-inverting mode of operation under the same conditions, the input impedance Z_i is expressed by

$$Z_i \approx \frac{1}{1/(A\beta Z_D) + 1/Z_{CM}} \quad (A15)$$

Since the input impedance in the non-inverting mode is limited only by the input characteristics of the operational amplifier itself (disregarding external leakage resistances and stray capacitances), it is the circuit configuration of choice when extremely high input impedance is required.

How realistic are the earlier assumptions that Z_D and Z_{CM} must be much greater than Z_2 ? To answer this question, consider the following cases: case (1) is a low-cost, integrated-circuit (IC), operational amplifier that has a minimum differential input impedance Z_D of $0.3 \times 10^6 \Omega$ and a common-mode input impedance of $10^8 \Omega$ shunted by 5 pF; and case (2) is an IC operational amplifier that uses field-effect transistors (FET) in the input stages to produce a Z_D of $10^{14} \Omega$ shunted by 2 pF and Z_{CM} of $10^{12} \Omega$ shunted by 2 pF. Both of the foregoing cases are typical descriptions of available, real operational amplifiers. In both cases, when $Z_D \gg Z_2$ then $Z_{CM} \gg Z_2$ is also true.

In case (1), $Z_D \gg Z_2$ is interpreted to mean that Z_D is at least two orders of magnitude greater than Z_2 ($Z_D > 100 Z_2$). For the minimum specified value of Z_D , the value of a resistive Z_2 must be

less than 3,000 Ω . For a closed-loop gain (low frequency) of $A = 100$, then R_1 is 30 Ω (derived from $A = R_2/R_1$). When this amplifier is used in the inverting mode, the closed-loop input impedance is approximately equal to 30 Ω . Under these conditions, when the voltage source e_1 has an internal impedance R_s of 350 Ω for a typical strain-gauge bridge, the actual gain equation is $A = R_2/(R_1 + R_s) \approx 8$. This gain of 8 is considerably different from the expected value of 100; the discrepancy is the result of the low input impedance.

If this same amplifier is used in the non-inverting mode for this example and $A\beta$ at low frequencies is 1,000, then the input impedance Z_i would from Eq. (A17) be equal to

$$\begin{aligned} Z_i &= 1/[1/(A\beta Z_D) + 1/Z_{CM}] \\ &\approx 1/[1/[(10^3)(3 \times 10^5)] + 1/10^8] \\ &\approx 75 \times 10^6 \Omega \text{ (at low frequency)} \end{aligned}$$

At this impedance level, the shunt capacitances can produce significant effects on the closed-loop performance at higher frequency in the form of additional capacitive feedback.

After reviewing the above example, the engineer may wonder why the non-inverting operational mode is not used for all applications. There are two major reasons: (1) many circuits cannot be implemented in the non-inverting mode, and (2) common-mode rejection is not as great for this mode of operation (see Effects of Finite Amplifier Common-Mode Rejection Ratio, in a following subsection).

In case 2, in which $R_D = 10^{11} \Omega$, R_2 could be very large and still meet the requirement that $R_2 \ll Z_D$. This means that even in the inverting mode of operation, where the effective amplifier input impedance is approximately equal to R_1 , this input impedance can still be very large. The use of high impedances in the feedback divider introduces serious limitations. The stray and shunt capacitances have a far greater effect at high impedance and high frequency. Also, the input bias currents (to be discussed next) have to be compensated.

A.6 EFFECTS OF INTERNAL VOLTAGE AND CURRENT BIAS

When an ideal operational amplifier is operated as a voltage amplifier, no output should exist for a zero input. In real amplifiers, this is never the case. When the input is zero, a steady-state output voltage exists which is called the output offset voltage. This output offset voltage is caused by three factors: (1) the input bias currents, (2) the input offset current, and (3) the input offset voltage. In flight-test applications, when an operational amplifier is used as a steady-state amplifier, the output offset voltage is often the most significant error parameter. The primary factor that causes output offset voltage variations is the ambient temperature changes which in turn cause deviations in the amplifier input offset voltage and in both the input and bias currents. The input bias currents, I_{B1} and I_{B2} , are steady-state currents that flow through the two input terminals of an operational amplifier. The bias currents at each input terminal are usually similar in magnitude; that is, the input bias current at the inverting terminal I_{B1} is approximately equal to the input bias current at the non-inverting terminal I_{B2} (see Fig. 111). These currents usually track one another and vary mainly as a function of the amplifier temperature.

From Fig. 111, the following equation can be derived:

$$e_{os} = I_{B1}R_2 - I_{B2}R_3(1 + R_2/R_1) \quad (A16)$$

Equation (A16) represents the output offset voltage, which is the result of input bias currents. The input offset voltage also contributes to the output offset voltage e_{os} and will be discussed later in this section. Normally $I_{B1} = I_{B2}$. If I_{B1} were equal to I_{B2} , the effects of the bias-current error voltage could be eliminated by setting R_3 to the parallel combination of R_1 and R_2 , as shown in

$$R_3 = (R_2 R_1)/(R_1 + R_2) \quad (A17)$$

for $I_{B1} = I_{B2}$. When the impedances R_1 , R_2 , and R_3 are large, the errors associated with bias currents are large, and it is more important to balance the two input impedances. The bias currents I_{B1} and I_{B2} are not usually equal, and the amplifier specification sheets often use the average bias current. The input offset current I_{os} is the difference between I_{B1} and I_{B2} and is usually at least an order of magnitude smaller than I_{B1} or I_{B2} . The average bias I_B current and the input offset current as I_{os} are given by

$$I_B = (I_{B1} + I_{B2})/2 \quad (A18)$$

$$I_{os} = I_{B1} - I_{B2} \quad (A19)$$

When R_3 is made equal to the parallel combination of R_1 and R_2 , and I_{B1} is not equal to I_{B2} , Eq. (A16) reduces to

$$e_o = I_{os}R_2 \quad (A20)$$

for $R_3 = R_1R_2/(R_1 + R_3)$. When R_3 is ignored ($R_3 = 0$), Eq. (A16) reduces to

$$e_{os} = I_{B1} R_2 \quad (A21)$$

In both cases, the output offset voltage is related to the feedback resistor R_2 ; however, in Eq. (A20), the offset voltage is proportional to the offset current I_{os} , which is usually much smaller than I_{B1} .

The output offset voltage error owing to I_B and I_{os} is a function of the input resistances, but the input offset voltage is not. Also, whereas I_B and I_{os} are specified as an initial value plus a temperature effect, the input offset voltage is usually specified as a function of temperature, power-supply voltage, and time. One method of measuring input offset voltage is shown in Fig. 112. The input offset voltage e_B is related to the output error voltage by the relationship

$$e_B = e_o/\beta(0) \quad (A22)$$

where $\beta(0)$ is the feedback factor at zero frequency. Note in Fig. 112 that the resistive impedances have been kept very low to reduce any effects from the input bias currents.

The initial output offset voltage can be nulled for a given set of conditions. In flight-test applications, the wide temperature excursions encountered cause drifts in e_B and I_B . The e_B value also is a function of the power-supply voltage and time. The power-supply dependence is usually specified as a direct function of the power-supply voltage level. The time-dependence is represented by a true random-walk function and as such, when the typical input offset voltage versus time is specified — for example as 20 $\mu\text{V}/\text{month}$ — then the variation for a year typically would be $\sqrt{12}$ 20 $\mu\text{V}/\text{year}$. The input offset voltage nulling process is accomplished by using the input termination provided by the manufacturer, or by adding a summing voltage at the feedback junction. Since the power supply voltage is normally controlled, the effect on the offset voltage is minimal. The drift with temperature contributes substantially to the offset-voltage variation. Some useful ways of reducing the drift are to (1) reduce the power supply voltage, which not only reduces e_B but also reduces I_B since it lowers self-heating; (2) provide a good heat sink for critical stages, which usually helps because the operational amplifier normally operates at temperatures above ambient; and (3) reduce the power output of critical stages, which also reduces the internally generated temperature.

Output offset voltage can also be generated from the rectification of very-high-frequency signals by the internal amplifier components. This type of offset voltage can only be reduced by preventing these high frequencies from reaching the amplifier. Radio frequency noise can enter the amplifier on any terminal, but is most common on the signal inputs, the power supply leads, and output leads. These leads are often the longest and thus the most susceptible to RF noise contamination.

A.7 EFFECTS OF FINITE AMPLIFIER COMMON-MODE REJECTION RATIO

The common-mode rejection ratio (CMRR) is a measure of how well an amplifier discriminates between the differential input voltage and the common-mode input voltage. A large CMRR is desirable and indicates the amplifier capability to amplify only differential input voltage and to exclude common-mode input voltage. The amplifier CMRR is defined from Fig. 113 as

$$\text{CMRR} = A_D/A_{CM} \quad (A23)$$

An amplifier can be adversely affected by its finite CMRR even though it has no external common-mode inputs. The finite CMRR, in many cases, can be a major source of nonlinearities and closed-loop gain errors for an operational amplifier used in the non-inverting mode. This is particularly true for the voltage-follower circuit shown in Fig. 114a. In this circuit the voltage at the inverting input is essentially e_1 :

$$e_{CM} = (e_1 + e_o)/2 \quad (A24)$$

(In an ideal operational amplifier the voltage at the inverting input would be identical to e_1 since both inputs must be at the same potential.) A finite CMRR causes this common-mode voltage to be amplified. Reference 10 derives the actual closed-loop gain of Fig. 114b to be

$$A = e_o/e_1 = (1 - 1/\text{CMRR})/(1 + 1/A^-) \quad (A25)$$

Equation (A25) is difficult to evaluate in an actual application because the CMRR is a function of such things as frequency and signal amplitude.

A.8 EFFECTS OF OTHER NON-IDEAL FACTORS

Other factors limit the real operational amplifier response such as slewing rate, full power response, and overload recovery time. These effects are well covered in the literature (Ref. 10) and are not addressed in detail in this volume; neither are these other factors ordinarily encountered in most flight-test applications.

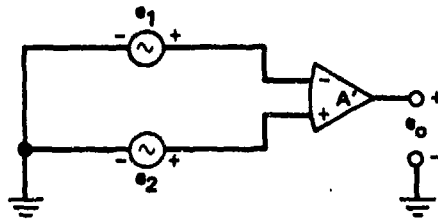
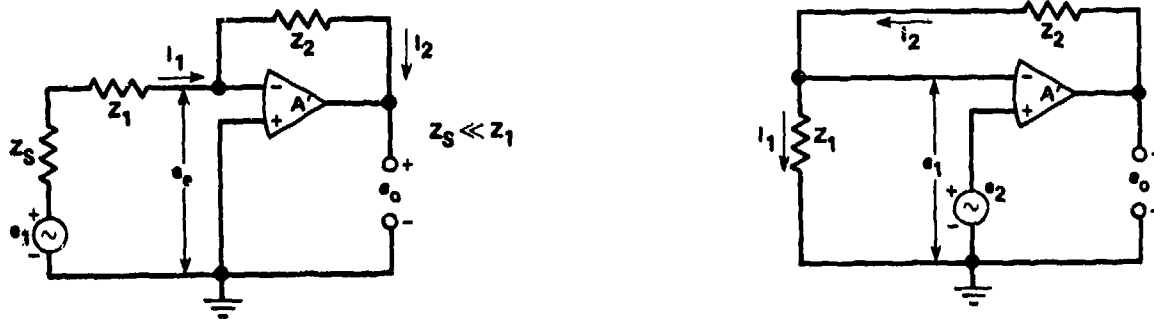


Figure 104. Differential operational amplifier



(a) Inverting amplifier

(b) Non-inverting amplifier

Figure 106. Inverting and non-inverting mode ideal operational amplifiers

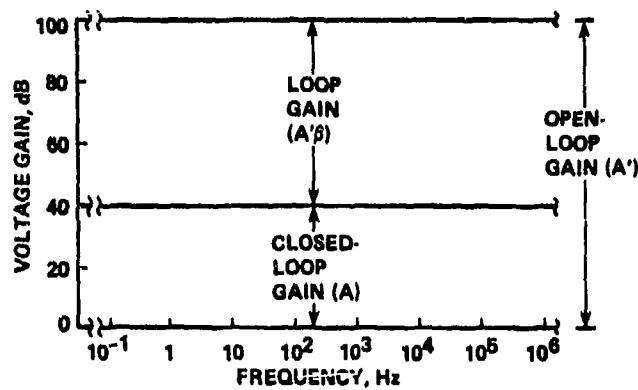


Figure 106. Gain characteristics of gain-limited ideal operational amplifier

$A'\beta \gg 1$

e_1 = INPUT VOLTAGE

e_0 = OUTPUT VOLTAGE

Z_L = LOAD IMPEDANCE

Z_o = OPEN-LOOP OUTPUT IMPEDANCE

Z_1, Z_2 = FEEDBACK IMPEDANCES

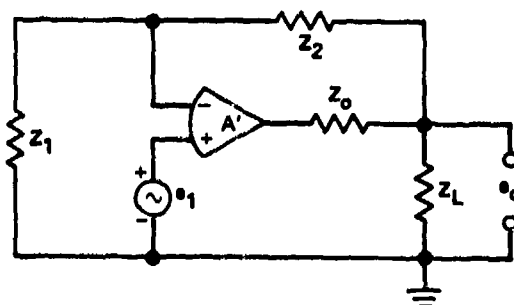
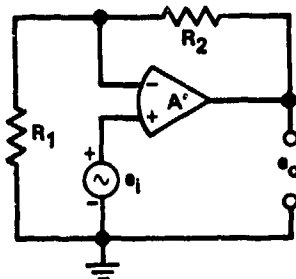
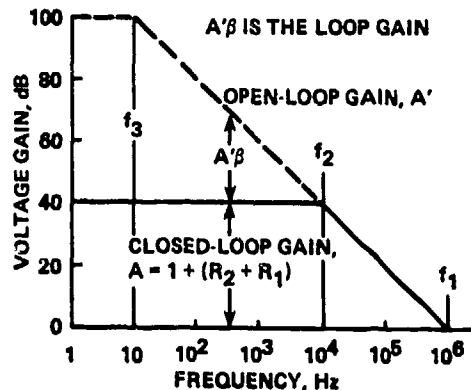


Figure 107. Model for calculating effective closed-loop output impedance

$A = 1 + (R_2/R_1)$; IN THIS EXAMPLE, A IS ASSUMED TO BE 100 (I.E., 40 dB)
 $A' = 100,000$ AT LOW FREQUENCIES
 e_i = INPUT VOLTAGE
 e_o = OUTPUT VOLTAGE
 f_1 = UNITY GAIN FREQUENCY; IN THIS EXAMPLE, f_1 IS ASSUMED TO BE 1 MHz

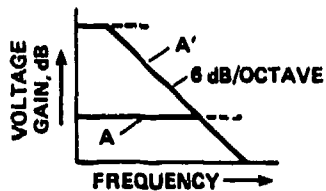


(a) Circuit representation

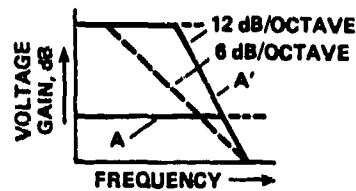


(b) Frequency-response characteristic

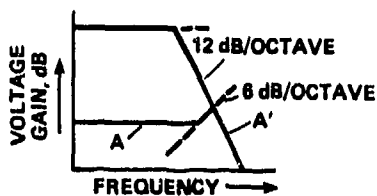
Figure 108. Operational amplifier and frequency-response characteristic



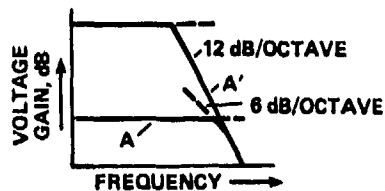
(a) Inherently stable amplifier



(b) Marginally stable amplifier



(c) Unstable amplifier



(d) Stable amplifier

Figure 109. Bode plots of operational amplifier characteristics

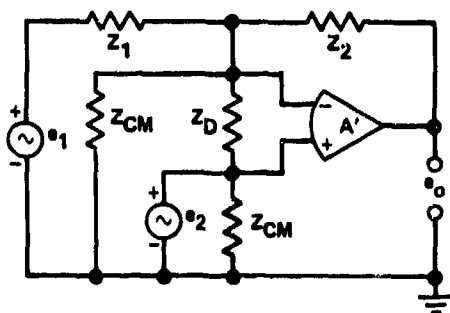


Figure 110. Finite input-impedance model

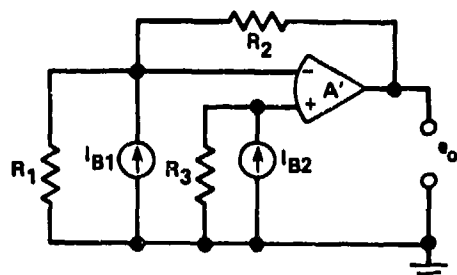


Figure 111. Finite input bias current model

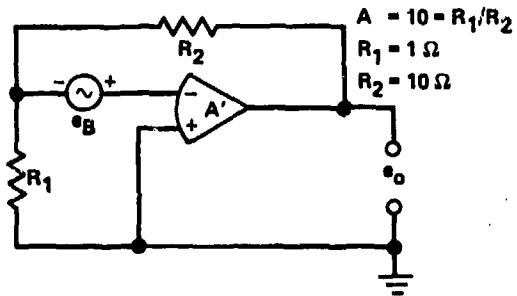


Figure 112. Input offset-voltage measuring circuit

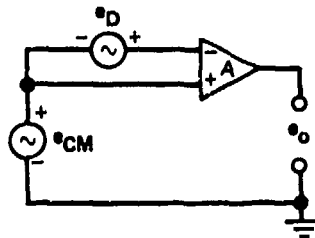
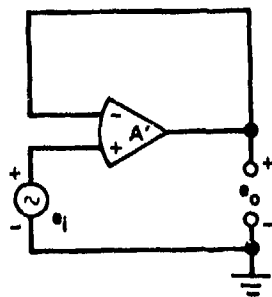
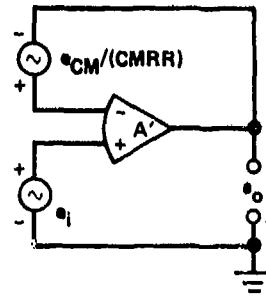


Figure 113. Common-mode rejection model



(a) Voltage-follower circuit



(b) Voltage-follower circuit including common-mode error

Figure 114. Gain reduction model for common-mode rejection ratio

APPENDIX B

SINGLE-ENDED VOLTAGE AMPLIFIER

A single-ended voltage amplifier is a voltage amplifier that has one signal input; the other input is the amplifier common. In this amplifier, one side of the input voltage source must be grounded to complete the electrical circuit.

The ideal Thévenized voltage signal source has an internal voltage generator that is directly proportional to the desired measurand and the source internal impedance is zero. In actual practice, a voltage source has a finite but usually low internal impedance. According to Thévenin's theorem, any two-terminal linear network containing one or more independent sources of voltage is equivalent to a simple voltage source having an internal impedance Z_0 . The generated voltage is the voltage that appears across the output terminals when no load impedance is connected, and Z_0 is the impedance that is measured between the terminals when all the independent voltage sources in the network are set to zero. Under these conditions, a source of voltage is represented as shown in Fig. 115 (which is similar to Fig. 7). Both the voltage source and the voltage amplifier output, as shown in Fig. 115, are equivalent voltage sources. In many actual applications, most of the impedances shown are subject to long-term drift and temperature variations. The output voltage e_0 in Fig. 115 is related to the source voltage e_s by the relationship

$$e_0 = A e_s [Z_i / (Z_s + Z_i)] [Z_L / (Z_0 + Z_L)] \quad (B1)$$

Examination of this relationship quickly reveals that if the output is to be independent of the variable circuit impedances, Z_i must be much larger than Z_s , and Z_L must be much larger than Z_0 . Under these conditions and with a stable amplifier gain A , the voltage across the load Z_L is directly proportional to the output of the voltage generator, e_s :

$$e_0 = A e_s \quad (B2)$$

From Fig. 115, it can also be seen that a voltage amplifier is an isolation amplifier to the extent that load variations do not affect the voltage source.

In the following circuit examples, extensive use will be made of operational amplifiers (see Appendix A) to illustrate various amplifier configurations.

B.1 THE SINGLE-ENDED INVERTING AMPLIFIER

The single-ended amplifier requires that one input be grounded. The inverting-mode amplifier is most often used (Fig. 116). This single-input, grounded configuration avoids certain internal common-mode errors (see Appendix A). The inverting amplifier, as distinguished from the non-inverting operational amplifier, also can produce gains that are less than 1. This is important in such applications as active filters and integrators, where portions of the frequency response must be attenuated to values less than 1. The negative feedback reduces the apparent input impedance at the inverting input to negligible proportions. This condition makes the effective input impedance equivalent to R_1 ; R_1 is in turn limited by the open-loop input impedance Z_i of the amplifier itself. As R_1 approaches and exceeds Z_i , the amplifier voltage drift and noise increase rapidly. The low input impedance can be very useful in applications such as current amplifiers (see Appendix E). At low closed-loop gains, degradation occurs in the output-voltage offset drift and noise (by as much as a factor of 2 at a gain of 1).

In the inverting amplifier shown in Fig. 116 the overall amplifier (closed-loop) gain A is

$$A = -e_0/e_s = -R_2/(R_1 + R_s) \quad (B3)$$

It is desirable, particularly when R_s is not constant, to have R_1 very much larger than R_s , and, since R_1 and R_2 can be precision resistors, the amplifier gain will also be very stable, as shown by the following:

$$A = R_2/R_1 \quad (B4)$$

In the typical voltage amplifier application, where R_2 is not very large (in this case large is determined by the basic operational amplifier input bias currents), and if $R_1 \gg R_s$, then R_3 should be zero. If, however, R_2 is of such a magnitude that the operational amplifier input bias currents can produce a substantial voltage across R_2 , then R_3 can be used to appreciably reduce this effect when it is made equal to the parallel combination of R_2 and $(R_1 + R_s)$. This relationship, when $R_s \ll R_1$, is

$$R_3 = R_1 R_2 / (R_1 + R_2) \quad (B5)$$

where $R_s \ll R_1$. This is possible because the input bias currents I_{B1} and I_{B2} at each input to the operational amplifier are approximately equal.

B.2 THE SINGLE-ENDED NON-INVERTING AMPLIFIER

The most useful characteristic of the non-inverting mode operational amplifier is its extremely high input impedance. An analysis of Fig. 117 shows that the effective input impedance Z_i of the non-inverting amplifier is

$$Z_i = \frac{1}{(1/A' \beta Z_D) + 1/Z_{CM}} \quad (B6)$$

A typical FET operational amplifier has the following specifications:

$$\begin{aligned} Z_D &= 10^{11} \Omega \text{ in parallel with } 2 \text{ pF} \\ Z_{CM} &= 10^{12} \Omega \text{ in parallel with } 2 \text{ pF} \\ A' &= 50,000 \end{aligned}$$

Under these conditions, the limiting effective input impedance (at low frequencies and for reasonable values of $A'\beta$) is Z_{CM} . Since Z_D and Z_{CM} are resistors shunted by a capacitance, both impedances will decrease with increasing frequency. Since the non-inverting amplifier is valued for its high input impedance, it follows that it is usually used in applications in which the source impedance R_S is very high; however, when R_S is very large, several application limitations must be observed. The major considerations are the following:

1. Closed-loop gain is scaled by the ratio $Z_D/(Z_D + Z_S)$. When the source impedance exceeds the amplifier open-loop differential input impedance, the closed-loop gain is substantially reduced. The reduction of the closed-loop gain reduces gain accuracy, gain stability, and closed-loop input impedance.
2. The input voltage offset and input voltage offset drift degrade as $(Z_D + Z_S)/Z_D$.
3. Input current noise is proportional to the magnitude of Z_S and can be quite high for large values of Z_S .
4. When Z_S is very large, the operational amplifier input bias currents can produce large output-voltage offsets and voltage-offset drifts.

Notice that for the non-inverting amplifier, performance degrades when the source impedance approaches the operational amplifier open-loop input impedance. With modern FET operational amplifiers, which often have input impedances in excess of $10^{11} \Omega$ in parallel with a nominal capacitance of 2 pF, this source impedance can be very large and still not degrade the performance significantly. Figure 118 shows a non-inverting circuit with provisions for nulling a large output-voltage offset owing to input bias current. Many operational amplifiers have internal provisions for nulling the initial offset voltage (Fig. 119). This provision should not be used to null offsets caused by input bias currents since this may cause increased input offset voltage drift which is often a more critical problem in flight-test applications.

One of the most popular variants of the non-inverting amplifier is the impedance converter (a voltage amplifier with a gain of 1) shown in Fig. 119. Figure 119 illustrates a very high input impedance amplifier circuit that uses a precision, low-drift, FET input operational amplifier. This circuit has an input impedance of approximately $10^{15} \Omega$ shunted by nominally 0.2 pF and uses a drive voltage for the input guard and for the transducer-to-amplifier shield. Pin 2 (the amplifier inverting input connection) is driven by the amplifier feedback to track the voltage on pin 3 (this voltage should be e_S when R_S is much smaller than the amplifier input impedance). This feedback voltage can be used to drive the amplifier metal case, the input wiring shield, and the guard ring around the signal input terminals to a potential equal to e_S . Several advantages derive from this guarding technique. The first is that current leakage paths are minimized. Since the potential differences between the coaxial cable center wire and its shield, between the amplifier input terminal and the surrounding printed circuit board (see Fig. 120), and between the amplifier and its case are very small, current leakage in the total circuit is considerably reduced. In addition, the guarding technique reduces noise contamination and capacitive loading from the source. Since there is very little capacitance that the source is required to charge, the apparent capacitance presented to the source is very small (the amplifier feedback charges the input circuit capacitance).

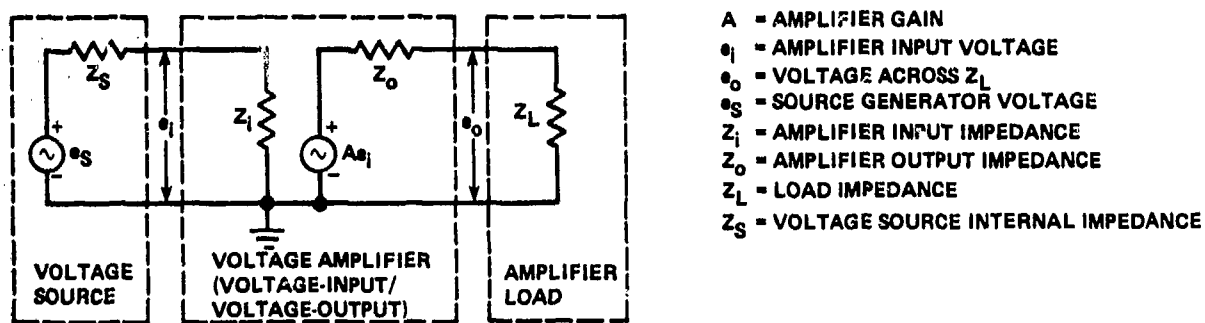


Figure 115. Voltage amplifier

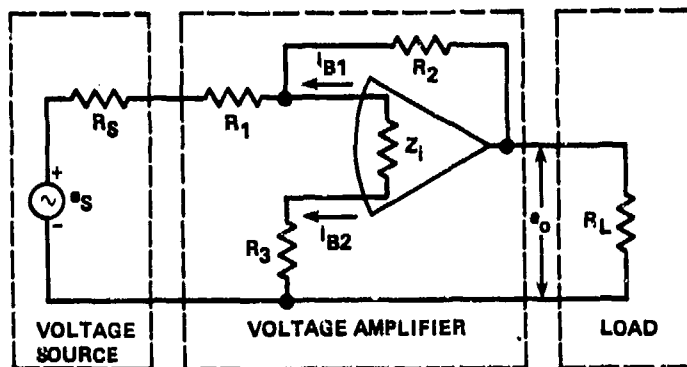


Figure 116. Inverting amplifier

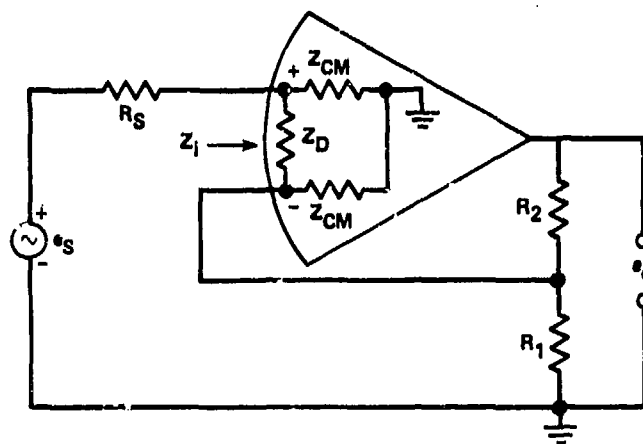


Figure 117. Single-ended non-inverting amplifier

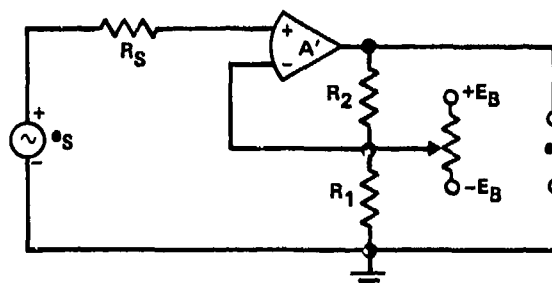


Figure 118. Non-inverting amplifier with input offset-voltage nulling provisions

(A) OPTIONAL CONNECTION. IMPROVES PERFORMANCE BUT MAY CAUSE AMPLIFIER INSTABILITIES WHICH ARE USUALLY CORRECTED BY PLACING A CAPACITOR FROM THE POSITIVE INPUT TO GROUND.

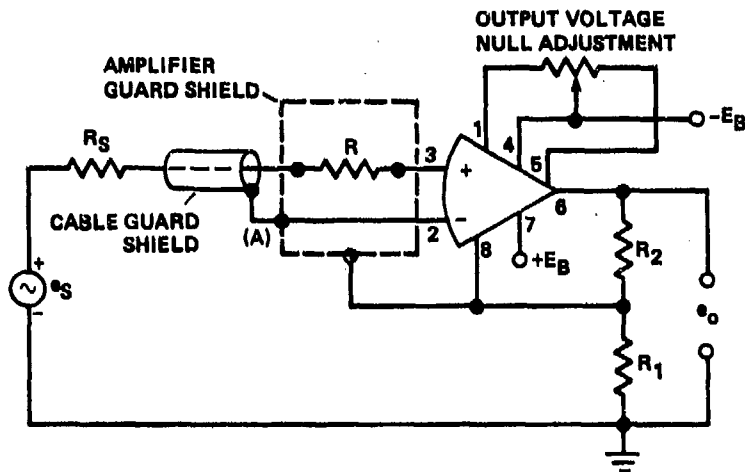
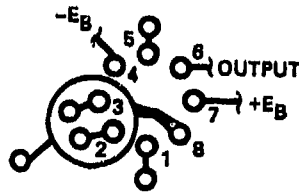
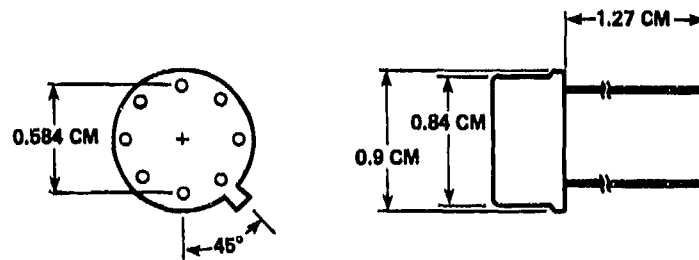


Figure 119. Very-high-impedance voltage amplifier with input guard and drive shield



(a) Printed circuit board, bottom view



(b) TO-99 exterior dimensions

Figure 120. TO-99 packaged operational amplifier (AD545) and circuit board layout

APPENDIX C

INSTRUMENTATION (DIFFERENTIAL) AMPLIFIER

The ideal differential amplifier amplifies only the difference between two input signals (see Fig. 121). This type of amplifier is useful for amplifying signals from resistive bridge circuits, which are above ground, and for rejecting common-mode noise signals.

The amplifier of Fig. 121 qualifies as a general-purpose instrumentation amplifier when it possesses the following: high input impedance; high common-mode voltage rejection; stable but easily variable voltage gain A ; low output impedance; adequate frequency bandwidth; and appropriate output drive capability. Integrated-circuit technology combined with the demand for large numbers of these types of amplifiers has made them available in potted modules and hermetically sealed, flat metallic packages which are ideally suited for flight-test voltage amplification purposes. It must be noted that even though instrumentation amplifiers have differential inputs, there must be a return path for the bias currents. When this is not provided, these bias currents will charge various stray capacitances, causing the amplifier output to drift uncontrollably. Particular care must be used when amplifying outputs of "floating" sources, such as transformers, ungrounded thermocouples, and ac-coupled sources, to provide a steady-state current path from such input to the common. (When this is not feasible, see Appendix D.)

Figure 122 shows an example of a ground return for a floating (ungrounded) thermocouple circuit. Typically, these integrated-circuit instrumentation amplifiers are cheaper to buy than to construct from discrete components or operational amplifiers; however, to promote a better understanding of the capabilities and to provide a connection to the discussion on operational amplifiers, the following discussion is included.

A differential-amplifier circuit constructed from a single operational amplifier is shown in Fig. 123. Ideally, the amplifier is completely insensitive to the common-mode voltage e_{CM} . In actual practice, R_2 and R_1 have to be very carefully matched to provide good common-mode rejection even when the source resistance R_{S1} and R_{S2} are zero. For real values of R_{S1} and R_{S2} , where R_{S1} exactly equals R_{S2} , the common-mode rejection ratio is unaffected but the gain changes, as shown in

$$G = e_o/e_d = e_o/(e_2 - e_1) = [R_2/(R_1 + R_{S1})] \quad (C1)$$

If R_{S1} is not equal to R_{S2} , then the common-mode rejection ratio is degraded. The principal disadvantages of the amplifier of Fig. 123 are the low input impedance and the difficulty in changing the gain.

Most of the limitations of the above differential amplifier can be eliminated by placing two non-inverting operational amplifiers in the inputs as shown in Fig. 124. In this amplifier circuit, R_p is a variable resistor which provides an easy (and very nonlinear) gain adjustment. The input impedance is very high, which minimizes the effects of imbalances in R_{S1} and R_{S2} . A mismatch between the two resistors labeled R produces a gain error without affecting the common-mode rejection of the circuit. For convenience, R_1 and R_2 are often made equal, because they must be very closely matched to achieve excellent common-mode voltage rejection. In this case, the final stage performs simply as a differential-input to single-ended output amplifier. Feedback resistors in all stages can be kept low to reduce the output-voltage offset caused by the various input bias currents. When most of the amplifier gain is in the first stage, the input offset voltages of these two input operational amplifiers determine the output-voltage offset. When the input voltage offsets of each input amplifier are equal and track one another, then the differential second stage cancels most of the input-voltage offset effects, including drift. The input bias currents associated with the non-inverting inputs of the first stage flow through R_{S1} and R_{S2} , and a mismatch between R_{S1} and R_{S2} or the two input bias currents will cause an output offset error.

An example of an instrumentation amplifier circuit that has been optimized for very high input impedance and high noise rejection is shown in Fig. 125. In this circuit, the common-mode input impedance is typically $10^{15} \Omega$ shunted by 0.2 pF. This value of input impedance is achieved by very careful attention to leakage paths, using input guarding, driven shields, and premium-grade FET-input operational amplifiers A_1 and A_2 . Amplifiers A_3 and A_4 are not as critical. In this example, the signal input to each amplifier (points 1 and 2), the input amplifier case (points 3 and 4), and the shield to the transducer (points 5 and 6) are driven at the common-mode voltage e_{CM} . This considerably reduces any common-mode leakage paths and reduces the common-mode capacitive coupling paths. When the shield capacitances are small, the buffer amplifier A_4 (and its associated resistor $1/2R_3$) can be replaced by a wire between points 7 and 8.

Normally, it is more economical to use mass-produced integrated-circuit instrumentation amplifiers than to construct them; however, specialized requirements may dictate the use of a custom-built instrumentation amplifier.

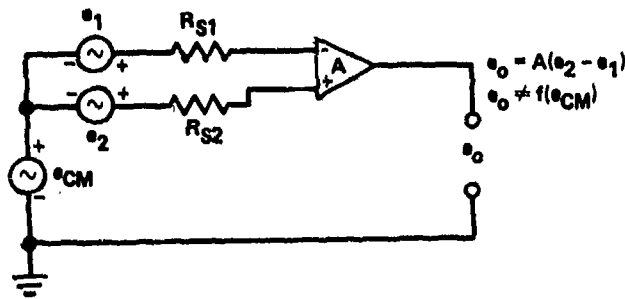


Figure 121. Ideal differential amplifier

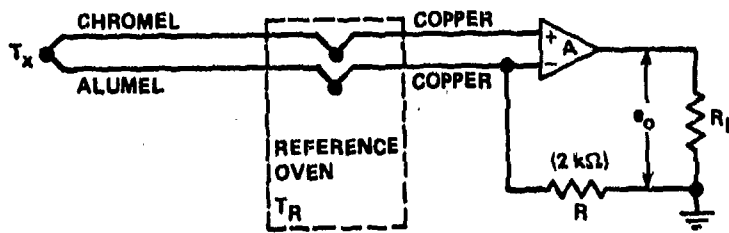


Figure 122. Instrumentation amplifier for ungrounded thermocouple circuit

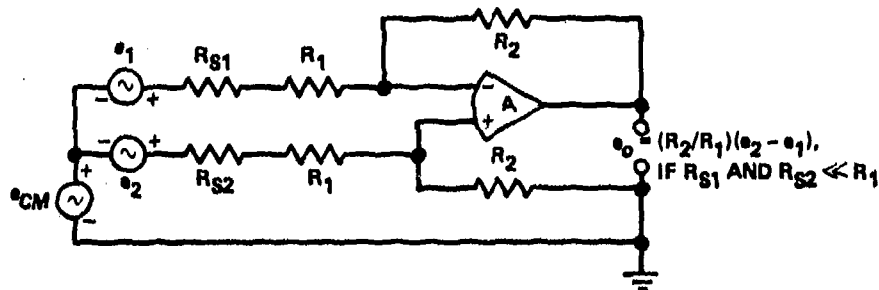


Figure 123. Simple differential amplifier

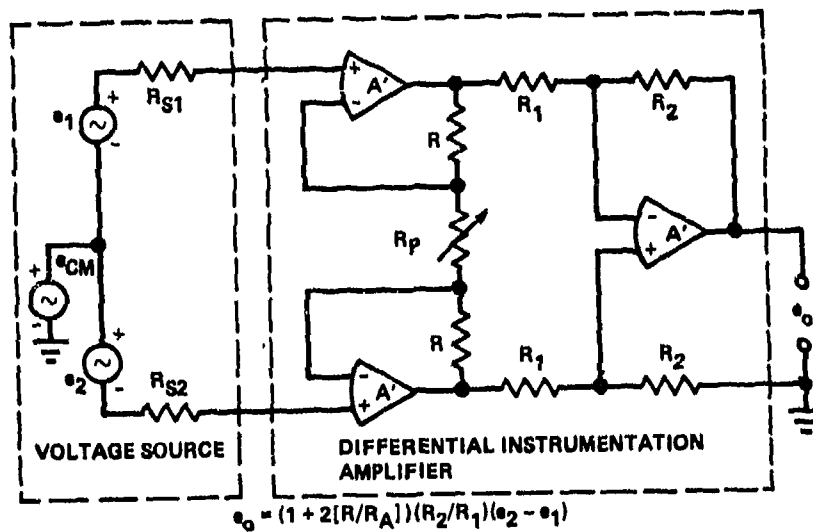


Figure 124. Instrumentation amplifier circuit constructed from three operational amplifiers

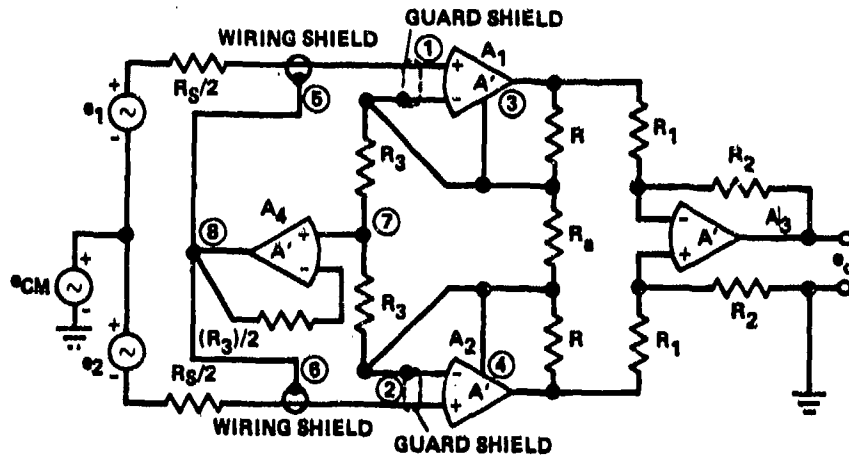


Figure 185. High-input-impedance amplifier (All similarly numbered resistors should be matched to within $\pm 0.1\%$.)

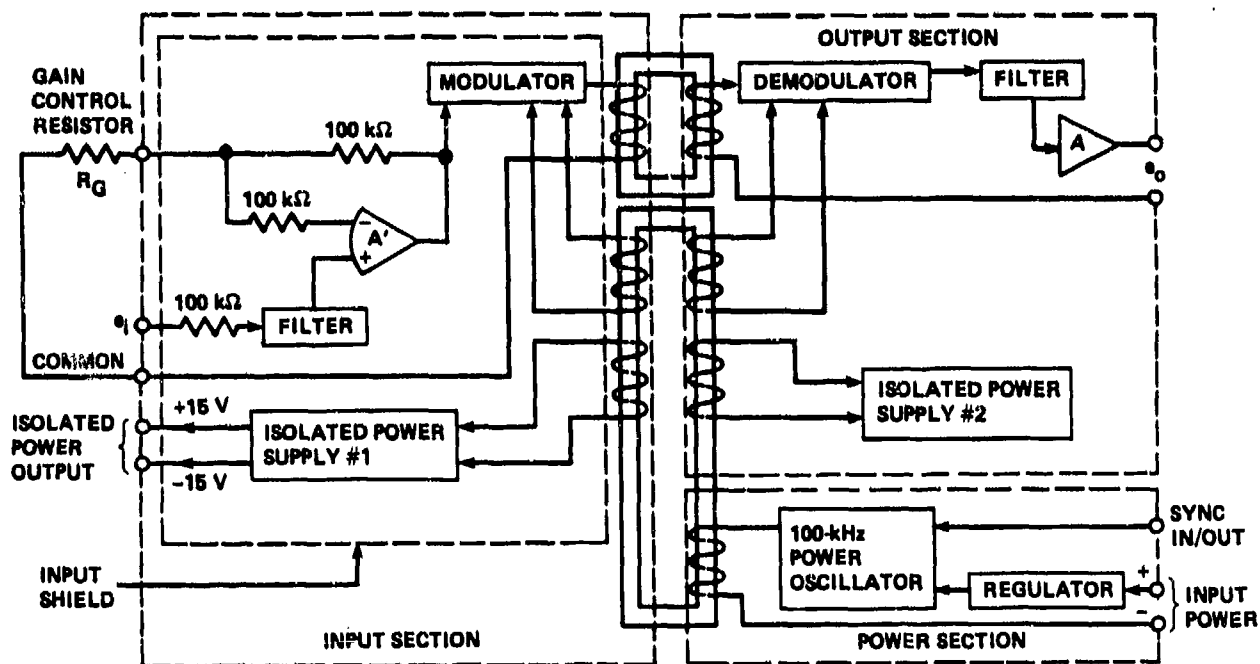
APPENDIX D
ISOLATION AMPLIFIER

An isolation amplifier is used when it is essential that the amplifier input and output signals be completely separated. Medical applications are typical situations in which extra isolation is warranted, although special measurement applications sometimes demand the use of isolation amplifiers to limit noise contamination or to protect critical system elements. An example of a commercially available frequency-modulated, transformer-coupled isolation amplifier is shown in Fig. 126 (taken from Ref. 41). For this amplifier, the best common-mode rejection performance can be achieved by using twisted, shielded-pair wires from the sensor to the amplifier terminals to reduce inductive and capacitive noise contamination. To further reduce effective cable capacitance, the cable shield should be connected to the common-mode guard drive as close to the input signal "low" as possible.

Although this circuit has many desirable features, it is still available in encapsulated modules that are only 3.8 cm long, 5.1 cm wide, and 2 cm high. As shown in Fig. 126, the input circuitry can sustain a $\pm 2,500$ -V potential difference between the input and the output circuits. The power-system ground portion of the amplifier can sustain full line voltages of 120 Vac with reference to output ground without disturbing the output. The input has its own isolated power supply which can be used to power, for example, transducers and floated operational amplifiers. When using more than one isolation amplifier in a system, the internal power oscillators in each unit can be synchronized to one another to prevent the oscillators from producing beat frequencies in the output of the amplifiers. The unit considered here has a calculated mean-time-between-failure (MTBF) of over 2 million hours. The MTBF is a very important parameter in amplifiers of this type.

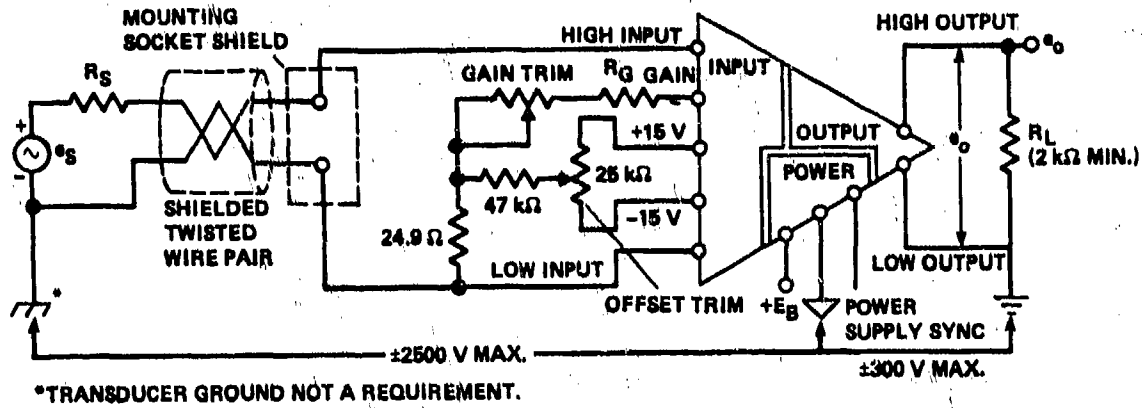
The amplifier in Fig. 126 has its input protected resistively. This input protection serves two functions: (1) protects the amplifier input against differential overloads, and (2) protects the sensitive input sources from supply voltage if the input amplifier malfunctions.

The device shown in Fig. 126 has the input configured as an instrumentation amplifier and its output is a buffered output amplifier. Other configurations are also available, the most common being an input that is configured as an operational amplifier. The operational amplifier input can be very useful for performing such functions as summing, integration, and differentiation while retaining all the desirable features of the isolation amplifier.



(a) Transformer-coupled isolation amplifier block diagram

Figure 126. Transformer-coupled isolation amplifier with power-supply synchronization capabilities



(b) Isolation amplifier functional diagram

Figure 126. Concluded

APPENDIX E

CURRENT AMPLIFIER

A current source has a very high internal impedance and is most appropriately matched with a current sensor that has a very low internal impedance. When operational amplifiers are used to implement the current-amplifier circuit, a very low effective input impedance can be achieved. For example, in the current-input/voltage-output (current-to-voltage) amplifier of Fig. 127a the input terminal marked (G) is a "virtual" ground and thus has essentially zero input impedance Z_i . In this example, the low input impedance of the inverting-mode amplifier is a distinct advantage. Since Z_s is typically very large, and Z_i is almost zero, all of the source current is available to the input terminal of the amplifier. The voltage output is not restricted, since R_2 can be any reasonable value, especially when FET or parametric bridge operational amplifiers are utilized. The gain of the amplifier for steady-state offset voltages and noise voltages is $(R_2 + Z_s)/Z_s \approx 1$. Thus, the error attributable to these parameters is small. The current noise, however, can be quite important because of the large impedances; therefore, it is good practice to include the capacitance C to reduce high-frequency current noise.

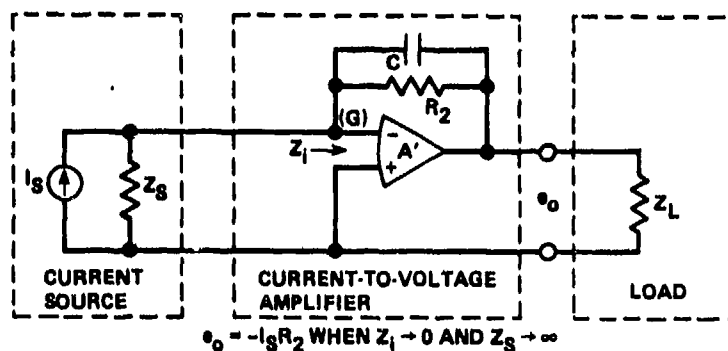
Figure 127b illustrates a simple voltage-to-current amplifier. In this configuration, the load must be ungrounded. The operational amplifier provides the current to drive the load, and R_1 can be made relatively large so as not to load the voltage source. If R_1 is made large, amplifier scaling can still be provided through R_3 . The circuit of Fig. 127b can readily be modified to a current-to-current amplifier, as shown in Fig. 127c. This circuit also must have an ungrounded load (the input and output may not have a common terminal).

When a current output is required that must be grounded, the circuit illustrated in Fig. 128 is often used. When the resistance ratios R_3/R_4 and R_2/R_1 are matched, the circuit will function as a true source of current with a very high internal impedance (this occurs because the circuit contains positive feedback). Any mismatch in the resistor ratios will appear as a reduction in the equivalent current-source internal impedance. The capacitor C_L is included to reduce noise and prevent oscillation. In normal use, R_1 and R_2 will be made large to prevent loading the input voltage source, and R_3 and R_4 will be made small to minimize voltage drops. There are two limitations with this circuit: (1) the operational amplifier must have the output voltage swing available to provide the necessary maximum load voltage plus the voltage drop across R_3 (keep R_3 small), and (2) unlike the circuits of Fig. 127, this circuit can have common-mode gain-deterioration errors (see Appendix A).

An example of picoampere current-to-voltage amplifier using a very high input impedance FET operational amplifier is shown in Fig. 129. This circuit uses guarding to reduce exterior noise inputs. In this case, the coaxial shield, the input terminal guard (see Appendix B for details), and the isolated metal container for the operational amplifier are all connected to ground. The 10-pF capacitor reduces high-frequency current noise. With the amplifier used in this example, if the transducer is not current-limited, amplifier failure can result from overheating owing to excess input currents. The resistance R is included under these conditions to limit the input current to the specified maximum overload current. Resistance R can be quite large without affecting the amplifier performance.

Under certain transducer failure modes, in some transducers, such as high-vacuum photomultipliers, a high voltage may appear at the input to the amplifier. The amplifier in Fig. 129 has a JFET input and its design requires protection when the source is not current-limited. (In a CMOS-input amplifier, over-voltage protection would be required.)

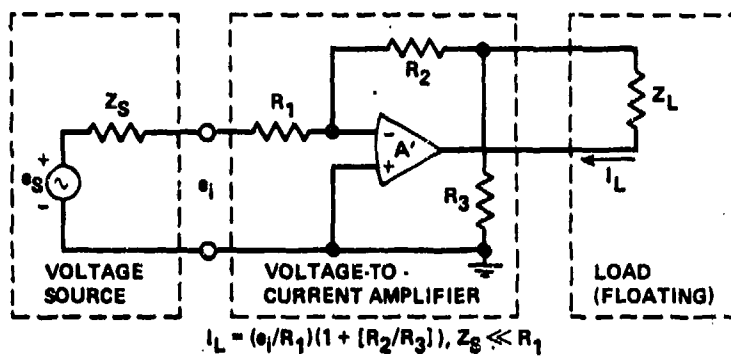
Most operational amplifiers that are used as current-output sources have very high feedback impedance which is often shunted with small capacitances. For example, if the feedback impedance is $10^{12} \Omega$ paralleled by 3 pF, the output is useful only at very low frequencies (the knee-frequency occurs at 0.05 Hz). Output guarding can be used to reduce this capacitive shunting.



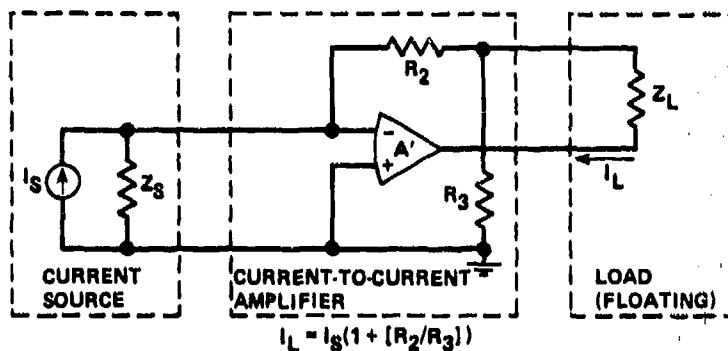
$$e_o = -I_s R_2 \text{ WHEN } Z_i \rightarrow 0 \text{ AND } Z_s \rightarrow \infty$$

(a) Current-to-voltage amplifier

Figure 127. Three current amplifier circuits



(b) Floating load voltage-to-current amplifier



(c) Floating load current-to-current amplifier

Figure 127. Concluded

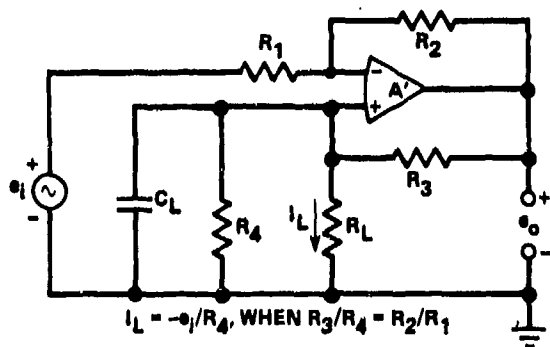


Figure 128. Voltage-to-current amplifier with grounded load

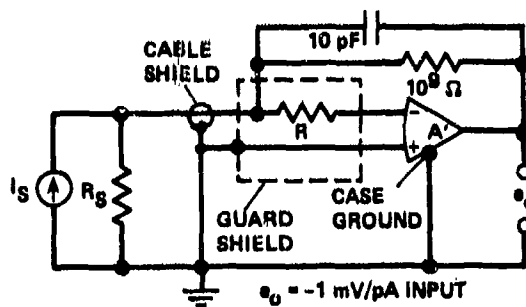


Figure 129. Picoampere current-to-voltage converter with input guarding

APPENDIX F

CHARGE AMPLIFIER

Many transducers, such as the piezoelectric transducer and the variable capacitor transducer, operate on the principle of converting of the measurement variable into an equivalent charge. The equivalent circuits of two such transducers are shown in Fig. 130. Both circuits are basic charge generators, that is, the measurand is expressed as a function of charge. The reason ΔQ is used in this figure is to stress that charge generators cannot be used for measuring static inputs.

The charge amplifier discussed here is the charge-to-voltage converter. This is by far the most popular charge amplifier for airborne applications (in industrial use, a charge-to-current converter is sometimes used to drive long lines and to match with existing current-sensitive systems). Figure 131 shows two versions of the charge amplifier constructed using operational amplifiers. In most cases, FET input operational amplifiers are used for this kind of application. The amplifiers shown in Fig. 131 are configured as integrators. The amplifier output e_0 is a function of the integral of the input current; that is, $Q = \int i dt$; therefore, the amplifier output voltage is a function of the charge input.

In Fig. 131, the shunt resistor R_f around C_f is required to provide a leakage path to amplifier common for the amplifier input bias currents. The resistors R_a and R_b are optional. The resistor R_b can be used to protect an amplifier that uses JFET inputs, as long as it is not so large as to cause undue voltage offset from the amplifier input bias current. The resistor R_a can be used also to protect the input, but it is most often used for its stabilizing effect since it provides a high-frequency filter effect, as shown in Fig. 132. Resistors R_a and R_b are not usually used together.

The amplifier configuration shown in Fig. 131b has no advantage over that in Fig. 131a and has the disadvantage that the common-mode effects can be significant, particularly at higher frequencies. The circuit of Fig. 131b suggests how two amplifiers can be combined to produce a differential charge amplifier. The amplifier of Fig. 131a will be used in the following discussion.

In Fig. 131a, the output voltage e_0 is exactly that required to deposit a charge on C_f , at the operational amplifier negative input terminal, that exactly equals the charge Q generated in the transducer. The charge stored in the feedback capacitor C_f is identical to Q , and this produces a voltage that is equal to the value of the charge input divided by the capacitance of the feedback capacitor C_f . Since the negative input terminal is a virtual ground, the voltage across C_f is e_0 and $e_0 = Q/C_f$ at midband frequencies. The overall frequency response is shown in Fig. 132 when the low-frequency cutoff f_{CL} is defined as

$$f_{CL} = \frac{1}{2\pi R_f C_f} \quad (F1)$$

Figure 132 also shows the high-frequency response cutoff f_{CH} .

The actual circuit transfer function, including the effects of the feedback resistance R_f , is

$$e_0/Q = \frac{-A'}{1 + A'} \frac{sR_f}{sR_f[(C_T + C_C)/(1 + A') + C_f] + 1} \quad (F2)$$

where

- A' = amplifier open-loop gain
- C_C = coaxial cable capacitance
- C_f = amplifier feedback capacitance
- C_T = transducer capacitance
- e_0 = charge amplifier output voltage
- Q = transducer charge
- s = Laplace mathematical operator (see Appendix I)
- R_f = feedback resistance

In normal applications, A' is a very large value so that $-A'/(A' + 1) \approx -1$. In general, $(C_T + C_C)/(1 + A')$ is much much smaller than C_f . This last relationship is true when the cable or the transducer capacitances are very small and the feedback capacitance C_f is very large. If the relationships $-A'/(A' + 1) \approx -1$ and $C_f \gg (C_T + C_C)/(1 + A')$ are valid, then the following equation is true:

$$e_0/Q = -sR_f/(sR_f C_f + 1) \quad (F3)$$

It is important to observe in Eq. (F3) that the output-versus-input transfer function is independent of C_T , C_C , R_{TL} , R_{CL} , and amplifier input impedances. The low-frequency cutoff is dependent only on R_f and C_f and not on the various shunting capacitances, the transducer leakage, the cable and connector leakages, and the uncontrolled amplifier input impedances. For these reasons, the charge-amplifier systems, unlike the voltage-amplifier systems, do not require end-to-end calibration (that is, the amplifier and transducer can be calibrated independently and cable effects neglected).

From Eq. (F3), it can be seen that when the feedback resistor is removed ($R_f = \infty$), the transfer function has a steady-state response. This conclusion is valid except for the practical limitations imposed by real operational amplifiers. Real operational amplifiers generate small offset and bias currents in the input stages. Without R_f , these bias currents would continue to charge the feedback capacitance until the charge amplifier saturates. Resistance R_f is very large in many cases ($10^8 \Omega$ is not unusual), and f_{CL} thus can often be made 0.1 Hz or smaller. In the interests of reduced noise, f_{CL} should in practice be no lower than actually required.

When charge amplifiers are driven into saturation, a recovery time is required. This recovery time is in actuality the low-frequency time-constant, τ_L of the charge amplifier, as shown by

$$\tau_L = R_f C_f = 1/(2\pi f_{CL}) \quad (F4)$$

For a typical cutoff frequency of 0.1 Hz, the recovery time is approximately 1.6 sec. No data are available during this recovery period. To avoid saturation, actual charge amplifiers are usually made with low gains. The rest of the gain is provided by a voltage amplifier as shown in Fig. 133. Using this technique, a charge amplifier can be built that will normally not saturate when driven by a signal that exceeds the full-scale input signal by more than a factor of 10. In test environments that have considerable noise inputs above $0.2 f_n$, input filters may be required since these signals may be outside the amplifier passband and cause the amplifier to saturate without showing any indications in the output signal that this has happened.

Figure 134 shows a charge amplifier with a noise source included to analyze the effects of input shunt capacitance on the amplifier performance. In this analysis, the effects of R_f have been ignored; however, these effects are covered in Ref. 19. The charge amplifier noise gain (e_o/e_n) is a function of the transducer and cable shunt capacitance:

$$e_o/e_n = (C_s + C_f)/C_f \quad (F5)$$

where

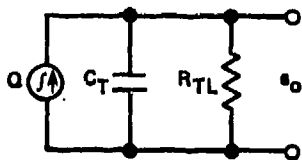
- C_f = amplifier feedback capacitance
- $C_s = C_T + C_C$ = total amplifier input shunt capacitances
- e_n = serial input noise voltage
- e_o = noise output voltage

These capacitance effects must be considered even though the charge amplifier gain is independent of these parameters. The noise gain derived from Fig. 134 (above the low-frequency cutoff) approaches the term shown in Eq. (F5) (Ref. 19), and as can be seen from the equation, the shunt input capacitances should not be permitted to increase indiscriminately if good noise rejection is to be retained.

When using charge amplifiers, the total external input shunt resistance is also important, because it affects the amplifier noise and stability. Many charge amplifiers do not operate properly with a shunt resistance below several hundred megohms. Although special charge amplifiers are available that can operate from sources with shunt resistances as low as 1 k Ω , from a noise standpoint it is desirable to avoid these special circuits. The noise gain of the amplifier at very low frequencies is proportional to $(R_f + R_s)/R_s$ (as long as this ratio does not approach the open-loop gain of the amplifier (Fig. 135)). This noise gain has a cutoff frequency $f_c = 1/2\pi R_s C_f$ and increases below f_c at 20 dB/decade until it reaches the low-frequency cutoff f_{CL} of the charge amplifier; at that point, the amplifier noise gain levels off at $(R_f + R_s)/R_s$ (Fig. 136, this curve taken from Ref. 19).

The charge amplifier is a very desirable remote signal conditioner for piezoelectric transducers. It has some very useful characteristics and very few limitations. When the limitations are observed, it is the most desirable remote signal-conditioning technique for piezoelectric and other charge-generating transducers.

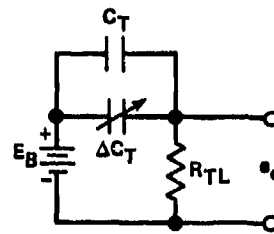
- C_T - TRANSDUCER CAPACITANCE
- E_B - BIAS VOLTAGE
- e_o - TRANSDUCER OUTPUT VOLTAGE
- K_1 - PIEZOELECTRIC CRYSTAL CHARGE SENSITIVITY
- K_2 - TRANSDUCER SENSITIVITY
- Q - TRANSDUCER CHARGE
- R_{TL} - TRANSDUCER LEAKAGE RESISTANCE
- ΔC_T - CAPACITIVE CHANGE PRODUCED BY THE MEASURAND CHANGE, ΔX
- ΔQ - CHARGE PRODUCED BY THE MEASURAND CHANGE, ΔX
- ΔX - DYNAMIC MEASUREMENT VARIABLE (MEASURAND)



$$\Delta Q = K_1 \Delta X$$

$$e_o = \Delta Q / C_T = K_1 \Delta X / C_T$$

(a) Piezoelectric transducer equivalent circuit



$$\Delta C = K_2 \Delta X$$

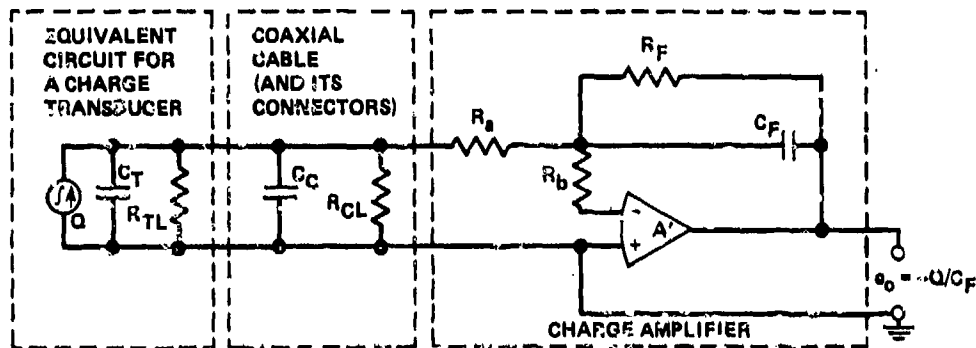
$$\Delta Q = E_B \Delta C_T = K_2 E_B \Delta X$$

$$e_o = E_B \Delta C_T / C_T = \Delta Q / C_T$$

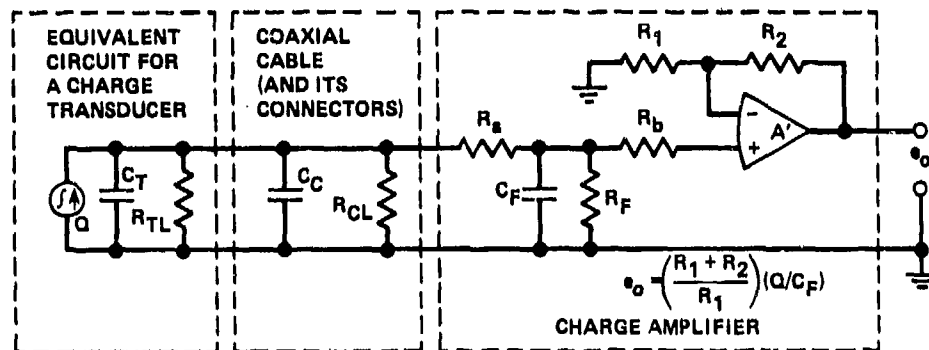
(b) Condenser microphone equivalent circuit

Figure 130. Examples of two charge-generating transducers

- A' = OPERATIONAL AMPLIFIER OPEN-LOOP GAIN
- C_C = COAXIAL AND CONNECTOR CAPACITANCE
- C_F = FEEDBACK CAPACITANCE
- C_T = TRANSDUCER CAPACITANCE
- e_o = MID-FREQUENCY AMPLIFIER OUTPUT VOLTAGE
- Q = TRANSDUCER CHARGE
- R_a AND R_b = OPTIONAL AMPLIFIER INPUT PROTECTION RESISTORS
- R_{CL} = COAXIAL CABLE AND CONNECTORS LEAKAGE RESISTANCE
- R_F = FEEDBACK RESISTANCE
- R_{TL} = TRANSDUCER LEAKAGE RESISTANCE
- R₁ AND R₂ = GAIN ADJUSTING RESISTORS



(a) Charge amplifier using an inverting operational amplifier



(b) Charge amplifier using a non-inverting operational amplifier

Figure 131. Charge amplifiers used with charge generator circuit

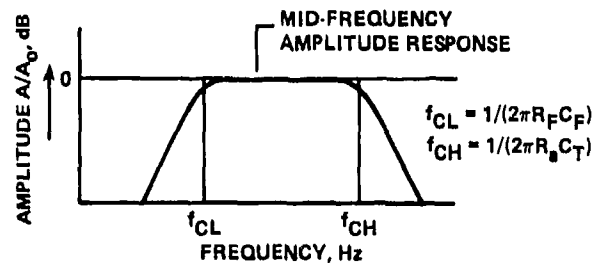


Figure 132. Charge-amplifier frequency-response curve

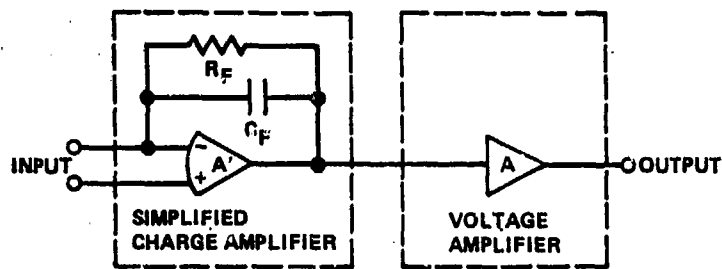


Figure 133. Technique for improving a charge-amplifier overload performance

$C_S = C_T + C_C$ (FROM FIG. 131)
 e_N = SERIES NOISE VOLTAGE
 e_o = OUTPUT NOISE VOLTAGE CAUSED BY e_N

C_F = FEEDBACK CAPACITANCE
 e_N = SERIAL INPUT NOISE VOLTAGE
 e_o = OUTPUT NOISE VOLTAGE
 R_F = FEEDBACK CAPACITOR SHUNT RESISTANCE
 R_S = TOTAL INPUT SHUNT RESISTANCE

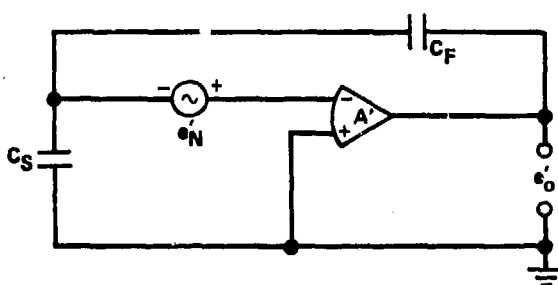


Figure 134. Charge-amplifier input shunt capacitance noise analysis circuit

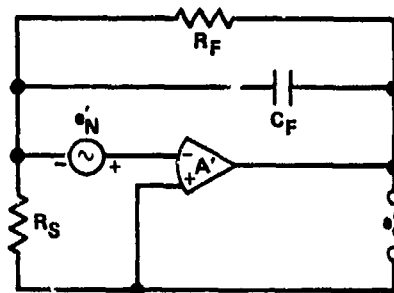


Figure 135. Charge-amplifier input shunt resistance noise analysis circuit

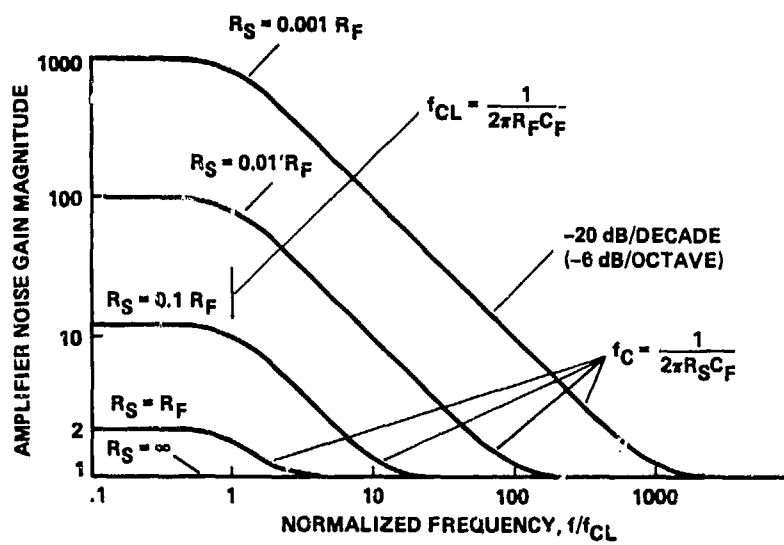


Figure 136. Charge-amplifier noise gain as a function of frequency and input shunt resistance

APPENDIX G

ALTERNATING CURRENT COUPLED AMPLIFIER

Instrumentation and operational amplifiers are both steady-state devices. Both types of amplifiers have more than adequate bandwidths to meet the usual requirements of flight data acquisition. As a general rule, it is not desirable to have bandwidths that are significantly larger than required to pass the data, since this allows the ever present noise to be amplified. One type of noise that is particularly troublesome is low-frequency drift, or level shift. Some transducers are prone to drift, and when the signal of interest is a low-level dynamic parameter, then an ac amplifier is desirable.

Figure 137 illustrates two operational amplifiers used as ac amplifiers, in both cases the source impedance is assumed to be insignificant relative to R_1 . In the amplifier of Fig. 137a, an operational amplifier is connected in the inverting mode. This amplifier has a low-frequency cutoff f_{CL} :

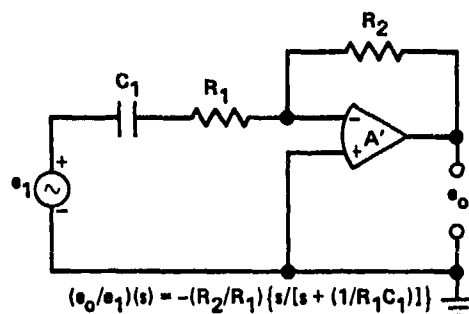
$$f_{CL} = 1/(2\pi R_1 C_1) \quad (G1)$$

Below f_{CL} , the attenuation with decreasing frequency approaches 6 dB/octave. The inverting mode ac amplifier has an input impedance of approximately R_1 in the passband. It is typical that when the source resistance is large, the source resistance tends to vary over a wide range of values. This variable-source resistance directly affects the gain (A) and frequency cutoff (f_{CL}). To overcome the effects of the source resistance, the amplifier shown in Fig. 137b is often used.

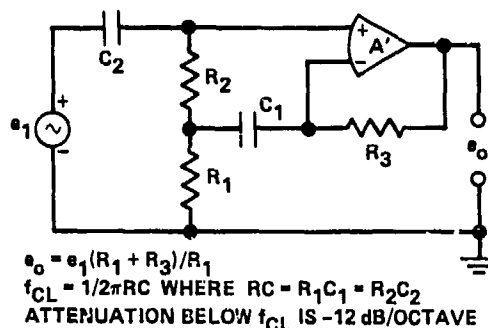
The amplifier of Fig. 137b uses feedback to generate a large amplifier input impedance. The input impedance of this circuit for an ideal operational amplifier (an operational amplifier with infinite gain at all frequencies) is

$$Z_i = R_1 + R_2 + (1/j\omega C_2) + j\omega C_1 R_1 R_2 \quad (G2)$$

As the frequency increases, the $j\omega C_1 R_1 R_2$ term becomes quite large and dominates the other terms in the equation. The open-loop gain of a real operational amplifier decreases as the frequency increases, which eventually causes the input impedance to decrease.



(a) Single-ended inverting mode ac amplifier



(b) Single-ended non-inverting mode ac amplifier

Figure 137. Amplifiers constructed from operational amplifiers

APPENDIX H
CARRIER-AMPLIFIER SYSTEM

The carrier-amplifier system has many desirable characteristics, particularly when it is used with non-self-generating transducers. A carrier-amplifier system can be implemented with various degrees of sophistication; however, the advent of economical integrated circuits, such as the phase-sensitive demodulator, has made the carrier system far easier to implement.

To be used with a carrier amplifier system, a self-generating transducer requires modulation. This modulation is most often accomplished with an integrated-circuit multiplier. The modulation process is illustrated by the following equations:

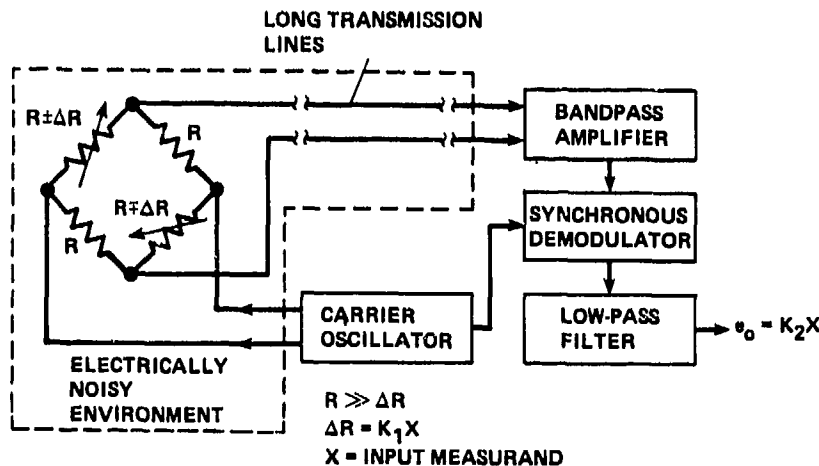
$$(C \sin \omega_c t)(A + B \sin \omega_s t) = (CA) \sin \omega_c t - (CB/2) \cos (\omega_c + \omega_s)t + (CB/2) \cos (\omega_c - \omega_s)t \quad (H1)$$

where $C \sin \omega_c t$ is the carrier signal, and $(A + B \sin \omega_s t)$ is the data signal. Note that this is a suppressed carrier-modulation system (the carrier does not exist in the output unless there is a steady-state component (A) in the signal). The signal frequency will appear as an upper sideband $(\omega_c + \omega_s)$ and a lower sideband $(\omega_c - \omega_s)$ around ω_c .

A non-self-generating transducer has a variable impedance as a function of the measurand of interest. In these transducers, the variable impedance is often used to implement the modulation. Figure 138 illustrates an example of a carrier-amplifier system which is used with a resistive strain-gauge bridge transducer. The measurand X is represented by a sinusoidal input, $X = K_3 \cos (2\pi f_s)t$. The bridge-excitation voltage is the carrier oscillator output voltage, $e_c = K_5 \cos (2\pi f_c)t$. The differential output voltage of the bridge e_A is the product of ΔR and i_c (the bridge excitation current). Various constants of proportionality (K_n) are used in Fig. 138 to simplify the equations.

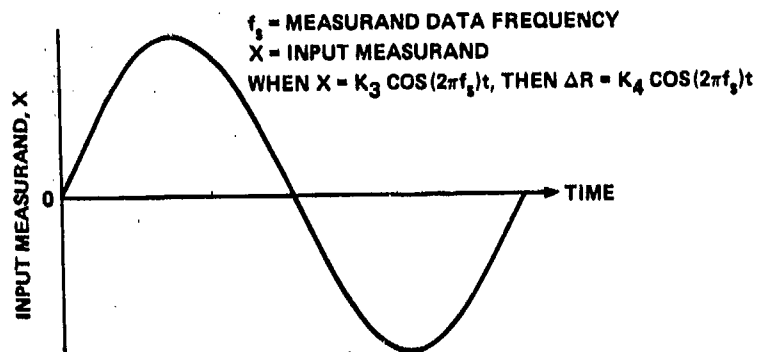
The advantages of using an ac bandpass amplifier to accomplish the system amplification are numerous: (1) using an ac amplifier avoids the amplifier noise sources such as output-voltage offset and low-frequency transistor flicker noise; (2) the noise pickup in the amplifier passband is small when the carrier frequency has been selected to lie in a portion of the frequency spectrum where there is relatively little electrical noise; (3) when $f_c \gg f_s$, the amplifier noise passband is also quite small, $(2f_s)$; and (4) the voltage gain of narrow-passband amplifiers can be made quite large and retain stability. The demodulator need not be a phase-sensitive demodulator if the input is unipolar. In this example, the transducer output is bipolar and a phase-sensitive demodulator is required. The phase-sensitive demodulator is more complicated than a simple half-wave rectification demodulator, but the phase-sensitive demodulator provides excellent noise-rejection characteristics in addition to its ability to demodulate bipolar signals.

When the output of the demodulator is passed through a low-pass filter that passes essentially the highest signal frequency of interest, then a signal proportional to the input measurand, as shown in Fig. 138f, will be seen at the filter output. Figure 139 illustrates one implementation of the band-pass filter, multiplier demodulator, and low-pass filter portion of the system. Other demodulator types include the switching demodulator and the rectifying demodulator.

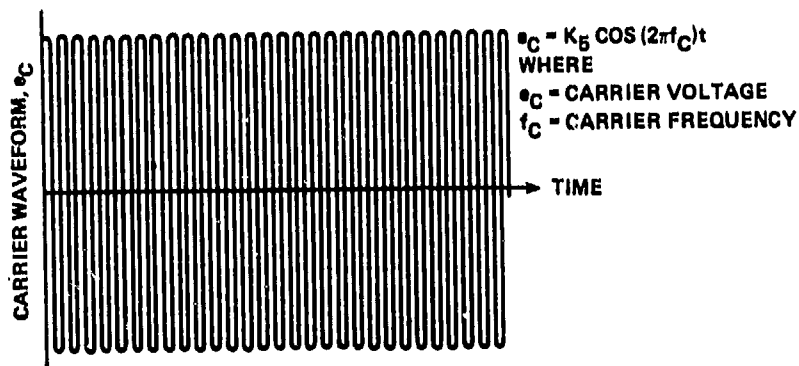


(a) Resistive-bridge transducer carrier-amplifier system

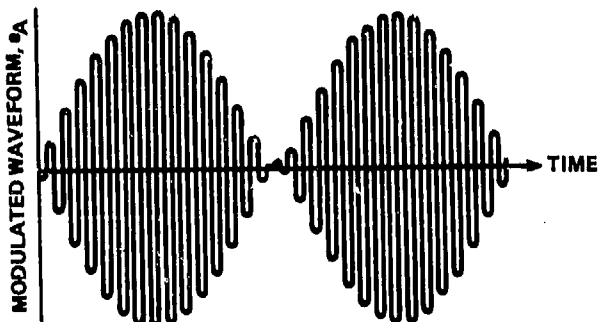
Figure 138. Carrier-amplifier system used with resistive-bridge transducer



(b) Bridge-transducer measurand input

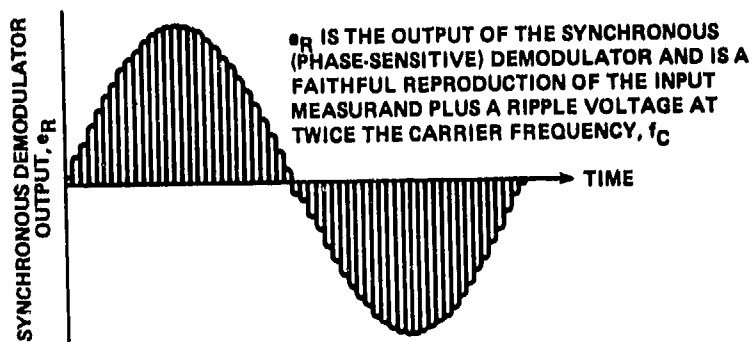


(c) Carrier waveform

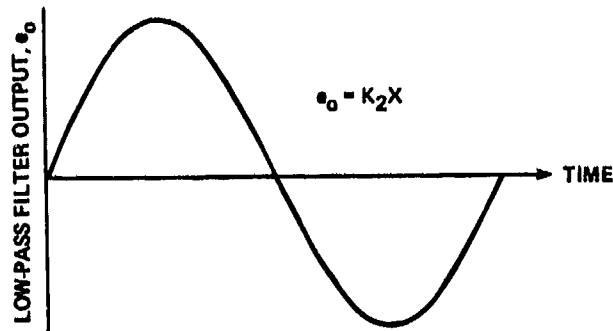


e_A = MODULATED WAVEFORM, WHEN $\Delta R \ll R$ THEN $e_A = K_6 E_C \Delta R$
 $e_A = K_6 [\cos(2\pi f_s)t] [\cos(2\pi f_c)t] = K_7 [\cos 2\pi(f_c - f_s)t + \cos 2\pi(f_c + f_s)t]$

(d) Bridge output waveform



(e) Phase-sensitive demodulator output



(f) Low-pass-filter output
Figure 138. Concluded

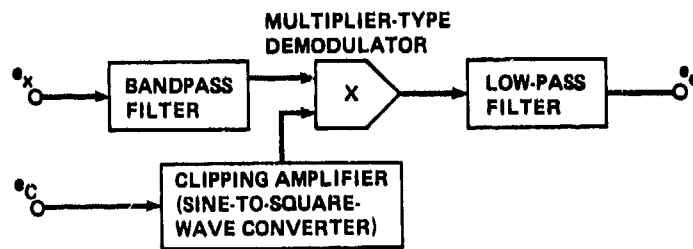


Figure 139. Phase-sensitive demodulator

APPENDIX I

THE ACTIVE FILTER

I.1 INTRODUCTION

This appendix contains background information on the use of the decibel in filter circuits and information on transfer functions as applied to filters. It also presents some actual filter circuits. The filter circuits include low-pass filters, high-pass filters, bandpass filters, and band-reject filters. In addition, techniques for scaling component values and frequencies are discussed, and a few comments are provided about desirable circuit components.

The emphasis herein is on active filters, because active filters are so useful as flight data-acquisition filters. These filters can be easily constructed in a small package to function at frequencies from 0.1 Hz to 1 kHz, the frequency range of most airborne data. Passive filters, designed for lower frequency operation, in contrast, are usually quite large and expensive.

First-order filters and the second-order Bessel, Butterworth, and Chebyshev filters are relatively easy to understand through an examination of the transfer function. The Cauer filter will also be discussed, but the transfer function is so mathematically complex that it is usually solved on a computer and the results presented in tabular form (see Ref. 42). Filters such as the equiripple approximation to the linear phase filter have no presently known closed-form solutions so an iterative procedure has been devised. Reference 12 provides listings for such types of passive filters. Fortunately, the most popular filters — the Bessel, Butterworth, and Chebyshev filters — are easy to analyze mathematically.

For the purpose of illustration, a parallel comparison of the active and passive filters will be made. Passive filters are constructed using resistors, capacitors, and inductors. The active filter is constructed of resistors, capacitors, and operational amplifiers. Active filters could use inductors as multioverorder passive filters do, but at low frequencies the inductors are large and expensive. In addition, because of physical constraints, inductors at low frequency are limited to low values of quality factor, Q . This limitation in Q values means that steep filter cutoff and narrow bandpass are not possible with low-frequency filters that contain inductors.

Active filters are smaller, lighter, and less expensive than passive filters; require little magnetic shielding (no inductor); have high input and low output impedances; provide selectable gain greater than 1; are easy to tune; and are of simple design. On the other hand, active filters require regulated power supplies; they introduce noise, drift, and offset; they become saturated at high amplitudes; and their efficiency is decreased at frequencies from 0.1-1 MHz.

Despite its disadvantages, the active filter is the most desirable airborne signal-conditioning higher-order filter. The ready availability of economical integrated circuit operational amplifiers and voltage regulators makes the use of active filters possible.

I.2 LOGARITHMIC RATIOS FOR DESCRIBING FILTER RESPONSE

The decibel (dB) is extensively used in filter applications. The power relationship in decibels is expressed as 10 times the logarithm of the ratio of the output power to the input power (see Eq. (11) and Fig. 140). A power ratio of 2 represents 3 dB, and a power ratio of 10 represents 10 dB, with a power ratio of 100 being expressed as 20 dB. Since passive filters display output-to-input power ratios less than 1, the description of the filter characteristic in decibels will be a negative number. Active filters are characterized by gains of either negative or positive values, since gains of both more than 1 and less than 1 are possible. The output-to-input ratio is important because logarithmic analysis may only be applied to dimensionless numbers.

Logarithmic ratios combined with a logarithmic frequency scale are very useful when representing filter characteristics in graphical form. To a first-order approximation, most filters can be represented on such a graphical format as a series of straight lines. Another, almost equally important advantage is that the frequency response can be quickly derived by simple observation of the filter transfer-function equation or, conversely, the filter transfer-function equation can be quickly approximated from observation of the experimentally derived frequency response.

To take the logarithm of a quantity that has dimensions, the quantity must be made dimensionless, which can easily be accomplished. For example, in Fig. 140, the output power P_L can be divided by the input power P_i :

$$\text{Power gain (dB)} = 10 \log_{10} (P_L/P_i) \quad (11)$$

The definition of the power ratio is the ratio of the input power P_i across the input impedance Z_i to the output power P_L across the load impedance Z_L , as in Eq. (11). However, when the voltage ratio is used,

$$P_L = (e_o^2/Z_L) \cos \theta_2 \quad (12)$$

and

$$P_i = (e_i^2/Z_i) \cos \theta_1 \quad (13)$$

By substituting Eqs. (12) and (13) into Eq. (11), the following equation is derived:

$$\text{Power gain (dB)} = 10 \log_{10}(e_0/e_1)^2 + 10 \log_{10}(Z_i/Z_L) + 10 \log_{10}(\cos \theta_1/\cos \theta_2) \quad (14)$$

In these equations, θ_1 and θ_2 are phase angles of the impedances Z_i and Z_L , respectively. When the impedances Z_i and Z_L are resistive ($\cos \theta_1/\cos \theta_2 = 1$), the last term in Eq. (14) is zero. Also, when the two impedances Z_i and Z_L are equal, the second term in Eq. (14) is zero. When both of these conditions are met, Eq. (14) reduces to an equation that is used to express the voltage gain of a filter:

$$\text{Voltage gain (dB)} = 20 \log(e_0/e_1) \quad (15)$$

In practice, equal phase angles and equal input and output impedances are rare. Equation (15) is widely used to represent power gain in terms of voltage gain; however, when the conditions of equal input and output impedance are not considered, Eq. (15) does not represent power gain. The voltage gain is a useful filter performance measure in its own right and is used throughout this volume to quantify filter performance. In this volume, unless otherwise specified, the term "gain" means voltage gain, even though expressing voltage gain in terms of decibels is not rigorously correct.

Using Eq. (15), it can be demonstrated that a voltage gain of 2 (that is $e_0/e_1 = 2$) corresponds to a gain of +6 dB. Also, when an input voltage to the circuit of Fig. 140 results in an output voltage that is half that of the input voltage, then from Eq. (15) the signal has been "amplified" by -6 dB. Thus, an output voltage that exceeds the input voltage, that is, a gain, is expressed as a positive number, and an attenuation is shown as a negative number.

1.3 TRANSFER FUNCTION AND FILTERS

The purpose of this section is to demonstrate how the equations that describe output-versus-input relationships of linear lumped-parameter filters can be written directly in an operational mathematical form called a transfer function. The approach used here is called the Heaviside technique after its originator. In this text, these transfer functions will be used to illustrate how specific features of a filter can be deduced from the transfer function (for example, its order and roll-off characteristics) and to derive the steady-state sinusoidal amplitude and phase response of the filter.

The reason that the transfer function is so popular in filter analysis is twofold: (1) s-plane techniques can be used to perform sophisticated analysis of filters under transient and other input/output conditions; and (2) considerable information can be determined about filter characteristics by inspection of its transfer function. In this text, the emphasis will be on the use of the transfer function by the person who is not a filter specialist.

When a voltage is applied to the lumped-parameter linear filter of Fig. 141, the transfer function is $H(s)$ and it is equivalent to $(e_0/e_1)(s)$, s being in general a complex mathematical operator having both real and imaginary parts; in this text, however, s will be equated to its steady-state sinusoidal equivalent ($j\omega$). Table 11 lists transfer functions for first- and second-order all-pole filters.

TABLE 11. — TRANSFER FUNCTIONS OF FIRST- AND SECOND-ORDER ALL-POLE FILTERS

Type of filter	Filter order ^a	
	First	Second
Low-pass	$K\omega_c/(s + \omega_c)$	$K\omega_c^2/(s^2 + d\omega_c s + \omega_c^2)$
Bandpass	None	$K\omega_c s/(s^2 + d\omega_c s + \omega_c^2)$
High-pass	$Ks/(s + \omega_c)$	$Ks^2/(s^2 + d\omega_c s + \omega_c^2)$

^a K = circuit gain; ω_c = filter cutoff frequency, rad/sec; s = Laplace operator and equals $j\omega$ for a steady-state sinusoidal input; d = filter damping factor.

In all lumped-parameter filters, that is, filters for which all the impedances are specific values of resistance and capacitance (no distributed parameters), the transfer function can be expressed as the ratio of two polynomials, $N(s)$ in the numerator and $D(s)$ in the denominator, such as

$$H(s) = N(s)/D(s) \quad (16)$$

The roots of the polynomial in the denominator $D(s)$ are referred to as poles, and the roots of $N(s)$, which are located in the numerator, are referred to as zeros. The denominator polynomial $D(s)$ can be expressed as

$$D(s) = s^n + a_1 s^{n-1} + a_2 s^{n-2} + \dots + a_{n-1} s + a_n \quad (17)$$

The order of the filter is the largest exponent of s in the polynomial.

In the all-pole filters of Table 11, the eventual filter attenuation is $(6n)$ dB/octave ($(20n)$ dB/decade). In all filters of a given type — for example, Bessel, Butterworth, Chebyshev, or Causer filters — the order n determines the sharpness of the filter roll-off outside the passband.

Figure 142 illustrates some simplified low-pass Butterworth filter amplitude response curves of various orders n . Circuit complexity tends to increase directly with the filter order, and diminishing returns are realized with higher-order filters.

The four most popular airborne signal-conditioning filters are the Bessel, Butterworth, compromise, and Chebyshev filters. These filters are often called all-pole filters because they have no polynomial series, such as $s + a$ or $s^2 + as + b$ in the numerator, and no attenuation ripple in the stop band. Note that all-pole bandpass and high-pass filters do have a simple zero in the numerator at $s = 0$. The popularity of the all-pole filters may have had its origins in the ease of mathematical analysis. In contrast, many of the recently evolved filters, such as the Cauer and equiripple phase-response filters, are usually solved with the aid of computers. All-pole filters are readily available and normally adequate for all but the most exacting applications.

Filters that have zeros in the numerator, such as the Cauer filter, can be tailored to have a very high rate of attenuation just beyond the filter cutoff frequency. This high rate of attenuation is achieved by placing a zero slightly outside the filter bandpass. A filter of this type will have a sharper band-edge attenuation than, for example, a Butterworth low-pass filter of the same order. A disadvantage of these filters is a rebound from the infinite attenuation zero and a lower overall stop-band attenuation than a Chebyshev or Butterworth filter (see Fig. 26) at higher frequencies. As explained in Sec. 3 (under Filters), sharp cutoff filters, although they perform very well with steady-state sinusoidal signals, produce wave-shape distortions in transient signals (the most common case in flight-test data).

The transfer function developed here utilizes the Heaviside technique, and is useful for transient analysis using the methods developed for the Laplace transform when all the circuit voltages are initialized to zero. This can easily be accomplished for a step or pulse input. For this type of analysis, refer to a text on Laplace transformations.

The simplified filter transfer function as a function of s is relatively easy to determine. The order of the filter can be readily determined by inspection of the simplified polynomial in the denominator, since the highest order of s in the denominator is the order of the filter. By replacing s with $j\omega$ and solving for the real and imaginary parts of the transfer function, the sinusoidal steady-state amplitude and phase response of the filter can be determined.

In this first example of how to derive and utilize a filter transfer function, the circuit of Fig. 143 will be used. This is a first-order, low-pass filter, with -6 dB/octave roll-off. The operational amplifier is assumed to be ideal (see Appendix A for background on operational amplifiers). Since the operational amplifier is ideal, $I_3 = I_4$ and, therefore,

$$(e_1 - e_2)/R_3 = e_2/(1/sC) \quad (18)$$

(Note that the equation is written directly with s replacing $j\omega$; this is the Heaviside technique.) Also by the same reasoning $I_1 = I_2$ and $e_2 = e_3$; therefore,

$$e_3/R_1 = (e_0 - e_3)/R_2 \quad (19)$$

By combining Eqs. (18) and (19), the transfer function $H(s)$ is

$$H(s) = (e_0/e_1)(s) = (1 + R_2/R_1) \frac{1/R_3C}{s + (1/R_3C)} \quad (110)$$

Table 11 lists some common transforms for various types of all-pole filters. By comparing the transfer function derived from Fig. 143 with those of Table 11, the derived transfer function corresponds to that of a first-order, low-pass filter when $K = (1 + R_2/R_1)$, which is the low-frequency gain of the non-inverting operational amplifier. Also, ω_c equals $1/R_3C$, that is, $f_c = 1/(2\pi R_3C)$, where f_c is the filter cutoff frequency as defined in Sec. 3.

To solve the transfer function for the steady-state sinusoidal response, $j\omega$ is substituted for s and ω_c for $1/R_3C$ in the transfer function; the result is

$$H(j\omega) = K \left[\frac{1}{1 + j\omega/\omega_c} \right] \quad (111)$$

where $H(j\omega)$ is the steady-state sinusoidal transfer function. To resolve $H(j\omega)$ into its real and imaginary parts, both the numerator and denominator are multiplied by the complex conjugate of the denominator, that is, by $1 - j(\omega/\omega_c)$. The transfer function for steady-state sinusoidal inputs, $H(j\omega)$, then becomes

$$H(j\omega) = K \left\{ \frac{1}{1 + (\omega/\omega_c)^2} \right\} - jK \left\{ \frac{(\omega/\omega_c)}{1 + (\omega/\omega_c)^2} \right\} \quad (112)$$

or

$$H(j\omega) = K(a - jb) \quad (113)$$

The complex transfer function $H(j\omega)$ may be represented as a vectorial quantity, as shown in Fig. 144; therefore, the magnitude of the gain $|H(j\omega)|$ or $G(\omega)$ is derived by taking the square root of the sum of the squares of the real and imaginary quantities a and b . These relationships in a and b (which are true for all transfer functions which have been resolved into real and imaginary parts) and the phase shift ϕ are shown in the following equations:

$$G(\omega) = |H(j\omega)| = k \sqrt{a^2 + b^2} \quad (I14)$$

$$\phi = -\arctangent(b/a) \quad (I15)$$

For the filter of Fig. 143 the magnitude of the steady-state sinusoidal amplitude response $G(\omega)$ is

$$G(\omega) = |e_0/e_1| = k \sqrt{\left[\frac{1}{1 + (\omega/\omega_c)^2}\right]^2 + \left[\frac{\omega/\omega_c}{1 + (\omega/\omega_c)^2}\right]^2} \quad (I16)$$

or

$$G(\omega) = \frac{k}{1 + (\omega/\omega_c)^2} \quad (I17)$$

The phase response as a function of ω is

$$\phi(\omega) = -\arctangent(\omega/\omega_c) \quad (I18)$$

In both of the above equations $\omega_c = 1/R_3C$, so the filter can be designed for any cutoff frequency ω_c . The filter response of Fig. 143 is plotted in Fig. 23 (note in this plot that k is assumed to be 1).

When R_3 and C in Fig. 143 are interchanged, the transfer function is found to be that listed in Table 11 for a first-order high-pass filter where ω_c equals $1/R_3C$. As shown in Table 11, there is no first-order bandpass filter.

The second example of how to derive a transfer function from an active filter will use the circuit of Fig. 145. Again, assuming that the operational amplifier is an ideal operational amplifier, then $i_1 = i_2 + i_3$ and $e_3 = e_0$, and, therefore,

$$\frac{e_1 - e_2}{R_1} = \frac{e_2 - e_0}{1/sC_1} + \frac{e_2 - e_0}{R_2} \quad (I19)$$

also $i_3 = i_4$, so

$$\frac{e_2 - e_0}{R_2} = \frac{e_0}{1/sC_2} \quad (I20)$$

Using Eqs. (I19) and (I20), which express the voltage relationship, e_2 can be eliminated and the transfer function e_0/e_1 is

$$H(s) = (e_0/e_1)(s) = \frac{1/(R_1R_2C_1C_2)}{s^2 + s[(R_1 + R_2)/R_1R_2C_1] + (1/R_1R_2C_1C_2)} \quad (I21)$$

When this is compared with Table 11, it is found to be in the format of a second-order, low-pass filter. For this filter, the cutoff frequency ω_c is

$$\omega_c = 1/\sqrt{R_1R_2C_1C_2} \quad (I22)$$

and $k = 1$. Thus, the cutoff frequency is now defined in terms of R_1 , R_2 , C_1 , and C_2 . The filter damping factor d can now be determined to be

$$d = (R_1 + R_2) \sqrt{C_2/(R_1R_2C_1)} \quad (I23)$$

A plot of the steady-state sinusoidal amplitude and phase shift responses have already been shown in Fig. 24 for three values of filter damping factors d . From Table 11, using the techniques explained in the previous example, the equations describing these curves are

$$G(\omega) = |(e_0/e_1)(\omega)| = 1/\sqrt{(\omega/\omega_c)^4 + (\omega/\omega_c)^2(d^2 - 2) + 1} \quad (I24)$$

and

$$\phi(\omega) = -\arctangent \left\{ d(\omega/\omega_c) / [1 - (\omega/\omega_c)^2] \right\} \quad (125)$$

Many applications call for high-order filters with a specific cutoff frequency. The natural initial approach to developing a filter of this type is to combine two lower-order filters. This is a feasible technique, but the combination is not a simple one. When the two Butterworth filters of Figs. 143 and 145, each with cutoff frequencies of f_c , are combined in series they will not produce a third-order, low-pass Butterworth filter with a cutoff frequency at f_c . Butterworth and Chebyshev polynomials for $n = 2$ through 8 or higher may be found in filter reference texts. These polynomials may be used in combination to match the desired filter order. These higher-order polynomials in the denominator can be factored into a combination of first- and second-order polynomials, which means that all filters can be synthesized entirely from first- and second-order sections. Figure 146 illustrates how two second-order filters can be combined to produce a fourth-order, 0.5-dB, peak-to-peak, ripple Chebyshev filter.

Manipulation of these polynomials to achieve a particular filter characteristic by trial and error is a very difficult task. In general, a circuit will be illustrated for a given family of filters. These circuits are usually specified at one frequency and at one set of resistances and capacitances. When it is desired to shift the frequency or component values, they can be scaled by the techniques shown next.

1.4 SCALING FILTER FREQUENCY AND IMPEDANCE

There are many reasons why it is desirable to scale filter impedance or frequency. The most common is that filters are tabulated to function at a specified frequency which is different from the desired operating frequency. When the frequency is scaled to the desired frequency, the component values may be impractical or difficult to locate, thus the impedances must often be scaled as well.

The filter in Fig. 147 is a specific application of the filter in Fig. 143 where R_3 is zero (that is the gain is 1), ω_c equals 1 rad/sec as a result of the specific R_1 and C_1 values. To use this filter at 40 Hz, use the rules in Table 12 and proceed as follows:

Rule 1: Since $f_c = \omega_c / (2\pi)$ and where $\omega_c = 1$, then $f_c = 40$ Hz, and $f_c / f_c' = 3.98 \times 10^{-3}$. The resistance values are multiplied by 3.98×10^{-3} , producing an $R' = 4 \times 10^{-3} \Omega$. In this example, the value C is not frequency-scaled as all the scaling is accomplished by scaling the R value.

Now the frequency is the desired 40 Hz, but 1 F is an impractically large capacitance and $4 \times 10^{-3} \Omega$ is too small to be usable. Rule 2 must now be used to adjust the circuit impedance to a more realistic value.

Rule 2: To adjust the circuit impedances, a constant K equal to 10^7 will be used. This produces a new impedance R'' and C'' where

$$R'' = KR' = 40 \text{ k}\Omega \quad (126)$$

$$C'' = C/K = 0.1 \text{ }\mu\text{F} \quad (127)$$

Both of these values are available as standard value components.

Table 12. — RULES FOR SCALING FILTER CIRCUITS

<p>Rule 1: To scale a filter frequency from f_c to a new frequency f_c', multiply the value(s) of the frequency-determining resistor(s) or capacitor(s) by f_c / f_c'.</p> <p>Rule 2: To scale filter impedances to obtain standard values of capacitance or resistance without changing the frequency response, select a constant K, multiply the values of the frequency-determining resistors, and divide the values of the capacitors by the constant K.</p>

It is important to note that for the filter of Fig. 147, the voltage source to the filter must provide a resistive path to ground for leakage currents. In addition, this voltage source internal impedance must be very much smaller than R'' if it is not to affect the frequency. When the voltage source impedance is resistive and stable, it can be included as a part of, or all of, R'' .

1.5 FILTER CIRCUITS

A limited number of active filter circuit categories will be addressed, since several different circuits can be used to implement each of the transfer functions. The following sections will illustrate those circuits that offer some particular virtues. These virtues include ease of tuning, low sensitivity to component variations, and high circuit isolation. The strengths and weaknesses of each included filter circuit will be briefly discussed.

The broad filter categories covered are (1) the low-pass filter, (2) the high-pass filter, (3) the tuned band-pass and band-reject filter. The high-pass filter would, in practice, normally be combined with the low-pass filter to form a broadband bandpass or broadband band-reject filter.

1.5.1 The Zero-Offset Low-Pass Filter

The typical direct-coupled, low-pass active filter has a voltage offset that causes an undesirable level shift which is troublesome when the filter has a low-level input voltage. Figure 148a is the schematic of a filter that eliminates any steady-state offset contributions from the operational amplifier. Figure 148b illustrates the use of the filter in a circuit. The circuit transfer function is derived in this case to demonstrate how the circuit functions.

To derive the transfer function, refer to Fig. 148b. Since $I_2 = I_3$ for an ideal operational amplifier, then assuming the voltage source resistance R_S is zero, the following equations representing the circuit voltage relationships can be used to solve for e_0/e_1 as a function of s by eliminating e_2 :

$$e_0 s C_1 = -e_2 / R_2 \quad (128)$$

Also, $I_2 = I_1 + I_5$, $I_4 = I_5 + I_6$ and $e_3 = 0$; therefore,

$$e_0 s C_1 = [(e_1 - e_0) / R_1] - (e_2 - e_0) s C_2 - e_0 / R_L \quad (129)$$

The transfer function $H(s)$ is

$$H(s) = (e_0/e_1)(s) = \frac{1/(R_1 R_2 C_1 C_2)}{s^2 + s[(C_1 + C_2)/R_2 C_1 C_2] + [1 + (R_1/R_L)]/R_1 R_2 C_1 C_2} \quad (130)$$

Now when R_L is very much larger than R_1 , the transfer function is

$$H(s) = \frac{1/(R_1 R_2 C_1 C_2)}{s^2 + s[(C_1 + C_2)/R_2 C_1 C_2] + 1/R_1 R_2 C_1 C_2} \quad (131)$$

This transfer function is identical to that derived for the circuit in Fig. 143 and is that of a second-order all-pole low-pass filter. As explained in Sec. 3, depending on the value assigned to the filter damping factor d , this type of filter can be made to function as a Bessel, compromise, Butterworth, or Chebyshev type filter. From the transfer function, it can be determined that

$$\omega_c = 1/\sqrt{R_1 R_2 C_1 C_2} \quad (132)$$

and

$$d = R_1(C_1 + C_2) / \sqrt{R_1 R_2 C_1 C_2} \quad (133)$$

In order to avoid interaction between the filter cutoff characteristics and the filter cutoff frequency, it is desirable to make the values of d and ω_c independent of each other. In this case, these parameters interact and are not independent. Since there are fewer standard values of capacitors, and since resistors are more easily trimmed than capacitors, it is often convenient to make all frequency-determining capacitors in the filter equal.

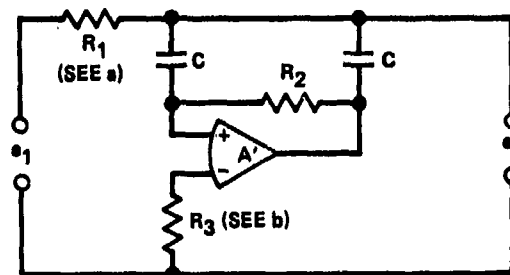
When $C_1 = C_2 = C$, then

$$2\pi f_c = \omega_c = 1/C\sqrt{R_1 R_2} \quad (134)$$

and

$$d = 2\sqrt{R_1/R_2} \quad (135)$$

The first step is to choose the filter damping factor d that defines the ratio of R_1 and R_2 . Then a value is selected for the capacitors C that provides appropriate values of R_1 and R_2 at the desired frequency f_c . Table 13 illustrates the above filter with some actual resistor and capacitor values selected to provide a cutoff frequency f_c of 1 kHz. For any other cutoff frequency, the scaling techniques are used that were covered earlier in Table 12.

TABLE 13. -- ZERO-OFFSET SECOND-ORDER LOW-PASS FILTER ($f_c = 1 \text{ kHz}$)

Filter type	Damping coefficient, d	R_1 , $k\Omega$	R_2 , $k\Omega$	C , μF
Bessel ^a	1.732	13.8	18.4	0.01
Compromise	1.564	12.5	20.4	0.01
Butterworth ^b	1.414	11.3	22.5	0.01
Chebyshev				
0.25-dB ripple	1.236	9.83	25.8	0.01
1-dB ripple	1.049	8.43	30.0	0.01

^aThis filter, unlike most low-pass active filters, does not require the source to provide a resistive return to amplifier common; however, it does require the source impedance R_S to be much much smaller than R_1 , or that R_S be a stable resistance and be included in R_1 . The load resistance should be much larger than $(R_1 + R_S)$.

^bResistance R_3 is optional and would be included to reduce the effects of the input bias currents. These input bias currents will not produce output offset in this filter; however, if the input bias current is large enough, it can cause the operational amplifier to saturate and the filter to become inoperative. If R_3 is used, then usually $R_3 \approx R_2$.

1.5.2 Voltage-Controlled Voltage-Source Low-Pass Filters

The voltage-controlled, voltage-source (VCVS) low-pass filter circuit has a high input impedance and low output impedance and, as a result, reduces circuit interaction. The circuits are easier to tune than most other circuit configurations and can be adjusted over wide ranges without substantial interaction of the critical parameters.

The circuit for the second-order low-pass VCVS filter is shown in Fig. 149. The transfer function for this circuit is

$$H(S) = (e_0/e_1)(s) = \frac{K/R_1R_2C_1C_2}{s^2 + s[(1/R_1C_1) + (1/R_2C_1) + (1 - K)/R_2C_2] + 1/R_1R_2C_1C_2} \quad (136)$$

This equation can be shown to be in the format of the second-order low-pass filter of Table 11. Using the format of Table 11, the following circuit relationships are derived:

$$K = (\text{circuit gain at } \omega = 0) = 1 + (R_a/R_b)$$

$$\omega_c = 2\pi f_c = 1/\sqrt{R_1R_2C_1C_2} \quad (137)$$

and

$$d = \sqrt{R_2C_2/R_1C_1} + \sqrt{R_1C_2/R_2C_1} + (1 - K)\sqrt{R_1C_1/R_2C_2} \quad (138)$$

Various assumptions can be made to simplify the above equations. It will be assumed that $R_1 = R_2 = R$ and that $C_1 = C_2 = C$. With these circuit constraints, the above circuit relationships simplify to

$$\omega_c = 2\pi f_c = 1/RC \quad (I39)$$

and

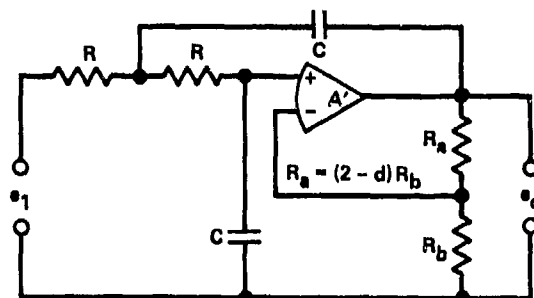
$$d = 3 - K \quad (I40)$$

This circuit is shown in Fig. 150. As can be observed, ω_c can be tuned independently of d and K , and d is a function only of the circuit gain K .

Note that in this type of low-pass filter, voltage offsets from the operational amplifier are added directly to the output signal and appear as data. This is normally not a major limitation when the input signals are large or when special low-output, offset-voltage operational amplifiers are utilized. Output offset voltages can also be reduced by applying proper circuit precautions (see Appendix A for a discussion of these techniques).

Tables 14-17 contain tabulated circuit values for the Bessel, Butterworth, and 0.5-dB, peak-to-peak, ripple Chebyshev filter responses. These filters were derived from tables in Ref. 10. The Bessel filters are frequency-normalized to unity group delay, that is $\tau(\omega) = 1$ sec at $\omega/\omega_c = 1$. The Butterworth filters are frequency-normalized to produce a steady-state amplitude response of -3 dB at ω_c . For the Chebyshev filter response, the cutoff frequency ω_c has been redefined from the earlier definition and is now defined as the frequency at which the amplitude response first exceeds the specified ripple (in this case, as it crosses 0 dB; see Fig. 146). The value of 0.5 dB was chosen because it represents a maximum deviation in the passband of about 6% (from $\omega = 0$ to $\omega = \omega_c$). This can be contrasted with the popular Butterworth filter. Although the Butterworth filter has no ripple in the passband (any all-pole filter with less damping than a Butterworth filter will have a ripple in the passband), it has an amplitude deviation of about 29% at ω_c .

TABLE 14. — SECOND-ORDER, VCVS, LOW-PASS FILTER CIRCUITS ($f_c = 1$ kHz)

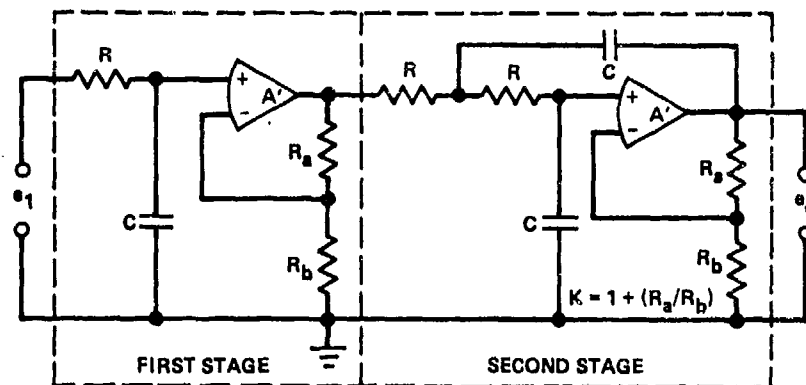


Filter response	Damping coefficient, d	R , k Ω	C , μF	Gain $K = 3 - d = 1 + R_A R_B$
Bessel ^a	$1.732 = \sqrt{3}$	9.189	0.01	1.268
Butterworth ^b	$1.414 = \sqrt{2}$	15.92	0.01	1.586
Chebyshev ^c (0.5-dB peak-to-peak ripple)	1.1578	12.93	0.01	1.842

^aThis Bessel filter is frequency-normalized to unity delay $\tau(\omega) = 1$ sec at $\omega/\omega_c = 1.0$.

^bThis Butterworth filter is frequency-normalized to be -3-dB response at $\omega/\omega_c = 1.0$.

^cThis Chebyshev filter is frequency-normalized so that the amplitude response at the band-edge passes through the lower boundary of the ripple band at $\omega/\omega_c = 1.0$.

TABLE 15. — THIRD-ORDER, VCVS, LOW-PASS FILTER CIRCUITS ($f_C = 1$ kHz)

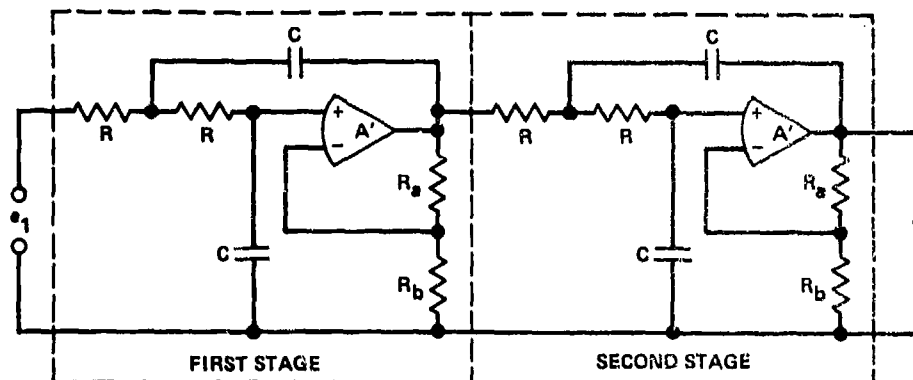
Filter response	Stage	Damping coefficient, d	R by stage, $k\Omega$	C , μF	Gain K
Bessel ^a	1	Real pole	6.854	0.01	(b)
	2	1.4471	6.262	0.01	1.553
Butterworth ^c	1	Real pole	15.92	0.01	(b)
	2	1.000	15.92	0.01	2.000
Chebyshev ^d (0.5-dB peak-to-peak ripple)	1	Real pole	25.41	0.01	(b)
	2	0.5861	14.89	0.01	2.414

^aThis Bessel filter is frequency-normalized to unity delay $\tau(\omega) = 1$ sec at $\omega/\omega_C = 1.0$.

^bAdjustable.

^cThis Butterworth filter is frequency-normalized to be -3-dB response at $\omega/\omega_C = 1.0$.

^dThis Chebyshev filter is frequency-normalized so that the amplitude response at the band-edge passes through the lower boundary of the ripple band at $\omega/\omega_C = 1.0$.

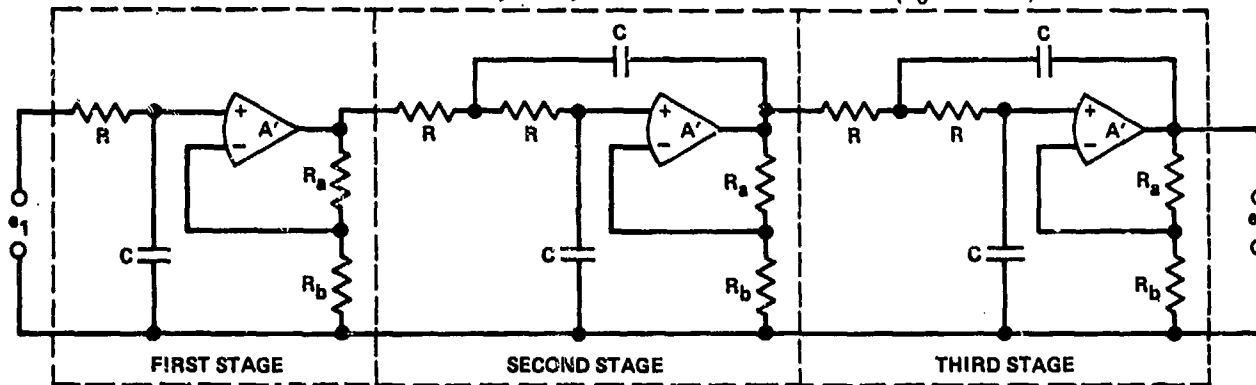
TABLE 16. — FOURTH-ORDER, VCVS, LOW-PASS FILTER CIRCUITS ($f_C = 1$ kHz)

Filter response	Stage	Damping coefficient, d	R by stage, $k\Omega$	C , μF	Gain (by stage) K
Bessel ^a	1	1.916	5.264	0.01	1.084
	2	1.2414	4.70	0.01	1.759
Butterworth ^b	1	1.848	15.92	0.01	1.152
	2	0.7654	15.92	0.01	2.235
Chebyshev ^c (0.5-dB peak-to-peak ripple)	1	1.418	26.66	0.01	1.582
	2	0.3401	15.43	0.01	2.660

^aThis Bessel filter is frequency-normalized to unity delay $\tau(\omega) = 1$ sec at $\omega/\omega_C = 1.0$.

^bThis Butterworth filter is frequency-normalized to be -3-dB response at $\omega/\omega_C = 1.0$.

^cThis Chebyshev filter is frequency-normalized so that the amplitude response at the band-edge passes through the lower boundary of the ripple band at $\omega/\omega_C = 1.0$.

TABLE 17. — FIFTH-ORDER, VCVS, LOW-PASS FILTER CIRCUITS ($f_c = 1$ kHz)

Filter response	Stage	Damping coefficient, d	R by stage, $k\Omega$	C , μF	Gain (by stage) K
Bessel ^a	1	---	4.364	0.01	(b)
	2	1.775	4.213	0.01	1.225
	3	1.0911	3.735	0.01	1.909
Butterworth ^c	1	---	15.92	0.01	(b)
	2	1.6180	15.92	0.01	1.382
	3	0.6180	15.92	0.01	2.382
Chebyshev ^d (0.5-dB peak-to-peak ripple)	1	---	43.93	0.01	(b)
	2	0.8490	23.05	0.01	2.151
	3	0.2200	15.64	0.01	2.780

^aThis Bessel filter is frequency-normalized to unity delay $\tau(\omega) = 1$ sec at $\omega/\omega_c = 1.0$.

^bAdjustable.

^cThis Butterworth filter is frequency-normalized to be -3-dB response at $\omega/\omega_c = 1.0$.

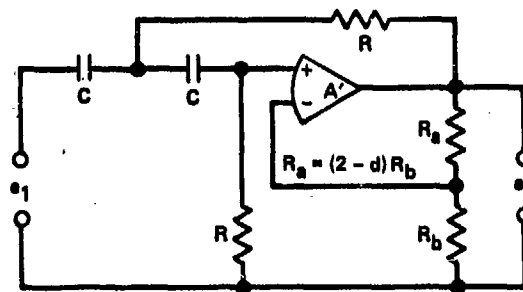
^dThis Chebyshev filter is frequency-normalized so that the amplitude response at the band-edge passes through the lower boundary of the ripple band at $\omega/\omega_c = 1.0$.

Higher-order filters are described in the other filter texts, such as in Refs. 10, 12, 42, and 43. Higher-order filters are not only more complex, but they also require more attention to the matching and accuracy of the components, filter-frequency tuning, and damping accuracy, and they should only be used when absolutely necessary. In this text, the tuning and damping of all the previous filter circuits and of the following all-pole high-pass circuits need be adjusted only to within $\pm 10\%$ for an acceptable filter accuracy. For contrast, a sixth-order, 3-dB, peak-to-peak ripple Chebyshev filter requires frequency tuning accuracy of $\pm 1\%$, an order of magnitude more difficult to achieve than that required for the circuits shown here.

1.5.3 Voltage-Controlled Voltage-Source High-Pass Filters

Tables 18-21 list the all-pole high-pass filters corresponding to the low-pass filters in Tables 14-17. It should be noted that the Bessel high-pass filter should probably be considered as only a highly damped filter since the linear phase which is characteristic of the low-pass Bessel filter is not attainable for the high-pass condition.

As discussed earlier in Sec. 3, high-pass filters are not usually recommended for use as signal-conditioning filters unless the high-frequency noise is limited by other system parameters. However, high-pass filters are combined with low-pass filters to produce very effective broadband filters. Figure 151 illustrates how this is accomplished.

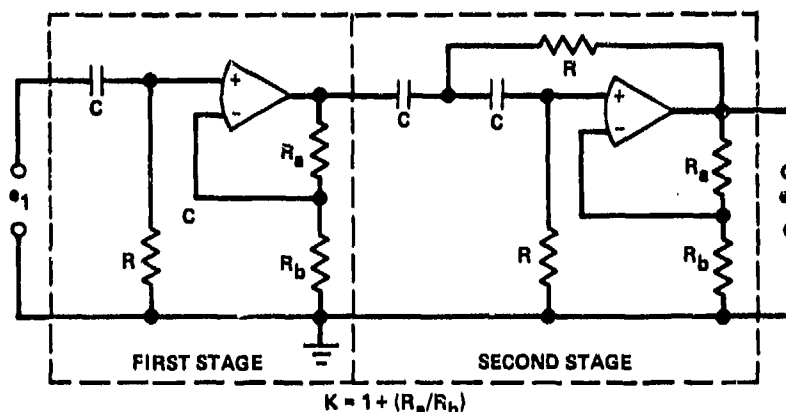
TABLE 18. — SECOND-ORDER, VCVS, HIGH-PASS FILTER CIRCUITS ($f_c = 1$ kHz)

Filter response	Damping coefficient, d	R , $k\Omega$	C , μf	Gain $K = 3 - d = 1 + (R_a/R_b)$
Bessel ^a	3	27.57	0.01	1.268
Butterworth ^b	2	15.92	0.01	1.586
Chebyshev ^c (0.5-dB peak-to-peak ripple)	1.1578	19.60	0.01	1.842

^aThis Bessel filter is frequency-normalized to unity delay $\tau(\omega) = 1$ sec at $\omega/\omega_c = 1.0$.

^bThis Butterworth filter is frequency-normalized to be -3-dB response at $\omega/\omega_c = 1.0$.

^cThis Chebyshev filter is frequency-normalized so that the amplitude response at the band-edge passes through the lower boundary of the ripple band at $\omega/\omega_c = 1.0$.

TABLE 19. — THIRD-ORDER, VCVS, HIGH-PASS FILTER CIRCUITS ($f_c = 1$ kHz)

Filter response	Stage	Damping coefficient, d	R by stage, $k\Omega$	C , μF	Gain (by stage) K
Bessel ^a	1	A real pole	36.96	0.1	(b)
	2	1.4471	40.45	0.1	1.553
Butterworth ^c	1	A real pole	15.92	0.1	(b)
	2	1.0000	15.92	0.1	2.000
Chebyshev ^d (0.5-dB peak-to-peak ripple)	1	A real pole	9.970	0.1	(b)
	2	0.5861	17.01	0.1	2.414

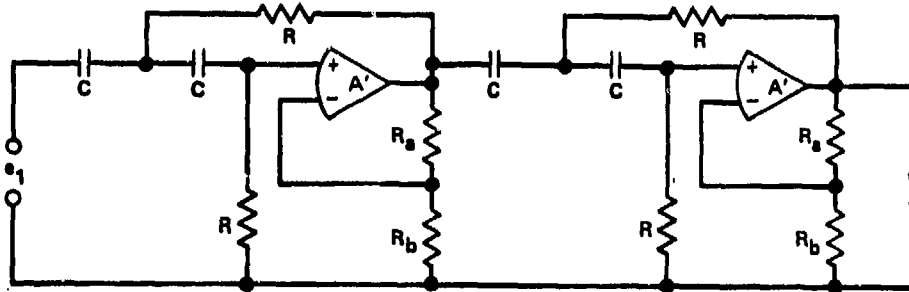
^aThis Bessel filter is frequency-normalized to unity delay $\tau(\omega) = 1$ sec at $\omega/\omega_c = 1.0$.

^bAdjustable.

^cThis Butterworth filter is frequency-normalized to be -3-dB response at $\omega/\omega_c = 1.0$.

^dThis Chebyshev filter is frequency-normalized so that the amplitude response at the band-edge passes through the lower boundary of the ripple band at $\omega/\omega_c = 1.0$.

TABLE 20. — FOURTH-ORDER, VCVS, HIGH-PASS FILTER CIRCUITS ($f_c = 1 \text{ kHz}$)



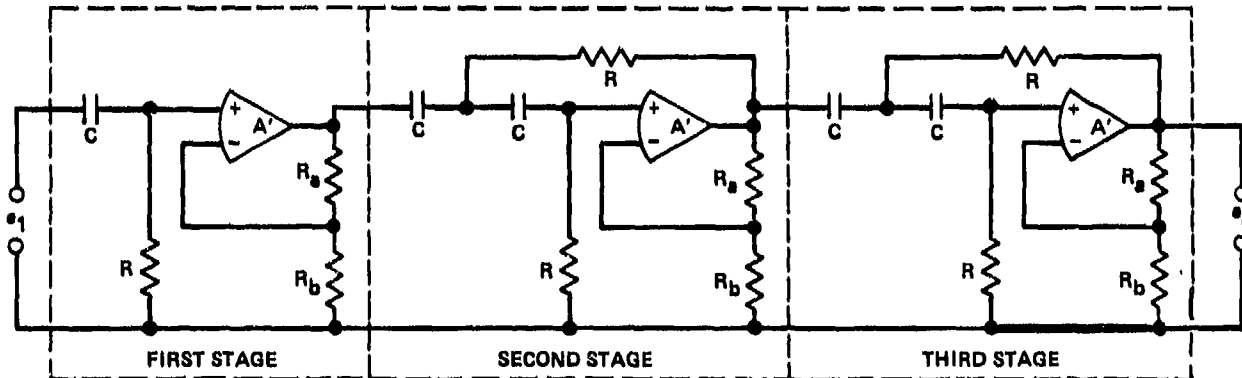
Filter response	Stage	Damping coefficient, d	R by stage, k Ω	C, μF	Gain (by stage) K
Bessel ^a	1	1.9159	48.15	0.01	1.034
	2	1.2414	53.94	0.01	1.759
Butterworth ^b	1	1.8476	15.92	0.01	1.152
	2	0.76537	15.92	0.01	2.235
Chebyshev ^c (0.5-dB peak-to-peak ripple)	1	1.4182	9.502	0.01	1.582
	2	0.34007	16.41	0.01	2.660

^aThis Bessel filter is frequency-normalized to unity delay $\tau(\omega) = 1 \text{ sec}$ at $\omega/\omega_c = 1.0$.

^bThis Butterworth filter is frequency-normalized to be -3-dB response at $\omega/\omega_c = 1.0$.

^cThis Chebyshev filter is frequency-normalized so that the amplitude response at the band-edge passes through the lower boundary of the ripple band at $\omega/\omega_c = 1.0$.

TABLE 21. — FIFTH-ORDER, VCVS, HIGH-PASS FILTER CIRCUITS ($f_c = 1 \text{ kHz}$)



Filter response	Stage	Damping coefficient, d	R by stage k Ω	C, μF	Gain (by stage) K
Bessel ^a	1	---	58.06	0.01	(b)
	2	1.775	60.14	0.01	1.225
	3	1.091	68.83	0.01	1.909
Butterworth ^c	1	---	15.92	0.01	(b)
	2	1.6180	15.92	0.01	1.382
	3	0.6180	15.92	0.01	2.382
Chebyshev ^d (0.5-dB peak-to-peak ripple)	1	---	5.768	0.01	(b)
	2	0.8490	10.99	0.01	2.151
	3	0.2200	16.20	0.01	2.780

^aThis Bessel filter is frequency-normalized to unity delay $\tau(\omega) = 1 \text{ sec}$ at $\omega/\omega_c = 1.0$.

^bAdjustable.

^cThis Butterworth filter is frequency-normalized to be -3-dB response at $\omega/\omega_c = 1.0$.

^dThis Chebyshev filter is frequency-normalized so that the amplitude response at the band-edge passes through the lower boundary of the ripple band at $\omega/\omega_c = 1.0$.

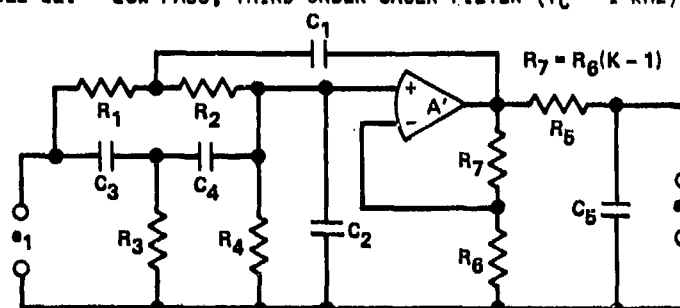
1.5.4 Cauer (Elliptic) High-Pass and Low-Pass Filters

The Cauer filters come very close to the ideal filter amplitude response. As shown in Fig. 26, the Cauer filter has a very steep attenuation outside the cutoff frequency f_c . This is possible because Cauer filters have a transmission zero (or zeros) just outside the passband. These transmission zeros can sometimes be placed at some discrete interference frequency to achieve very high attenuation. Figure 152 illustrates the important design parameters of a fifth-order Cauer filter.

As for the Chebyshev filters of Tables 14 through 21, the cutoff frequency for the Cauer filter is defined as the point at which the filter attenuation first exceeds R_{dB} . Both the Cauer and Chebyshev filters have ripple in the passbands; however, the Cauer filter also has ripple in the stop-band. The attenuation term (A_{dB}) is defined for the Cauer filter as the difference in decibels between the 0-dB level and the maximum stop-band ripple. The first time the filter achieves A_{dB} outside the passband is called f_s .

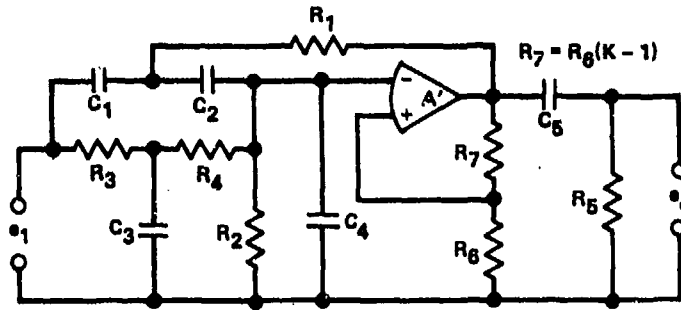
The third-order Cauer low-pass filter of Table 22 and the similar high-pass filter of Table 23 were designed from tables given in Ref. 42. This particular implementation of the Cauer filter requires many diverse values of resistors and capacitors, but only uses one operational amplifier. A tolerance of 1.0% on the resistor and capacitor values is adequate for most applications. A ripple (R_{dB}) of 0.01 dB is recommended for transient data, and a ripple (R_{dB}) of 0.28 dB is advised for nontransient data.

TABLE 22. — LOW-PASS, THIRD-ORDER CAUER FILTER ($f_c = 1$ kHz)



Load impedance must be high and the input impedance low.

Filter parameters	Attenuation (A_{dB})		
	50 dB	40 dB	30 dB
f_s	7,185 Hz	5,241 Hz	3,628 Hz
K	1.148	1.206	1.343
Gain	1.098	1.111	1.141
R_1	3.487 k Ω	3.620 k Ω	3.922 k Ω
R_2	6.974 k Ω	7.240 k Ω	7.844 k Ω
R_3	50.45 k Ω	28.05 k Ω	14.80 k Ω
R_4	227.0 k Ω	126.2 k Ω	66.62 k Ω
R_5	10.00 k Ω	10.00 k Ω	10.00 k Ω
C_1	0.03848 μ F	0.03724 μ F	0.03474 μ F
C_2	8,553 pF	8,274 pF	7,721 pF
C_3	1,182 pF	2,136 pF	4,090 pF
C_4	591.1 pF	1,068 pF	2,045 pF
C_5	0.0100 μ F	9,856 pF	9,498 pF
f_s	4,134 Hz	2,924 Hz	2063 Hz
K	1.319	1.410	1.603
Gain	1.247	1.263	1.297
R_1	3.525 k Ω	3,719 k Ω	4,119 k Ω
R_2	7.050 k Ω	7,438 k Ω	8,238 k Ω
R_3	40.84 k Ω	21.42 k Ω	11.65 k Ω
R_4	183.8 k Ω	96.38 k Ω	52.43 k Ω
R_5	10.00 k Ω	10.00 k Ω	10.00 k Ω
C_1	0.05936 μ F	0.05631 μ F	0.05095 μ F
C_2	0.01319 μ F	0.01251 μ F	0.01132 μ F
C_3	2,278 pF	4,345 pF	8,002 pF
C_4	1,139 pF	2,172 pF	4,001 pF
C_5	0.02091 μ F	0.02040 μ F	0.01929 μ F

TABLE 23. — HIGH-PASS THIRD-ORDER CAUER FILTER ($f_c = 1$ kHz)

The load impedance must be high and the input impedance should be low.				
Filter parameters	Attenuation (A_{dB})			
	50 dB	40 dB	30 dB	
f_s	139 Hz	191 Hz	276 Hz	
K	1.148	1.206	1.343	
Gain	0.0505	0.0955	0.2015	
R_1	4.136 k Ω	4.274 k Ω	4.581 k Ω	
R_2	18.61 k Ω	19.23 k Ω	20.61 k Ω	
R_3	134.6 k Ω	74.52 k Ω	38.91 k Ω	
Ripple (R_{dB}) = 0.01 dB	R_4	269.3 k Ω	149.0 k Ω	77.82 k Ω
	R_5	15.90 k Ω	16.15 k Ω	16.76 k Ω
	C_1	0.04564 μ F	0.04397 μ F	0.04058 μ F
	C_2	0.02282 μ F	0.02198 μ F	0.02029 μ F
	C_3	3,155 pF	5,674 pF	0.01754 μ F
	C_4	701 pF	1,261 pF	2,389 pF
	C_5	0.01592 μ F	0.01592 μ F	0.01592 μ F
f_s	242 Hz	342 Hz	485 Hz	
K	1.319	1.410	1.603	
Gain	0.0717	0.146	0.306	
R_1	2.681 k Ω	2.826 k Ω	3.124 k Ω	
R_2	12.06 k Ω	12.74 k Ω	14.06 k Ω	
R_3	69.88 k Ω	36.63 k Ω	19.89 k Ω	
Ripple (R_{dB}) = 0.28 dB	R_4	139.8 k Ω	73.26 k Ω	39.78 k Ω
	R_5	7.610 k Ω	7.800 k Ω	8.251 k Ω
	C_1	0.04515 μ F	0.04279 μ F	0.03864 μ F
	C_2	0.02258 μ F	0.02140 μ F	0.01932 μ F
	C_3	3,897 pF	7,430 pF	0.01366 μ F
	C_4	865.9 pF	1,651 pF	3,036 pF
	C_5	0.01592 μ F	0.01592 μ F	0.01592 μ F

Note that there are two gains (K and Gain) given in Tables 22 and 23. The gain K is the closed circuit gain of the operational amplifier and is equal to

$$K = 1 + (R_7/R_6) \quad (I41)$$

The gain K must be set to the value shown in the tables for proper functioning. Resistors R_7 and R_6 are not frequency determining resistors and therefore are not scaled as the other resistors in the filter. The gain value shown in the tables is the overall circuit gain and is smaller than K since the input resistors form an input voltage divider. This voltage-divider effect is particularly detrimental in the high-pass-filter format.

When a higher-order Causer filter is required, the multioperational amplifier filter implementation shown in Ref. 44 is recommended. The spread of component values is less and, therefore, the filter is easier to implement and tune.

I.5.5 Commutating Bandpass and Band-Reject Filter

A useful special-purpose filter is the commutating filter. The filter illustrated here is the one presented by Deboo (Ref. 43) and the following description is based on Deboo's text.

The commutating filter is mainly of use in applications such as phase-sensitive detection systems where a critical clock frequency is already available. With the commutating filter, a very high Q bandpass filter can be constructed which tracks the fundamental clock frequency; thus component and frequency drifts are not relevant factors in filter performance.

The principle of the commutating filter can best be understood by referring to Fig. 153. In Fig. 153a, a commutator sequentially switches n capacitors; it illustrates how the basic commutating filter is implemented. In actual practice, the mechanical switch used in the illustration is replaced with an electronic switch, as shown in Fig. 154.

Figure 153b illustrates the bandpass response of this type of filter at various frequencies. In this figure, $f_s = 8 f_c = 8$ kHz, where f_s is the commutating (sampling) frequency, and $f_c = 1$ kHz is the center frequency of the desired bandpass. As can be seen in Fig. 153, this filter actually passes frequencies near zero with slightly more gain than those at 1 kHz. The filter continues to produce passbands with decreasing gain at multiples of $f_c = 1$ kHz until zero gain is reached at the switching frequency, $f_s = 8$ kHz. Above f_s , the gain of each bandpass window starts to increase again. Nulls occur at each whole multiple of 8 kHz, for example, at 8 kHz, 16 kHz, and 24 kHz.

The actual output of the basic commutating filter of Fig. 153a to a 1-kHz input is shown in Fig. 153c. This figure shows, as expected, that there are eight samples per cycle. This also explains why the 2- and 3-kHz windows are not used (they would provide even fewer samples per cycle). The larger the number of samples per cycle, the better the original input waveform can be reconstructed. The passband windows at 4 kHz and higher produce output frequencies that are not the same as the input frequencies and are thus to be avoided.

In Fig. 154, the analog input bandpass filter eliminates the steady input and drastically reduces the inputs that are harmonics of 1 kHz. The output analog filter removes the high-frequency "step" response introduced by the switching process. A spectral response of the filter in Fig. 154 is shown in Ref. 43 and shows no detectable passband responses other than at 1 kHz. This spectral response curve indicates a final attenuation of greater than 50 dB, which is very good for an active filter. With analog filters in the input and output, the filter tracking is limited to variations within the input and output filter bandwidth.

The commutating filter can also be configured as a notch filter. The input and output of the commutating filter are in phase and of equal amplitude. The output signal is inverted and then summed with the input, which produces a notch filter by the resulting cancellation. A commutating notch filter of this type is described in Ref. 45.

I.6 SELECTING COMPONENTS FOR AN ACTIVE FILTER

The choice of an active-filter resistor is dictated by the application requirements. In airborne applications, temperature variations often cause unacceptable resistance changes. Carbon-film resistors are adequate for many applications where the temperature variations are limited and overall component accuracy is not critical. For example, a carbon composition resistor with a temperature coefficient, TC, of 400 parts per million per °C (ppm/°C) will have a 1% change with a 25°C temperature change. Metal-film resistors (TC of 100 ppm/°C) are a good cost compromise between carbon composition resistors (TC of 250 to 500 ppm/°C) and high grade wire-wound resistors (TC of a few ppm/°C).

The choice of suitable filter capacitors is often more difficult than the choice of resistors. Cost, performance, and size are important in the selection of capacitors for filter use. The polystyrene capacitor has high temperature stability, but it is large and its temperature-limited to about 85°C. Metalized Mylar capacitors, although physically smaller, have a larger TC and power factors but have limited temperature range. High-quality mica capacitors are physically large at larger capacitance values, but they have a very low TC and low loss. Teflon capacitors have a temperature range of -60°C to +150°C with a temperature coefficient of -250 ppm/°C and very low loss. Glass and silver mica capacitors are stable, but are useful mainly for low values of capacitance. The temperature-compensated ceramic capacitors are very small, but have poor stability and exhibit high electrical loss. Tantalum oxide capacitors are attractive because of their high capacitances per unit volume; however, they should only be used with great care, because the initial value of capacitance can vary markedly.

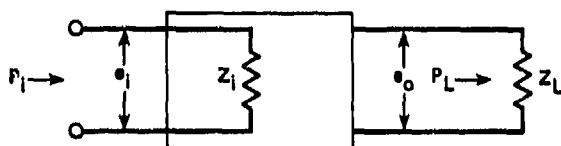


Figure 140. Illustration of factors used in definition of the decibel



Figure 141. Block diagram of lumped-parameter linear filter

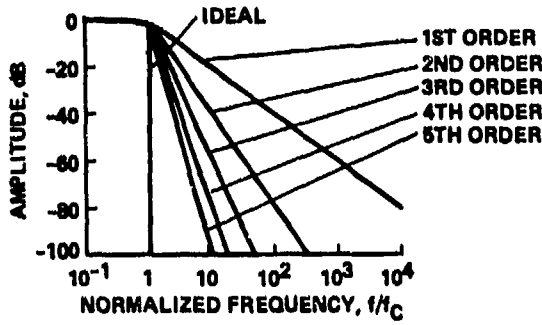


Figure 142. Amplitude response curves for Butterworth low-pass filters

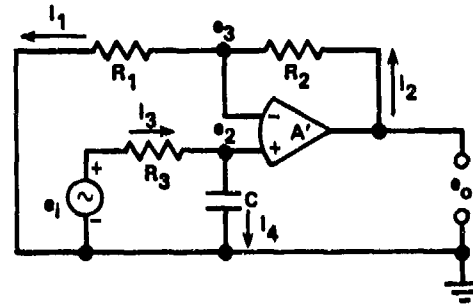


Figure 143. First-order low-pass active filter

- a = REAL PART OF $H(j\omega)$
- b = IMAGINARY PART OF $H(j\omega)$
- $H(j\omega)$ = STEADY-STATE SINUSOIDAL TRANSFER FUNCTION
- j = SQUARE ROOT OF -1
- ϕ = TRANSFER FUNCTION PHASE ANGLE

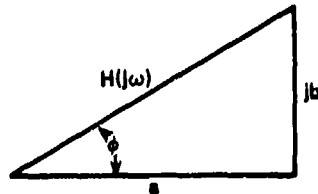


Figure 144. Vectorial representation of $H(j\omega)$

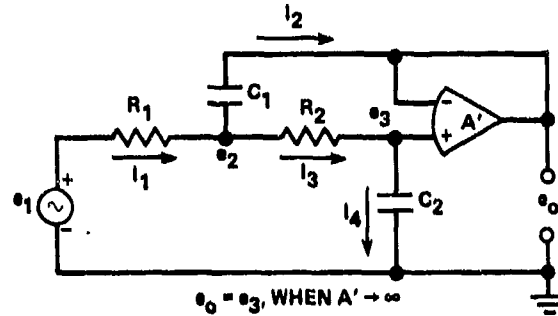
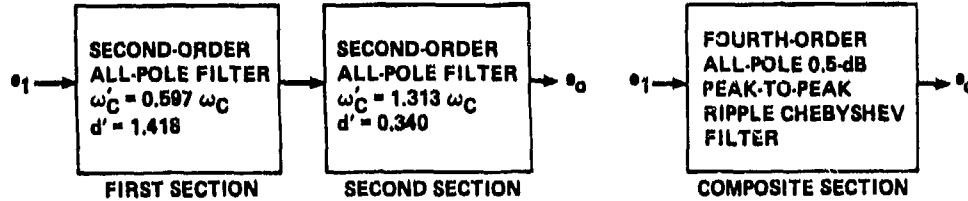
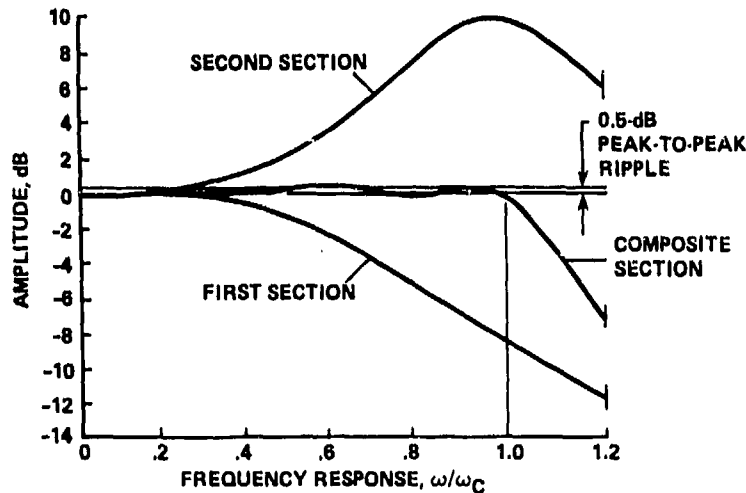


Figure 145. Second-order low-pass active filter

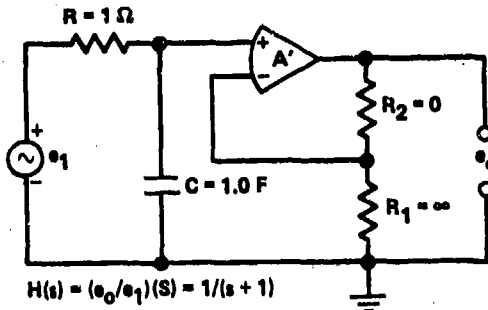


(a) Using two second-order filters to produce a fourth-order filter

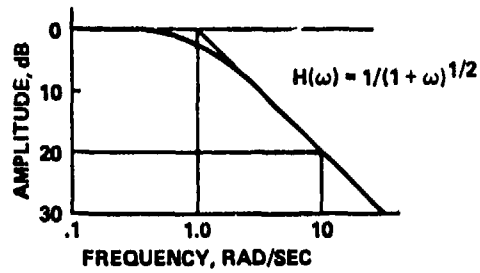


(b) Combined amplitude filter response

Figure 146. Constructing a high order filter from two lower order filters

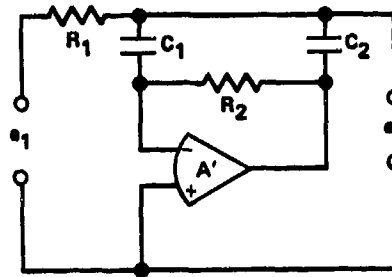


(a) First-order low-pass active filter

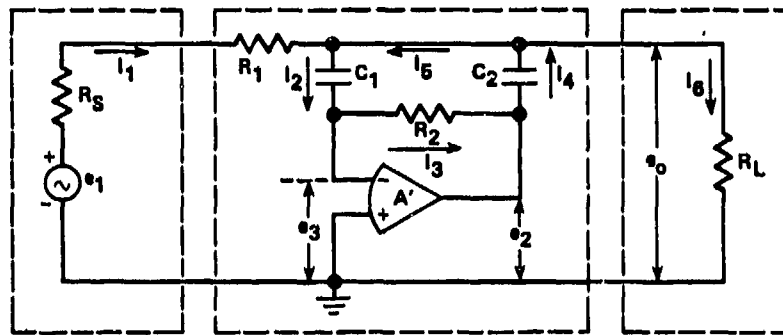


(b) Amplitude response

Figure 147. First-order low-pass active filter and amplitude response



(a) Schematic diagram of zero-offset low-pass active filter



(b) Zero-offset low-pass active filter in a circuit

Figure 148. Zero-offset low-pass active filter

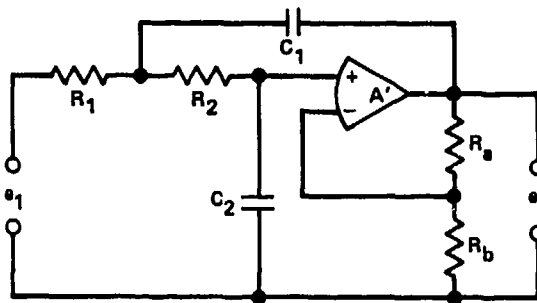


Figure 149. Second-order low-pass filter for voltage-controlled voltage source

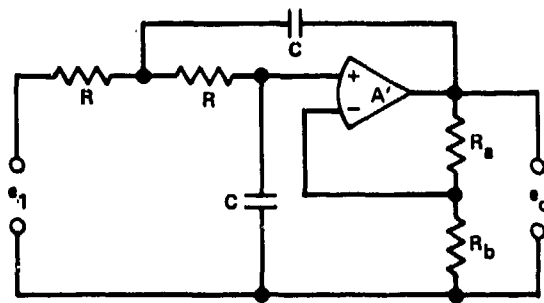
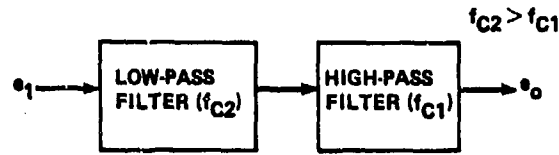
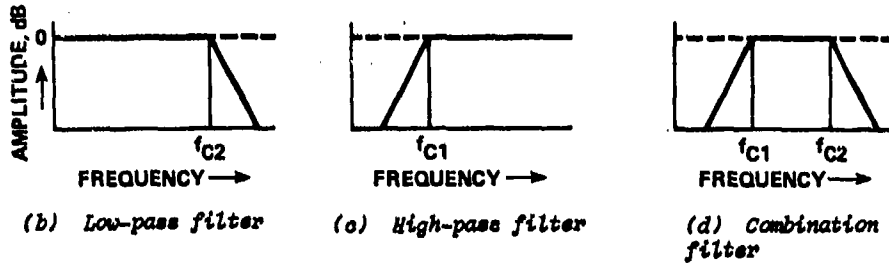


Figure 150. Equal component value of second-order low-pass filter for voltage-controlled voltage source



(a) Series high-pass and low-pass filters



(b) Low-pass filter

(c) High-pass filter

(d) Combination filter

Figure 151. A broad-band bandpass filter

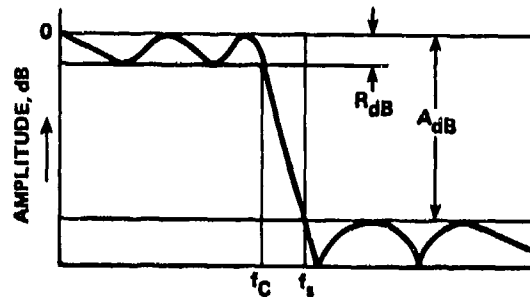
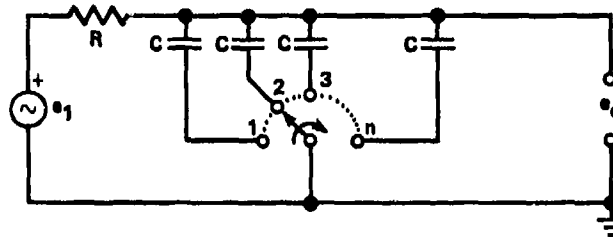
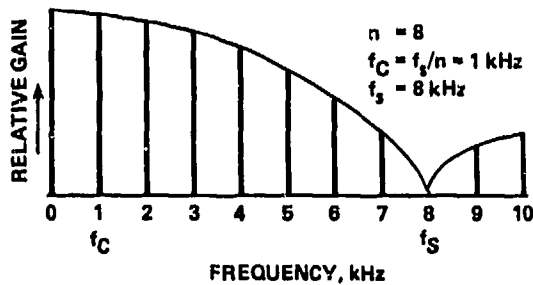


Figure 152. Design parameters of fifth-order Chebyshev filter

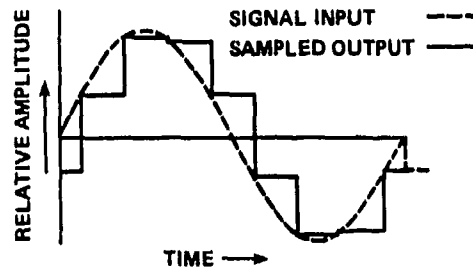


$$f_s = n f_c$$

(a) Switched capacitor commutating filter

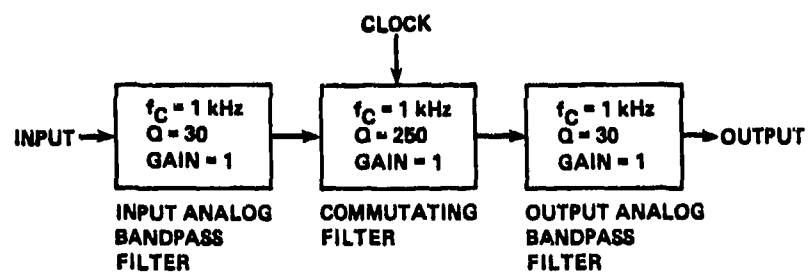
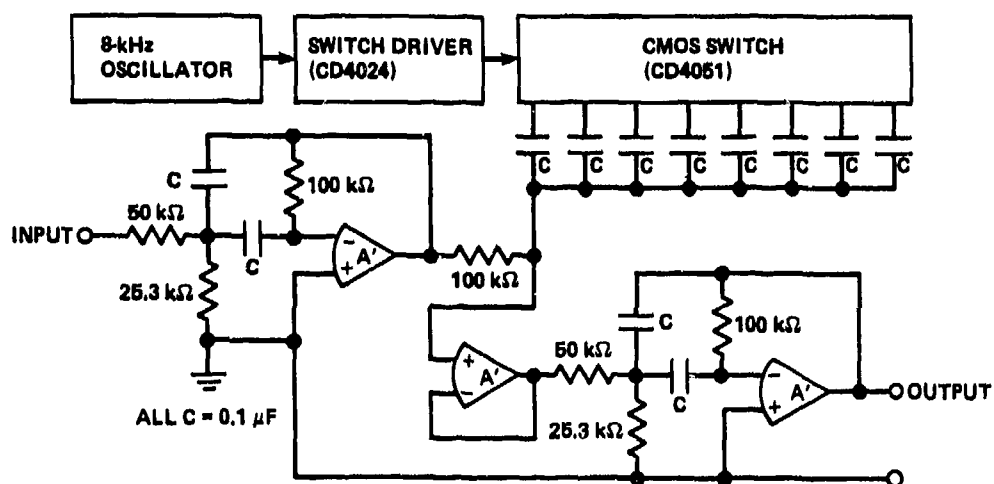


(b) Commutating filter bandpass response



(c) Commutating filter input-output waveforms

Figure 153. A 1-kHz bandpass commutating filter

(a) *Commutating filter block diagram*(b) *Commutating filter circuit*Figure 154. *Practical 1-kHz commutating filter*

APPENDIX J

THERMOCOUPLE PATTERN-CIRCUIT TECHNIQUE

A pattern circuit for analyzing thermocouple circuits was devised by Dr. Robert J. Moffat of Stanford University (Stanford, California). This technique is the most effective one known to the author for thermocouple circuit analysis. Dr. Moffat's technique was first described in Ref. 24, which was later published in Ref. 23. The following discussion draws extensively on Dr. Moffat's work and uses his techniques.

Dr. Moffat states in Ref. 24 that ". . . It can be shown from either the free-electron theory of metals or from thermodynamic arguments alone, that the output of a thermocouple can rigorously be described in terms of the contribution from each of the lengths of material comprising the circuit; the junctions are merely electrical connections between the wires."

This can be easily illustrated by a minor change in Eq. (30) to yield

$$e_{AB} = \int_{T_2}^{T_1} (e_1 - e_2) dT \quad (J1)$$

Equation (J1) could be viewed as indicating that the thermoelectric voltage originates in the wire instead of at the junction. This interpretation does not negate or contradict any of the findings of Peltier, Thompson, or Seebeck; rather, it is entirely consistent with their results. Such a view offers a great operational advantage, for it opens the way to graphic analysis of thermocouple circuits. Graphic analysis is used with the pattern-circuit concept to analyze the behavior of the most complex thermocouple circuits. When a thermocouple circuit can be reduced to the pattern circuit, the calibration tables provided for the two materials are applicable. The pattern technique requires a method of graphically relating the voltage output e_0 of Fig. 155 to the temperatures T_1 and T_R . For graphic analysis of this nature, the curves of Fig. 156 are used. These curves are a linearized version of those in Fig. 46 where the metals shown are calibrated against platinum.

The use of linearized approximations of the actual thermocouple outputs versus temperature in no way limits the pattern-circuit technique as used in this document. The purpose of this technique is not to derive the system output voltage, but to demonstrate graphically that a complex thermocouple circuit performs identically to the pattern circuit. In fact, arbitrary curve slopes can be used in the graphic analysis as long as different slopes are used for each thermoelectrically unique material. When using arbitrary slopes, it is desirable to keep the relative slope magnitude proportional to the actual magnitude. Once the relationship has been established between the actual circuit and the pattern circuit, the tables and equations representing the thermocouple circuit output are applicable to the complex circuit.

Figure 157a illustrates a typical laboratory thermocouple measuring system which uses a null-balance millivoltmeter to measure the thermocouple voltage. When the null-balance millivoltmeter output voltage exactly counters the Seebeck voltage, no current flows in the thermocouple circuit. This circuit can now be represented by that of Fig. 157b. This is the pattern circuit. To analyze the circuit graphically, a voltage-versus-temperature curve is constructed, as shown in Fig. 157c. The following procedure is used to construct this curve:

1. Locate point (1) at zero voltage and T_R .
2. Using the voltage-versus-temperature slope for Chromel (EP or KP) from Fig. 156, draw a line using an increasing voltage until it intercepts T_1 at point (2).
3. From point (2), use the slope for Alumel (KN) and proceed back to point (3) which is at the reference temperature T_R as was point (1).
4. Point (3) on the ordinate is the pattern-circuit output voltage, $e_p = e_0$.

Now that the pattern circuit has been demonstrated, a simple example will be used to analyze three "laws" of thermocouples which are useful to instrument engineers. Figure 158 illustrates the law of interior temperatures. In Fig. 158a, a candle is shown heating point (2) of material A. The effects are illustrated graphically in Fig. 158b. To analyze the circuit, the following procedure is used:

1. Starting at point (1) (T_R and zero voltage), proceed to point (2) at T_2 , along the voltage-versus-temperature curve for material A.
2. From point (2), move down the same slope to point (3) at T_3 .
3. From point (3), move along the slope for material B to point (4) at T_R .

The circuit output is identical to that of the pattern circuit that would overlay Fig. 158 from point (1) to (3) to (4). Thus, it is concluded that temperature gradients along a wire do not affect the output voltage. (In actual practice, wire is tested for homogeneity by this method. A sharp temperature gradient is passed along the wire and if an output is generated, the wire is defined as inhomogeneous.)

Figure 159 illustrates the law of inserted materials. In this figure, a material C has been inserted into the material-A portion of the circuit. As can be observed from Fig. 159b, as long as points (2) and (4) are at the same temperature, the inserted material will produce no variances from the ideal pattern circuit. It is important to notice that the analysis in Figs. 158 and 159 is done with arbitrary materials that have fixed but arbitrary output slopes. This is very convenient when analyzing a complex circuit and in no way invalidates the comparison. In this case the pattern circuit lies along the lines (1) to (5) and (5) to (6).

Figure 160 illustrates the law of intermediate materials. In this example, a material C has been inserted between the two materials A and B at the measurement junction. This is different from Fig. 159 in that the inserted material is now located at one of the measurement junctions.

As can be seen from the graphic analysis of Fig. 160, when T_2 and T_4 are the same, there is no deviation from the ideal pattern circuit, that is points (1) to (2) to (5). The law of intermediate materials is of great practical importance in that it deals with how thermocouple junctions can be manufactured. In practice, a thermocouple junction is soldered, brazed, or welded (the welding process itself produces a new material). As long as the new material begins and ends at the same temperature (isothermal), no extraneous voltage is generated in the circuit. This isothermal condition is usually accomplished by designing the thermocouple junction installation to avoid thermal gradients. When a thermocouple junction is installed in a strong temperature gradient or the installation itself introduces a sharp temperature gradient (non-isothermal condition) it will invalidate the conditions for the above illustration and re-design will be required.

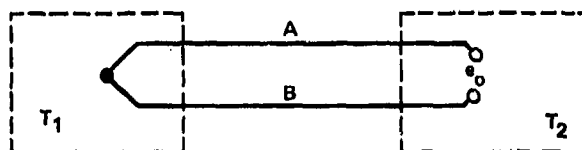


Figure 155. Pattern circuit for analyzing thermocouple circuit techniques

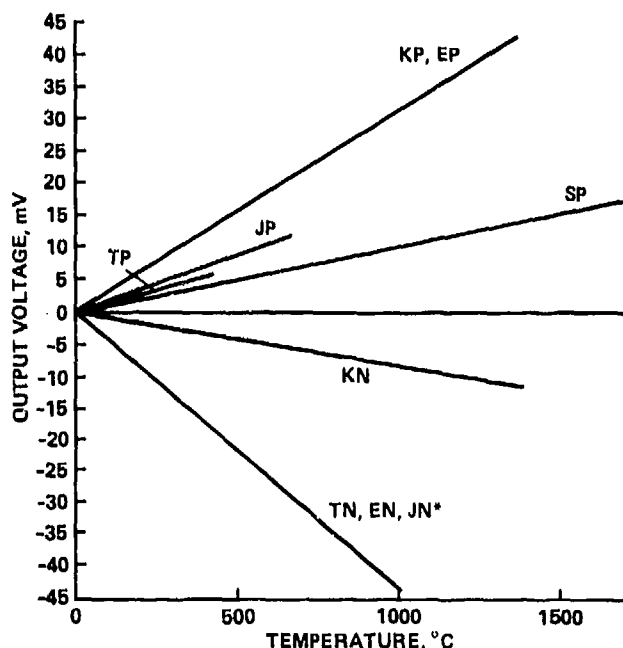
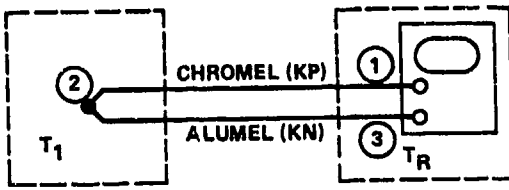
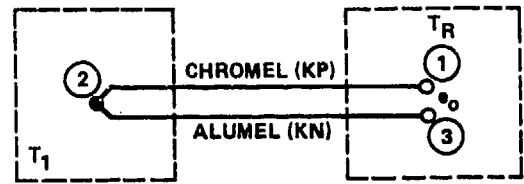


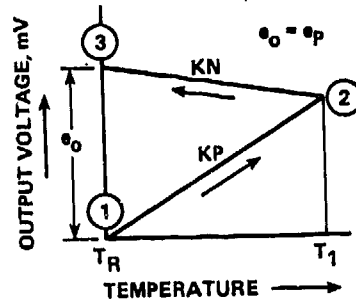
Figure 158. Voltage-temperature curves for various thermocouple materials, straight-line approximation (Refer to Table 2. JN has slightly lower output than TN and EN and is limited to a maximum temperature of 780°C.)



(a) Null-balance millivoltmeter used with thermocouple

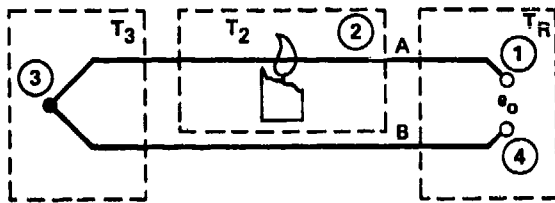


(b) Equivalent thermocouple circuit at balance

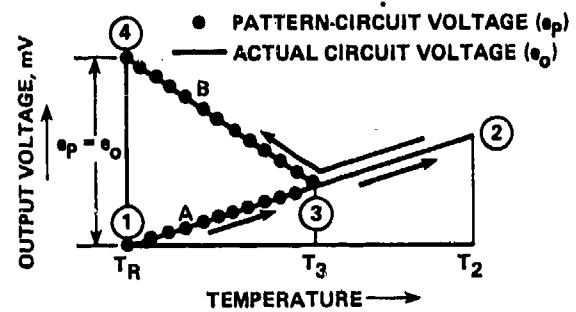


(c) Pattern circuit analysis of (b)

Figure 157. Laboratory null-balance thermocouple temperature measurement system

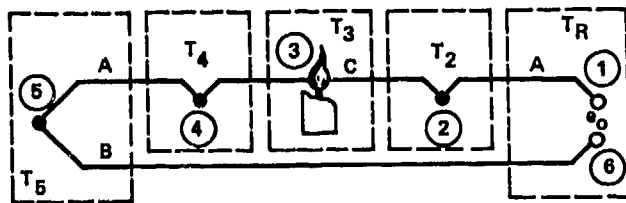


(a) Thermocouple circuit with heated material A

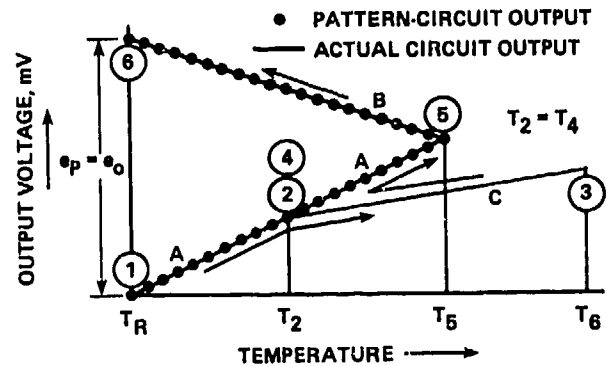


(b) Graphic analysis of (a)

Figure 158. Illustration of the law of interior temperatures

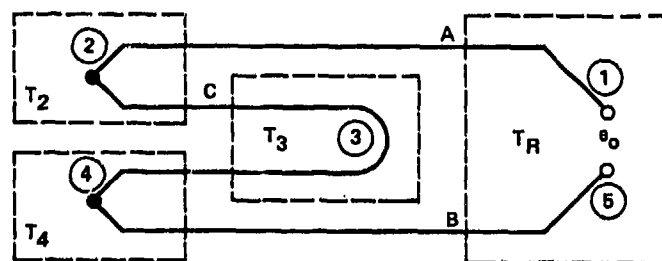


(a) Thermocouple circuit with three materials (Note heated material C.)

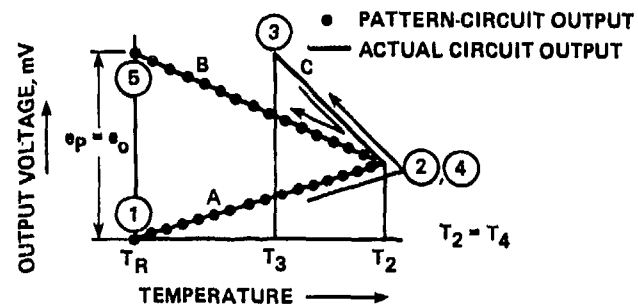


(b) Graphic analysis of (a)

Figure 159. Illustration of the law of inserted materials



(a) Thermocouple circuit with third material added



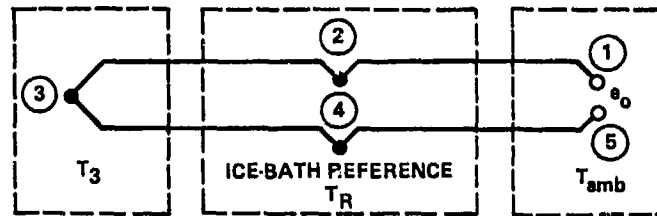
(b) Graphic analysis of (a)

Figure 180. Illustration of the law of intermediate materials

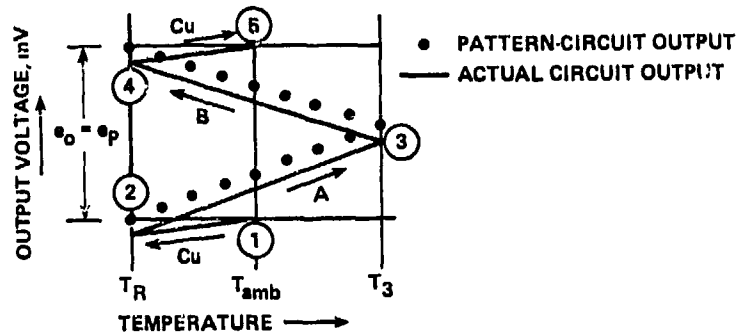
APPENDIX K

ANALYSIS OF AN ICE-BATH REFERENCE

Figure 161 illustrates a temperature-measuring system using an ice-bath reference. Figure 161a illustrates the open-circuit equivalent of this circuit. A major advantage of this circuit, and of other temperature-reference systems, is that copper wiring can be used from the ice-bath reference to the measurement system. Note that in the open-circuit case, a temperature difference between points (1) and (5) in Fig. 161a must also be avoided if this circuit is to agree exactly with the pattern circuit. Fortunately, the thermoelectric sensitivity of copper is low, which minimizes this potential error source. Figure 161b is a pattern circuit of the ice-bath reference.



(a) Thermocouple circuit using ice-bath reference



(b) Graphic analysis of (a)

Figure 161. Analysis of ice-bath reference thermocouple circuit

APPENDIX L

PROPORTIONAL-CONTROL HEATER FOR THERMOCOUPLE REFERENCE OVENS

The correctly designed proportional-control heater produces much less electrical noise than either the on-off thermostatically controlled or electronic-pulsed input ovens. Since thermocouples typically have very low output, it is important to reduce the coupling of switching noise into these sensitive circuits.

Inside the reference oven, the thermocouple junctions are mounted to an isothermal reference bar. The thermocouple junctions should be electrically insulated from, but closely coupled thermally, to the isothermal bar. Any good thermal conductor such as silver or copper will make a good isothermal bar. The bar should be well isolated from external heat sources, and the temperature should always be monitored. A platinum-type resistive-temperature gauge serves well as a monitor. The thermocouple wires should be routed through the insulation in a manner that avoids producing excessive temperature gradients and temperature losses. In cases in which extra heating capabilities are required, the power transistor can be mounted inside the insulated area.

The circuit shown in Fig. 162 was initially used to control the temperature of a precision force-rebalance altimeter and was adapted for use as a thermocouple reference-oven temperature controller. This circuit is not a state-of-the-art design, but it is well proved and is used here for illustration purpose.

It is the author's opinion that the on-off thermostat should be avoided because of its electrical-noise generation potential. Although the bimetal thermostat is basically very simple, it lacks acceptable accuracy and repeatability for normal applications. The mercury column "thermometer"-type thermostat is accurate ($\pm 0.5^\circ\text{C}$) and is a desirable alternative to the bimetal thermostat; however, for flight-test applications, the mercury column often separates under shock and vibration and results in very erratic switching points.

$Q_1, Q_2, Q_3 = 2\text{N}2180\text{A DUAL TRANSISTORS}$
 $Q_4 = 2\text{N}328\text{A TRANSISTOR}$
 $Q_5 = 2\text{N}1208\text{ TRANSISTOR}$
 $R_1 = 100\ \Omega\ \text{RESISTIVE TEMPERATURE SENSOR}$

ALL RESISTORS ARE 1/4-W, 10% RESISTORS EXCEPT
 THOSE MARKED WITH AN * OR **.
 *DENOTES A 1%, PRECISION RESISTOR.
 **DENOTES A 2-W RESISTOR.

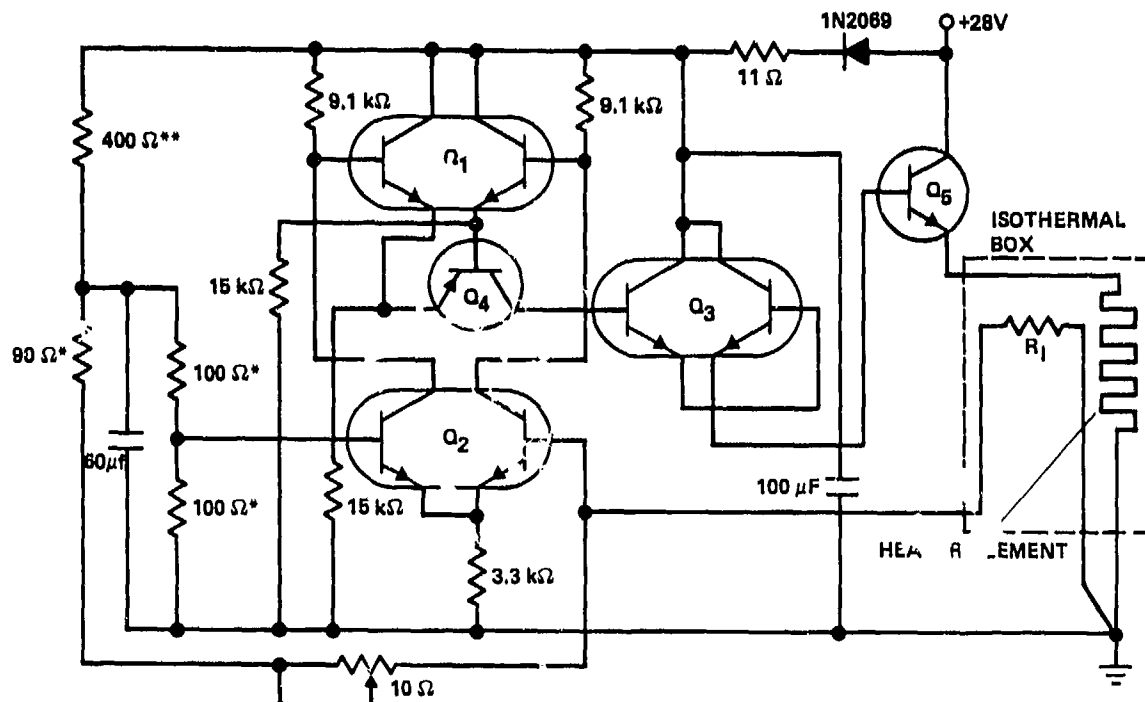


Figure 162. Proportional-control oven temperature regulator

APPENDIX M

THERMOCOUPLE REFERENCE-JUNCTION COMPENSATOR

A thermocouple reference-junction compensator is often used in place of an ice bath or a reference oven to provide a reference for a thermocouple circuit. In one technique for constructing a reference-junction compensator, a temperature-sensitive bridge is used.

The reference-junction compensator of Fig. 163 is designed to compensate a type-K (Chromel-Alumel) thermocouple. This same technique can be used for any of the common metal-type thermocouples. Note that if the thermocouple is grounded, E_B must be isolated from ground. Also when either the power supply or the thermocouple is grounded, the amplifier connected to the output should be an isolation- or differential-type amplifier. The technique used in this appendix is based on the one used in Ref. 46.

To analyze the implementation of the circuit shown in Fig. 163, proceed as follows:

1. Assume that the desired reference temperature T_R is 20°C and that it is desired to compensate for reference-junction ambient temperature variations of $\pm 20^\circ\text{C}$; therefore, where T_{amb} is the ambient temperature,

$$T_{\text{amb}} = T_R \pm 20^\circ\text{C} \quad (\text{M1})$$

2. Approximate the copper-wire/resistance-temperature relationship using the following equation:

$$R_T = R_{20} + \alpha R_{20} (T_{\text{amb}} - 20^\circ\text{C}) \quad (\text{M2})$$

In Eq. (M2), R_{20} is the value of R_T at 20°C , T_{amb} is the temperature of the compensator reference zone, and α is the temperature coefficient of resistivity. For annealed copper, α is specified as $0.00393/^\circ\text{C}$ at 20°C . In this example, R_{20} is arbitrarily set at 15Ω . Over the temperature range of 0°C to 40°C , the temperature sensitivity of a type-K thermocouple, S_K , is $40 \mu\text{V}/^\circ\text{C}$.

3. Assume T_X is, for convenience, temporarily fixed at 20°C . Now, when T_{amb} is also at 20°C and when $R_1 = R_2$ and $R_3 = R_T = R_{20} = 15 \Omega$, the bridge output e_B is zero.

4. Allow the reference-junction temperature T_{amb} to drift away from 20°C , and both the bridge and the thermocouple reference junction will generate voltage outputs that are constrained to cancel each other (remember that T_X is still held at the desired reference temperature, that is, 20°C).

For the reference-junction compensator to function properly under these conditions, the thermocouple error voltage and the bridge voltage e_B should exactly cancel each other. The thermocouple error voltage e_K can be expressed as

$$e_K = S_K(T_{\text{amb}} - 20^\circ\text{C}) \quad (\text{M3})$$

where S_K is the thermocouple sensitivity in volts per degree.

To simplify the bridge design, R_1 and R_2 are made equal. Resistors R_1 , R_2 , and R_3 should be high-quality, metal-film resistors or precision wire-wound resistors. Resistors R_1 and R_2 are selected to be much larger than R_T and R_3 , thus making the current through R_T essentially independent of small variations in R_T . Resistors R_1 and R_2 are arbitrarily chosen to be $5,000 \Omega$ for this exercise.

The bridge-generated output voltage can be expressed as

$$e_B = \alpha R_{20}(T_{\text{amb}} - 20^\circ\text{C})I_T \quad (\text{M4})$$

Since e_B and e_K must be equal and opposite when the junction compensation is effective, the following relationship can be used to calculate I_T , which sets the bridge sensitivity:

$$e_K = S_K(T_{\text{amb}} - 20) = e_B = \alpha R_{20}(T_{\text{amb}} - 20^\circ\text{C})I_T \quad (\text{M5})$$

This equation is then solved for I_T as follows:

$$I_T = S_K/(\alpha R_{20}) \quad (\text{M6})$$

(Note that the relationship shown does not place any limitations on the variation of T_{amb} . This is misleading, since these equations are linear approximations of what is basically a nonlinear process. Large divergences of T_{amb} from 20°C cause errors because of the accumulated nonlinearity.)

In the selected example, the following terms have been defined:

$$\begin{aligned} S_K &= 40 \times 10^{-6} \text{ V/}^\circ\text{C} \\ \alpha &= 39.3 \times 10^{-4}/^\circ\text{C} \\ R_{20} &= 15 \Omega \end{aligned}$$

Therefore, I_T can be calculated from Eq. (M6) as

$$I_T = 40 \times 10^{-6} / (39.3 \times 10^{-4})(15) = 0.679 \text{ mA}$$

The bridge current I_B is equal to $2I_T$, or 1.36 mA. When the bridge power supply E_B is available as 5 V, then R_B is

$$R_B = (5/I_B) - [(R_1 + R_3)(R_2 + R_T)/(R_1 + R_2 + R_3 + R_T)]$$

or

$$R_B = 1,169 \Omega$$

This design can be adapted to other thermocouple types by merely substituting the appropriate value of thermocouple sensitivity for the thermocouple under consideration (for S_K in the above equations). Other materials can be used for the temperature-sensitive element by using an appropriate α .

The accuracy of this technique is limited by three major factors: (1) the linearity of S_K , (2) the linearity of α , and (3) the bridge nonlinearity for large changes in R_T . The practical design would incorporate a technique for setting the initial system to zero. Figure 164 illustrates one method of accomplishing this adjustment for the previously derived compensator.

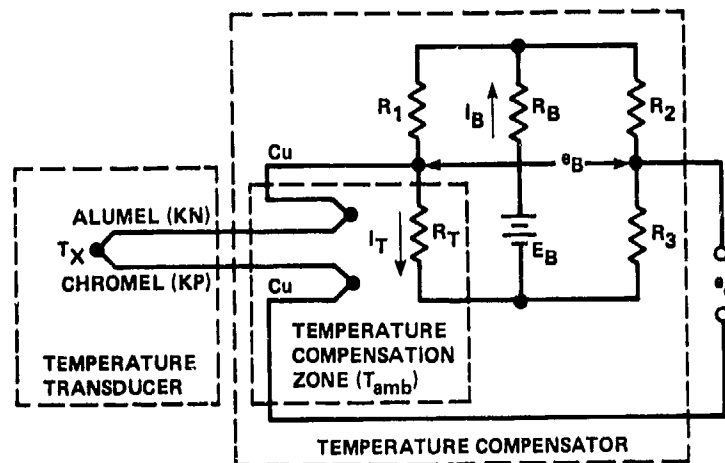


Figure 163. Bridge-type thermocouple reference-junction compensator circuit

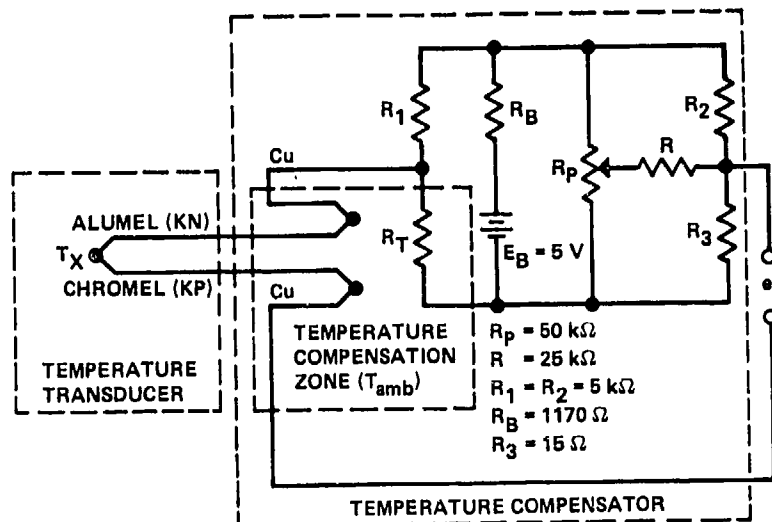
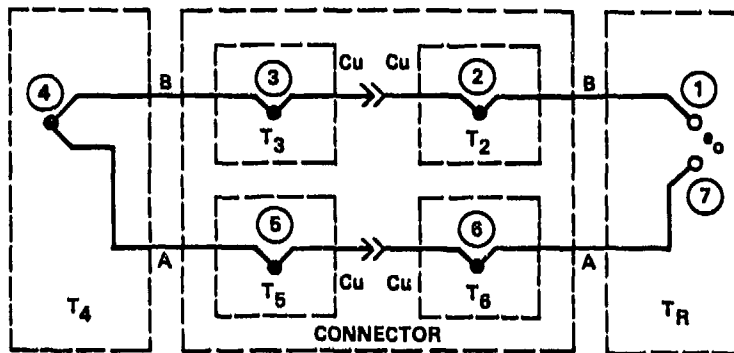


Figure 164. Type-K thermocouple reference-junction compensator with zero adjustment circuit

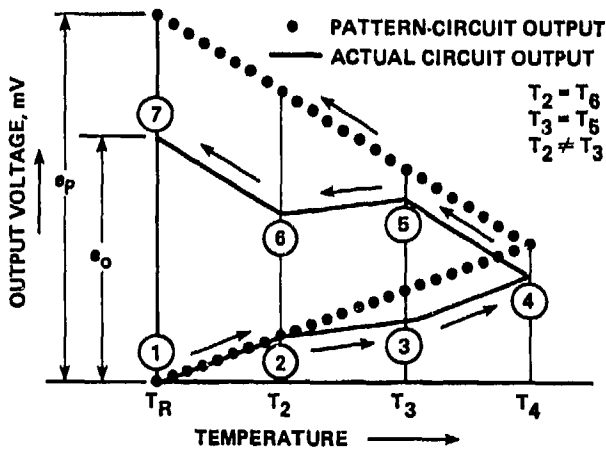
APPENDIX N

ANALYSIS OF A STANDARD COPPER CONNECTOR IN A THERMOCOUPLE WIRING CIRCUIT

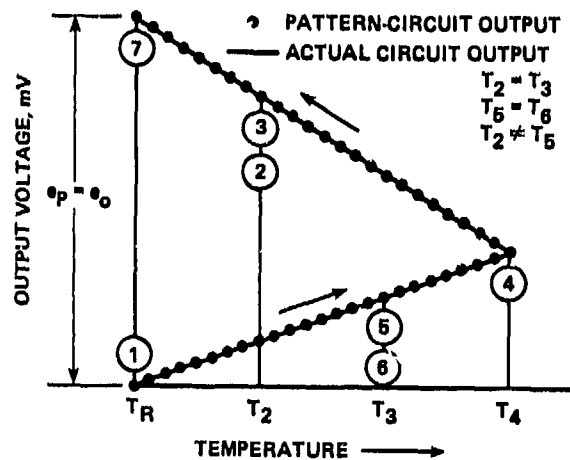
Provisions are often required for a wiring disconnect in a thermocouple circuit. Since different metals and assembly materials are involved, there is a potential for introducing substantial errors into the thermocouple temperature measurement. The most common technique for making a disconnect is to use a standard flight-qualified connector which would normally be used for copper wiring (a plug using copper pins). When certain system restrictions are possible, this approach is the easiest to implement. Figure 165 illustrates this connector problem for two common situations. Figure 165b illustrates a common temperature distribution for a bulkhead disconnect where there are different ambient temperatures on each side of the bulkhead. In this case, significant errors can be introduced into the thermocouple circuit. Figure 165c represents an application of the "law" of inserted materials. (See Appendix J for a more thorough treatment.) Even when thermocouple wires A and B are passed through different plugs, that are at different temperatures (that is, $T_2 \neq T_5$), no errors are introduced as long as there is no temperature gradient between the ends of each connector pin.



(a) Thermocouple circuit with copper connector pins



(b) Temperature gradient along connector pins



(c) Temperature difference between connector pins

Figure 165. Thermocouple circuit with intermediate copper connector pins

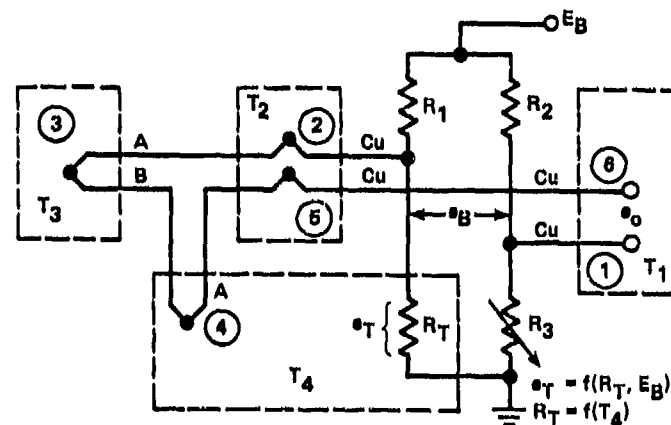
APPENDIX O

THE PATTERN-CIRCUIT ANALYSIS TECHNIQUE FOR COMPLEX THERMOCOUPLE CIRCUITS

The pattern-circuit method is a valuable one for analyzing complex thermocouple circuits. This appendix presents an analysis of two common circuit situations to illustrate how the pattern-circuit method is used. The technique for constructing a thermocouple reference-junction compensator is presented in Ref. 46. In that reference, a circuit (Fig. 166a) is presented that is similar to the one in Fig. 50. The pattern-circuit analysis of Fig. 166b confirms that the circuit is properly mechanized and that the circuit of Fig. 166a should have the same output as the pattern circuit; however, the graphic solution seems overly complex. It is not immediately clear why two isothermal zone boxes are required and, indeed, only one reference is actually required. When the redundant zone box is eliminated, the graphic analysis of Fig. 166c results. Visual inspection shows that the thermocouple wire from point (4) to point (5) is in this case redundant. The result is the simplified circuit of Fig. 163 which has eliminated one junction and one isothermal zone box.

When a commutating switch is used in conjunction with a number of thermocouples and zone boxes, an innovative technique of adding a reference junction may be applied. Figure 167 illustrates two methods of adding a reference junction to commutated thermocouples of a single type and also provides a pattern-circuit analysis of each method. In these cases, the reference-junction voltage is successively added to each sampled thermocouple sensor. Electrically, each circuit agrees with the pattern circuit.

An example of how to use the pattern-circuit technique to locate errors is examined in Fig. 168, assuming that the reference junction was reversed as shown. In Fig. 168b, it is clearly shown that the pattern voltage e_p does not equal the actual circuit output voltage e_o .



(a) Bridge circuit compensator

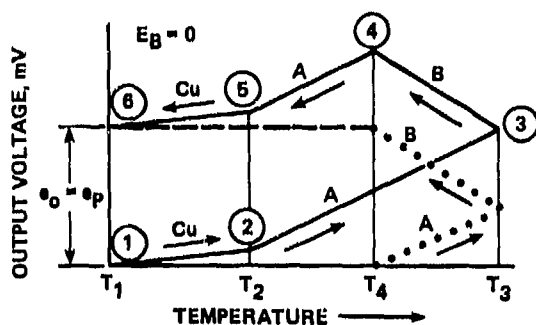
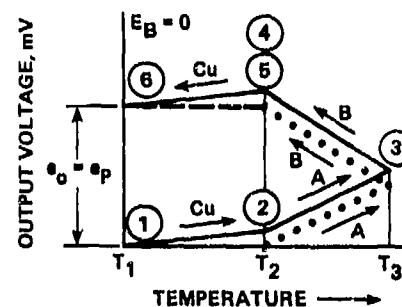
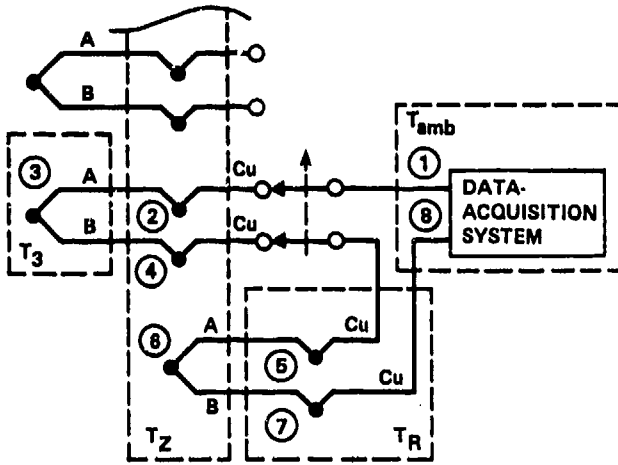
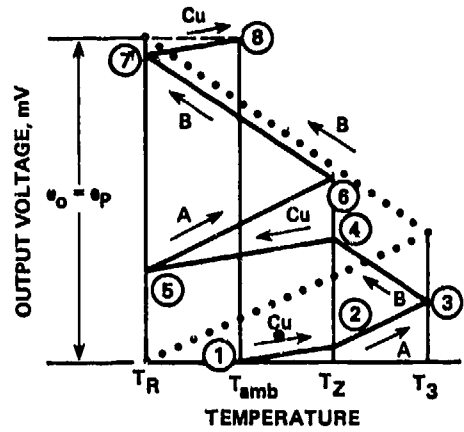
(b) Graphic analysis of (a) with $E_B = 0$ (c) Graphic analysis of (a) with $E_B = 0$ and $T_2 = T_4$

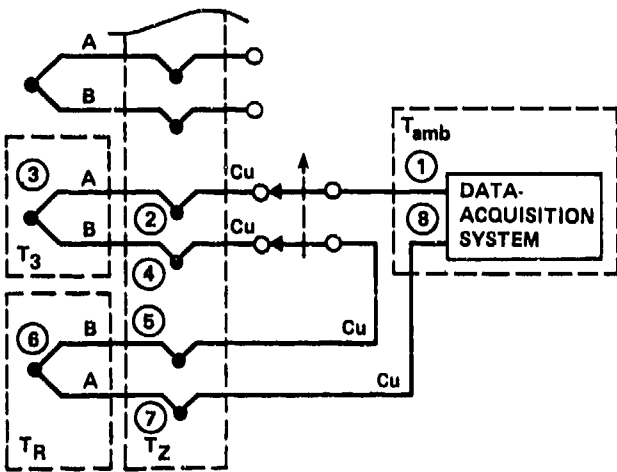
Figure 168. Bridge circuit thermocouple reference-junction compensator



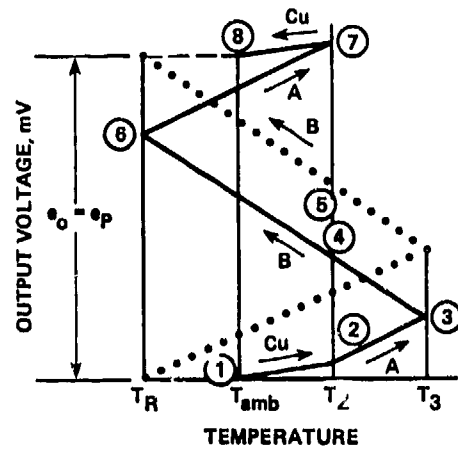
(a) Commutated thermocouple reference technique No. 1



(b) Analysis of technique No. 1

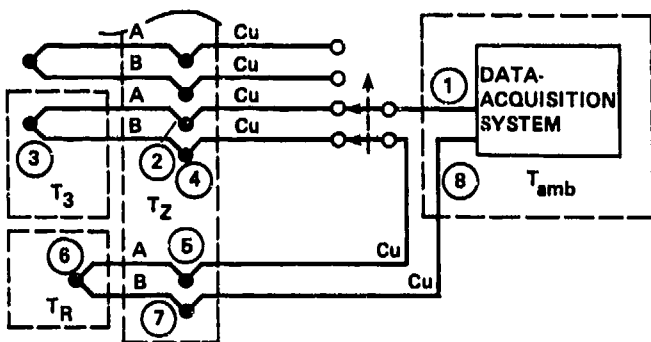


(c) Commutated thermocouple reference technique No. 2

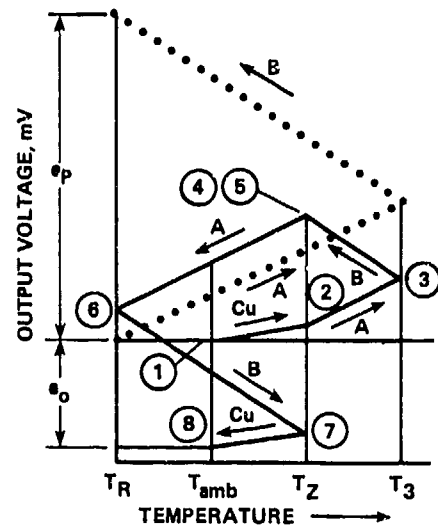


(d) Analysis of technique No. 2

Figure 187. Commutating and referencing thermocouples with some boxes



(a) Commutated multiple-thermocouple system



(b) Graphic analysis of commutated multiple-thermocouple system

Figure 188. Analysis of incorrectly connected reference oven

REFERENCES

1. Pool, A.; and Bosman D., eds.: Basic Principles of Flight Test Instrumentation Engineering. AGARDograph No. 160, vol. 1, 1974.
2. Standard 315-1975: Symbols. Inst. of Elec. & Electron. Eng., 1975.
3. Borek, Robert: Practical Aspects of Instrumentation System Installation. AGARDograph No. 160, vol. 13, 1981.
4. Wilner, Douglass O.: AIFTDS Stand-Along RMDU Flight Test Report. NASA TM-72866, 1979.
5. Wilner, Douglass O.: Results of a Remote Multiplexer/Digitizer Unit Accuracy and Environmental Study. NASA TMX-56043, 1977.
6. Morrison, Ralph: Grounding and Shielding Techniques in Instrumentation. Second ed. John Wiley & Sons, Inc., New York, 1972.
7. Ott, Henry W.: Noise Reduction Techniques in Electronic Systems. John Wiley & Sons, Inc., New York, 1976.
8. Bergh, H.; and Tijdemann, H.: Theoretical and Experimental Results for the Dynamic Response of Pressure Measuring Systems. Report NLR-TR F.238, National Aeronautical Laboratory, Amsterdam, 1965.
9. Ferrell, K.R.: Helicopter Flight Test Instrumentation. AGARDograph No. 160, vol. 10, 1980.
10. Graeme, Jerald G.; et al., eds.: Operational Amplifiers: Design and Applications. McGraw-Hill Book Co., Inc., New York, 1971.
11. Graeme, Jerald G.: Application of Operational Amplifiers, Third Generation Techniques. McGraw-Hill Book Co., Inc., New York, 1973.
12. Zverev, Anatol I.: Handbook of Filter Synthesis. John Wiley & Sons, Inc., New York, 1967.
13. Rabiner, L.R.; and Gold, B.A.: Theory and Application of Digital Signal Processing. Prentice Hall, Inc., Englewood Cliffs, N.J., 1975.
14. Oppenheim, Alan V.; and Schaffer, Ronald W.: Digital Signal Processing. Prentice Hall, Inc., Englewood Cliffs, N.J., 1975.
15. Aircraft Internal Time Division Command/Response Multiplex Data Bus. MIL-STD-1553B, 1978.
16. Brockman, D.M.: A Flight Test Real-Time GW-CG Computing System. International Instrum. Symposium, Instrumen. Soc. America, Seattle, Wash., 1980, vol. 2, pt. 2, pp. 583-589.
17. Lieberman, William S.: Use of On-Board Real-Time Flight Test Analysis and Monitor System - A Progress Report. AGARD Conference Proc. No. 223, 1976, pp. 24-1 to 24-10.
18. Hix, C.F., Jr.; and Alley, R.P.: Physical Laws and Effects. John Wiley & Sons, Inc., New York, 1958.
19. Shock and Vibration Measurement Technology. Rev. ed. Endevco Dynamic Instrument Div., San Juan Capistrano, Calif., Nov. 1980.
20. Wilson, John: Noise Suppression and Prevention in Piezoelectric Transducer System. Sound and Vibration, Apr. 1979.
21. Change, N.D.: Integrated-Circuit Piezoelectric Instrumentation. Measurements and Control. Jan.-Feb. 1977.
22. Herzfeld, C.M., ed.: Temperature, Its Measurement and Control in Science and Industry. Reinhold Publishing Corp., New York, and Chapman and Hall, Ltd., London, 1962, vol. 3, pt. I and II.
23. Moffat, Robert J.: The Gradient Approach to Thermocouple Circuitry. Proc. of Fourth Symposium on Temperature, Its Measurement, and Control in Science and Industry; American Inst. Phys., Instrum. Soc. America, and NBS, 1961.
24. Moffat, Robert J.: 1976 Measurement Systems Engineering Short Course: Thermocouple Theory and Practice. Sixth ed. Stein Engineering Services, Phoenix, Ariz., 1976.
25. Powell, Robert L.; et al.: Thermocouple Reference Tables Based on IPTIS-68. NBS Monograph 125, 1974.
26. Thermocouple Measurements with the 3050B. Hewlett Packard Corp., Palo Alto, Calif., 1968.

27. Doebelin, Ernest O.: Measurement Systems: Application and Design. McGraw-Hill Book Co., Inc., New York, 1975.
28. Kottkamp, K.; Wilhelm, H.; and Kohl, D.: Strain Gauge Measurements on Aircraft. AGARDograph No. 160, vol. 7, 1976.
29. Condon, E.V.; and Odishaw, Hugh, eds.: Handbook of Physics. McGraw-Hill Book Co., Inc., New York, 1958.
30. Synchro Conversion Handbook. Second ed. Data Device Corp., N. Hollywood, Calif., 1979.
31. Giannini Optical Shaft Encoder. Bulletin 001, Giannini Corp., Monrovia, Calif., 1965.
32. Morris, Harold D.: A Low Cost Precision Inertial-Grade Accelerometer. Deutsche Gesellschaft für Ortung und Navigation Symposium, Braunschweig, Germany, 1976.
33. Vernier Range Extender, Model 4409. Tech. Bull. 1090, Systron-Donner Corp., Concord, Calif., 1964.
34. Telemetry Standards Document 106-80. Telemetry Group, Inter-Range Instrumentation Group, Range Commanders Council. Secretariat, Range Commanders Council, White Sands Missile Range, N. Mex., 1980.
35. Telemetry FM/FM Baseband Structure Study. AD-621139 and AD-621140, vol. I and II. Department of Defense, 1962.
36. Maury, Jesse L.; and Styles, Frederick J.: Development of Optimum Frame Synchronization Codes for Goddard Space Flight Center PCM Telemetry Standards. National Telemetry Conference Proc., June 1964.
37. Crowley, L.D.: Evolution of the Douglas Flight-Test Data System. International Telemetry Conference Proc., vol. X, 1976, pp. 186-187.
38. Bennett, G.E.: Magnetic Recording of Flight Test Data. AGARDograph No. 160, vol. 5, 1979.
39. Kalll, Ford, ed.: Magnetic Tape Recording for the Eighties. NASA RP-1075, 1982.
40. Nichols, Myron H.; and Rauch, Lawrence L.: Radio Telemetry. Second ed. John Wiley & Sons, Inc., New York, 1960.
41. Sheingold, Daniel H., ed.: Transducer Interfacing Handbook: A Guide to Analog Signal Conditioning. Analog Devices Inc., Norwood, Mass., 1980.
42. Williams, Arthur B.: Design Active Elliptical Filters Easily. Electronic Design, vol. 19, no. 21, Oct. 14, 1971.
43. Deboo, Gordon J.: An RC Active Filter Design Handbook. NASA SP-5104, 1977.
44. Lancaster, Don: Active-Filter Cookbook. Howard W. Sams and Co. Inc., Indianapolis, Ind., 1980.
45. Kaufman, M.: Get Notch Q's in the Hundreds. Electronic Design, vol. 22, no. 16, Aug. 2, 1974, p. 96.
46. Ben-Yaakob, S.; and Sanandago, Y.: Don't Sweat with Thermocouple Thermometers. Electronic Design, vol. 24, no. 24, Nov. 22, 1976, pp. 142-148.

Annex 1

AGARD FLIGHT TEST INSTRUMENTATION AND FLIGHT TEST TECHNIQUES SERIES

1. Volumes in the AGARD Flight Test Instrumentation Series, AGARDograph 160

<i>Volume Number</i>	<i>Title</i>	<i>Publication Date</i>
1.	Basic Principles of Flight Test Instrumentation Engineering by A.Pool and D.Bosman	1974
2.	In-Flight Temperature Measurements by F.Trenkle and M.Reinhardt	1973
3.	The Measurement of Fuel Flow by J.T.France	1972
4.	The Measurement of Engine Rotation Speed by M.Vedrunes	1973
5.	Magnetic Recording of Flight Test Data by G.E.Bennett	1974
6.	Open and Closed Loop Accelerometers by I.Mclaren	1974
7.	Strain Gauge Measurements on Aircraft by E.Kottkamp, H.Wilhelm and D.Kohl	1976
8.	Linear and Angular Position Measurement of Aircraft Components by J.C.van der Linden and H.A.Mensink	1977
9.	Aeroelastic Flight Test Techniques and Instrumentation by J.W.G.van Nunen and G.Piazzoli	1979
10.	Helicopter Flight Test Instrumentation by K.R.Ferrell	1980
11.	Pressure and Flow Measurement by W.Wuest	1980
12.	Aircraft Flight Test Data Processing — A Review of the State of the Art by L.J.Smith and N.O.Matthews	1980
13.	Practical Aspects of Instrumentation System Installation by R.W.Borek	1981
14.	The Analysis of Random Data by D.A.Williams	1981
15.	Gyroscopic Instruments and their Application to Flight Testing by B.Stieler and H.Winter	1982
16.	Trajectory Measurements for Take-off and Landing Test and Other Short-Range Applications by P.de Benque d'Agut, H.Riebeck and A.Pool	1985
17.	Analogue Signal Conditioning for Flight Test Instrumentation by D.W.Veatch and R.K.Bogue	1986

At the time of publication of the present volume the following volume was in preparation:

Microprocessor Applications in Airborne Flight Test Instrumentation
by M.Prickett

2. Volumes in the AGARD Flight Test Techniques Series

<i>Number</i>	<i>Title</i>	<i>Publication Date</i>
AG 237	Guide to In-Flight Thrust Measurement of Turbojets and Fan Engines by the MIDAP Study Group (UK)	1979

The remaining volumes will be published as a sequence of Volume Numbers of AGARDograph 300.

<i>Volume Number</i>	<i>Title</i>	<i>Publication Date</i>
1.	Calibration of Air-Data Systems and Flow Direction Sensors by J.A.Lawford and K.R.Nippres	1983
2.	Identification of Dynamic Systems by R.E.Maine and K.W.Iliff	1986
3.	Identification of Dynamic Systems Applications to Aircraft Part 1: The Output Error Approach by R.E.Maine and K.W.Iliff	1985
4.	Determination of Antenna Patterns and Radar Reflection Characteristics of Aircraft by H.Bothe and D.Macdonald	1986
5.	Store Separation Flight Testing by R.J.Arnold and C.S.Epstein	1986

At the time of publication of the present volume the following volumes were in preparation:

Identification of Dynamic Systems. Applications to Aircraft
Part 2: Nonlinear Model Analysis and Manoeuvre Design
by J.A.Mulder and J.H.Breeman

Flight Testing of Digital Navigation and Flight Control Systems
by F.J.Abbink and H.A.Timmers

Techniques and Devices Applied in Developmental Airdrop Testing
by H.J.Hunter

Aircraft Noise Measurement and Analysis Techniques
by H.H.Heller

Air-to-Air Radar Flight Testing
by R.E.Scott

The Use of On-Board Computers in Flight Testing
by R.Langlade

Flight Testing under Extreme Environmental Conditions
by C.L.Hendrickson

Flight Testing of Terrain Following Systems
by C.Dallimore and M.K.Foster

Annex 2

AVAILABLE FLIGHT TEST HANDBOOKS

This annex is presented to make readers aware of handbooks that are available on a variety of flight test subjects not necessarily related to the contents of this volume.

Requests for A & AEE documents should be addressed to the Defence Research Information Centre, Glasgow (see back cover). Requests for US documents should be addressed to the Defense Technical Information Center, Cameron Station, Alexandria, VA 22314 (or in one case, the Library of Congress).

<i>Number</i>	<i>Author</i>	<i>Title</i>	<i>Date</i>
NATC-TM76-ISA	Simpson, W.R.	Development of a Time-Variant Figure-of-Merit for Use in Analysis of Air Combat Maneuvering Engagements	1976
NATC-TM76-3SA	Simpson, W.R.	The Development of Primary Equations for the Use of On-Board Accelerometers in Determining Aircraft Performance	1977
NATC-TM-77-IRW	Woomer, C. Carico, D.	A Program for Increased Flight Fidelity in Helicopter Simulation	1977
NATC-TM-77-2SA	Simpson, W.R. Oberle, R.A.	The Numerical Analysis of Air Combat Engagements Dominated by Maneuvering Performance	1977
NATC-TM-77-1SY	Gregoire, H.G.	Analysis of Flight Clothing Effects on Aircrew Station Geometry	1977
NATC-TM-78-2RW	Woomer, G.W. Williams, R.L.	Environmental Requirements for Simulated Helicopter/VTOL Operations from Small Ships and Carriers	1978
NATC-TM-78-1RW	Yeend, R. Carico, D.	A Program for Determining Flight Simulator Field-of-View Requirements	1978
NATC-TM-79-33SA	Chapin, P.W.	A Comprehensive Approach to In-Flight Thrust Determination	1980
NATC-TM-79-3SY	Schiflett, S.G. Loikith, G.J.	Voice Stress Analysis as a Measure of Operator Workload	1980
NWC-TM-3485	Rogers, R.M.	Six-Degree-of-Freedom Store Program	1978
WSAMC-AMCP 706-204	—	Engineering Design Handbook, Helicopter Performance Testing	1974
NASA-CR-3406	Bennett, R.L. and Pearsons, K.S.	Handbook on Aircraft Noise Metrics	1981
—	—	Pilot's Handbook for Critical and Exploratory Flight Testing. (Sponsored by AIAA & SETP — Library of Congress Card No. 76-189165)	1972
—	—	A & AEE Performance Division Handbook of Test Methods for Assessing the Flying Qualities and Performance of Military Aircraft. Vol.1 Airplanes	1979
A & AEE Note 2111	Appleford, J.K.	Performance Division: Clearance Philosophies for Fixed Wing Aircraft	1978

<i>Number</i>	<i>Author</i>	<i>Title</i>	<i>Date</i>
A & AEE Note 2113 (Issue 2)	Norris, E.J.	Test Methods and Flight Safety Procedures for Aircraft Trials Which May Lead to Departures from Controlled Flight	1980
AFFTC-TD-75-3	Mahlum, R.	Flight Measurements of Aircraft Antenna Patterns	1973
AFFTC-TIH-76-1	Reeser, K. Brinkley, C. and Plews, L.	Inertial Navigation Systems Testing Handbook	1976
AFFTC-TIH-79-1	—	USAF Test Pilot School (USAFTPS) Flight Test Handbook. Performance: Theory and Flight Techniques	1979
AFFTC-TIH-79-2	—	USAFTPS Flight Test Handbook. Flying Qualities: Theory (Vol.1) and Flight Test Techniques (Vol.2)	1979
AFFTC-TIM-81-1	Rawlings, K., III	A Method of Estimating Upwash Angle at Noseboom-Mounted Vanes	1981
AFFTC-TIH-81-1	Plews, L. and Mandt, G.	Aircraft Brake Systems Testing Handbook	1981
AFFTC-TIH-81-5	DeAnda, A.G.	AFFTC Standard Airspeed Calibration Procedures	1981
AFFTC-TIH-81-6	Lush, K.	Fuel Subsystems Flight Test Handbook	1981
AFEWC-DR 1-81	—	Radar Cross Section Handbook	1981
NATC-TM-71-ISA226	Hewett, M.D. Galloway, R.T.	On Improving the Flight Fidelity of Operational Flight/Weapon System Trainers	1975
NATC-TM-TPS76-1	Bowes, W.C. Miller, R.V.	Inertially Derived Flying Qualities and Performance Parameters	1976
NASA Ref. Publ. 1008	Fisher, F.A. Plumer, J.A.	Lightning Protection of Aircraft	1977
NASA Ref. Publ. 1046	Gracey, W.	Measurement of Aircraft Speed and Altitude	1980
NASA Ref. Publ. 1075	Kalil, F.	Magnetic Tape Recording for the Eighties (Sponsored by: Tape Head Interface Committee)	1982

The following handbooks are written in French and are edited by the French Test Pilot School (EPNER Ecole du Personnel Navigant d'Essais et de Réception ISTRES — FRANCE), to which requests should be addressed.

<i>Number EPNER Reference</i>	<i>Author</i>	<i>Title</i>	<i>Price (1983) French Francs</i>	<i>Notes</i>
2	G.LebLANC	L'analyse dimensionnelle	20	Réédition 1977
7	EPNER	Manuel d'exploitation des enregistrements d'Essais en vol	60	6ème Edition 1970
8	M.Durand	La mécanique du vol de l'hélicoptère	155	1ère Edition 1981
12	C.Laburthe	Mécanique du vol de l'avion appliquée aux essais en vol	160	Réédition en cours
15	A.Hisler	La prise en main d'un avion nouveau	50	1ère Edition 1964
16	Candau	Programme d'essais pour l'évaluation d'un hélicoptère et d'un pilote automatique d'hélicoptère	20	2ème Edition 1970
22	Cattaneo	Cours de métrologie	45	Réédition 1982

<i>Number EPNER Reference</i>	<i>Author</i>	<i>Title</i>	<i>Price (1983) French Francs</i>	<i>Notes</i>
24	G.Fraysse F.Cousson	Pratique des essais en vol (en 3 Tomes)	T 1 - 160 T 2 - 160 T 3 - 120	1ère Edition 1973
25	EPNER	Pratique des essais en vol hélicoptère (en 2 Tomes)	T 1 - 150 T 2 - 150	Edition 1981
26	J.C.Wanner	Bang sonique	60	
31	Tarnowski	Inertie-verticale-sécurité	50	1ère Edition 1981
32	B.Pennacchioni	Aéroélasticité -- le flottement des avions	40	1ère Edition 1980
33	C.Lelaie	Les vrilles et leurs essais	110	Edition 1981
37	S.Allenic	Electricité à bord des aéronefs	100	Edition 1978
53	J.C.Wanner	Le moteur d'avion (en 2 Tomes) T 1 Le réacteur T 2 Le turbopropulseur	85 85	Réédition 1982
55	De Cennival	Installation des turbomoteurs sur hélicoptères	60	2ème Edition 1980
63	Gremont	Aperçu sur les pneumatiques et leurs propriétés	25	3ème Edition 1972
77	Gremont	L'atterrissage et le problème du freinage	40	2ème Edition 1978
82	Auffret	Manuel de médecine aéronautique	55	Edition 1979
85	Monnier	Conditions de calcul des structures d'avions	25	1ère Edition 1964
88	Richard	Technologie hélicoptère	95	Réédition 1971

REPORT DOCUMENTATION PAGE

Recipient's Reference	2. Originator's Reference AGARD-AG-160 Volume 17	3. Further Reference ISBN 92-835-1520-X	4. Security Classification of Document UNCLASSIFIED				
5. Originator	Advisory Group for Aerospace Research and Development North Atlantic Treaty Organization 7 rue Ancelle, 92200 Neuilly sur Seine, France						
6. Title	ANALOGUE SIGNAL CONDITIONING FOR FLIGHT TEST INSTRUMENTATION						
7. Presented at							
8. Author(s)/Editor(s)	D.W.Veatch and R.K.Bogue edited by R.K.Bogue		9. Date April 1986				
10. Author's/Editor's Address	Various		11. Pages 178				
12. Distribution Statement	This document is distributed in accordance with AGARD policies and regulations, which are outlined on the Outside Back Covers of all AGARD publications.						
13. Keywords/Descriptors	<table border="0"> <tr> <td>Flight tests</td> <td>Data acquisition</td> </tr> <tr> <td>Recording instruments</td> <td>Signal processing</td> </tr> </table>			Flight tests	Data acquisition	Recording instruments	Signal processing
Flight tests	Data acquisition						
Recording instruments	Signal processing						
14. Abstract	<p>✦ This Flight-Test Instrumentation AGARDograph in the 160 Series addresses the application of analog signal conditioning to flight-test data-acquisition systems. Emphasis is placed on practical applications of signal conditioning for the most common flight-test data-acquisition systems. A limited amount of theoretical discussion is included to assist the reader in a more complete understanding of the subject matter.</p> <p>Nonspecific signal conditioning, such as amplifications, filtering, and multiplexing, is discussed. Signal conditioning for various specific transducers and data terminal devices is also discussed to illustrate signal conditioning that is unique to particular types of transducers.</p> <p>The purpose of this document is to delineate for the flight-test instrumentation engineer the various signal conditioning technique options, together with tradeoff considerations, for commonly encountered flight-test situations.</p> <p>This AGARDograph has been sponsored by the Flight Mechanics Panel of AGARD.</p>						

<p>AGARDograph No.160 Volume 17 Advisory Group for Aerospace Research and Development, NATO ANALOGUE SIGNAL CONDITIONING FOR FLIGHT TEST INSTRUMENTATION by D.W.Veach and R.K.Bogue, edited by R.K.Bogue Published April 1986 178 pages</p> <p>This Flight-Test Instrumentation AGARDograph in the 160 Series addresses the application of analog signal conditioning to flight-test data-acquisition systems. Emphasis is placed on practical applications of signal conditioning for the most common flight-test data-acquisition systems. A limited amount of theoretical discussion is included to assist the reader in a more</p> <p>P.T.O</p>	<p>AGARD-AG-160-Vol.17</p> <p>Flight tests Recording instruments Data acquisition Signal processing</p>	<p>AGARDograph No.160 Volume 17 Advisory Group for Aerospace Research and Development, NATO ANALOGUE SIGNAL CONDITIONING FOR FLIGHT TEST INSTRUMENTATION by D.W.Veach and R.K.Bogue, edited by R.K.Bogue Published April 1986 178 pages</p> <p>This Flight-Test Instrumentation AGARDograph in the 160 Series addresses the application of analog signal conditioning to flight-test data-acquisition systems. Emphasis is placed on practical applications of signal conditioning for the most common flight-test data-acquisition systems. A limited amount of theoretical discussion is included to assist the reader in a more</p> <p>P.T.O</p>	<p>AGARD-AG-160-Vol.17</p> <p>Flight tests Recording instruments Data acquisition Signal processing</p>
<p>AGARDograph No.160 Volume 17 Advisory Group for Aerospace Research and Development, NATO ANALOGUE SIGNAL CONDITIONING FOR FLIGHT TEST INSTRUMENTATION by D.W.Veach and R.K.Bogue, edited by R.K.Bogue Published April 1986 178 pages</p> <p>This Flight-Test Instrumentation AGARDograph in the 160 Series addresses the application of analog signal conditioning to flight-test data-acquisition systems. Emphasis is placed on practical applications of signal conditioning for the most common flight-test data-acquisition systems. A limited amount of theoretical discussion is included to assist the reader in a more</p> <p>P.T.O</p>	<p>AGARD-AG-160-Vol.17</p> <p>Flight tests Recording instruments Data acquisition Signal processing</p>	<p>AGARDograph No.160 Volume 17 Advisory Group for Aerospace Research and Development, NATO ANALOGUE SIGNAL CONDITIONING FOR FLIGHT TEST INSTRUMENTATION by D.W.Veach and R.K.Bogue, edited by R.K.Bogue Published April 1986 178 pages</p> <p>This Flight-Test Instrumentation AGARDograph in the 160 Series addresses the application of analog signal conditioning to flight-test data-acquisition systems. Emphasis is placed on practical applications of signal conditioning for the most common flight-test data-acquisition systems. A limited amount of theoretical discussion is included to assist the reader in a more</p> <p>P.T.O</p>	<p>AGARD-AG-160-Vol.17</p> <p>Flight tests Recording instruments Data acquisition Signal processing</p>

<p>complete understanding of the subject matter.</p> <p>Nonspecific signal conditioning, such as amplifications, filtering, and multiplexing, is discussed. Signal conditioning for various specific transducers and data terminal devices is also discussed to illustrate signal conditioning that is unique to particular types of transducers.</p> <p>The purpose of this document is to delineate for the flight-test instrumentation engineer the various signal-conditioning technique options, together with tradeoff considerations, for commonly encountered flight-test situations.</p> <p>This AGARDograph has been sponsored by the Flight Mechanics Panel of AGARD.</p> <p>ISBN 92-835-1520-X</p>	<p>complete understanding of the subject matter.</p> <p>Nonspecific signal conditioning, such as amplifications, filtering, and multiplexing, is discussed. Signal conditioning for various specific transducers and data terminal devices is also discussed to illustrate signal conditioning that is unique to particular types of transducers.</p> <p>The purpose of this document is to delineate for the flight-test instrumentation engineer the various signal-conditioning technique options, together with tradeoff considerations, for commonly encountered flight-test situations.</p> <p>This AGARDograph has been sponsored by the Flight Mechanics Panel of AGARD.</p> <p>ISBN 92-835-1520-X</p>
<p>complete understanding of the subject matter.</p> <p>Nonspecific signal conditioning, such as amplifications, filtering, and multiplexing, is discussed. Signal conditioning for various specific transducers and data terminal devices is also discussed to illustrate signal conditioning that is unique to particular types of transducers.</p> <p>The purpose of this document is to delineate for the flight-test instrumentation engineer the various signal-conditioning technique options, together with tradeoff considerations, for commonly encountered flight-test situations.</p> <p>This AGARDograph has been sponsored by the Flight Mechanics Panel of AGARD.</p> <p>ISBN 92-835-1520-X</p>	<p>complete understanding of the subject matter.</p> <p>Nonspecific signal conditioning, such as amplifications, filtering, and multiplexing, is discussed. Signal conditioning for various specific transducers and data terminal devices is also discussed to illustrate signal conditioning that is unique to particular types of transducers.</p> <p>The purpose of this document is to delineate for the flight-test instrumentation engineer the various signal-conditioning technique options, together with tradeoff considerations, for commonly encountered flight-test situations.</p> <p>This AGARDograph has been sponsored by the Flight Mechanics Panel of AGARD.</p> <p>ISBN 92-835-1520-X</p>